UNIVERSITÀ DEGLI STUDI DI TRIESTE

# UNIVERSITÀ DEGLI STUDI DI TRIESTE

## XXXIV CICLO DEL DOTTORATO DI RICERCA IN

**Earth Science, Fluido Dynamics, Mathematics. Methodic interactions**

# The Messinian Salinity Crisis in the Adriatic Sea

Settore scientifico-disciplinare: GEO/11 Geofisica Applicata


DOTTORANDA

**Alessandra Lanzoni**

COORDINATORE

**PROF. Stefano Maset**

SUPERVISORE DI TESI

**PROF. Michele Pipan**

CO-SUPERVISORE DI TESI

**PROF. Anna Del Ben**


**ANNO ACCADEMICO 2020/2021**

# Table of Contents

# Abstract

The framework of this thesis investigated the effect of the Messinian Salinity Crisis (MSC; 5.97-5.33 Ma) in the Adriatic Sea, one of the most controversial geological events that occurred in the Mediterranean Basin. The main objectives included the analysis of surfaces and units of the MSC to evaluate the thickness of the MSC deposits and their relationships with the effect of different phenomena such as erosion, non-deposition, and Plio-Quaternary deformation, all related to the geological evolution of the Adria plate and its role as Apennine foreland. Moreover, the Adriatic Sea represents a not fully understood problem in the framework of the MSC and its connection with the other Mediterranean basins.

The Adriatic Sea is one of several restricted basins located in the Mediterranean Basin. It represents the foreland of three orogenic belts: The Southern Alps to the North, active since the Cretaceous time; the Dinarides to the East, active during the Eocene; and the Apennines to the West, active since the Paleogene.

For the aim of this thesis, more than 10000 km long 2D multichannel seismic profiles were analyzed, calibrated by 218 boreholes, covering almost the whole Adriatic Sea in the Italian and partially Croatian offshore. The interpretation of the seismic lines in the Adriatic Sea has been carried out thanks to the IHS Kingdom Suite software. A precise and careful seismo-stratigraphy analysis was performed to recognize the different facies of the sedimentary sequence, focusing on the MSC expression.

Analysis of the MSC surfaces and unit allowed to produce of the map of the base of the Plio-Quaternary sequence and the thickness of the evaporites. In particular, the Adriatic Sea was divided into three main geographical areas based on the occurrence of the MSC. Our results showed that the Northern Adriatic Sea during the MSC experienced subaerial exposure in front of the Trieste and Venice Gulfs. At the same time, evaporite deposition occurred in the modern Rimini foredeep. The Central Adriatic Sea shows the combined effect of deposition and erosion, with several channel incisions in this area, are related to paleo-drainage systems. The Southern Adriatic Sea shows an intense erosion on the carbonate platform, while MSC evaporites are present and eroded along the margins of the South Adriatic Basin.

Following the MSC, the east migration of the Apennine Chain was covered with the external thrust and obliterated part of the MSC. From the Late Pliocene, the Adriatic Sea underwent different evolutionary steps. Boreholes calibration highlight the presence of locally very thin Pliocene

succession in the entire Adriatic Sea. The main effect of the Apennines' eastward migration occurred during the Lower Pliocene, as testified by the regional tilting of the MSC reflectors, onlapped by Plio-Quaternary (PQ) parallel reflectors. The Southern Adriatic Sea was affected, starting from the Pliocene, by the Albanides orogenesis, as testified by the eastward foreland tilting, where PQ sediments onlap the MSC unconformity.

# Chapter 0 - Introduction

During the Messinian Salinity Crisis (MSC) (5.97 – 5.33 Ma; Krijgsman et al., 1999b; Roveri et al., 2014b), massive paleo-oceanographic and environmental changes affected the Mediterranean area (Hsü et al., 1973b). In the framework of the Mediterranean Sea, such changes lead to the deposition of kilometers-thick evaporites, mainly composed of halite, in the deep basins, or to a widespread erosional surface (Ryan and Cita, 1978) in the upper margins. This work focuses on the MSC effects in the Adriatic Sea, which during the Messinian age represented a peculiar basin in the Mediterranean context.

The Adriatic Sea is considered a marginal basin, where evaporite deposition is mainly characterized by a few tens/two hundred meters of gypsum at most, often topped or replaced by an erosional surface. The geodynamic context was a basin interposed between the Apennine and Dinard folds and thrust belts. The distribution of the MSC surfaces and unit in the Adriatic area has been a matter of several studies in the past years (Roveri et al., 2001, 2004, 2006; Ghielmi et al., 2010, 2013; Amadori et al., 2018; Manzi et al., 2020). Most of the research focused on the Northern Apennine outcrop data (Roveri et al., 2001, 2004, 2006), while few studies based on 2D and 3D seismic data are available (Ghielmi et al.,2010, 2013; Rossi et al., 2015; Amadori et al., 2018), localized in the Po Plain and Northern Adriatic Sea.

Since the end of the XIX century, the intensive hydrocarbon exploration in the Adriatic Sea and Po Plain produced several tens of wells that crossed the Messinian sequence or the relative unconformity. A few years ago, seismic data and exploration boreholes were made available through the ViDEPI (Visibility of petroleum exploration data in Italy) project, covering the entire Italian offshore and onshore territory. On the same time, several papers furnished new seismic data and geological information on the east Adriatic Sea. Identification of MSC events in the seismic profiles is favored by peculiar seismic facies of the surfaces and units, highlighted by a top marked by a high amplitude reflector with positive polarity.

Interpreting the Messinian surfaces and units considers the effect of the hypothesized sea-level drawdown during the MSC (Ryan and Cita, 1978), which also triggered an isostatic adjustment, especially in the deeper part. However, in the Adriatic Sea, the effect of the eastward Apennine migration during the Pliocene partially obliterated and deformed the MSC deposits and surfaces.

This paper aims to interpret more than 10000 km of 2D seismic profiles calibrated by exploration wells, to recognize the MSC seismic expression in the Adriatic Sea and the different meanings it

assumes in the study area, through the composition of structural and isopach maps related to the MSC event.

## Objective of the thesis

In this PhD thesis, I focused on the MSC surfaces and unit in the Adriatic Sea. So far, a complete work analyzing the effect of the MSC in the entire Adriatic Sea using 2D seismic lines is not available in the literature. Ghielmi et al. (2010, 2013) and Amadori et al. (2018) focused on the Po Plain and Northern Adriatic Sea, while the Central Adriatic Sea was studied by analyzing exploration boreholes (Manzi et al., 2020). Many local and extemporary considerations about the MSC have been made by various Authors who have analyzed the geological development of the Adriatic Sea, also through the peculiar seismic marker of the MSC (eg: Finetti et al., 1987; Argnani et al. 1996; Grandic et al., 1999, 2001; Geletti et al., 2008; Scisciani and Calamita, 2009; Argnani, 2013; Spelic et al., 2020; Mancinelli and Scisciani, 2020)

The primary out comes that I was going to obtain from this work were:

1. Precise analysis of the MSC surfaces and unit in the entire Adriatic Sea;
2. Paleo-geographical reconstruction of the Adriatic Sea area during the MSC;
3. Post-MSC analysis of the study area.

Moreover, some questions I tried to answer in this PhD works were:

- Was the Adriatic foreland completely subaerially exposed during the MSC sea-level drawdown acme?
- Was the Adriatic Sea disconnected from the rest of the Mediterranean Sea?

I used a geophysical approach to address these objectives and questions, analyzing the available 2D seismic dataset and mapping the MSC surface and unit thickness. In order to calibrate the seismic profiles, a large number of exploration boreholes (ViDEPI) were used. Mapping of the MSC surfaces and unit results in the production of several line drawings connecting the Italian-Croatian offshore, a structural map of the MSC surfaces and an isopach map of the MSC unit where evaporites were recognized.

Consideration of the post-MSC evolution of the study area was made, through the flattening of some selected seismic profiles, in order to understand how the Plio-Quaternary tectonics influenced and modified the MSC depositional environment.

Based on the interpretation, I produced a paleo-geographical reconstruction of the study area before and during the MSC, considering previous publications and paleo-geographical reconstruction.

## Outline of the Thesis

The thesis consists in 6 chapters:

Chapter 1 introduces the State of the art about the Messinian Salinity Crisis, starting from the basic knowledge concerning evaporites deposition, to the main outcrop and offshore discoveries until the most recent advancements, with the intent to focus on the Adriatic Sea. Explanation of the ongoing critical points and controversies in the MSC community are highlighted.

Chapter 2 focuses on the geological setting of the study area; it spans from the Triassic time to the Pleistocene. A brief geological evolution of the Adriatic Sea and how the surrounding orogenic chains (Alps, Dinarides and Apennines) contributes to its formation. I conclude summarizing how the basin evolution contributes to the modern physiography.

Chapter 3 presents the dataset I used in this work, composed by different 2D multichannel seismic profiles from several datasets, merged to cover the Italian and partially the Croatian offshore. Available boreholes in the ViDEPI database are used for calibration. Chronological and lithological classifications were explained.

Chapter 4: the seismo-stratigraphy analysis of selected unit and surfaces is illustrated. Apart from the MSC, four more units were used for the purpose of this thesis work.

Chapter 5 illustrates the results described through 10 selected transects connecting the Italian-Croatian offshore. Each profile presents a non-interpreted section and its line drawing. The interpretation is carried out following the seismo-stratigraphy subdivision showed in Chapter 4. Moreover, a structural map of the MSC surface and an isopach map of the MSC unit was produce and described in this chapter.

Chapter 6 contains the discussion and the main outcomes of the PhD: results are interpreted and explained in the MSC context. I provide answer to the research question postulated at the beginning

of the dissertation and discuss the implication of my results, trying to propose some future steps timprove the understanding of the Messinian Salinity.

# Chapter 1 – State of the Art

## 1.1 Overview of the Messinian Salinity Crisis

The Messinian Salinity Crisis (MSC) is one of the most controversial geological events in the Mediterranean Sea (Fig. 1.1). More than a million cubic kilometer of evaporites composed by salt and gypsum accumulated on the Mediterranean seafloor over a short period of time occured in the late Miocene and corresponding to less than 600 ky (Roveri et al., 2014b).

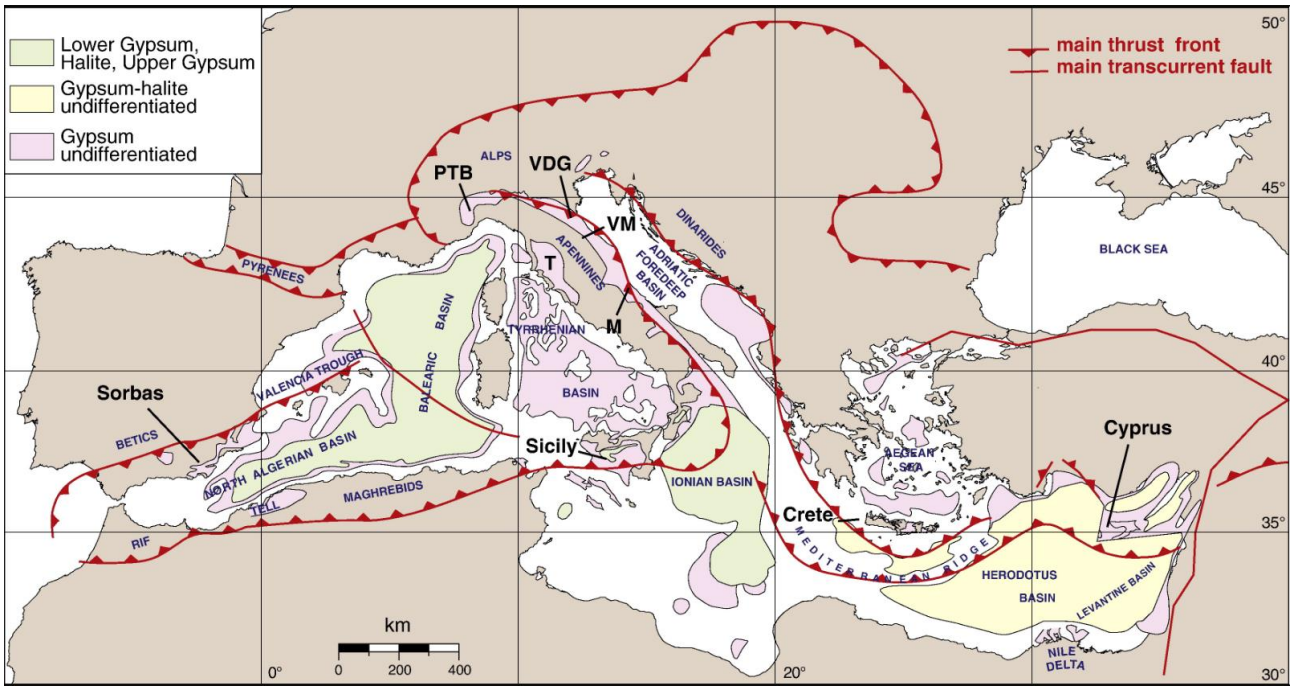


*Figure 1.1: Distribution of the Messinian evaporites in the Mediterranean regione. PTB: Piedmont Tertiary Basin; VDG: Vena del Gesso; VM: Val Marecchia; T: Tuscan Basin; M: Maiella (modified from Lugli et al., 2010).*

Gypsum ($CaSO_4$ $2H_2O$) is known to be formed by the chemical precipitation resulting from the seawater evaporation. The ionic component of $SO4^{2-}$ and $Ca^{2+}$ are among the most abundant dissolved ions in the seawater (Stumm et al., 1996). Modern salinity in the ocean, despite small spatial changes, is geographically homogeneous due to the rapid mixing of water masses. Subsequently, the sequence of mineral precipitation during seawater evaporation is constant

(Usiglio, 1849; Valyashko, 1972; Hermann et al., 1973). Firstly, calcite ($CaCO_3$) precipitates, followed by gypsum (in case of loose of the water molecules Anhydrite) (Fig. 1.2). Halite (NaCl) and, finally, a series of "bitter salts" as Sylvite (KCl), carbakkute ($KMgCl3\ 6H_2O$), Kainite ($KMg(SO_4)Cl\ 3H_2O$), (Camerlenghi and Aloisi, 2020) precipitate from the residual brine (Fig. 1.2). In the current scenario, gypsum deposition is expected when the salinity has risen to about three times the value of the modern seawater in a saturation range of 110-320 g/kg (Harvie, 1980; Hardie et al., 1984).

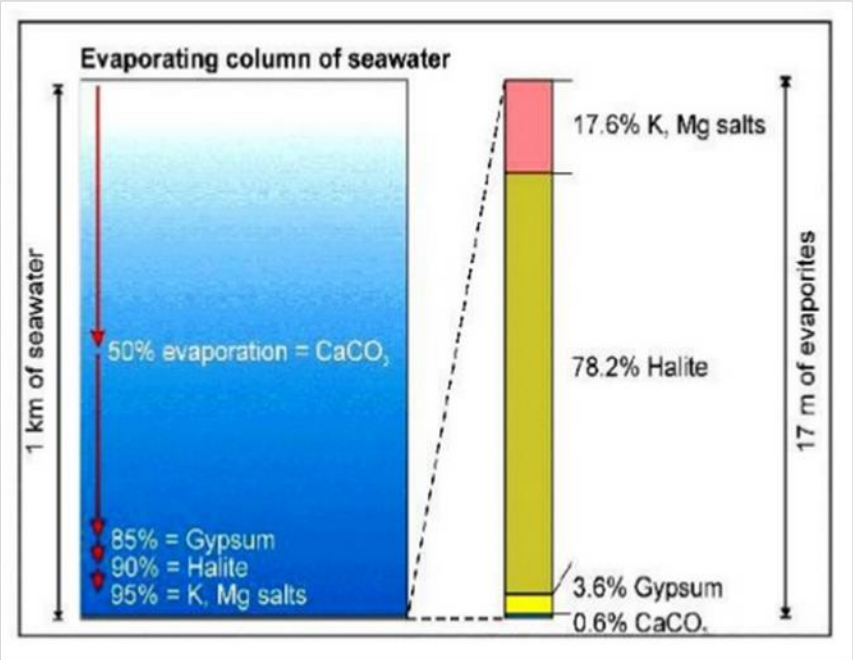


*Figure 1.2: Scheme of the seawater column evaporation and evaporation sequence. With 85% reduction of the water column we observe the deposition of less than a meter of gypsum (from Warren, 2006)*

The precipitation sequence that deposited gypsum and rock salt from seawater evaporation led Selli (1954) to the idea of the desiccation of the Mediterranean Sea and the hypothesis of the MSC. Based on outcropping gypsum deposits in the Northern Apennine (Fig. 1.3), he proposed that a significant disruption of the salinity in the Mediterranean Sea occurred during the Messinian stage. A first controversy of the MSC emerged in 1973, when evidence of evaporitic rocks was drilled during the Deep Sea Drilling Project (DSDP): evaporites were buried below the seafloor of the Mediterranean Sea and considered to be coeval with the evaporites formation outcropping in the Northern Apennine (Ryan, 1973).

*Figure 1.3: Panoramic view of the geological Formation "Vena del Gesso" in the Northern Apennine (Italy) (personal archive).*

Onshore and subsequent offshore research developed through the recognition of hyper- and ipo-saline environments, all around the Mediterranean Sea, during the Late Miocene (Selli, 1960; Hsü, 1972; Hsü et al., 1973b). Nevertheless, since the presence of the Salt Giant was recognized in the deeper basins of the Mediterranean Sea, controversies related to total (Hsü 1972; Hsü et al., 1973b) or partial (Sonnenfield and Finetti, 1985; Hardie and Lowenstein, 2004) desiccation were and are still ongoing (Fig. 1.4). Two main observations support the theory of total desiccation: 1) samples of gypsum evaporites contain algal stromatolites that needed light to survive, suggesting a shallow or even a subaerial sabkha environment; 2) geological and geophysical investigation on the margin of the Mediterranean Sea shows incision and erosional valleys.

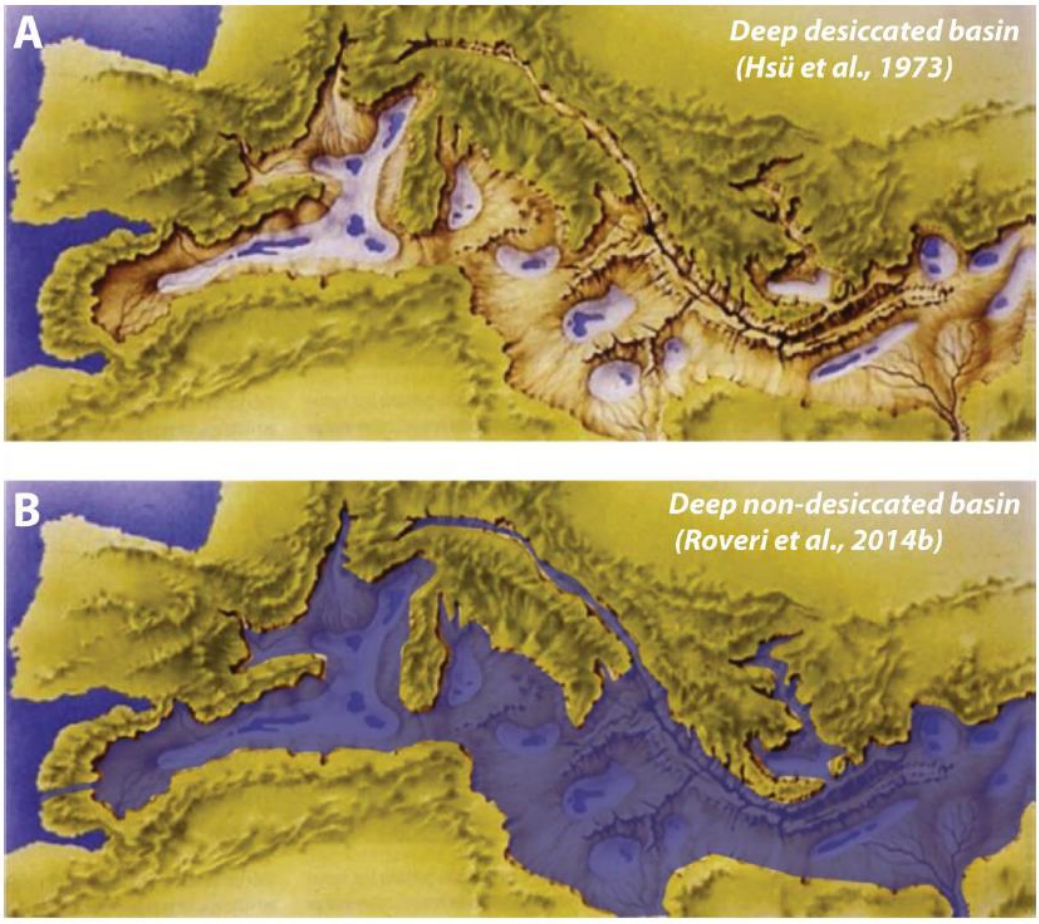


*Figure 1.4: Two different models of the Mediterranean Sea during the MSC: A) based on total desiccation hypothesis; B) Based on a non-desiccated basin hypothesis (from Krijgsman et al., 2018). Paleogeographic reconstruction of the peri-Adriatic area is not realistic due to the western position of the Apennine at that time.*

The Messinian is marked by two GSSP (Global Stratotype Section Points): the base at 7.25 Ma was identified in Western Marocco (Hilgen et al., 1995), while its top, at 5.33 Ma, was identified in Sicily (Van Couverung et al., 2000). The onset of deposition of the evaporites in different parts of the Mediterranean Sea is still discussed, and it is not clear if the onset of the MSC was (partially) diachronous or synchronous. Rouchy (1982), Rouchy and Saint Martin (1992), Butler et al. (1995), and Clauson et al. (1996b) proposed a diachronous model, with initial evaporite deposition in marginal basins, successively migrated into deeper basins following the sea level drawdown. Hilgen et al. (1995), and Hilgen and Krijgsman (1999b) hypothesized a synchronous deposition model in the entire Mediterranean area through cyclostratigraphy and astronomical data analysis, comparing the onset in different basins, and hypothesizing a start at 5.96 (+- 0.02) Ma. More consensus regards

the end of the MSC, fixed by Van Couvering et al. (2000) at 5.33 Ma, when the reestablishment of the Atlantic-Mediterranean connection and the so-called Zanclean reflooding occurred (Garcia-Castellanos et al., 2009).

In order to find a consensus, several MSC experts gathered together at CIESM (Mediterranean Science Commission, 2008) trying to define a common stratigraphic model. Three depositional stages, inspired by the two-stage model proposed by Clauzon (1996b), were proposed and later partially modified by Roveri et al. (2014b) (Fig. 1.5):

- Stage 1 (5.97-5.60 Ma): marks the onset of the MSC with the deposition of the Primary Lower Gypsum (PLG) in shallow marginal basins (Krijgsmann et al., 1999b; Lugli et al., 2010).
- Stage 2 (5.60 – 5.55 Ma): halite deposited in intermediate and deep basins, following the sea-level drawdown (Lugli et al., 1999b). PLG in the shallower basin underwent subaerial erosion and re-deposition (Roveri et al., 2006).
- Stage 3 (5.55 – 5.33 Ma): characterized by the deposition of the Upper Evaporites in intermediate and deep basins (Rouchy and Caruso, 2006; Manzi et al., 2009a) and followed by the "Lago-Mare" phase, characterized by sediments containing Para-Tethyan brackish fauna.

Nesteroff (1973) supports the hypothesis of shallow Mediterranean basins with depth varying between 200-500 m; on contrast the recovery of evaporites from the DSDP disproved the shallow basin theories by favouring the deep Mediterranean Sea theory (Hsu et al., 1973b; Ryan, 1976). Evaporites show similar characteristics to the modern sabkha deposits, containing evidence of subaerial exposure (e.g., desiccation cracks, karstification).

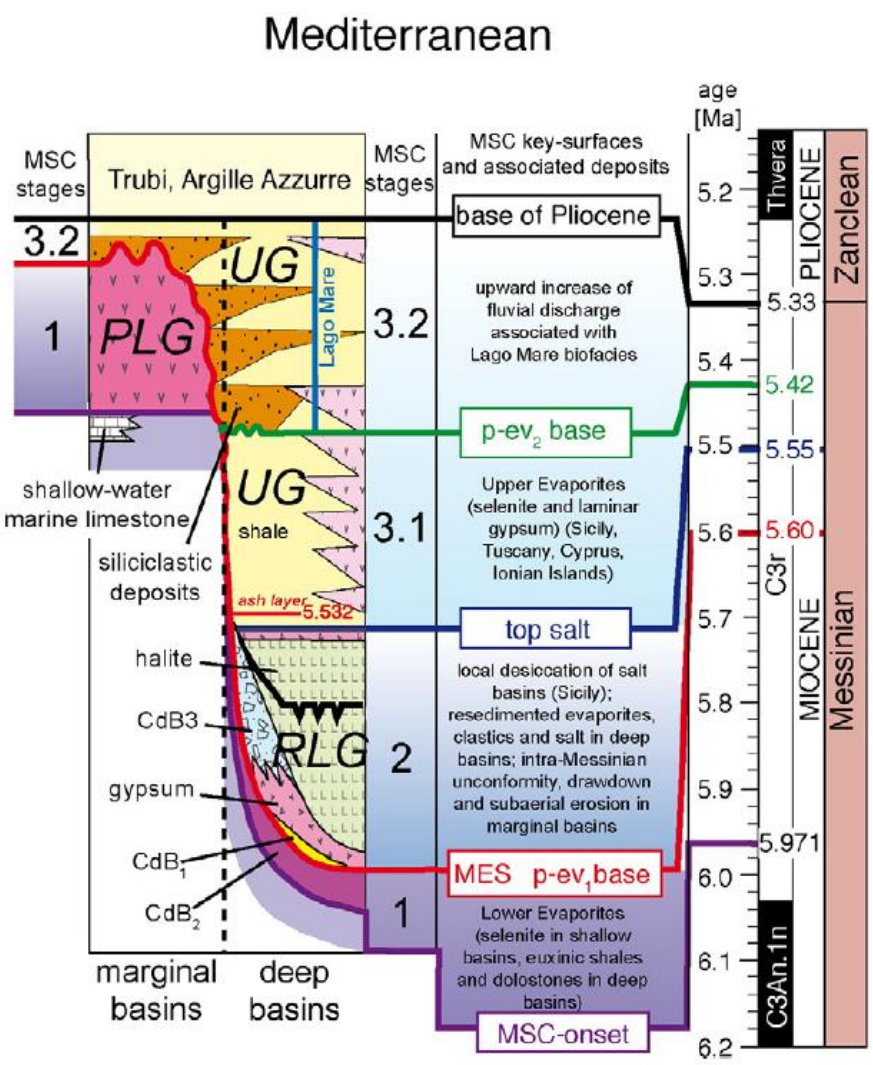


*Figure 1.5: Chronostratigraphy of Late Miocene to Early Pliocene highlighting the 3 stages of the MSC (modified from CIESM, 2008 and Roveri et al., 2014b). The Adriatic Sea is a marginal basin, consequently stage 2 and 3.1 are missed and replaced by a widespread erosional surface.*

## 1.2 The MSC in the present Onshore area

In the Adriatic Sea, which is considered to be a marginal basin (Fig. 1.6), the onset of the MSC is marked by the deposition of gypsum (Primary Lower Gypsum, PLG), recognized as the so-called Vena del Gesso formation in the Northern Apennines (Vai and Ricci Lucchi, 1977a) (Fig. 1.3). The PLG deposition during the stage 1 of the MSC is influenced by (i) precession driven cycles that produces the deposition of 16 gypsum-marls couple layers (Krijgsman et al., 1999b, Lugli et al., 2010; Manzi et al., 2013), and (ii) seasonal/annual cycles, that produced the lamination in the selenite crystal of the gypsum layer (Dela Pierre et al., 2015; Reghizzi et al., 2018).

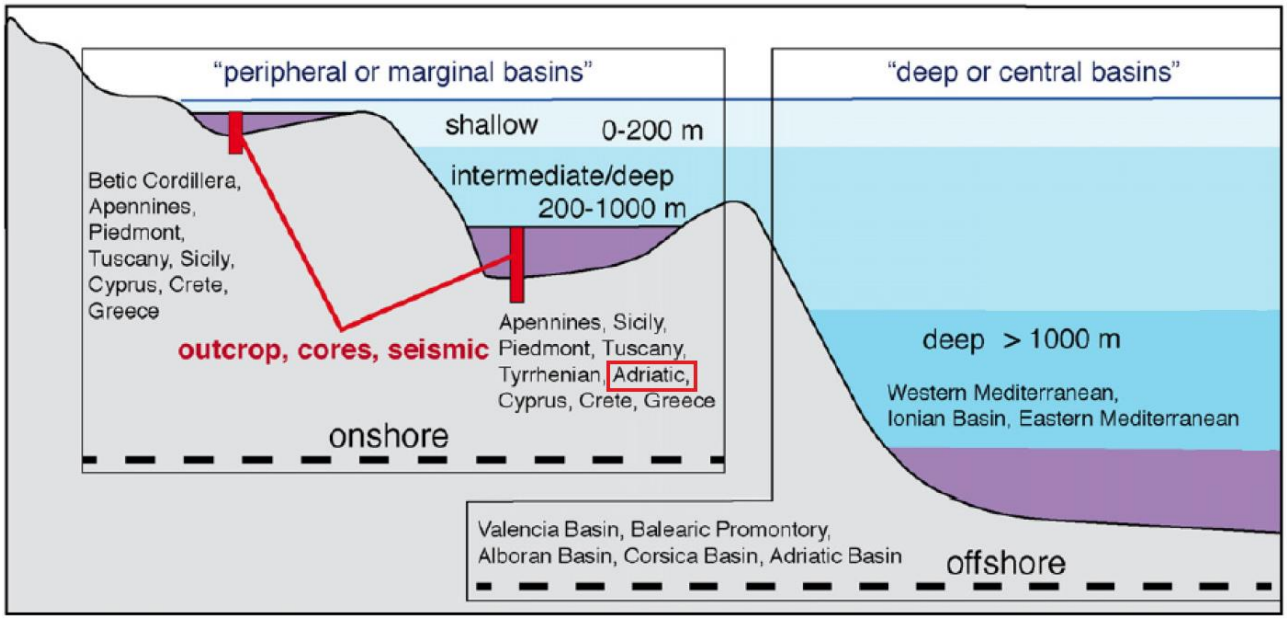


*Figure 1.6: Schematic representation of the MSC basin in the peri-Mediterranean area. Marginal/peripheral basins include both shallow and intermediate water. Intermediate water basin such as the Adriatic Sea is classified both in onshore and offshore settings (modify from Roveri et al., 2014b).*

Selenitic gypsum in m-thick beds was deposited during precession maxima (insolation minima), represented by arid period when the hydrogeological cycle decreased (Fig. 1.7), driving vertical mixing events in the water column (Aloisi et al., 2022). Gypsum precipitation may be enhanced by

the production and availability of dissolved $Ca^{2+}$ and $SO_4^{2-}$ from bearing runoff, producing supersaturation of a millimeter-thick gypsum lamina (Aloisi et al., 2022).

Marls intercalated in between the gypsum beds deposited during minima precession (maxima insolation), when the hydrological cycle in the marginal basin (such as the Adriatic one) was enhanced (Fig. 1.7), receiving the highest continental runoff (Lugli et al., 2010; Topper et al., 2014; Dela Pierre et al., 2011; Aloisi et al., 2022). This alternation between marls and gypsum reflected a water column stratification, resulting in bottom water anoxia that enhances the preservation of organic matter (Aloisi et al., 2022).

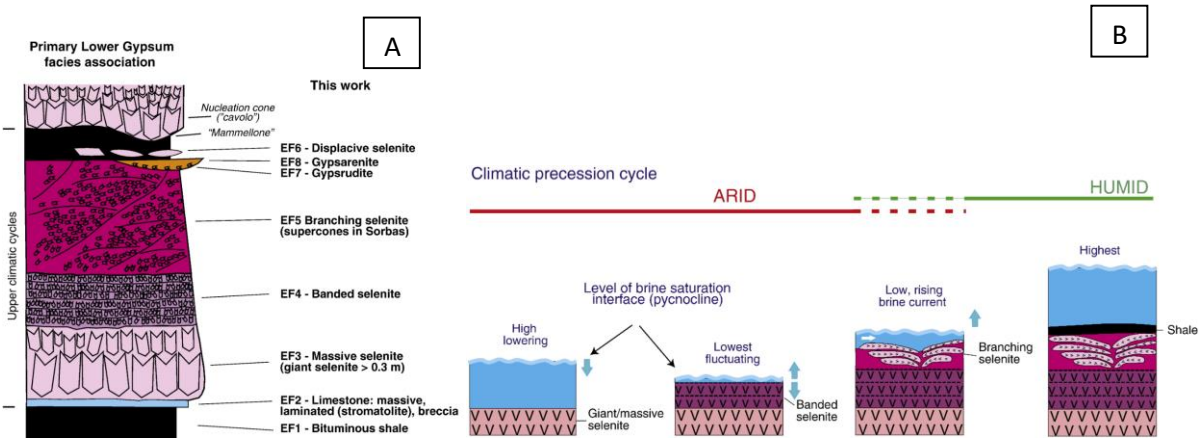


*Figure 1.7: A) Sedimentological facies and interpretation of the Vena del Gesso formation; B) Growth of different types of gypsum as a function of brine saturation level and climatic cycles (modify from Lugli et al., 2010).*

Moreover, Lugli et al. (2010) proposed that gypsum deposition in the Adriatic area is basin-scale controlled, favored by silled/close basins with a maximum paleo-depth of about 200 m. The presence of photic zone micro-organisms supports this hypothesis (e.g., cyanobacteria) contained inside the selenite crystals of the Vena del Gesso Fm. (Vai and Ricci Lucchi, 1977a; Panieri et al., 2010). However, other authors (Natalicchio et al., 2014; Dela Pierre et al., 2015; Pellegrino et al., 2021) interpreted the same micro-organism as sulfide-oxidizing bacteria able to survive in a wide range of water depths, not only in the first 200 m of the water column (Bailey et al., 2009; Natalicchio et al., 2021).

Furthermore, PLG salinity values obtained from fluid inclusion in the selenite crystals represent another critical point. Bigi et al. (2022) analyzed fluid inclusion from different PLG spatially distributed in the Mediterranean, suggesting that the gypsum precipitated from a mostly saline water

body susceptible to seasonal changes. Nevertheless, post-depositional processes may have damaged the fluid inclusion by introducing secondary low or high salinity fluids. Samples from the Vena del Gesso Fm. indicate a low salinity below the modern Gypsum saturation threshold; however, secondary low salinity fluid intrusion has to be considered. In contrast, Natalicchio et al. (2014) and Aloisi et al. (2022) strongly support the low-salinity theories based on the selenite crystal's fluid inclusion analysis from the Piedmont and the Vena del Gesso Basins. Gypsum precipitates from hybrid mixed water (seawater enriched with freshwater input), multiple factors that include ions dissolution from bearing runoff and the biogeochemical sulfur cycle may have provided gypsum supersaturation conditions (Aloisi et al., 2022, Guibourdenche et al., 2022), supporting the hypothesis of the different chemical composition of the Messinian gypsum, not comparable to the current gypsum precipitation (Natalicchio et al., 2014; Aloisi et al., 2022).

The nonmarine composition of the gypsum fluid inclusion raises new questions about paleo-hydrogeological models for the PLG by considering short-term changes in the hydrological budget of marginal basins (Manzi et al., 2012; Natalicchio et al., 2014; Aloisi et al., 2022).

Theories of mixed freshwater and seawater condition are also upheld by Sr isotopic analysis of gypsum fluid inclusions and gypsum-bound water (Muller and Mueller, 1991), previously discovered in the Piedmont basin (Dela Pierre et al., 2011; Natalicchio et al.,2014; Aloisi et al., 2022). These suggest that marginal basin gypsum formed from low-to moderate-salinity water masses (5 - 60 ‰) rather than from high-salinity brines (130 - 320 ‰) (Aloisi et al., 2022). Thus, it might indicate again that evaporites sedimented in a closed basin where the hydrological budget freshwater runoff was higher than evaporation, supporting the possibility of a mixed water body that precipitated the PLG.

Lastly, another PLG critical point regards the Resedimented Lower Gypsum (RLG) unit, firstly introduced by Roveri et al. (2006). This unit, present in the Northern Apennine (Roveri et al., 2003, 2006; Manzi et al., 2005b), consists of deep water resedimented gypsum resulting from the erosion or gliding of the PLG (Roveri et al., 2008). The RLG appears to be thicker in the main depocenter of the basin, thinning toward the margins, displaying lateral changes in the sedimentary facies (Roveri et al., 2006). Moreover, Manzi et al. (2020) highlighted that PLG mass-wasting unit points to large-scale collapses, probably favored by strong mechanical contrast between the gypsum selenite and the marls lithological facies (Roveri et al., 2003). However, several alternative theories for the mechanism formation are still debated. Decima and Wezel (1971) consider the possibility of intra- or post-Messinian tectonic deformation of the PLG unit, associated with intense active

tectonics alongside the growing thrust belts. Another possibility for the RLG formation regards the Messinian fluvial drainage; Bache et al. (2012) and Rouchy and Caruso (2006) hypothesized a subaerial drainage network able to cut the PLG unit, while Fortuin et al. (1995) and Manzi (2020), suggests that RLG unit results from large-scale subaqueous instability processes and mass-transport deposits. Moreover, Rouchy and Caruso (2006) interpreted the RLG unit due to evaporite dissolution.

It is well known in the literature that carbonate and evaporites develop karstification phenomena in which combined chemical and mechanical weathering dissolve the dense gypsum's structure. In the framework of the MSC, gypsum evaporites deposition occurred in a shallow-water column that progressively decreased into a Sabhka environment, with a cyclic variation of the humid and arid period (Manzi et al., 2011, 2016; Roveri et al., 2014b; Perri et al., 2017; Borrelli et al., 2021). The high solubility of the gypsum ranges between 0.4 mm/yr and 1.0 mm/yr (Cucchi et al., 1998) and is enhanced by weathering, which heavily affects the structure of the gypsum in case of subaerial exposure. Moreover, Calligaris et al. (2019) demonstrate that in a fluctuating water level condition, the evaporites dissolution rate rises to 2.8 mm/yr, allowing the formation of fractures in the evaporites. In such conditions, PLG may be highly eroded and mobilized, triggering the formation of the RLG unit.

Due to the complexity of the event, the MSC in the Adriatic Sea was divided into three main stages (CIESM, 2008; Manzi et al., 2013; Roveri, et al., 2014b), building on the model of Cluazon et al. (1996) (Fig. 1.5):

- Stage 1 (5,97-5,60 Ma; 370 ky): it marks the onset of the MSC and is characterized by deposition of the Gessoso-Solfifera, Vena del Gesso Formation (PLG), which displays 16 evaporites cycles related to astronomically forced climate changes up to form 200 m thick succession (Vai and Ricci Lucchi, 1977a; Marabini and Vai 1985; Vai, 1997b; Krijgsman et al., 1999b; Hilgen et al., 2007, Lugli et al., 2010; Manzi et al., 2020).

- Stage 2 (5,60-5,55 Ma; 50 ky): in the modern Adriatic offshore a hiatus is recorded by exploration wells due to uplift and deep erosion (Roveri et al., 2020). Thus, it is represented by a regional scale unconformity referred to as the Messinian Erosion Surface (Cita and Corselli, 1990). The widespread erosional surface is being observed in the entire basin, in different stratigraphic positions above paleo-margins and topographic high. RLG unit was most probably emplaced during this phase of the MSC. In the Mediterranean Sea, this stage is characterized by halite and potash bodies deposited in intermediate to deep basins following the major sea-level drawdown.

- Stage 3 (5,55-5,33 Ma; 220 ky): deposition of the ipohaline microfauna ascribed to para-Tethyan freshwater LagoMare type biofacies (Krijgsman et al., 1999b, Andreetto et al., 2020, 2021) characterizes this stage. In particular, the wells from ViDEPI calibrated three different formations: Fusignano Fm. onshore in the Northern Adriatic, Colombacci Fm. in the entire Adriatic offshore (where not eroded), and a peculiar conglomeratic carbonatic layer located in the Gargano onshore area known as the Casalbordino Breccia (Santantonio et al., 2013).

The return of fully marine conditions occurred after 5,33 Ma, with the so-called Zanclean megaflood. The end of the MSC was marked by an abrupt sedimentary change (Van Couvering et al., 2000) into the widespread silico-clastic succession of the "Argille Azzurre". Bache et al. (2012) debate the possibility of two or more reflooding events in the Mediterranean Sea through the Gibraltar Strait, which caused a deeply eroded channel in the Alboran Basin and associated chaotic deposits (Garcia-Castellanos et al., 2020; Micallef et al., 2018).

## 1.3 The MSC Offshore

The MSC offshore deposits constitute more than 90% of the MSC deposits in the entire Mediterranean area, with an overall volume of about 1.2 million $km^3$ (Ryan, 1976; Haq et al., 2020) **(**Fig. 1.1**)**. After the DSDP which calibrated the Ionian Sea (it represents the nearest DSDP of the Adriatic Sea, never intersected by this project), many industrial boreholes were drilled in the Adriatic Sea area, primarily for hydrocarbon exploration, reaching and cutting through the Messinian evaporites.

Although several controversies have been already discussed, the most disputed regard the amplitude of the sea-level drawdown, the timing and duration of the changes and how the base-level changed. The widespread erosional surfaces in the Mediterranean area are interpreted as subaerial exposure of the Messinian evaporites, supporting the theory of a sea-level drop of more than 1500 m (e.g., Ryan, 1976; Lofi et al., 2005; Camerlenghi et al., 2019, Heida et al., 2022). Moreover, adjustment of river profiles (Chumakov, 1973; Clauzon, 1978), presence of clastic fans at the output of incised valley (Lofi et al., 2005; Bache et al., 2009b; Micallef et al., 2018), deep incisions at the Gibraltar strait – supporting the reflooding theory – (Garcia-Castellano et al., 2009; 2018; 2020), contributes to the quasi-desiccated Mediterranean thesis. Several studies have been produced about the Adriatic offshore, mainly regarding the North Adriatic Sea and the Po Plain (Ghielmi et al., 2010, 2013; Amadori et al., 2018; 2019, Manzi et al., 2020), suggesting a sea-level drawdown of about 800-1300 m.

A different hypothesis claims that the amplitude of the sea-level drawdown did not vary strongly during the MSC, with an acme of about -200 m, supporting a non-desiccated Mediterranean thesis. The presence of subaqueous facies such as the RLG (Roveri et al., 2001; 2004; Hardie and Lowenstein, 2004, Lugli et al., 2013), the mismatch between Sr isotope ratios (Roveri et al., 2014; Andreetto et al., 2020) and sulfate values reflecting a clear Atlantic water signal (Garcia-Veigas et al., 2018b), may indicate a moderate sea-level drop.

The MSC surfaces and units were named considering the geometrical relationship between pre-Messinian units and the Plio-Quaternary sedimentary cover (Lofi, 2005, 2018; Lofi et al., 2011). The aim was a nomenclature that offers a global and consistent terminology, usable in the entire Mediterranean Sea (Fig. 1.8). However, only significant surfaces and units are present in the Adriatic offshore. Marginal basin terminology refers to its position with respect to the Messinian deep basins (present-day Mediterranean slope and bathyal plain; Roveri et al., 2014a,b).

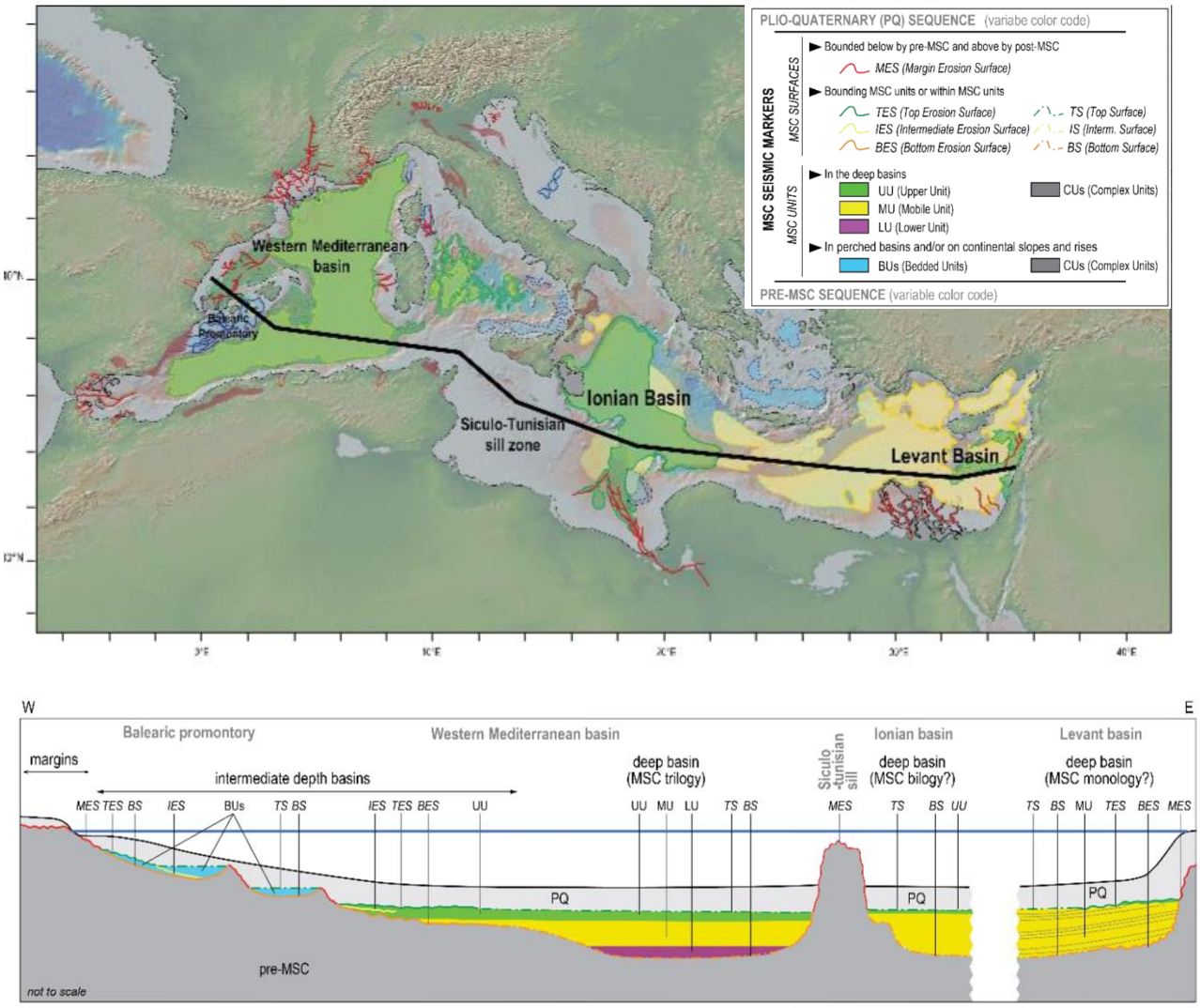


*Figure 1.8: Schematic cross section of the Mediterranean basin illustrating the present day distribution of the MSC surfaces and units (modified from Lofi, 2018).*

As Lofi (2018) clearly described relatively to the entire Mediterranean Sea, the MSC event can be distinguished in areas represented by an erosional truncation called MES (Margin Erosion Surface). MES unconformity often takes away a critical thickness of the pre-Messinian sedimentary sequence, juxtaposing the Lower Pliocene with pre-MSC sequences. The unconformity sometimes reaches the basement as in the Alboran Sea (Do Couto et al., 2014), in the Algero-Balearic Basin (Camerlenghi et al., 2018), in the Balearic Promontory (Maillard et al., 2006, 2018; Raad et a., 2021), in the Catalan Margin (Garcia Castellanos et al., 2018, 2020), in the Sardinia margins (Lymer et al., 2018; Del Ben et al., 2018). It is commonly interpreted as the result of subaerial

erosion and drainage action (Lofi et al., 2005). Reconstruction of the paleobathymetries of the MES reveals the existence of Messinian paleo-drainage and fluvial networks, such as in the Po Plain (Ghielmi et al., 2010, 2013; Amadori et al., 2019). Other examples come from the major modern river system such as the Ebro margin (Stampfli and Hocker, 1989; Urgeles et al., 2011) and the Gulf of Lyon (Guennoc et al., 2000; Bellucci et al., 2021). The MSC determined the deposition of a mainly evaporitic thickness in other basins, topped by the continuous non-erosional surface called TS (Top Surface). Such surface is present in the Algero-Balearic Basin (Camerlenghi et al., 2018; Maillard et al., 2018) and in the Ionian basin (Camerlenghi et al., 2019). When the MSC thickness has been partly eroded in its upper part, the TS surface becomes TES (Top Erosion Surface), a heavily eroded high-amplitude reflector.

Terminology for MSC-related units is based on the seismic facies and the geometrical relationship of the Units (Lofi, 2018). In the deeper basins of the Mediterranean Sea, complex stacked geometry of the MSC deposits is observed. In the Western Mediterranean Sea, a trilogy is composed of Lower Unit (LU), Mobile Unit (MU), and Upper Unit (UU) (Lofi, 2018; Del Ben et al., 2018, Camerlenghi et al., 2018) (Fig. 1.8). However, the trilogy mentioned above presents lateral changes in the Mediterranean Sea, expressed as a "bilogy" composed by MU and UU in the Algero-Provenzal basin (Camerlenghi et al., 2018) and in the Algerian basin (Kherroubi et al., 2018; Bouyahiaoui et al., 2018), or a MU "monology" in the Levant Basin (Lofi, 2018; Gvirtzman et al., 2017) (Fig. 1.8).

In this work, we indicate the top of the Messinian or the Plio-Quaternary base as the "Messinian surface" (M), further subdivided into the surfaces, when the seismic resolution allows it (Fig. 1.8):

- **MES** (Margin Erosion Surface) observed on the margin and slope in absence of MSC related units;
- **TES** (Top Erosion Surface) observed on slope and in the the deep portion of the basin at the upper boundary of the MSC unit;
- **TS** (Top Surface) non erosive surface in basins at the upper boundary of the MSC unit;
- **BS** (Bottom Surface) observed on slope and basins underlying the MSC unit.

The offshore MSC unit recognized in the Adriatic is the **BU** (Bedded Unit), the offshore analogue of the onshore “Vena del Gesso” formation. This unit is topped by the TES or TS surface and underplayed by the BS.

The exploration borehole calibrates the Messinian evaporites in the Adriatic Sea offshore (Table 3.1). However, its distribution might be underestimated: 2D seismic lines provide a comprehensive spatial resolution of the BU area; however, seismic resolution is not always able to detect its presence.

The connection between the Adriatic Sea and the deep Ionian Basin is still unclear. Mapping the BU and relatives MSC surfaces and understanding the Messinian Adriatic Basin's evolution will be the target of this thesis.

# Chapter 2 – Geological setting

## 2.1 Evolution of the Adria Plate

The Adriatic Sea is a narrow epicontinental basin, with dimensions of approximately 200x800 km, located at the center of the Mediterranean Sea (Trincardi et al., 2014) (Fig. 2.1).

The relationship between Adria and Africa Plates remained for many years controversial: geomagnetic data suggested to some authors that Adria extends as a promontory of the African Plate into the Adriatic region (Mele, 2001). However, there are more evidence that Adria would be an independent micro-plate between Africa and Eurasia (Nocquet and Calais, 2003). Battaglia et al. (2004) used GPS data to test the proposed models and showed that present-day velocities are best fitted by considering Adria as an independent micro-plate (Fig. 2.2). Structural (Finetti, 1982) and paleomagnetic (Wortmann et al., 2001) evidence shows that it has undergone and still undergoes motion relative to stable Africa in the Cenozoic (van Hinsbergen et al., 2020).

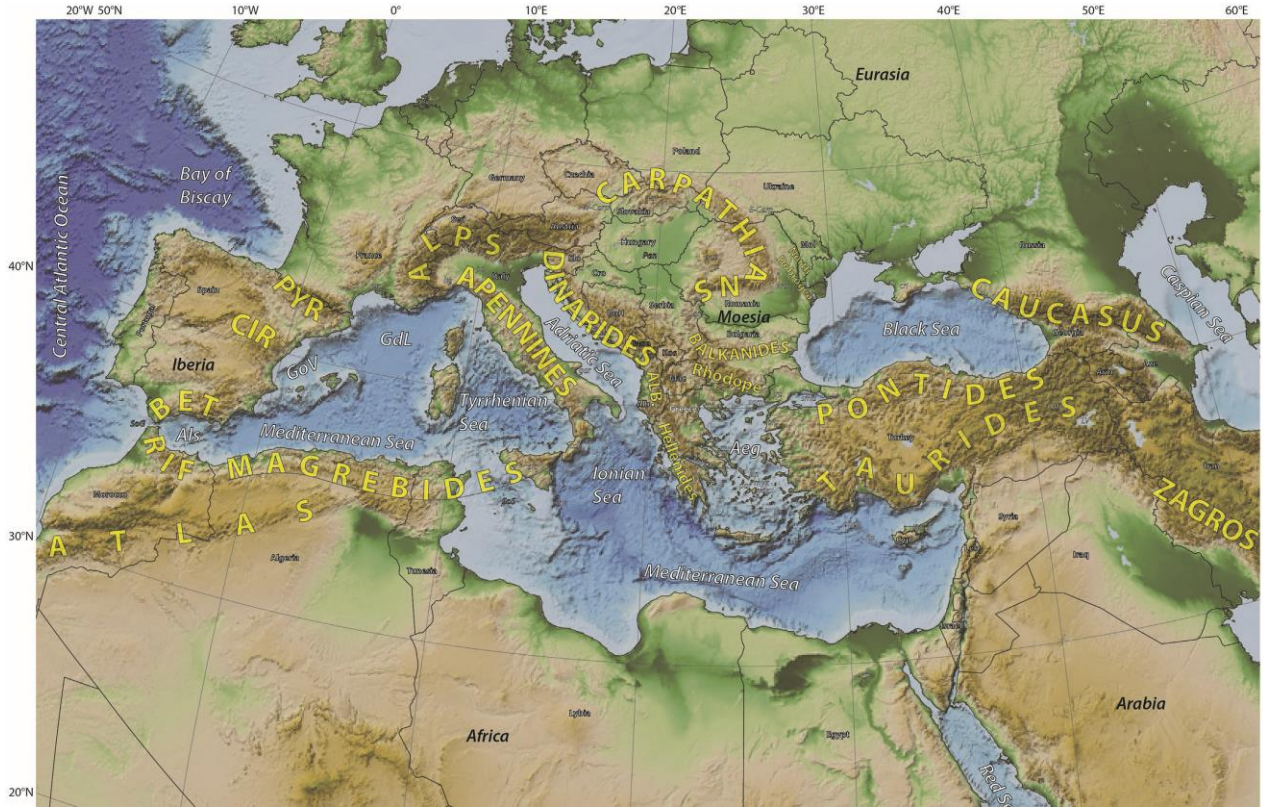


*Figure 2.1: Localization of the Adriatic Sea in the Mediterranean context, with indication of the main orogenic belts and basins, Key to abbreviations: Aeg = Aegean Sea; Alb = Albania; Alb. = Albanides; Als = Alboran Sea; ana = Anaximander Seamount; apu = Apuseni Mountains; Arm = Armenia; att = Attica; Aze = Azerbaidjan; bal = Baleares; BET = Betic Cordillera; big = Biga Peninsula; BoH = Bosnia and Herzegovina; cal = Calabria; cha = Chalkidiki Peninsula; CIR = Central Iberian Ranges; cor = Corsica; cri = Crimea; Cro = Croatia; cyp = Cyprus; EAHP = East Anatolian High Plateau; E-Carp = East Carpathians; era = Eratosthenes Seamount; evv = Evvia; flo = Florence Rise; GdL = Gulf de Lion; GoV = Gulf of Valencia; gar = Gargano Peninsula; goc = Gulf of Corinth; gs = Gran Sasso Mountains; ibi = Ibiza; isa = Isparta Angle; Kos = Kosovo; Kyr = Kyrenia Range; Leb = Lebanon; lig = Ligurian Alps; LV = Lake Van; Mac = North Macedonia; mal = Mallorca; me = Malta Escarpement; Mol = Moldova; Mon = Montenegro; myk = Mykonos; nax = Naxos; pro = Provence; par = Paros; Pan = Pannonian Basin; pel = Peloponnesos; po = Po Plain; pug = Puglia; PYR = Pyrenees; rho = Rhodos; sam = Samothraki Island; sar = Sardinia; S-Carp = South Carpathians; sic = Sicily; Slo = Slovenia; sma = Sea of Marmara; SoG = Strait of Gibraltar; SoS = Strait of Sicily; Swi = Switzerland; tat = Tatra Mountains; tin = Tinos; tra = Tracia; UK = United Kingdom; vra = Vrancea area; W-Carp = West-Carpathians, (from van Hinsbergen et al., 2020).*

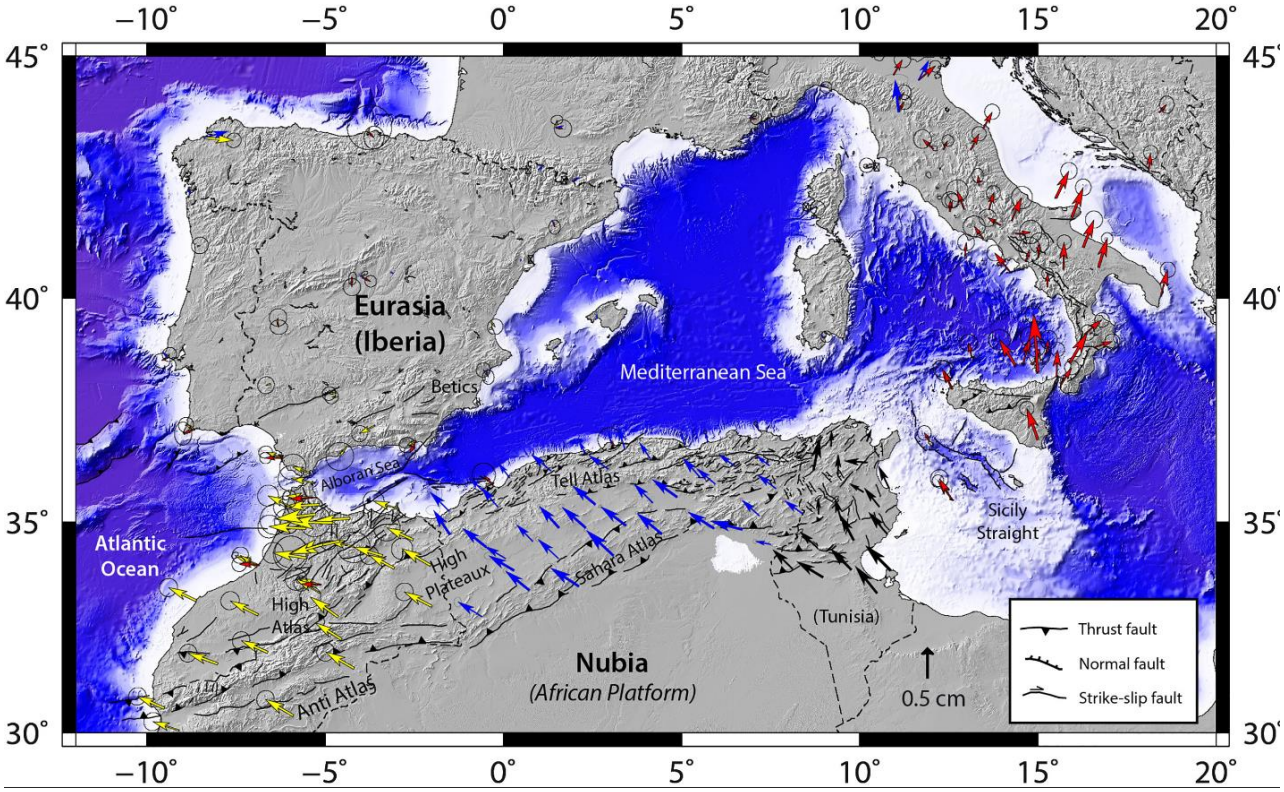


*Figure 2.2: Map of the horizontal GPS velocities in the Eurasian-fixed frame of the Maghrebian thrust belt and related Western Mediterranean geodynamics. Fault traces are from* **Meghraoui and Pondrelli (2012) and Meghraoui et al. (2016).** *Tunisian GPS results (black velocities) are combined to Italian GPS result (red velocities) from* **Serpelloni et al., 2007; Algerian and Lybian GPS results (blue velocities) from Bougrine et al., 2019; and Moroccan GPS velocities (yellow velocities) from Koulali et al., 2011, covering the 1996 to 2018 time** *span; (from Bahrouni et al., 2020).*

Since the early Pangea's break up in Triassic time (Fig. 2.3A), in the convergence between the African and Eurasia plate, the Adria plate was considered as microplate separated from the African plate (Finetti, 1985; van Hinsbergen et al., 2020). The modern Adriatic Sea is only part of the Adria microplate that, from the Cretaceous, represents a wide foreland for the belts produced after the collision of Adria and Europe. Three main orogenic belts border this foreland: to the north the Southern Alps from the Cretaceous; to the east the Dinarides/Albanides/Hellenides from theEocene; to the west the Apennines from theOligocene (Fig. 2.1).

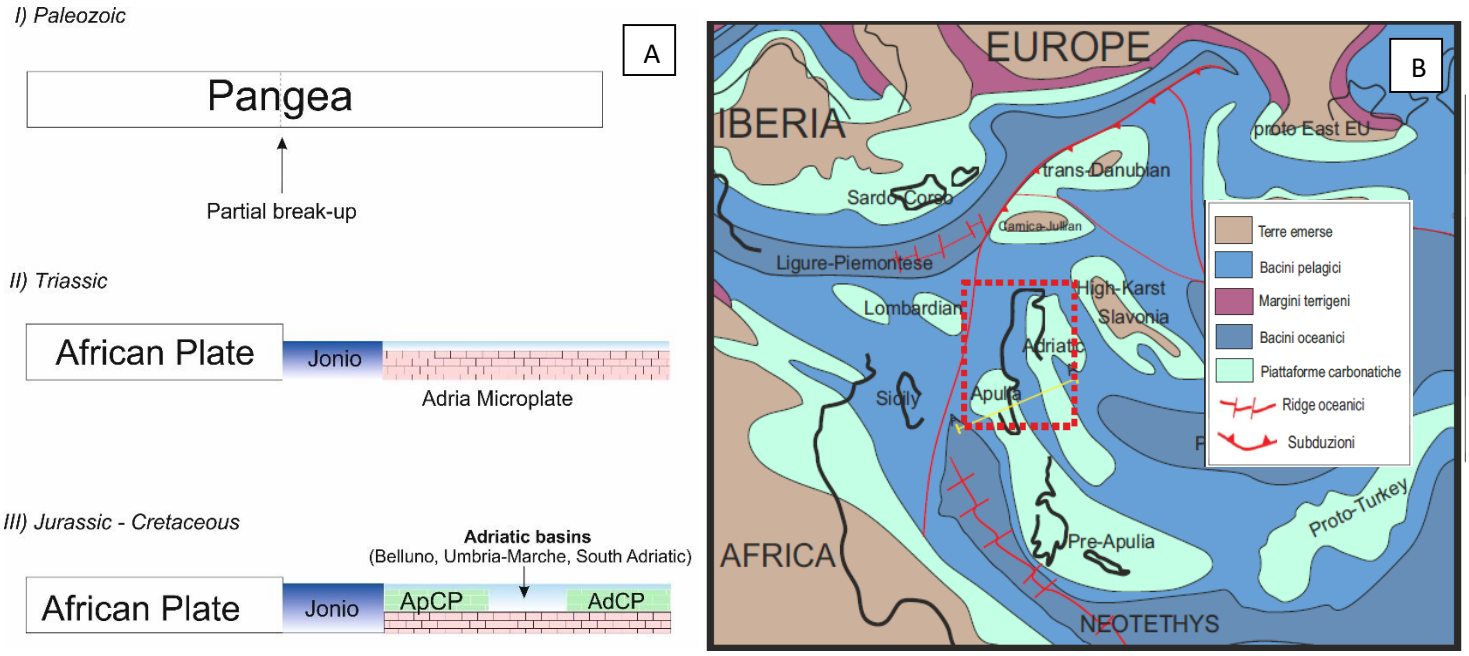


*Figure 2.3: (A) Schematic evolution of the Adria plate from the Paleozoic; I) break-up of the Pangea; II) Drifting of the Adria microplate from the African plate with the opening of the Ionian basin; above Adria, deposition of a widespread carbonatic platform occurred; III) Extensive tectonics produced deep and shallow basins (modified from Vlahović et al., 2005); (B) Paleogeographic reconstruction of the Mediterranean area in the Jurassic time (modify from Stampfli., 2005).*

During the Carnian-Norian time, the opening of the Central Atlantic Ocean pushed the Adria sector of the Gondwana toward tropical latitude and caused the deposition of a thick carbonate and evaporites sequence, mainly composed of Dolomia Principale and Burano evaporites (mostly salt evaporites) (Cati et al., 1987b; Mattavelli et al., 1991; Zappaterra, 1992), (Fig. 2.4). The Dolomia Principale and Burano formations create a huge isolated southern Tethyan Mega platform (Vlahović et al., 2005) that represents the basement of the future Mesozoic carbonate platforms in the periadriatic area. The Sinemurian break-up of the Triassic carbonate platform created a horst and graben configuration (Cati et al., 1987b; Mattavelli et al., 1991), alternating deep basins to shallow water domains (Fig. 2.3, 2.4). Examples of this setting are present in the north-eastern Adria plate, where shallow water domains created the Friuli/Adriatic carbonate platform (AdCP) to the northeast (Bosellini et al., 1981; Cati et al. 1987b, Grandić, 1999, Velić et al., 1995), and the Apulia Carbonate Platform (ApCP) to the southwest (Fig. 2.4). The deeper drowned domains were

connecting the Ionian with the Lagonero and the Umbria-Marche Basins and, to the north, the Belluno Basin and the Slovenian Through (Vlahović et al., 2005). The ApCP borders with the South Adriatic Basin on the NE (De Alteriis and Aiello, 1993; De Alteriis, 1995; Nicolai and Gambini, 2007), with the South Apulia basin on the SE (Del Ben et al., 2015), the East-Ionian basin on the E with (Aubouin et al., 1970), and with the Ionian oceanic basin on the SW (Finetti, 1982).

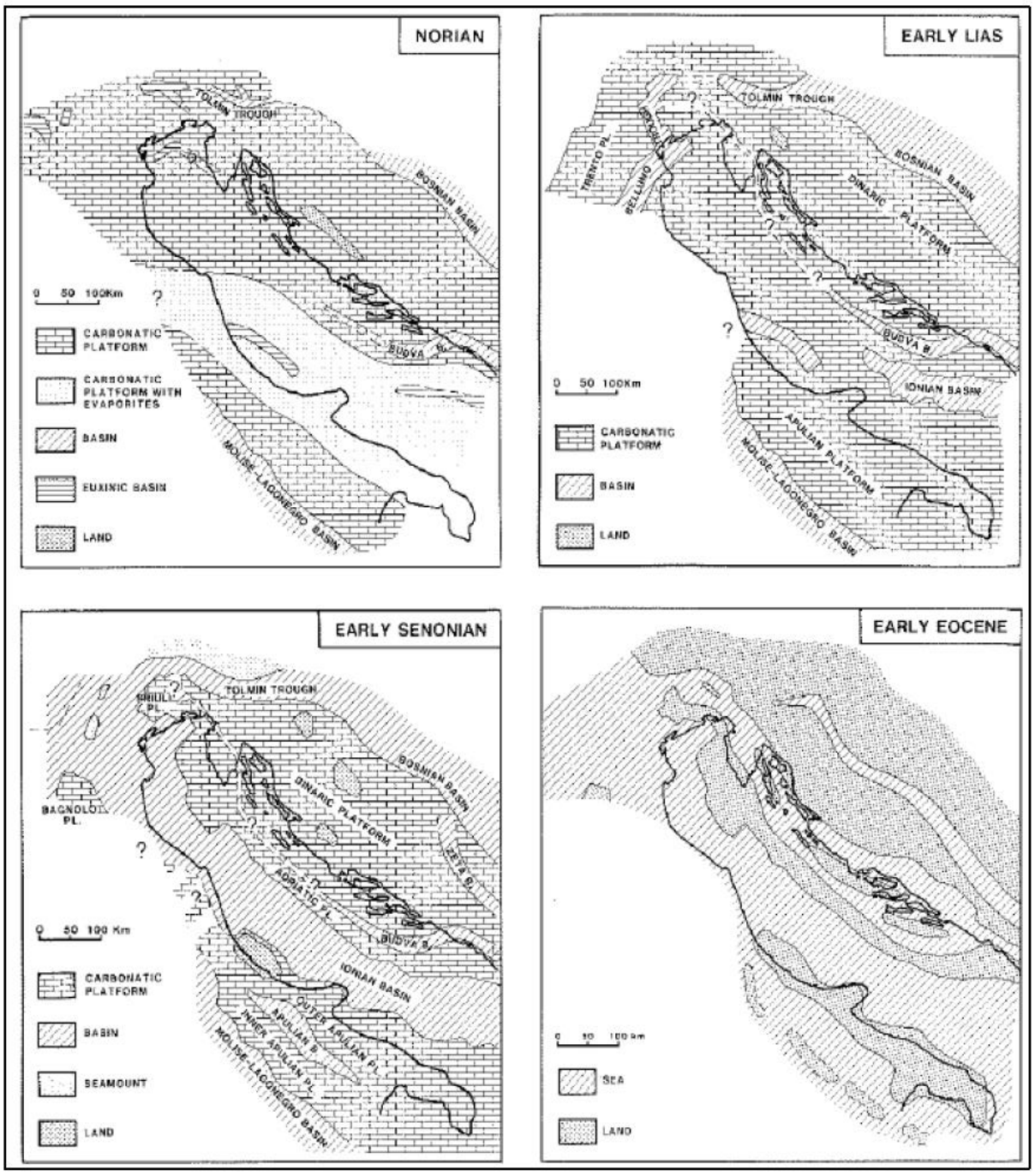


*Figure 2.4: paleo-geographic evolution of the Peri-Adriatic area, from Upper Triassic to late Eocene (from Cati et al., 1987b).*

The compressive tectonics is still active, as testified by the distributed seismicity along the Adria margins (Fig. 2.5). Furthermore, it triggered the halokinetic processes that affect the evaporitic succession of the Triassic Burano Formation (Mattavelli et al., 1991; Finetti and Del Ben, 2005; Geletti et al., 2008), producing the Mid Adriatic Ridge (MAR, Fig. 2.10). This structure system is located approximately along the Central Adriatic Sea axis, from the Conero structure to the northeast Gargano offshore. Geletti et al. (2008) interpreted it as the effect of the deep salt domes triggered by the Paleogene Dinaric compression, and they partially crossed and still deform the covering sedimentary sequence. Scisciani and Calamita (2009) consider the MAR as an effect of crustal compression due to the linkage between the two opposite-verging Apennines and South Dinarides belts, while Scrocca et al. (2007) interpreted it as an effect of the subducting Adria plate below the Apennine frontal accretionary wedge.

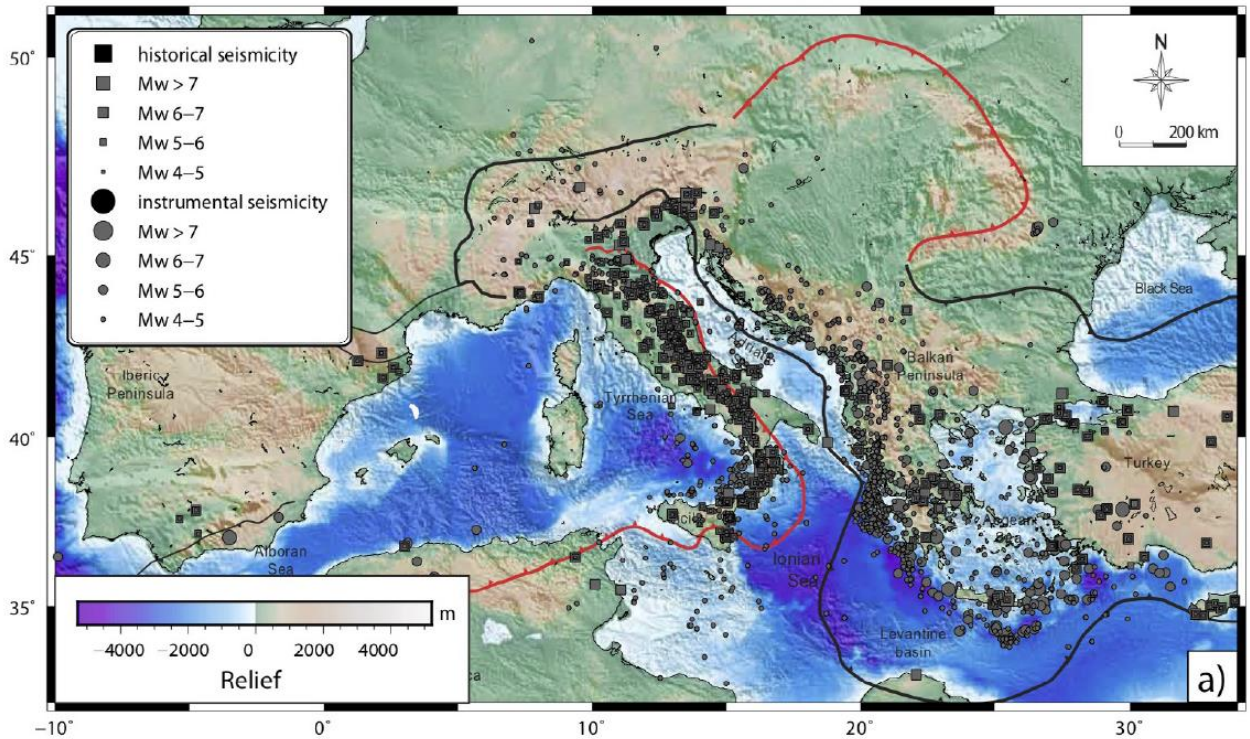


*Figure 2.5: Seismicity map of the Euro-Mediterranean region (from Doglioni and Carminati, 2007).*

Since the Serravallian (~13-11 Ma), roto-translation of the Sardo-Corso block and subsequent extension between Sardinia and the Calabrian block allowed the Eastward migration of the Apennine Chain (Faccennna et al., 2002; Mattei et al., 2002; Milia and Torrente, 2014) (Fig. 2.6). The Apennines represent the skeleton of the Italian Peninsula (Fig. 2.1), forming two curved belts

(Speranza et al., 1997). Growth of the Apennines orogenic system was caused by the extension and crustal attenuation in the Tyrrhenian Sea. The Apennines, with a NW-SE striking, represent a NE verging fold-and-thrust belt in the Northern Apennine, and a SE verging fold-and-thrust belt in the Southern Apennine. Both belts comprise ocean and continent-derived sedimentary and crystalline rock units thrust upon the still undeformed Adria continental crust (e.g., Dewey et al., 1989; Bernoulli, 2001; Scrocca, 2006; Calamita et al., 2011). The current front of the Northern Apennines is buried below the sediments of the Po Plain and Adriatic Sea (Fig. 2.7).

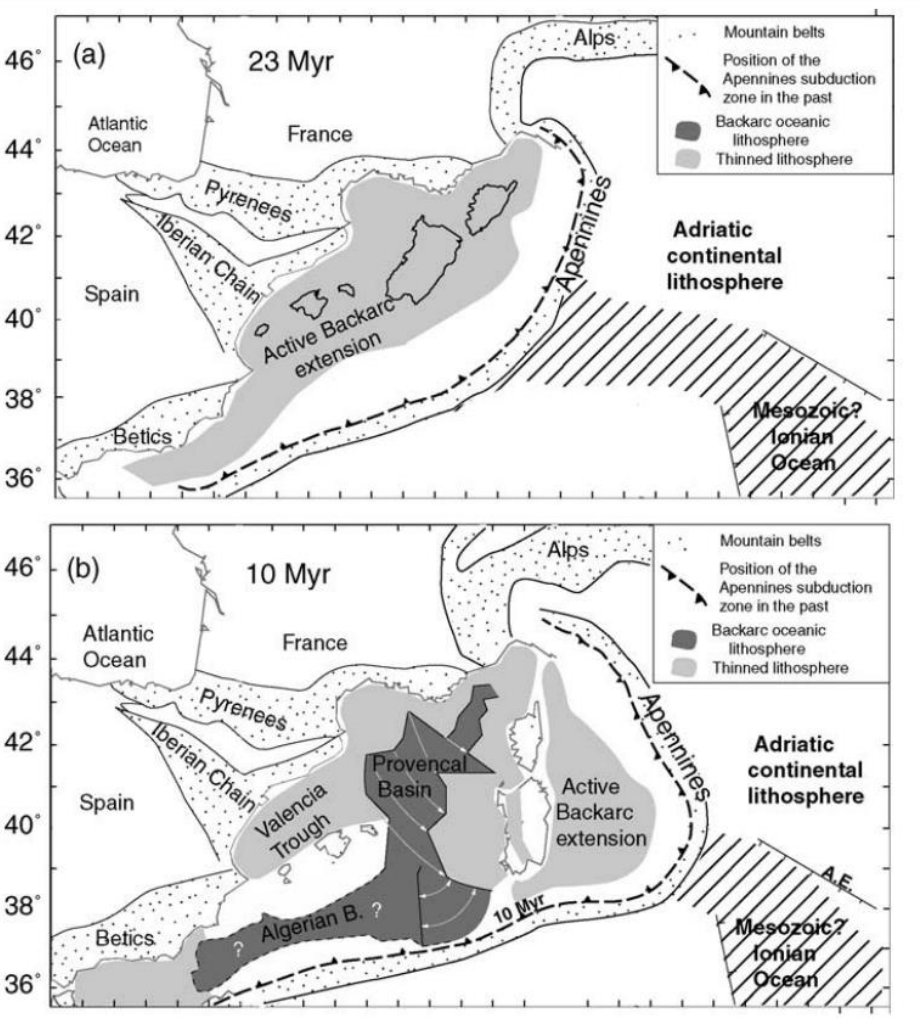


*Figure 2.6: Anticlockwise rotation of the Sardo-Corso block during Lower Miocene, and of the Apennines, since the Upper Miocene with consequent extension of the Tyrrhenian basin (Scrocca., 2006).*

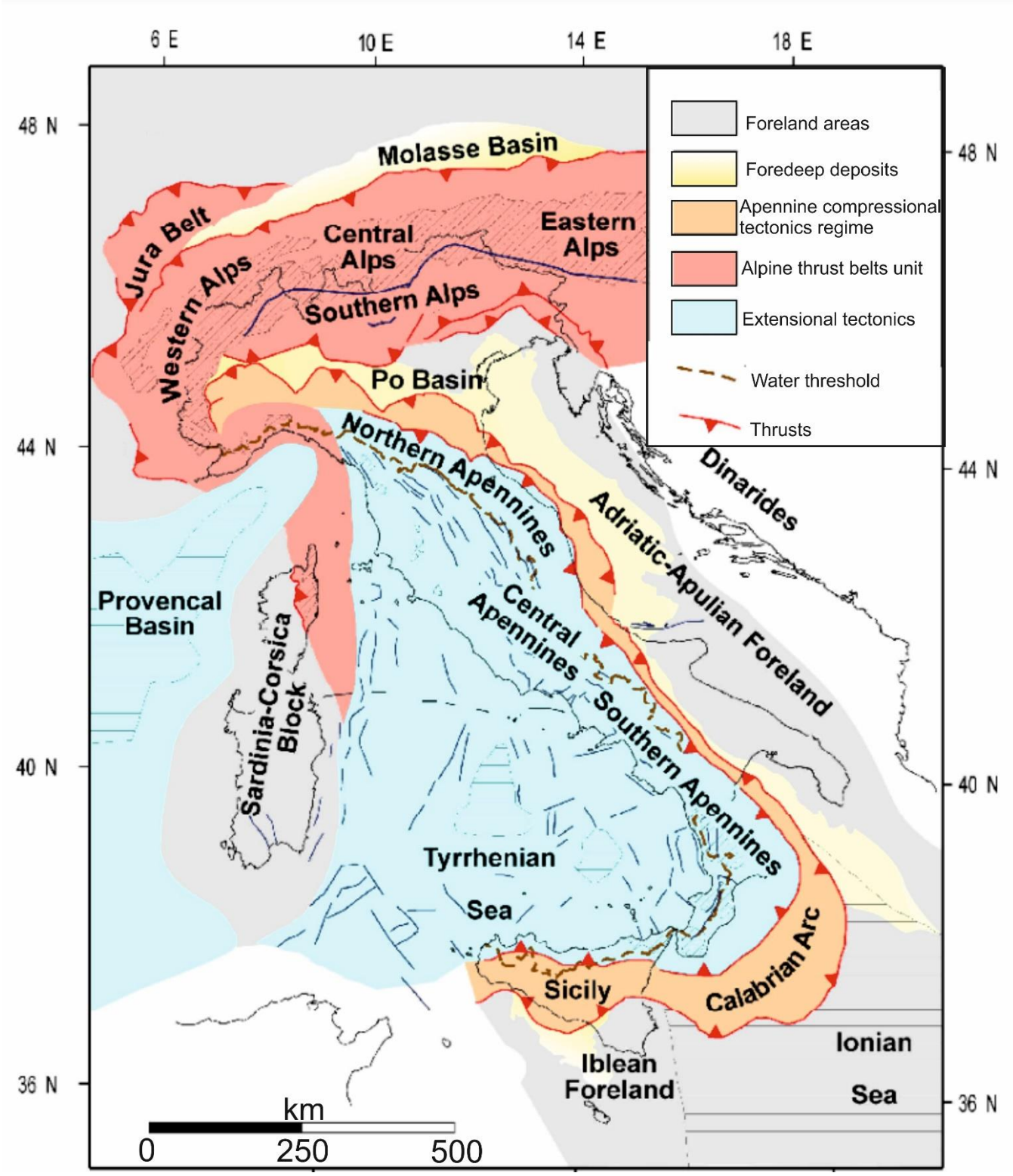


*Figure 2.7: Apennine and Alpine fronts in the peri-Adriatic area. External Apennines reaches the Central Adriatic Sea (modified from Carminati et al., 2004).*

The Southern Alps represent a retrowedge chain, southward thrusting onto the undeformed Adriatic foreland (west) and Dinarides (east) occurred in the Neogene age (Miocene) (Castellarin et al., 1992; Tomljenović et al., 2008; van Hinsbergen et al., 2020). Laterally, it gradually changes or transfers its offset to the dominantly dextral shearing displacement of the peri-Adriatic lineament, that marks the transition to the Dinarides (Tomljenović and Csontos, 2001; Žibret and Vrabec, 2016). The Southern Alps bound the Dinarides to the northwest, which structurally overprints the pre-existing Dinarides during Neogene-time (Castellarin et al., 1992; Tomljenović et al., 2008; van Hinsbergen et al., 2020).

The Dinarides, Albanides, and Hellenides (Fig. 2.1) comprise a large thin-skinned NW-SE trending and SW verging fold and thrust belt overlaying the Adriatic foreland or, to the south, the Ionian oceanic crust (van Hinsbergen et al., 2020).

In the Central and Southern Apennines, the orogenic wedge is thrusted over carbonate units of the Apulian Platform. The thrust front forms a tight curvature changing from a NW-SE to E-W direction toward the Sicily. The Central Apennines present a complex deformation pattern composed by high angles folds and thrusts in the Gran Sasso area (Speranza et al., 2003; Satolli et al., 2005). Growth of the Apennine orogenic system by thrusting was for much of the Neogene accompanied by extension and crustal attenuation in the Tyrrhenian Sea in the back-arc, with both compressive and extensional fronts migrating towards the foreland over time (Malinverno and Ryan, 1986; Casero et al., 1988; Patacca et al., 1990; Cello and Mazzoli, 1998; Faccenna et al., 1997, 2001b; Rosenbaum and Lister, 2004b; Nicolosi et al., 2006;). The three orogens produced changeable thicknesses of clastic deposits.

For the purpose of this work the description of the tectonic setting of Adriatic Sea is divided in three areas: Northern, Central and Southern Adriatic Sea.

## 2.2 The Adriatic Sea

### 2.2.1 Northern Adriatic Sea

The structural setting of the Northern Adriatic Sea results from two different tectonic stages: i) a Mid-Late Jurassic and Early Cretaceous extensional phase and ii) a complex Cenozoic compressional regime (Donda et al., 2015). From Late Cretaceous the Adria Plate represented the foreland for the South Alpine chain related to a southeast-directed subduction. Successively it was involved in the NE-directed Dinaric subduction (Di Stefano et al., 2009) and, from late Oligocene to Miocene, in the Apennines westward subduction (Carminati et al., 2003; Cuffaro et al., 2010). In particular, the Gulf of Trieste represents a double polarity foredeep related to the External Dinarides chain and to the Southern Alps (Carulli et al., 1980; Casero et al., 1990; Fantoni et al., 2003; Castellarin et al., 2006) (Fig 2.8). As a consequence of the compressional events, several inflection phases took place in the area and produced up to 8000 m-thick sediment accumulation in the foredeep basins, filled with clastic sequences in the Romagna offshore (Fantoni and Franciosi, 2010; Ghielmi et al., 2010, Donda et al., 2013). Faster subsidence during the Pleistocene along the western side of the northern Adria margin is recorded. This asymmetry has been associated with the Apennines subduction hinge retreat, which is still moving toward the northeast (Devoti et al., 2008). The stratigraphy of the study area is composed of a Cretaceous-Paleocene carbonate succession, comprising the Maiolica, Marne a Fucoidi, and Scaglia formations, overlain by the Eocene-Late Miocene turbidite deposits belonging to the Gallare Marls formation (Zecchin et al., 2017). Its top is marked by an erosional unconformity, corresponding to the wide Messinian Unconformity produced by sea-level drawdown during the Messinian Salinity Crisis (Ghielmi et al., 2010). The structural setting of the northern Apennines plays a crucial role in the depositional and paleogeographic evolution of the study area (Zecchin et al., 2017): from the Pliocene, the Apennines controlled the deformation processes, subsidence and sediment supply, tilting the Adria foreland.

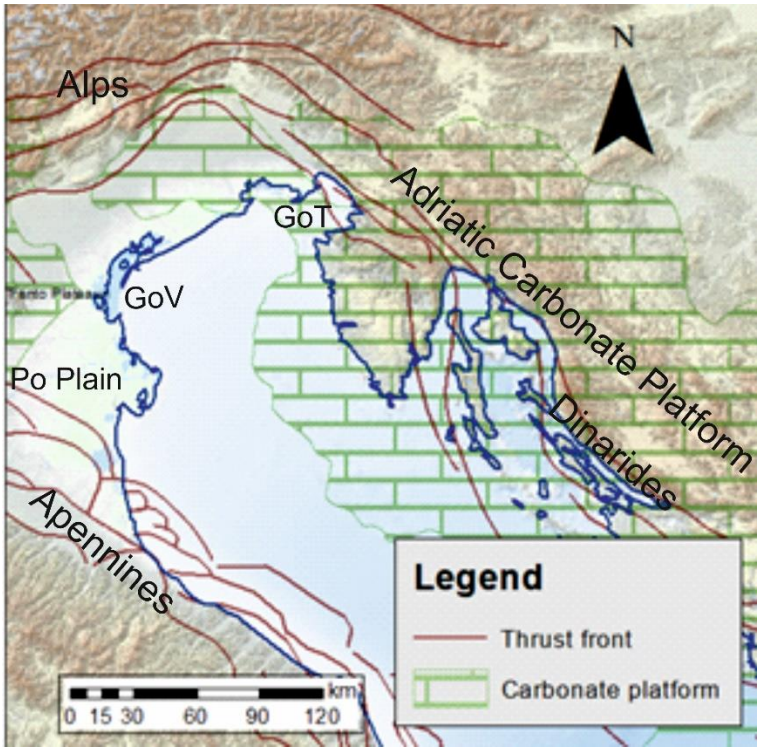


*Figure 2.8: Northern Adriatic Sea area, GoV: Gulf of Venice; GoT: Gulf of Trieste.*

As part of the Northern Adriatic Sea, the Istria Peninsula, i.e. the north-western portion of the Adriatic Carbonate Platform (AdCP) (Figs. 2.1, 2.4, 2.8, 2.9), extends through Slovenia and Croatia Karst up to Bosnia – Herzegovina and Mentenegro (External Dinarides) is part of the Northern Adria Plate (Vlahović et al., 2005). From a geological point of view, it is mainly composed of a very thick carbonate succession that ranges in age from Triassic until the Eocene (Velić and Vlahović, 1994; Vlahović et al., 2005). Paleogene carbonates show the transition to the turbiditic facies of the Eocene Flysch deposits (Velić and Vlahović, 1994; Velić et al., 1995; Vlahović et al., 2005).

This platform carbonate succession is more than 8000 m thick (Tišljar et al., 2002; Velić et al., 2002a, Vlahović et al., 2005). Nevertheless, only deposits from the Lower Jurassic age to the top of the Cretaceous can be attributed to the AdCP (Vlahović et al., 2005), with a thickness varying between 3500-5000 m. In Late Cretaceous, the platform was characterized by gradual disintegration, due to collisional processes causing differentiation of sedimentary environments (Vlahović et al., 2005) developed during different emersion stages. The Eocene maximum deformation of the AdCP resulted in the formation of the Dinaric mountain belt culminated with the uplift of Oligo-Miocene time (Vlahović et al., 2005). Compressional tectonics with a maximum stress-oriented SW-NE resulted in the final uplift of the Dinarides (AdCP included). Main tectonic

events favored the development of flysch deposits infilling the Adriatic foredeep and coming from the dismantling of the platforms.

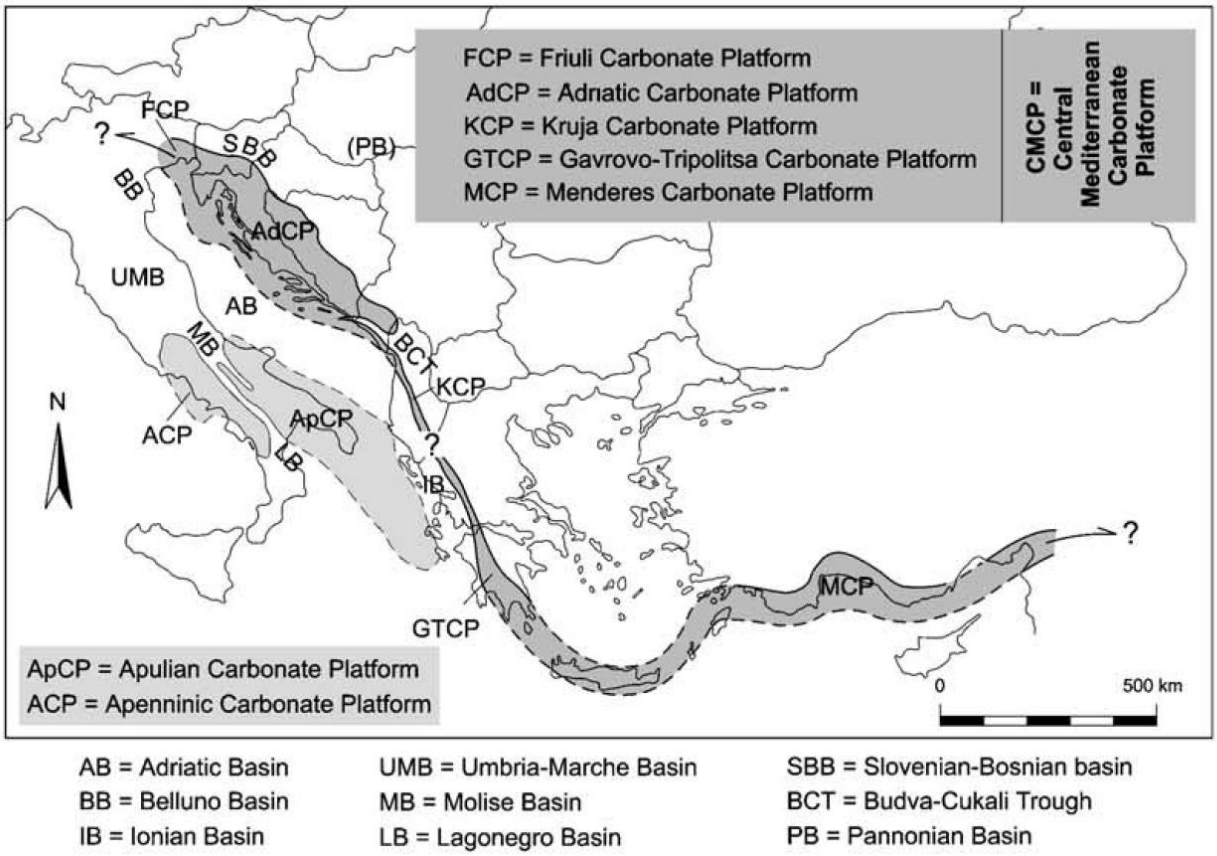


*Figure 2.9: modern extension of the Mesozoic carbonatic platform in the peri-Mediterranean area (from Vlahovic et al., 2005).*

## 2.2.2 Central Adriatic Sea

The Central Adriatic Sea (Fig. 2.10) underwent a slightly different evolution than the Northern Adriatic Sea. it shows three main domains: The Pescara foredeep, the Mid Adriatic Ridge (MAR), and the Ombrina-Rospo Plateau (Fig. 2.10). The counter-clockwise rotation of the Sardo-Corso block ended 14 Ma ago (Fig. 2.6), and from the Serravallian to the Present time, a South Tyrrhenian extension between Sardinia and Calabria occurred (Fig. 2.6).

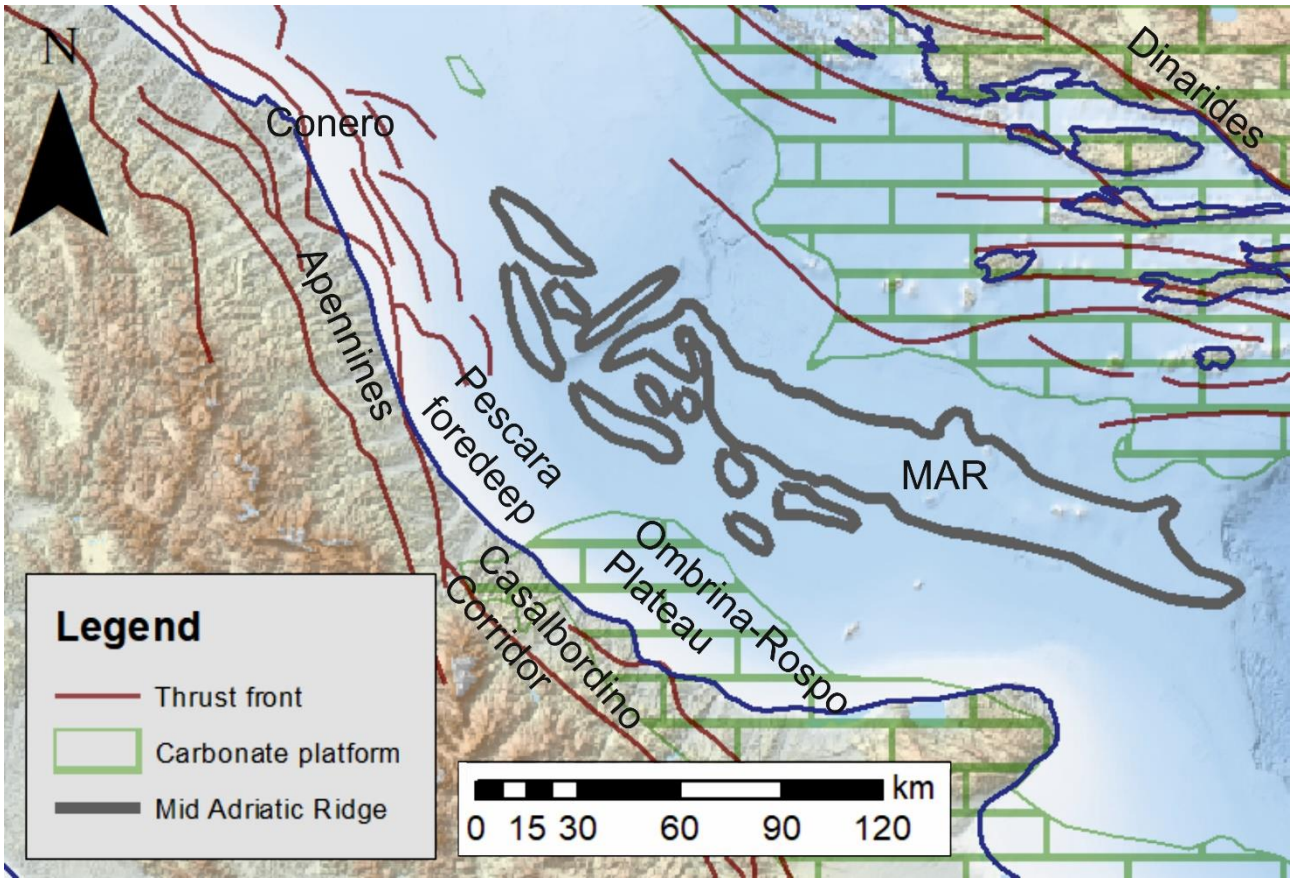


*Figure 2.10: Location of the Central Adriatic Sea, main tectonic features are indicated.*

Extension of the Tyrrhenian was coeval to the thrusting of the Northern and Central Apennines units above the western Adriatic foreland (Casero et a., 1988; Patacca et al., 1990; Faccenna et al., 1997). One of the main effects of this eastward migration of the Apennine chain is represented by the formation of the Pescara foredeep (Fig. 2.10): a terrigenous sedimentary wedge progressively E-ward onlapping a slightly tilted foreland ramp (Carruba et al., 2006; Scisciani and Calamita, 2009; Del Ben and Oggioni, 2016). Moving toward East, the Central Adriatic Sea is characterized by the presence of the MAR (Fig. 2.10), showing a general NW-SE orientation and extending for more

than 300 km in length and for 30-60 km in width (Finetti et al., 2005b). The origin of the MAR is doubtful: the onset of the halokinesis of the Burano evaporites that originated the MAR is alternatively ascribed to the compressional regime of the Dinarides (Finetti et al., 2005b; Geletti et al., 2008) or of the Apennines (Argnani and Frugoni, 1997; Scrocca, 2006). According to Scisciani and Calamita (2009) initial deformation is due to Paleogenic normal faults, subsequently re-activated during the Pliocene and Pleistocene. Other authors think that MAR's formation is due to the prolonged period of stress generated by the interaction between the two orogenic belts or by a peripheral bulge, which produced the vertical extrusion of salt (de Alteriis, 1995; Grandic et al., 1999; Scisciani and Calamita, 2009).

The Ombrina Rospo plateau, bordering to South-East the Central AS, (Fig. 2.10) represents a buried northward stretch of the ApCP (Santantonio et al., 2013). The carbonate platform shows tectonic re-activation of the Jurassic extensional fault during the Late Cretaceous, when a subsiding fault-bounded through known as the "Casalbordino Corridor" accommodated a thick marine succession (Santantonio et al., 2013) (Fig. 2.10). The western margin of the Ombrina-Rospo plateau represents the development of the Apennine foredeep basin (Patacca et al., 2008), where deep and shallow marine domains were present. Intense tectonics related to the compressional Apennine regime and sea-level drawn during the MSC may have disconnected the Ionian-Lagonegro Basin from the Central Adriatic Sea (Manzi et al., 2020). The East-migration of the Apennine chain brought a flexure hinge of the Adria plateau (Patacca and Scandone, 2008), which was incorporated in the Plio-Pleistocene foredeep and filled by onlapping sediments of the terrigenous sequence. Sedimentological characteristics of the Ombrina-Rospo plateau are related to the proper ApCP, as described in the further chapter.

During the Messinian Salinity Crisis, evaporites were deposited in the CAS area (Lugli et al., 2010; Lofi et al., 2011; Roveri et al., 2016; Lofi, 2018); this evaporites are generally referred to as the first evaporitic deposition which reached a maximum thickness of about 200 m (Roveri et al., 2008). Throughout Pliocene, tectonic shortening affected the Adria plate due to the opening of the Tyrrhenian Sea (Malinverno and Ryan, 1986; Boccaletti et al., 1990; Calamita et al., 1990; Fantoni et al., 2003; Toscani et al., 2014). This tectonic phase partially deformed the MSC deposits, particularly in the internal foreland, present below the chain. Fully marine conditions occurred in the Apennine foredeep basin, filled with turbidites onlapping a thin Early Pliocene, which parallelly covers the MSC unconformity (Carruba et al., 2006; Del Ben and Oggioni, 2016).

## 2.2.3 Southern Adriatic Sea

The Southern Adriatic Sea is generally considered the foreland of the opposite verging chains: Apennines and Dinarides/Albanides/Hellenides (Fig. 2.11). The two foredeep basins, respectively the Bradanic Trough of Plio-Pleistocene age and the eastern South Adriatic Basin of Mio-Pliocene age, are separated by the ApCP (Fig. 2.11).

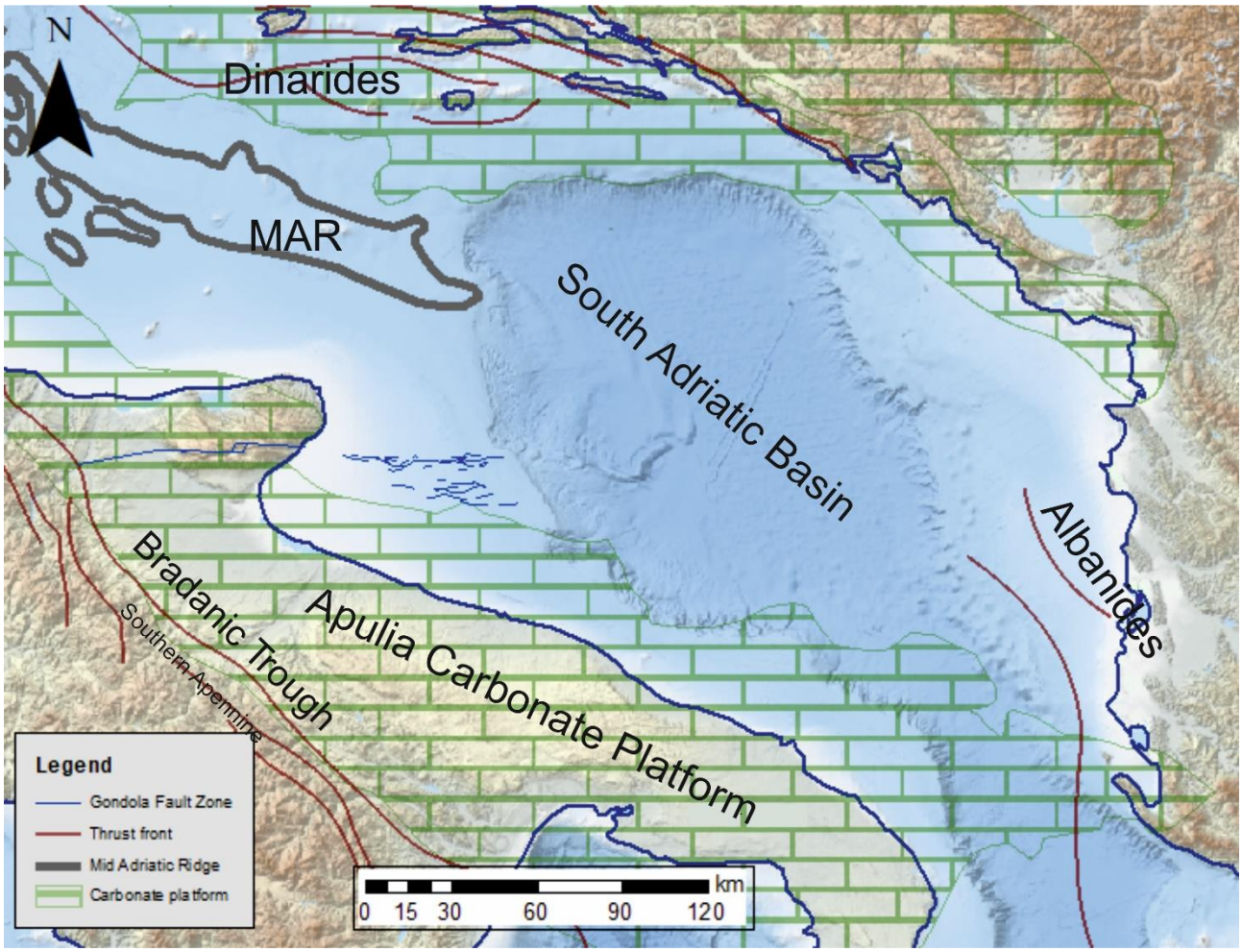


*Figure 2.11: Location of the Southern Adriatic Sea, main tectonic features are indicated.*

The Bradano Trough, in particular, is the effect of the Adria subduction below the Apennine chain (Nicolai and Gambini, 2007). The ApCP is composed by more than 7000 m of shallow-water carbonates deposited since the Triassic time (Merlini and Mostardini, 1986; Mattavelli et al., 1991; Patacca et al., 2008). The Triassic carbonate platform is composed by the very thick Dolomia Principale formation, while the Cretaceous carbonate is mainly constituted by the Cupello

formation, intercalated by bauxitic levels developed on a regional scale on all the peri-Adriatic platforms, testifying long-periods of subaerial exposure. The shallow-water Cretaceous carbonate is generally covered by a thin Miocene carbonate succession known as the Bolognano formation. The extension and geometry of the ApCP are still a matter of debate: it crops out in the Gargano promontory (Bosellini et al., 1993) and almost in the entire Puglia region (Fig. 2.11). It continues southeastward, buried below the Plio-Quaternary sediments, through the Otranto Channel and outcrops in the Karaburun peninsula (Argnani et al., 1996; Ballauri et al., 2002; Mocnik, 2008) with fold and thrust tectonics that led to widespread exposure of the ApCP (Le Goff et al., 2019). The pre-Apulia zone (Renz, 1940) is commonly recognized as an extension of the Apulian Platform with time-equivalent carbonate series described from the Salento coast (Chanell et al., 1979; Zappaterra, 1992; Le Goff et al., 2019). The succession exposed in the Karaburun peninsula comprises nearly 3000 m of Lower Cretaceous to Paleocene carbonates, NE tilted and extended for 40 km (Le Goff et al., 2019). The southern margin of the ApCP is considered a transition between the ApCP and the Ionian/South Adriatic basin. The first reconstruction of the Apulia platform margin in the East Salento offshore (Mocnik, 2008) delineated a complex outline and an isolated platform in the pelagic domain of the South Apulia Basin (Del Ben et al., 2015).

The ApCP was mainly exposed during the MSC, causing a non-depositional / erosional hiatus (De Alteriis and Aiello, 1993). In the South Adriatic Basin, evaporites are deposited and preserved in the Albanian offshore (Del Ben et al., 1994; De Alteriis, 1995; Argnani, 2013). Along the current SE Salento coast and across the Otranto Channel the platform margin developed until the Messinian with coral reef structures (Bosellini et al., 2001) until the Albania coast (Del Ben et al., 2010; 2015).

## 2.3 Oceanography setting

The Adriatic Sea has a surface area of 138600 km$^2$ and a water volume of 35000 km$^3$ (Fig. 2.12). It is connected with the Mediterranean Sea through the Strait of Otranto, a relatively wide and deep inlet (72 km wide and 780 m deep), that play an important role in water exchange circulation between the Ionian Sea and the Adriatic Sea (Gacic et al., 2001). The bathymetry is characterized by a transversal and longitudinal asymmetry, due to different morphology of the coasts: the Italian coastline is relatively smooth and regular, while the Croatian coastline is composed by archipelagos with irregular and steep surface (Fig. 2.12).

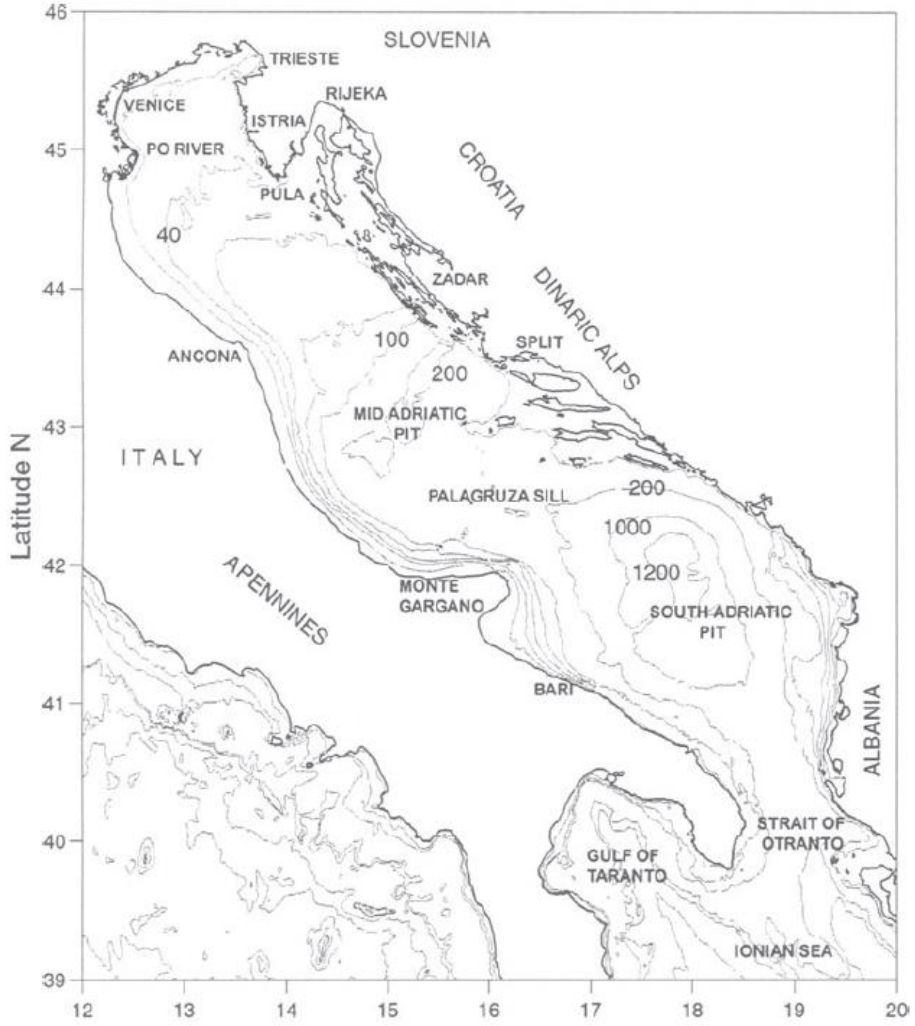


*Figure 2.12: Geography and bathymetry of the Adriatic Sea. Depth contours are in meters (from Gacic et al. 2001).*

In longitudinal direction, the Adriatic Sea is divided into three geographical regions namely: Northern, Central, and Southern Adriatic Sea. The northern portion is very shallow, starting with a depth of few m along the Venice-Trieste coastline, deepening slowly southward and abruptly reaching 270 m in the Mid Adriatic Pit (MAP), also known as "Pomo depression" or Jabuka Pit or Mid Adriatic Depression (Gacic et al., 2001; Trincardi et al., 2014) (Fig. 2.13). The northern edge of the depression was created by the ends of the last Glacial maximum progradation (Trincardi et al., 1994). Southward, the Palagruza Sill separates the MAP from the South Adriatic Basin, an abyssal depression reaching a maximum depth of about 1200 m (Fig. 2.13).

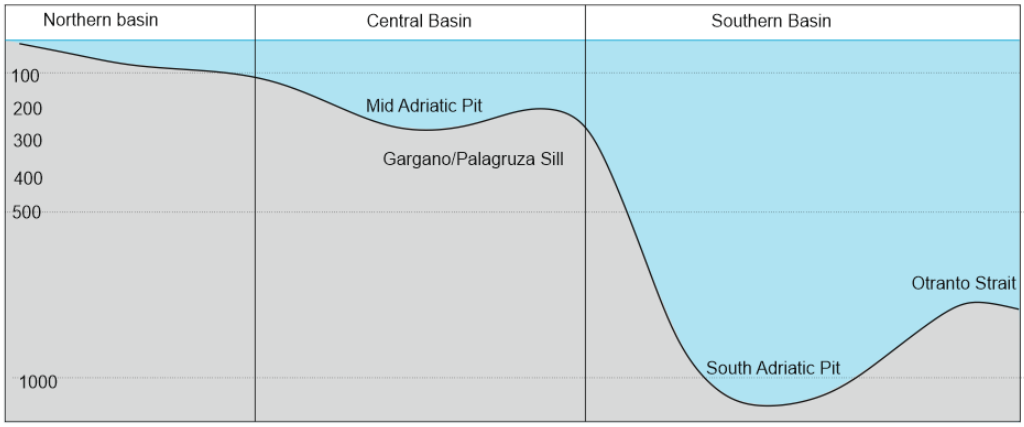


*Figure 2.13: Schematic cross section of the Adriatic Sea bathymetry (modify from Gacic et al., 2001).*

The northern part of the section is characterized by average values of depth of about 35 m, salinity of 37-38‰, and temperature of 25°C. The central and southern Adriatic Sea is characterized by average salinity of 38.4-38.9‰ and temperature of 18° (Gacic et al., 2001).

Several rivers are discharging into the Adriatic Sea (Fig. 2.14), such as the Po and the Adige rivers, responsible for the high freshwater discharge. Also underground freshwater seepings along the eastern coast contribute to the freshwater discharge. River discharge affects both the sedimentation and the water circulation along the coasts, and its effect is particularly evident in the Northern Adriatic Sea with the Po River, and in the Southern Adriatic Sea with the Neretva and others Albanian rivers (Brambati et al., 1983). Most of the input comes from the Po river, which is the largest Italian river and supplies over the 11% of the total freshwater flowing into the Mediterranean Sea, 28% flowing in the entire Adriatic Sea, and the 50% flowing into its northern part (Degobbis et al., 2000). Moreover, both rivers and submarine springs along the Balkan coast

contribute with another 29% of freshwater in the Adriatic Sea. This high input determines the low salinity of the Adriatic Sea, and the flow of low salinity water toward the Ionian Sea through the Otranto Strait (Gacic et al., 2001).

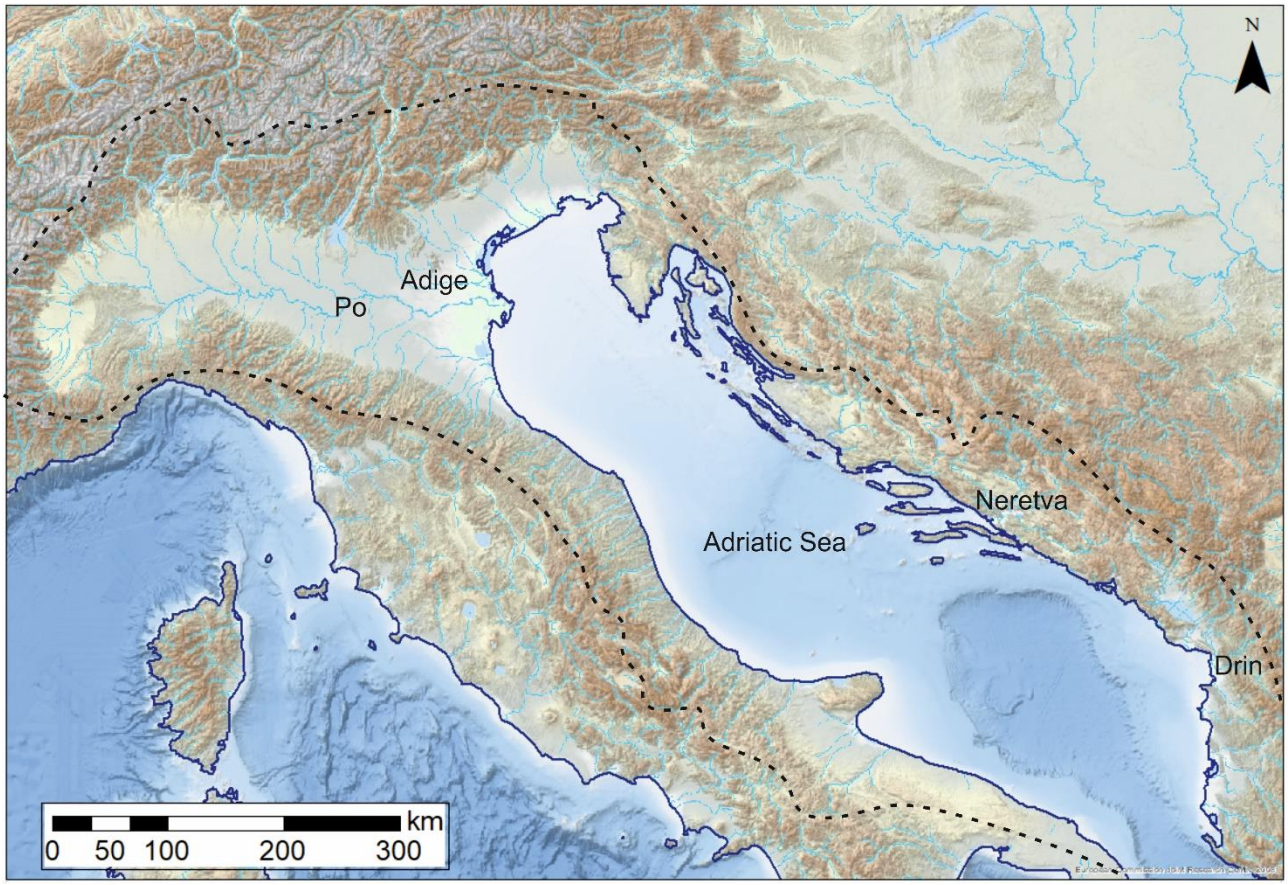


*Figure 2.14: Drainage basin discharging into the Adriatic Sea and related major rivers; the dashed black line represents the watershed line of the Adriatic Sea (adapted from Sekulic and Vertacnik, 1997).*

A cyclonic superficial water circulation characterizes the Adriatic Sea: the waters flow northward along the Croatian coast and southward along the Italian coast (Gacic et al., 2001) (Fig. 2.15). Cyclonic gyres could be formed in each of the three sub-basins, with different intensities depending on the season and the freshwater inputs. There is also some evidence of local anticyclonic cells (Gordini, 2012, and references therein). Tidal phenomena are more critical in the Adriatic than in the rest of the Mediterranean Sea, reaching amplitudes around 150-200 cm in the northern part (Gacic et al., 2001). Meteorological factors (such as winds and pressure conditions) and the geological-morphological characteristics as presence of seiches, strongly influence short-term sea-

level changes. Seasonal and long-term fluctuation of oceanographic and biological conditions occur, mainly due to atmospheric forcing, freshwater discharges, variable intrusion of high salinity waters, and a variable and complex circulation (Gacic et al., 2001).

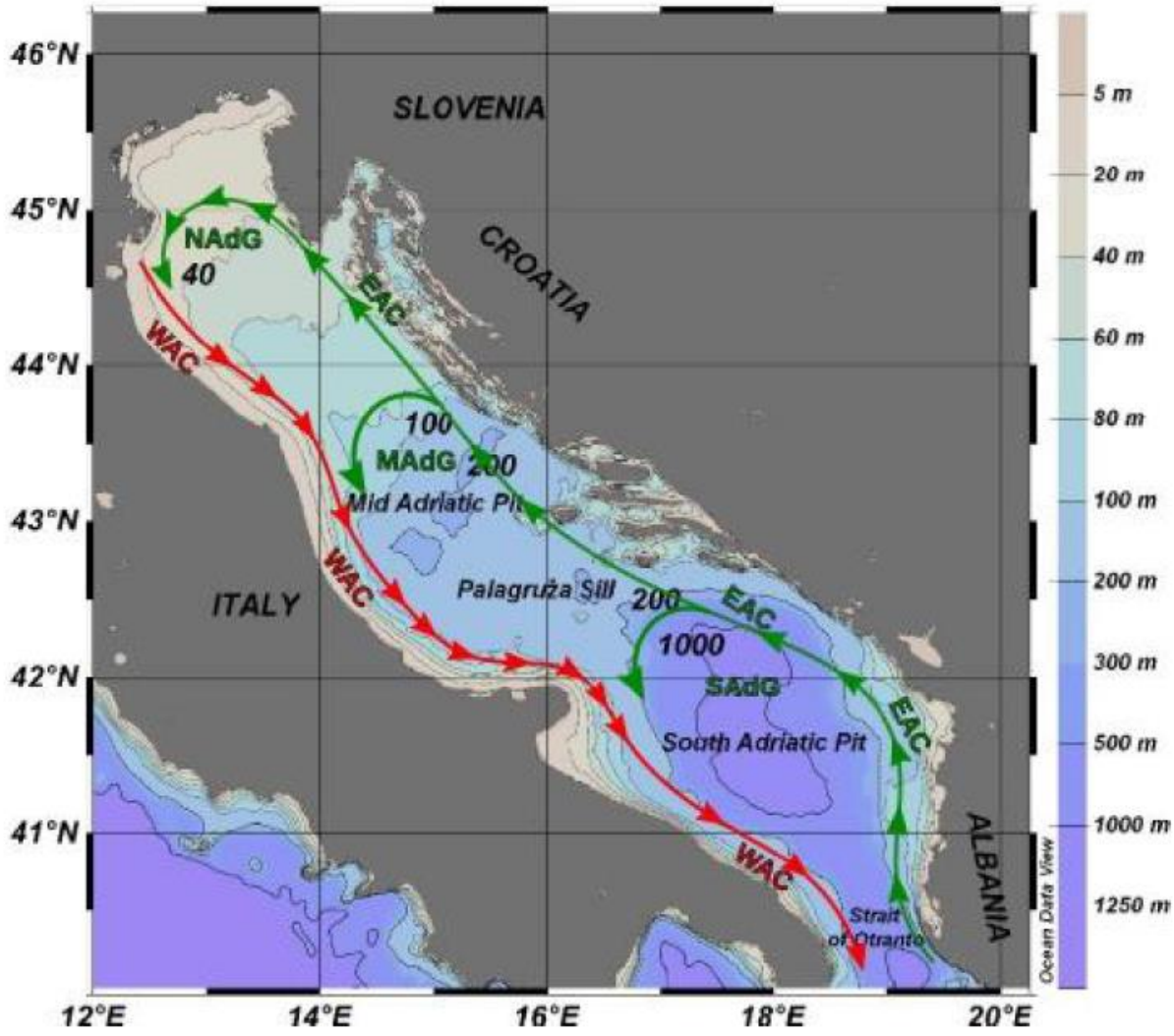


*Figure 2.15: Bathymetry, morphology and main surface circulation of the Adriatic Sea. EAC: Eastern Adriatic Current; WAC: Western Adriatic Current; NAdG: North Adriatic Gyre; MAdG: Middle Adriatic Gyre; SAdG: South Adriatic Gyre (from Lipizer et al., 2014).*

# Chapter 3 - Data and Methods

## 3.1 Principles of seismic reflection

Seismic reflection surveying is one of the most widely used and well known geophysical methods. Marine reflection seismic is a geophysical exploration technique that utilizes the principles of seismology to derive the properties of the ocean floor's surface and subsurface. Seismic exploration consists of three main stages: data acquisition, processing, and interpretation.

The technique is based on progradation of an elastic wave through a medium (e.g. water or sediment). Wave progradation with velocity V can be described by the d'Alambert wave equation (1), in one dimensional space: this partial differential equation describes the temporal (t) and spatial (x) dependence of variable u (pressure).

$$\frac{\partial^2 u}{\partial x^2} = \frac{1}{V^2}\frac{\partial^2 u}{\partial t^2} \qquad (1)$$

The velocity of a compressional wave (P-wave) depends on the properties of the medium and is a measure of the connectivity of medium elements. The P-wave velocity $V_p$ is given by:

$$V_p = \sqrt{\frac{K + \frac{4}{3}\mu}{\rho}} \qquad (2)$$

where K is the bulks modulus, μ the shear modulus and ρ the density. Shear waves were recorded in the old marine reflection seismology, because the shear modulus in fluid is zero. In the last decades, the 4C technique, using geophones sited on the sea bottom, recorders S-waves converted.

The data acquisition starts with an “explosion”, below the sea level, that produces an expanding compressional wavefront, that can be see as a seismic pulse. This seismic pulse, called "source wavelet", is produced usually by a gun, which is towed behind the vessel and shoots out compressed and highly pressurized air or water from pneumatic chambers at defined time intervals.

The source wavelet is transmitted through the water and the rocks as an elastic wave, which transfers his energy by the movement of the rock particles (Badley, 1985). Each rock type or lithology, shows behavior susceptibility to particles motion and a characteristic velocity when the seismic waves cross them.

The predictable and characteristic acoustic properties of a rock are defined as its "acoustic impedance" (Z), which is the product of density (ρ) and velocity ($V_P$).

$$Z = \rho VP \tag{3}$$

Reflection is generated at the interfaces that are characterized by a strong impedance contrast, like the seafloor, or the changes in lithological sequences (Yilmaz, 1987). The wavefront, when encounters the seafloor (different impedance between water and shallow sediments) splits: part of the acoustic energy is reflected back toward the surface, where it can be recorded with a chain of hydrophones (streamer) with different distances from the source (offset), and part is transmitted/refracted to continue the downward path (Fig. 3.1).

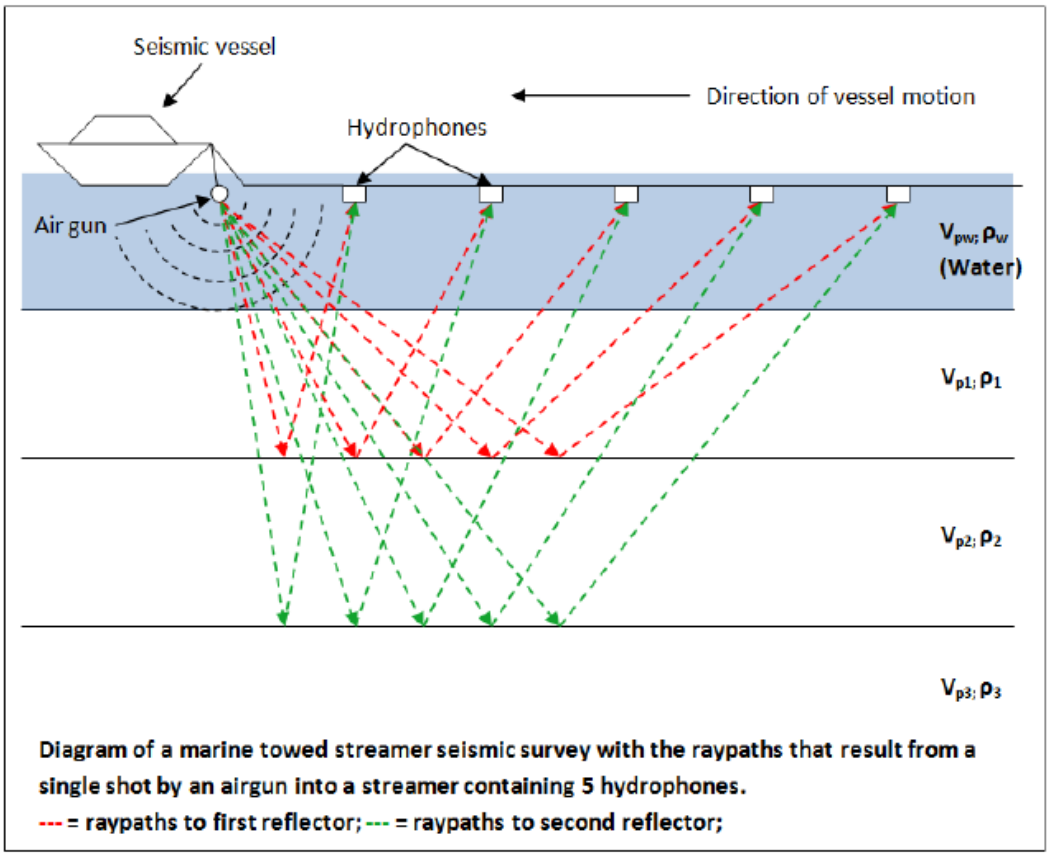


*Figure 3.1: schematic diagram of 2D marine seismic reflection acquisition (reproduced from Nwhit (2012).*

The wavefront split occurs exactly at the boundary between the two different sequences. The strength of reflected signal depends on the magnitude of the impedance contrast at the interface of two layer (also known as the Reflection coefficient).

The source wavelet is characterized by the superposition of several harmonic waves of different frequencies, amplitudes and phases (Hatton et al., 1996). The one dimensional convolutional model states that the recorded seismic trace is simply the result of the convolution of the Earth's reflectivity with the source wavelet plus a noise component, as shown in Figure 3.2 and Equation 4:

$$s(t) = w(t) * r(t) + n(t) \quad (4)$$

where *s(t)* is the seismic trace, w(t) is the seismic wavelet, r(t) the Earth reflectivity and n(t) the noise component.

The resolution of a seismic signal is highly affected by its dominant frequency. The resolution describes how far apart two interfaces (vertical resolution) or two features involving a single interface (horizontal resolution) must be, in order to recognize them in seismic images as two individual reflectors or features, respectively. Other factors controlling the resolution are the signal to noise ratio (S/N), the sample rate and the experience of the interpreter (Sheriff and Geldart, 1995). Seismic data are recorded in time, meaning that the vertical dimension of seismic images is two-way travel time (TWTT).

The maximum vertical resolution capability of a seismic signal is defined by the Rayleigh Criteria: “the minimum resolvable thickness of a layer must exceed at least a quarter of the dominant wavelength ($\lambda/4$) in order to be recognized as two separated reflectors”. This means that is not possible to determine the thickness of a layer from the wave shape (Sheriff and Geldart, 1995).

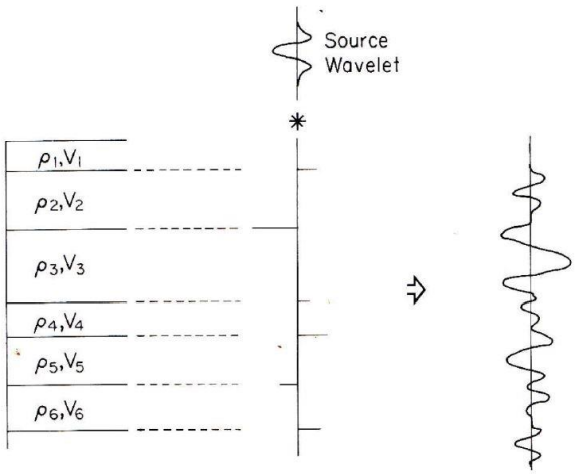


*Figure 3.2: Convolution of the source wavelet with the Earth's reflectivity and the resulting seismic trace (Hutton et al., 1986).*

Horizontal resolution in migrated profile is defined by the "Fresnel Zone". If the seismic signal is considered as a ray, it is reflected at a single at the surface. However, the seismic energy spreads out spherically and hence, it should be considered a wave front rather than a ray. Thus, energy is reflected at a relatively large area of the reflective surface (Fig. 3.3; Sheriff and Geldart, 1995). The lateral resolution of seismic images is limited by the trace sampling interval, the processing and imagine workflow, and the bandwidth of the seismic source.

The size of this area (Fresnel Zone) is defined by the travel time at which the returning signal has a phase difference of no more than a quarter wavelength, allowing constructive interference in this zone. The radius is calculated with Equation (5), where V is the velocity, t the arrival time and f the frequency in TWTT.

$$r_f = \frac{V}{2} \cdot \sqrt{\frac{t}{f}} \qquad (5)$$

After migration, seismic images collapse the Fresnel zone by summing contributions from many adjacent traces, meaning that migrated images have maximum lateral resolution of around half of the dominant wavelength (Chen and Schuster, 1999).

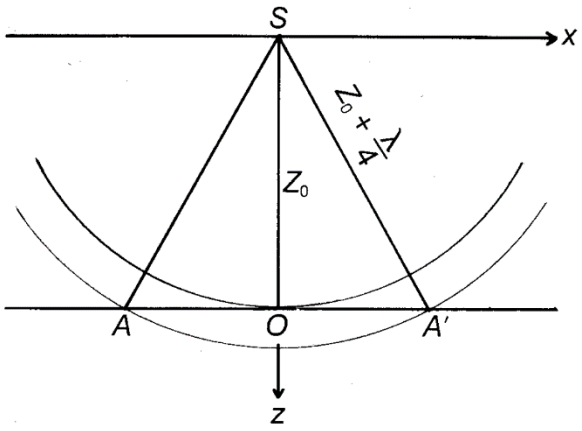


*Figure 3.3: Fresnel Zone (AA´) for coincident source and receiver (Yilmaz, 1987).*

The relationship between dominant frequency (f), propagation velocity (v) and wavelength (λ) is described in Equation 6:

$$\lambda = V/f \qquad (6)$$

Low-frequency signals (long wavelength) have a deep penetration but low resolution, while signals of high-frequency (short wavelength) provide high-resolution seismic profiles, which explore the shallow sequences. However, the attenuation of high frequencies during the travel time is stronger than for low-frequency waves. Therefore, resolution generally decreases with depth (Fig. 3.4; Brown, 1999). Seismic reflection techniques are fundamentally limited in depth penetration by seismic attenuation. Attenuation describes amplitude losses due to geometrical spreading of the wavefront.

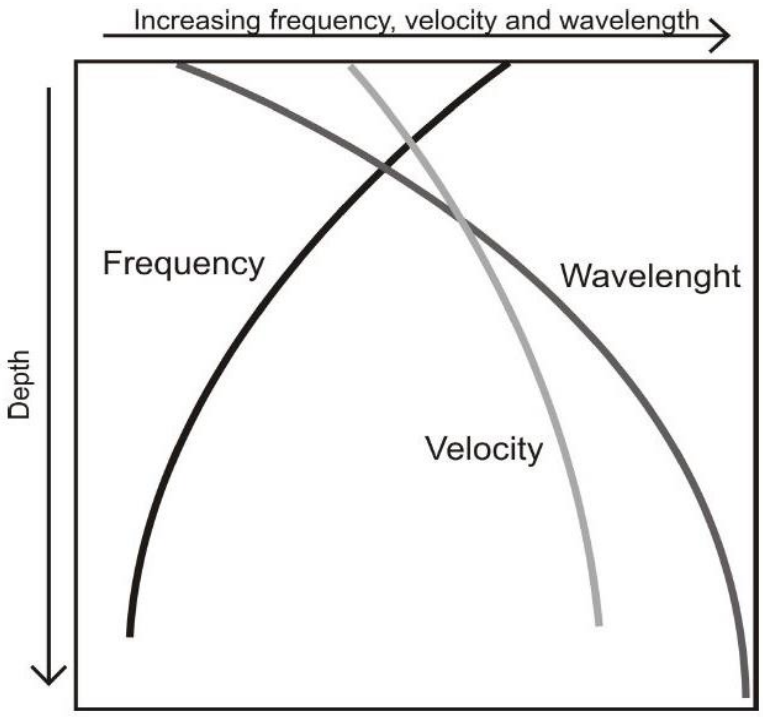


*Figure 3.4: Relation between frequency, wavelength and velocity. In general, the frequency decrease with depth (redrawn after Brown, 1999).*

The seismic-reflection method is based on the recording and measurement of reflection from interface boundaries. Seismic streamers are towed behind the ship and they detect reflected energy using pressure sensitive devices known as "hydrophones", which then convert the pressure signals into electrical signals. These, in turn, transmitted via the streamers to the recording system onboard the vessel. Processing of these recorded information allows to obtain data, consisting of two-way travel times (TWT), amplitudes, frequencies and to create a 2D subsurface image.

## 3.2 Italian public vintage seismic data

The Adriatic Plate is a hydrocarbon-producing area in Italy and Southern Europe (Bertello et al., 2010), where discoveries of biogenic gas fields are concentrate in the Po Plain and in the Northern and Central Adriatic Sea (Fig. 3.5), while in the southern Adria Plate oil fields occurrence are more present (Cazzini et al. 2015). The first Italian gas field (Caviaga field) was discovered in 1944 in the Po Plain, marking the beginning of the modern hydrocarbon exploration. Discoveries of other onshore gas field led to the intensification of exploration, that moved offshore in the 60's. First offshore discovery occurred in the Northern Adriatic Sea, targeting the subsurface anticline structure of Barbara biogenic gas field with peak production of gas in 1994 (Cazzini et al., 2015). Introduction in the 80's of seismic profiles techniques resulted in the discovery of hundreds of potential hydrocarbon traps. Exploration of Central and Southern Adriatic Sea begun in the 70's, pursuing 17 oil field discovered, only 6 currently producing (Cazzini et al., 2015). New discoveries began to decline from the early 2000, a trend continuing nowadays. Until the 2012, a total of 127 (Fig. 3.5) discoveries are reported in the Adriatic Sea offshore, which represent the 22% of the whole 582 Italian discoveries (Cazzini et al., 2015). In 2015, 54 out of 110 gas fields are producing or under development, the other 56 are on hold, abandoned, or non-economical discoveries.

Vintage geophysical data from hydrocarbon exploration purpose represent a huge heritage for the scientific community. These were acquired during the first development of the multichannel seismic reflection techniques, and are generally characterized by high penetration and regional extension. According to the Italian legislation (law n. 6 11/1/1957) documents related to mineral prospecting project must become public after one year from the termination of the royalties. Unfortunately, the original acquired data are no more available, so they can be recovered through their scanner acquisition (ViDEPI). Recovery and reprocessing of multichannel seismic vintage data depends largely on the quality of the original raster files, which in turn comes from the scanning of old papers (Diviacco et al., 2015). Processing was mainly aimed at attenuating the artifact introduced during the scanning and the conversion process of the raster files. Nevertheless, digitalization of the vintage seismic data permits to interpret all the data available in the Italian offshore, converting them into a Seg-y format. Seg-y is a digital format developed in the 1975, enable the storage of seismic profiles on magnetic tape. This format includes a header of metadata including identification of profiles (e.g., survey, year, coordinates, length…) and a navigation part associating at each shot point a geographical coordinate in metric format.

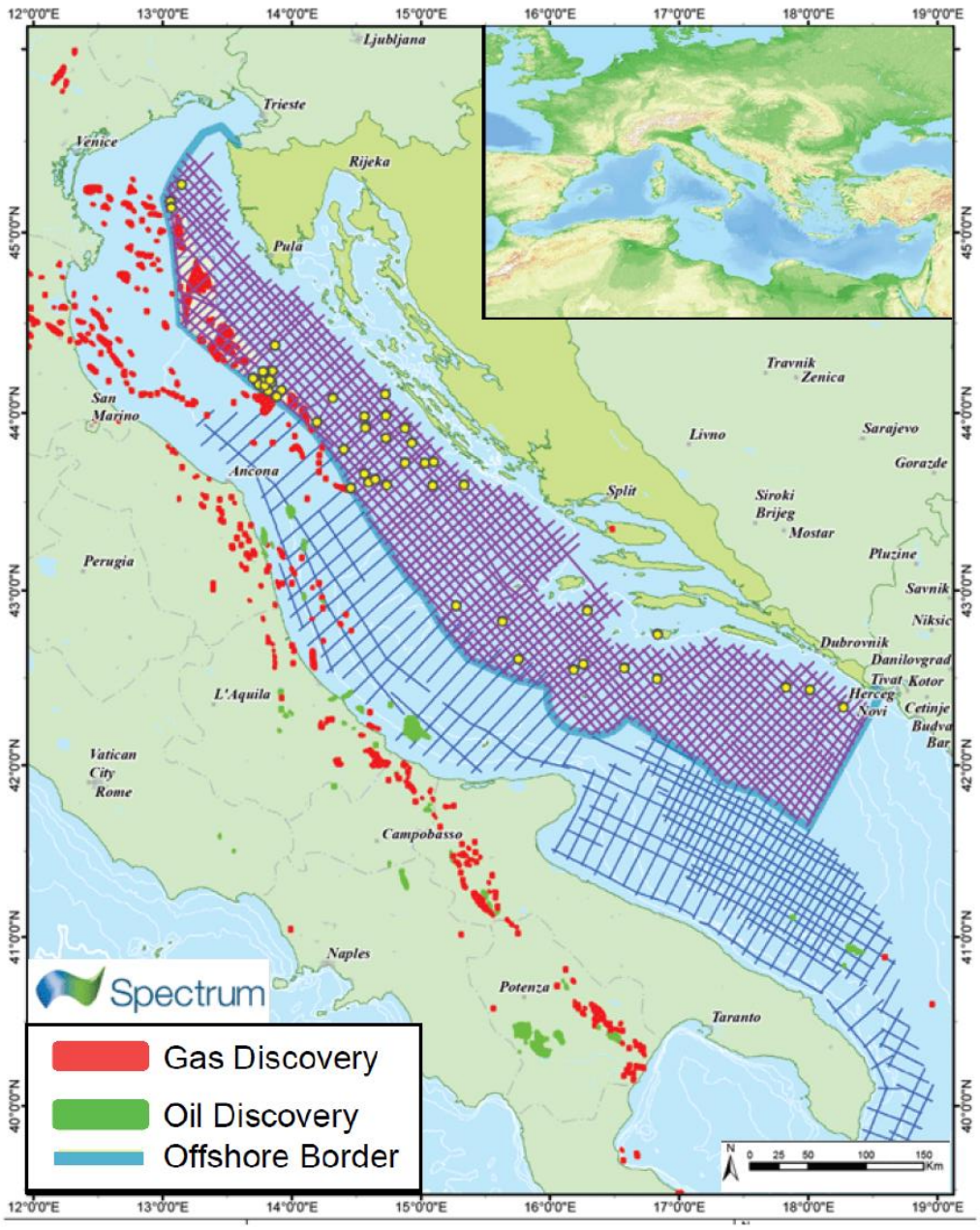


*Figure 3.5: Location of the hydrocarbon discovery in the Adriatic Sea and Italian peninsula (from Wrigley et al., 2015).*

For the aim of this thesis we merge data from different dataset analyzing more than 10000 km long profiles (Fig. 3.6):

— SNAP (Seismic data Network Access Point): zona A, B, D and F restore vintage seismic data from the Italian offshore; the ViDEPI database consists in the public documentation concern expired mining permit and concession. The dataset includes 2D multichannel seismic data from hydrocarbon exploration (mostly ENI, former

AGIP). The study area is covered by Zone A and B, it was acquired during the 60's; Zone D and F in the 60's and 70's. All the multichannel seismic survey were acquired by AGIP. The dataset consists of vintage low-resolution profiles, made available by the Ministry of Economic Development. The data, successfully converted from .TIFF to SEG-Y, were associated to their navigation coordinates (Diviacco et al., 2019). Processing sequence improved the "signal to noise ratio" possible on post-stack data.

— STENAP "Stratigraphic and Tectonic Evolution of the Northern Adriatic Sea in the Plio-Quaternary" acquired in 2009 with R/V OGS Explora. The cruised acquired 820 km of 2D multichannel seismic profiles (Donda et al., 2015);

— GANDI "GAs emission in the Northern ADrIatic Sea" acquired in 2014 with R/V OGS Explora. The cruise collected approximately 450 km of multichannel seismic lines;

— CROP "CROsta Profonda" deep penetration reflection profiles acquired by the R/V Explora from 1988 to 1995. Data provided deep crustal tectono-stratigraphic information. The basic processing sequence focused on the amplitude correction, multiple removal, deconvolution, velocity analysis, stacking, post stack migration and filtering (Finetti, 2005);

— Literature seismic profiles available in pdf format localized in the Croatian offshore had to be transformed into Seg-y in order to be integrated in Kingdmon Suite software. The publication includes: Grandic et al. (2001, 2010), Argnani (2013), Pellen et al. (2017), Scisciani et al. (2018), Wrigley et al (2015), Mazzuca et al. (2015), Spelic et al. (2021). These lines were integrated into the dataset in order to create transects crossing orthogonally the Adriatic Sea.

Although in some area the coverage of the seismic lines is not very dense, as for instance in the Albanian offshore, the strength of this dataset is due to its regional distribution with many available profiles that allow a connection between the Italian and Croatian offshore.

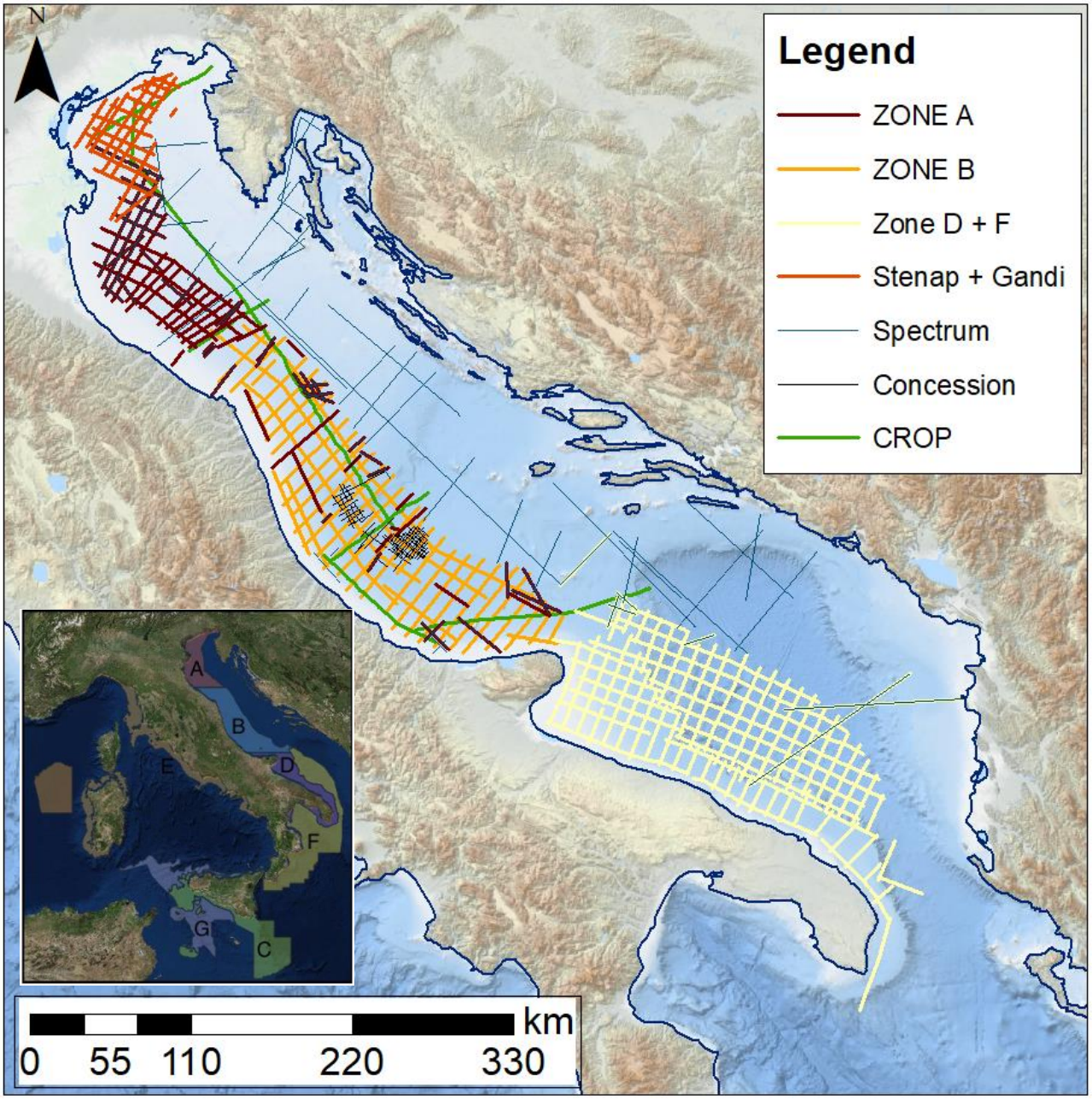


*Figure 3.6: Seismic dataset used for the seismic interpretation.*

## 3.3 Borehole data

All the well log data used for the seismic lines calibration in this thesis are from the ViDEPI database (Fig. 3.7). The buried sedimentary sequence of the Adriatic Sea was widely investigated by industrial and exploration wells (Fig. 3.7). In ViDEPI website a total of 218 boreholes are available in the Adriatic Sea (62 in zone A, 99 in zone B, 38 in zone D and 19 in zone F). Well data consists of composite logs charts which differently contain information about: age constrain, formation name, lithology (derived from cuttings), depth, lithostratigraphy, fluid occurrence, depositional environment, biostratigraphy, petrography information (e.g., Gamma-ray, resistivity, Sonic log, velocity). However, they are not always acquired or available. Moreover, the available technical reports concerning the exploration permits to provide technical information on the drilling parameters and on the local geological and structural setting around the drilling sites.

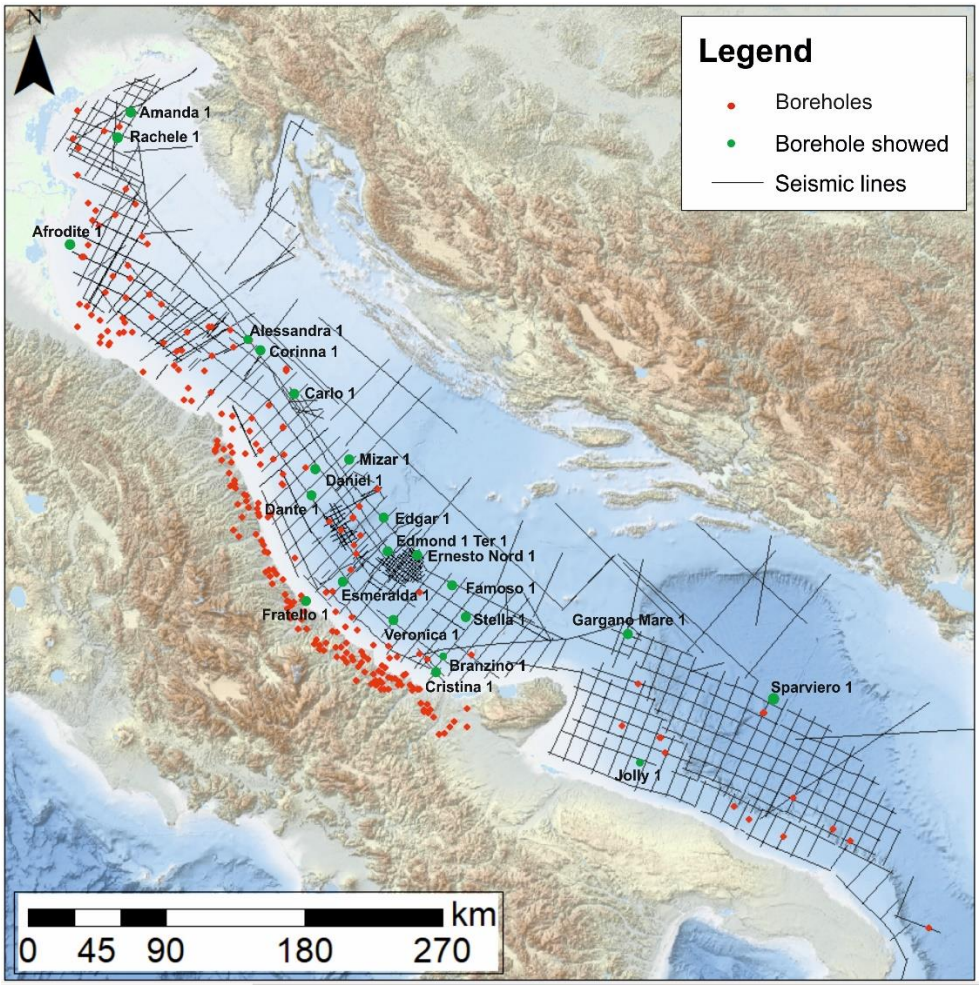


*Figure 3.7: Seismic lines and exploration boreholes (ViDEPI), in red location of all the boreholes investigate for the seismic calibration; in green boreholes showed in this work, schematized in figure 3.9.*

The main sedimentological formations present low variability from North to South, except for the thickness, which varies due to the neotectonic effect of the Apennine chain. The stratigraphic setting of the Adriatic area is summerized in figure 3.8. For the purpose of this thesis, only the recognized formations are shortly described below, and the reported features come from Finetti et al. (2005) and the CGT (*Carta Geologica D'Italia* 1:50000).

Plio-Pleistocene succession (Fig. 3.8, 3.9):

- **Asti Sand** (former *Carola* formations), Pleistocene**:** Clayely sand, sandy clays and silt. Gradually passing from one litotype to the other. These deposits show shallow marine, coastal, alluvional deposition during the filling of the accommodation spaces in the basins, organized in several transgressive-regressive cycles. Thicknesses vary greatly due to the neotectonic reaching over 4000 m thick succession (e.g. Afrodite -001). The formation is widely present in the Northern Adriatic Sea;
- **Argille Azzurre/Santerno Clay** (ENI subsurface lithostratigraphy, former *Porto Corsin*i, P*orto Garibaldi* formations), Pliocene: clay, clay marly and marly clay, without a clear internal stratification. Few levels with a higher composition in sand or conglomerates. In the Adriatic Sea the formation onlap the Messinian unconformity. Deposition occurred in marine environment is characterize by great variability in depth, however ascribed to the neritic environment. Thicknesses vary greatly, due to the neotectonics, reaching over 4000 m thick succession (e.g. Fratello-001). Widely distribute in the Adriatic Sea;
- **Eraclea Sand** (Lower Pliocene): sandy deposits with intercalation of clay. Bottom limit is covering (in onlap geometry) the Miocene succession, where conglomerates can be observed. Generally observed in the Northern Adriatic Sea.

Miocene succession (Fig. 3.8, 3.9):

- **Gessoso Solfifera Fm.** (Late Messinian): characterized by great lithological variability, composed by evaporites (gypsum), intercalated by marls. Thicknesses of the formation vary from zero to almost 200 m (e.g., Cristina-001). In several boreholes (e.g., Amanda-001, Alessandra-001, Jolly-001), this formation is absent, and an angular unconformity bounds the Pliocene formation from the pre-MSC formations. Depositional environment of the formation is still debated, but generally related to a sea level drop.

Listed below in Table 3.1, boreholes from the ViDEPI database used for the calibration of the Gessoso Solfifera Formation in the Adriatic Sea.

| Name | Total depth | BU (Y/N) | Depth (m) | Thickness (m) | MES | Depth (m) |
|---|---|---|---|---|---|---|
| AFROTIDE 1 | 3767 | Y | 3722 | 45 | Y | 3722 |
| AGUGLIA 1 | 2102 | N | - | - | N | - |
| ALBERTINA 1 | 1800 | N | | | Y | 1517 |
| AMANDA 1 BIS | 7305 | N | | | Y | 1210 |
| AMETISTA 1 | 2856 | N | | | Y | 2792 |
| AMIRA 1 | 2957 | N | | | Y | 1435 |
| ANCONA MARE 1 | 2304 | Y | 767 | 21 | Y | 767 |
| ARAGOSTA MARE 1 | 1113 | N | - | - | N | - |
| ARCOBALENO 1 | 1943 | N | | | Y | 1880 |
| ARLECCHINO 1 | 1658 | N | | | Y | 1626 |
| ASSUNTA 1 | 4747 | N | | | Y | 1554 |
| BALENA MARE 1 | 2013 | Y | 550 | 35 | ? | - |
| BARBAROSSA 1 | 2020 | Y | ? | ? | Y | 337 |
| BEATRICE 1 | 2200 | N | - | - | N | - |
| BOHEME 1 | 1666 | Y | 1634 | 32 | N | - |
| BONAVENTURA 1 | 3000 | Y | 1108 | 17 | Y | 992 |
| BORA 1 | 2500 | Y | 1423 | 149 | N | - |
| BR-48-IR I DIR | 1922 | N | - | - | N | - |
| BRANZINO 1 | 2022 | Y | 1290 | 52 | Y | 1284 |
| BREZZA 1 | 1000 | N | - | - | N | - |
| CARLO 1 | 2066 | N | - | - | Y | 1340 |
| CARLO 2 | 1300 | N | - | - | N | - |
| CARLOTTA 1 | 536 | N | - | - | N | - |
| CARMEN 1 | 1442 | Y | 798 | 43 | Y | 697 |
| CASSANDRA 1 | 1293 | N | - | - | N | - |
| CINZIA 1 | 3105 | N | | | Y | 3094 |
| CLAUDIA 1 | 1976 | N | | | Y | 1932 |
| COLOSSEO 1 | 1734 | Y | 1108 | 10 | Y | 1108 |
| CONRAD 1 | 3250 | Y | 1694 | 98 | Y | 1694 |
| CONRAD SUD OVEST 1 | 2683 | Y | 1390 | 95 | Y | 1390 |
| CONTESSA 1 | 2382 | Y | 1353 | 233 | N | - |
| CORINNA 1 | 3276 | N | - | - | N | - |
| CORNELIA 1 | 3998 | Y | 812 | 103 | Y | 812 |
| CRISTINA 1 | 1524 | Y | 1235 | 129 | Y | 1222 |
| DAFNE 1 | 1640 | N | - | - | N | - |
| DALILA 1 | 2105 | Y | 1052 | 222 | N | - |
| DANIEL 1 | 4950 | Y | 484 | 100 | Y | 464 |
| DANIELA 1 | 2635 | N | | | Y | 2614 |
| DANTE 1 | 1654 | Y | 1069 | 54 | N | - |

| | | | | | | |
|---|---|---|---|---|---|---|
| DORA 2 DIR A | 1422 | Y | 1439 | 30 | Y | 1411,5 |
| DORA 1 | 1865 | N | - | - | N | - |
| DORA 2 | 1595 | Y | 1122 | 28 | Y | 1102,5 |
| EDGAR 1 | 2276 | Y | 700 | 54 | Y | 700 |
| EDGAR 2 | 2100 | Y | 678 | 42 | Y | 663 |
| EDMOND 1A | 915 | Y | 808 | 107 | N | - |
| EDMOND 1TER | 4195 | Y | 850 | 107 | Y | 836 |
| ELGA 1 | 2700 | Y | 852 | 53 | N | - |
| ELISA 1 | 2193 | Y | 1010 | 82 | N | - |
| ELIZABETH 1 | 1583 | Y | 1356 | 74 | N | - |
| ELSA 1 | 4841 | | | | | |
| ENIGMA 1 | 2228 | Y | 1632 | 45 | Y | 1620 |
| ERNESTO NORD 1 | 6173 | Y | 684 | 39 | Y | 658 |
| ESMERALDA 1 | 3837 | Y | 2250 | 50 | N | - |
| ESTER 1 | 860 | N | - | - | N | - |
| ETERNO 1 | 2446 | | | | | |
| EURIDICE 1 | 1506 | N | - | - | Y | 1320 |
| FABIANA 1 | 1276 | N | - | - | N | - |
| FAMOSO 1 | 4479 | Y | 816 | 88 | N | - |
| FIONA 1 | 3517 | Y | 1650 | 162 | Y | 1650 |
| FIORELLA 1 | 1613 | N | - | - | N | - |
| FLAVIA 1 | 2212 | N | - | - | N | - |
| FRATELLO 1 | 4351 | Y | 4320 | 31 | N | - |
| FULVIA 1 | 1270 | N | - | - | N | - |
| GABRIELLA MARE 1 | 2417 | Y | 1103 | 22 | N | - |
| GARGANO MARE 1 | 2205 | N | - | - | N | - |
| GENDA 1 | 2050 | N | | | Y | 1956 |
| GILDA 1 | 3013 | Y | 1427 | 99 | N | - |
| GINA 1 | 1256 | N | - | - | N | - |
| GLORIA 1 | 2380 | Y | 414 | 108 | Y | 394 |
| GRETA 1 | 3180 | N | - | - | N | - |
| IRMA 1 | 2508 | Y | 2508 | 3 m | Y | 2505 |
| ISABELLA 1 | 1642 | N | | | Y | 1601 |
| JUDITH 1 | 1870 | N | - | - | N | - |
| MALACHITE 1 | 2488 | N | - | - | N | - |
| MANILA 1 | 3110 | Y | 1453 | 207 | N | - |
| MARIANGELA 1 | 2030 | N | | | Y | - |
| MARIELLA 1 | 2135 | N | - | - | N | - |
| MARILENA 1 | 2702 | N | - | - | N | - |
| MARTINSICURO MARE 1 | 3978 | N | - | - | N | - |
| MILLI 1 | 1909 | N | - | - | N | - |
| MIZAR 1 | 4000 | Y | 1166 | 109 | Y | 1166 |
| MIZAR 2 | 1962 | N | - | - | N | - |
| MONICA 1 | 1470 | Y | 1293 | 66 | Y | 1275 |
| OMBRINA MARE 1 | 2360 | N | - | - | Y | 2074 |
| PATRIZIA 1 | 1648 | Y | 829 | 69 | Y | 814 |

| | | | | | | |
|---|---|---|---|---|---|---|
| PESARO MARE 1 | 1919 | Y | 890 | 20 | N | - |
| PESARO MARE 3 | 1501 | N | - | - | N | - |
| PESARO MARE 4 | 4271 | N | - | - | N | - |
| PUNTA DELLA PENNA MARE 1 | 1450 | N | - | - | N | - |
| RACHELE 1 | 1640 | N | | | Y | 1523 |
| RAFFAELLA 1 | 1955 | N | | | Y | 1923 |
| REGOLO 1 | 2601 | N | - | - | N | - |
| RICCIONE MARE 3 | 3321 | N | | | Y | 3232 |
| RIGEL 1BIS | 2335 | Y | 977 | 29 | N | - |
| RITA 1 | 3590 | N | | | Y | 3542 |
| ROMBO MARE 1 | 4125 | Y | 2103 | 21 | N | - |
| ROSELLA 1 | 2455 | Y | 387 | 90,5 | Y | 384 |
| S.SALVO MARE 1 | 1372 | N | - | - | N | - |
| S.STEFANO MARE 2 | 1765 | N | - | - | N | - |
| SABRINA 1 | 1444 | Y | 1277 | 65 | Y | 1277 |
| SCORPENA MARE 1 | 1563 | N | - | - | N | - |
| SILVANA 1 | 5221 | Y | 3530 | 22 | Y | 3520 |
| SILVIA 1 | 5122 | Y | 2363,5 | 76 | Y | 2363,5 |
| SIMONA 1 | 1500 | Y | 1276 | 60 | Y | 1256 |
| SONIA 1 | 2121 | Y | 1536 | 35 | N | - |
| SPINELLO MARE 1 | 5889 | Y | 2520 | 50 | N | - |
| SQUALO 1 | 305 | N | - | - | N | - |
| SQUALO 1BIS | 2569 | N | - | - | N | - |
| STEFANIA 1 | 1944 | Y | 1330 | 105 | N | - |
| STELLA 1 | 3000 | Y | 1310 | 140 | N | - |
| TAMARA 1 | 3216 | N | - | - | Y | 3040 |
| TRACHINO MARE 1 | 4221 | Y | 1153 | 90 | N | - |
| TRIGLIA MARE 1 | 1845 | N | | | Y | 1435 |
| VALERIA 1 | 2200 | Y | 611 | 81 | Y | 603 |
| VANESSA 1 | 3330 | N | - | - | N | - |
| VASTO MARE 1 | 1655 | N | - | - | N | - |
| VASTO MARE 2 | 1367 | Y | 1253 | 34 | Y | 1253 |
| VERONICA 1 | 3265 | N | - | - | N | - |
| VIRGINIA 1 | 1856 | N | - | - | N | - |

*Table 3.1: Collection of all the boreholes where MSC surfaces and unit are recognized. Boreholes data are from ViDEPI database.*

- **Schlier Fm.** (Langhian – Early Messinian**)** constituted by an alternation of marls, silty marls, marly-limestone. Layers show a great variability in thickness from decimeter to meters thinks, with a total thickness of more than 400 m of the succession. The base of the Schiler Fm is seismically hardly identifiable, and coincides with a lithological change since the succession lies on limestone and marly limestone of the Bisciaro Fm. Its top corresponds either to the Messinian related erosion or to the conctact with the Gessoso-solfifera Fm. The formation sedimented on a continental slope through low-density turbiditic flows coming from the Austro-Alpine domains. This formation is widely present in the entire Adriatic Sea.

- **Bolognano Fm.** (Tortonian): sandy limestone with a relevant bioclastic component, which led to recognize this formation from the Bisciaro one. Thicknesses vary, reaching a maximum of about 30 meters. A lenticular geometry characterized this formation. Deposition occurred on a carbonate ramp in a low energy environment. It has been widely recognized in the Southern Adriatic Sea above the ApCP, often directly overlaying Cretaceous deposits.

- **Bisciaro Fm** (Burdigalian): clay marls and marly limestone with some thin glauconitic layers; the higher amount of clay minerals led to recognize the Bisciaro formation form the Schlier and Scaglia succession. Thicknesses vary from 15 to more than 200 m according to the paleo-morphology of the basin. This formation is widely present in the entire Adriatic Sea.

Eocene-Miocene succession (Fig. 3.8, 3.9):

- **Gallare Marls** (Early Eocene - Late Miocene: marls or clay with thinner arenaceous beds, related to turbidite processes and sedimented in a transitional environment between neritic and batial. This formation is localized in the Northern Adriatic Sea only.

- **Flysch** (Middle Eocene): distal turbidite sediments infilling the External Dinaric foredeep and mafe up of a dense alternation of marl and arenite. Marl intervals show a thickness varying from millimeter- to decimeter-, while arenaceous intervals show a thickness varying from centimeters- to meters; some carbonate clasts are present. The

Lower limit of the Flysch corresponds to a transitional environment of the Dinaric foredeep. The Upper limit is the Messinian angular unconformity that put in contact the Flysch unit to the Pliocene units. The Flysch is present in the Northern Adriatic Sea, in front of the Dinaric thrust of the AdCP.

Eocene – Jurassic succession (Fig. 3.8, 3.9):

- **Scaglia Succession** (Middle Cretaceous - Oligocene): represented by the following formations: *Scaglia Alpina, Scaglia Variegata, Scaglia Cinerea, Scaglia Rossa*; these are composed of Calcareous mudstone, marly limestone, marls with clay. The succession deposited in a pelagic environment, reaching a thickness of more than 1000 meters in the Central and Southern Adriatic Sea.

- **Marne a Fucoidi Fm.** (Albiano – Aptiano, Middle Cretaceous): alternation between malrs or clay-marls characterized by a variable color. The whole formation is 45-90 m thick; the base corresponds to the contact with the Maiolica Formation, while the top in is the passage to the Scaglia Succession. This formation is widely recognized in the Mesozoic pelagic domains of the Adriatic Sea; it represents a stratigraphic marker, due to its high amplitude reflection.

- **Calcare di Cupello** (Cretaceous): whitish to greyish stratified limestone (mudstone/wackstone), deposited in a carbonate tidal flat eteropic with a carbonate ramp. In the deeper portion of the basin, it is heteropy with the Pelagic carbonate succession.

- **Carbonate Pelagic Succession** (Late Jurassic - Late Creataceous): Corresponding to the: *Maiolica, Rosso Ammonitico, Corniola, Massiccio* Formations. It is a fine fine grained limestone showing a variable colors and the presence of flint nodules. This succession is the result of the deposition of mud and microcrystalline carbonate in a pelagic basin.

Triassic succession (Fig. 3.8, 3.9):

- **Dolomia Principale:** Organized in peritidal cycle made up to dolostones with traces of pedogenetic structures. Depositional environment was a tidal flat and lagoon.

- **Burano evaporites**: composed of an alternation of anhydrites and dolostone, the anhydrites are often recognized as well crystalized salt with thin layer of clay and

organic matter. Thickness vary greatly due to tectonic process; it spans from few hundreds of meters to kilometer thick succession. Deposition occurred in a sabkha environment with hypersaline water.

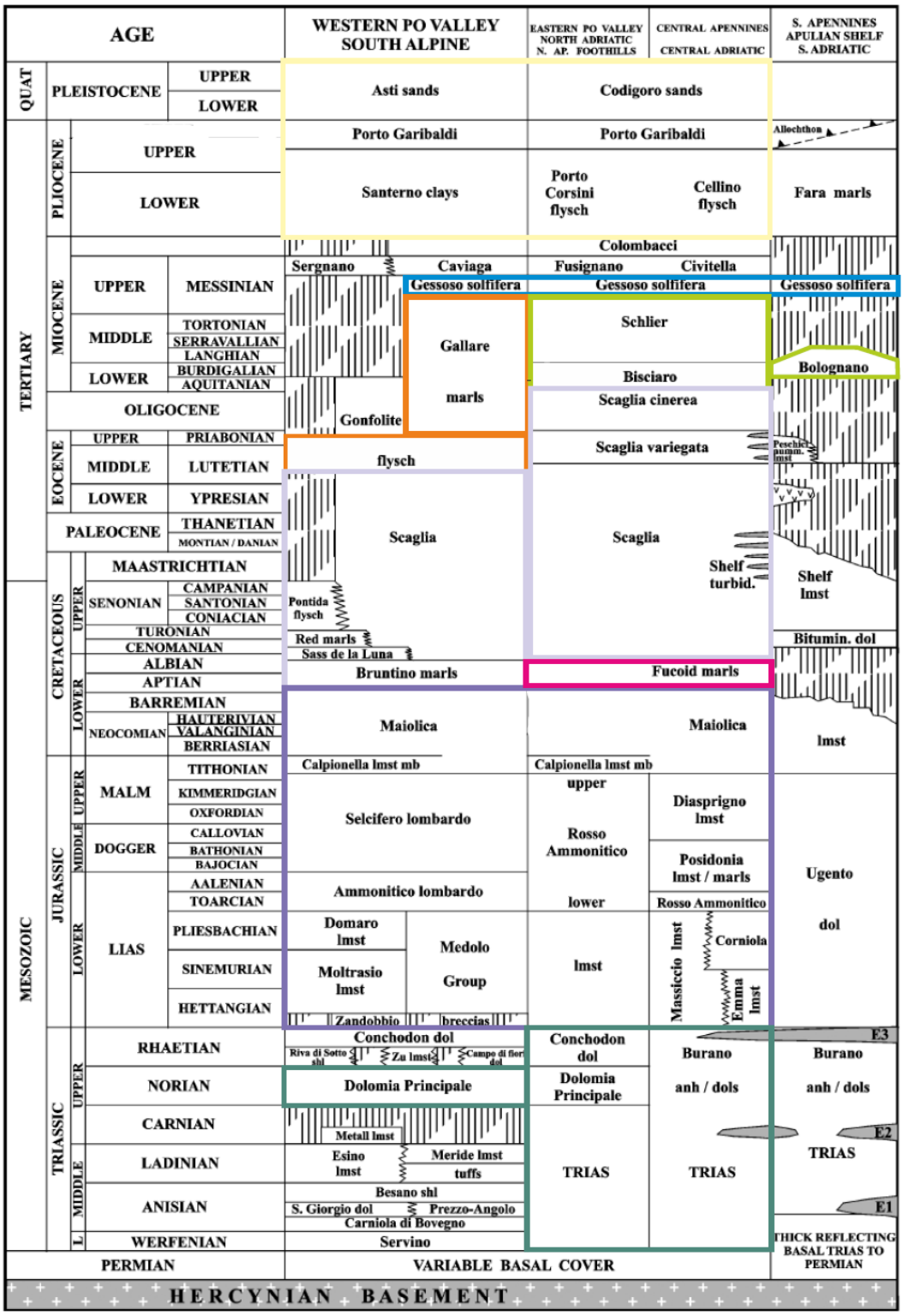


*Figure 3.8: Indicative stratigraphic chart of the Adriatic – Po Valley and Apulia foreland and adjacent Apenninic front areas (modify from Finetti et al., 2005b).*

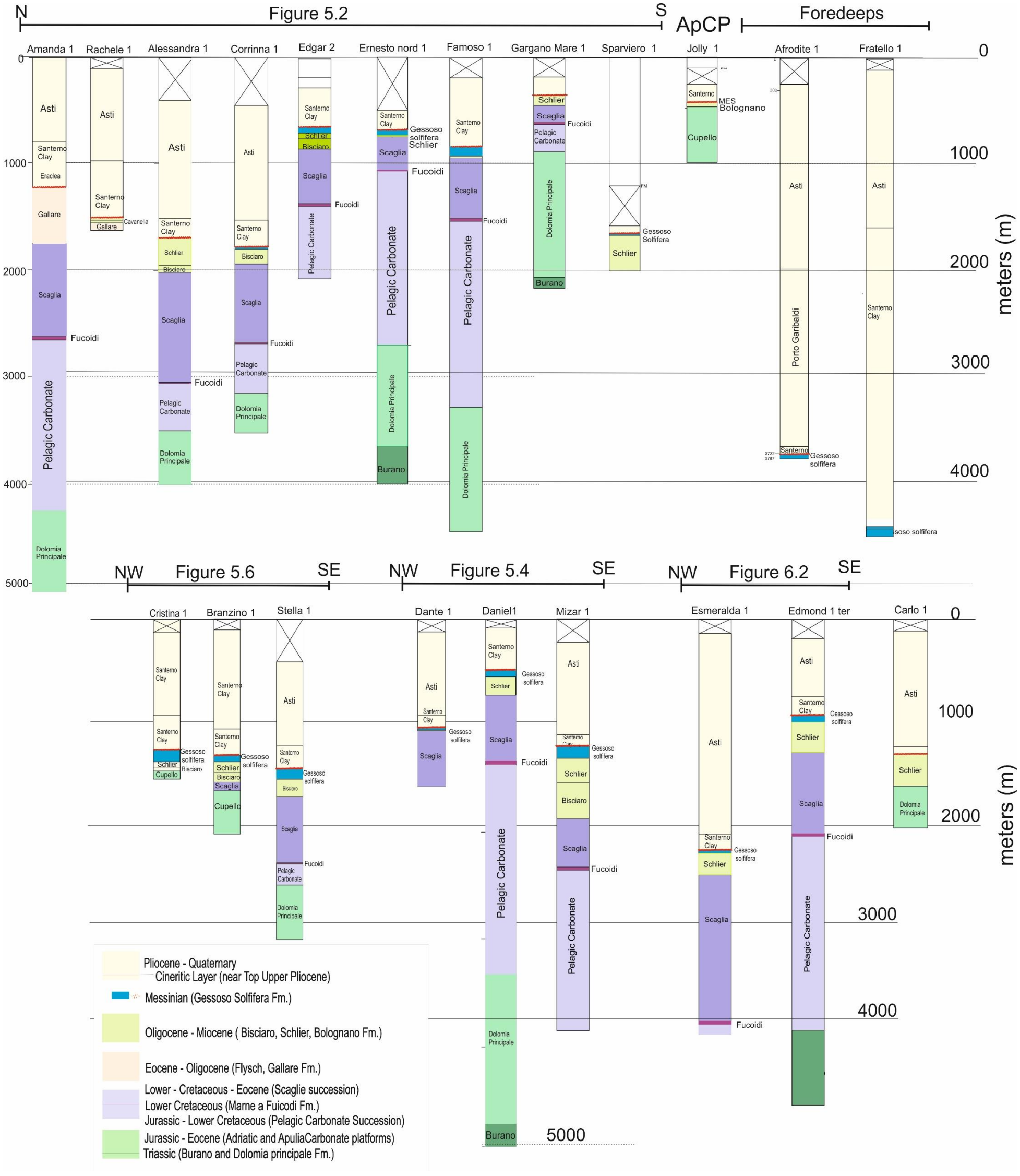


*Figure 3.9: Schematic representation in scale of significant exploration well in the Adriatic Sea, location in figure 3.7.*

## 3.4 Methodology for producing the Maps

Construction of structural and thickness map of the MSC surfaces and unit goes through some phases that were applied for each reflector:

- Firstly, we defined and interpreted the different seismic markers following the stratigraphic concepts published in Mitchum and Vail (1977), i.e. defining different seismic facies on the base of the sedimentology calibrated by the boreholes (Seismo-stratigraphy is described in Chapter 4).
- Later, the interpretation of horizons was carried out using the Kingdom Suite software, exported as a xyz (time) file, projected in UTM32 WGS 84. The results were then re-projected and interpolated on GMT (Generic Mapping Tool) to create the depth and thickness maps in TWT.

GMT Software (Wessel and Smith, 1995; 1998; Wessel et al., 2019) provides a useful tool to map and interpolate seismic horizons. The software allows a good control of the interpolation step. In this case study we used the *near neighbor* method with an interpolation of 1 km for each interpreted point.

# Chapter 4 - Seismo-Stratigraphy

## 4.1 Seismic stratigraphic approach

The interpretation of the seismic lines in the Adriatic Sea was carried out using the IHS Kingdom Suite software. The interpretation was performed by manually picking the investigated horizons on the base of seismic stratigraphy principles. Furthermore, conventional interpretation involves mapping of the structures characterizing the horizons of interest. Seismic stratigraphy involves the subdivision of the sedimentary sequence into units of peculiar seismic expression (Keary et al., 2002). Horizon picking involves identification of specific reflection events, calibrated through boreholes, and corresponding to top and base of sedimentary sequences whose facies can be recognized based on their termination and geometries (Mitchum and Vail, 1977) (Fig. 4.1). The reflection terminations can be erosional truncations, onlaps, downlaps, configurations that allow the identification and definition of the seismic units and boundaries. Moreover, it is necessary to describe and identify internal configuration of the sedimentary facies (seismic facies), a concept introduced by Sheriff (1976) (Fig. 4.2).

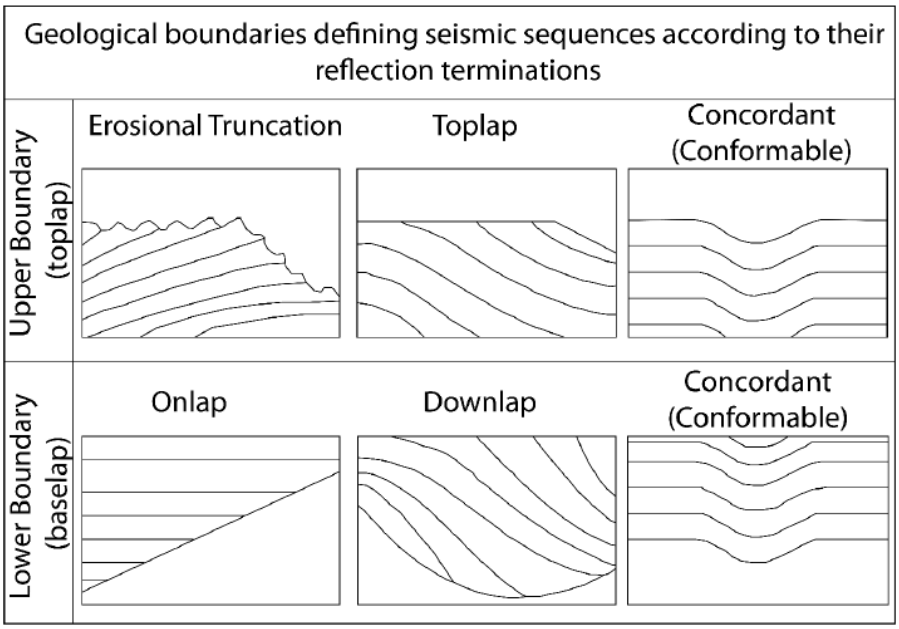


*Figure 4.1: Classification of the geometries and boundaries in seismic sequences (Mitchum and Vail, 1977)*

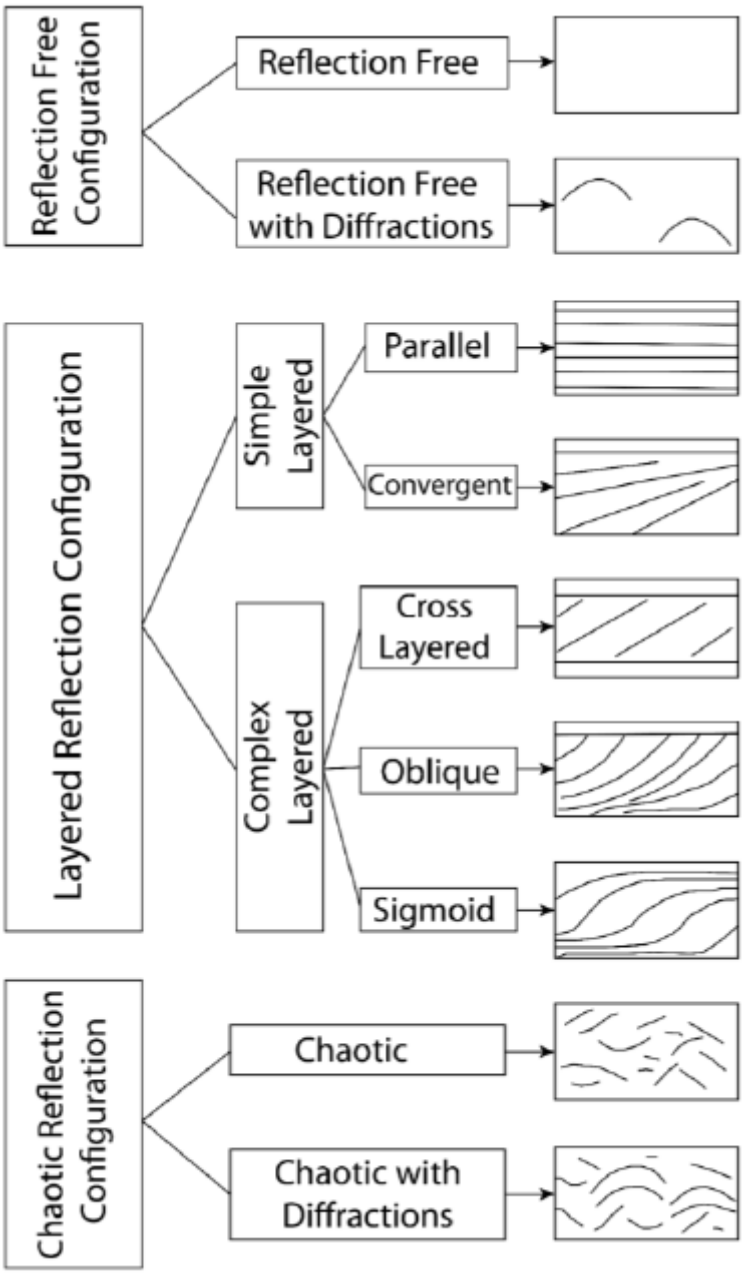


*Figure 4.2: Classification of the internal bedforms and seismic reflection (Sheriff, 1976)*

The built dataset was not available for reprocessing; consequently, I identify the geological formations through the borehole calibration method and correlation of seismo-stratigraphic facies.

Although the acoustic impedance of the MSC units was higher than the surrounding formations, part of the formations could be below resolution. For example, due to the similar acoustic impedance, surface separating the Schlier and Bisciaro formations (Early Miocene) is affected by low amplitude, and the two units were incorporated in the same seismic facies. The same approach was applied to the Scaglia Succession and to the Carbonate Pelagic succession.

## 4.2 Seismo-stratigraphy horizons and facies

### 4.2.1 Plio-Quaternary Succession

The Plio-Quaternary (PQ) units show a significant thickness variability, due to the post-Messinian tectonic evolution of the Adriatic region (Fig. 3.7). The outermost Apennine foredeep collected more than 4000 m of Plio-Pleistocene sediments, mainly composed of terrigenous sediments (e.g., Afrodite 1, Fratello 1, see Fig. 3.9). Calibration of the Pliocene and Pleistocene (Fig. 4.3) was made up using line B419 and Veronica 1 exploration borehole. The PQ unit shows very high variability; two sub-units were identified (Fig. 4.4):

- The lower unit, identified as the Pliocene unit (e.g., Argille Azzurre/Santerno Clays) directly onlaps and covers the Miocene unit (Del Ben and Oggioni, 2016) (Fig 4.4). Seismic characteristics show a transparent facies with few weak discontinuous internal reflectors (Fig. 4.4 A, B, D). The Pliocene unit reaches its maximum thickness in the Apennine foredeep (3.8 s TWT, Fig.4.4 A) while it thins eastwards, following the west-ward flexure of the Adriatic foreland. In the Central Adriatic Sea, a high-amplitude negative polarity reflector, called Cineritic Layer (CL), identified as a volcanic event (tephra lithology), is used as a seismic marker located in the upper part of the Upper Pliocene unit (Fig. 4.3, 4.4 A, B, D,). The boundary between the Piocene and Pleistocene units shows a gradual change in the seismic facies (Fig. 4.3, 4.4A, B), from low to higher amplitude reflectors, and displays parallel to convergent geometries often disrupted and discontinuous.

- The upper unit, identified as the Pleistocene unit, is generally characterized by sigmoidal geometries on the western part of the Adriatic Sea (Fig. 4.4 C). Clinoform geometries were produced as the response to the Pleistocene uplift and dismantlement of the Central Apennines and Apulia Carbonate Platform (Del Ben and Oggioni, 2016). This thick progradational sequence is covered by the Po fluvial system deposited during the Last Glacial Maximum (LGM) on the northern Adriatic Sea until the northern margin of the Mid-Adriatic Depression (Trincardi and Correggiari, 2000). The upper Holocene sediments are not calibrated by wells and are very thin; the thickness is generally below the seismic

resolution. At the top, the seafloor shows a very high amplitude reflector characterized by positive polarity (Fig. 4.3)

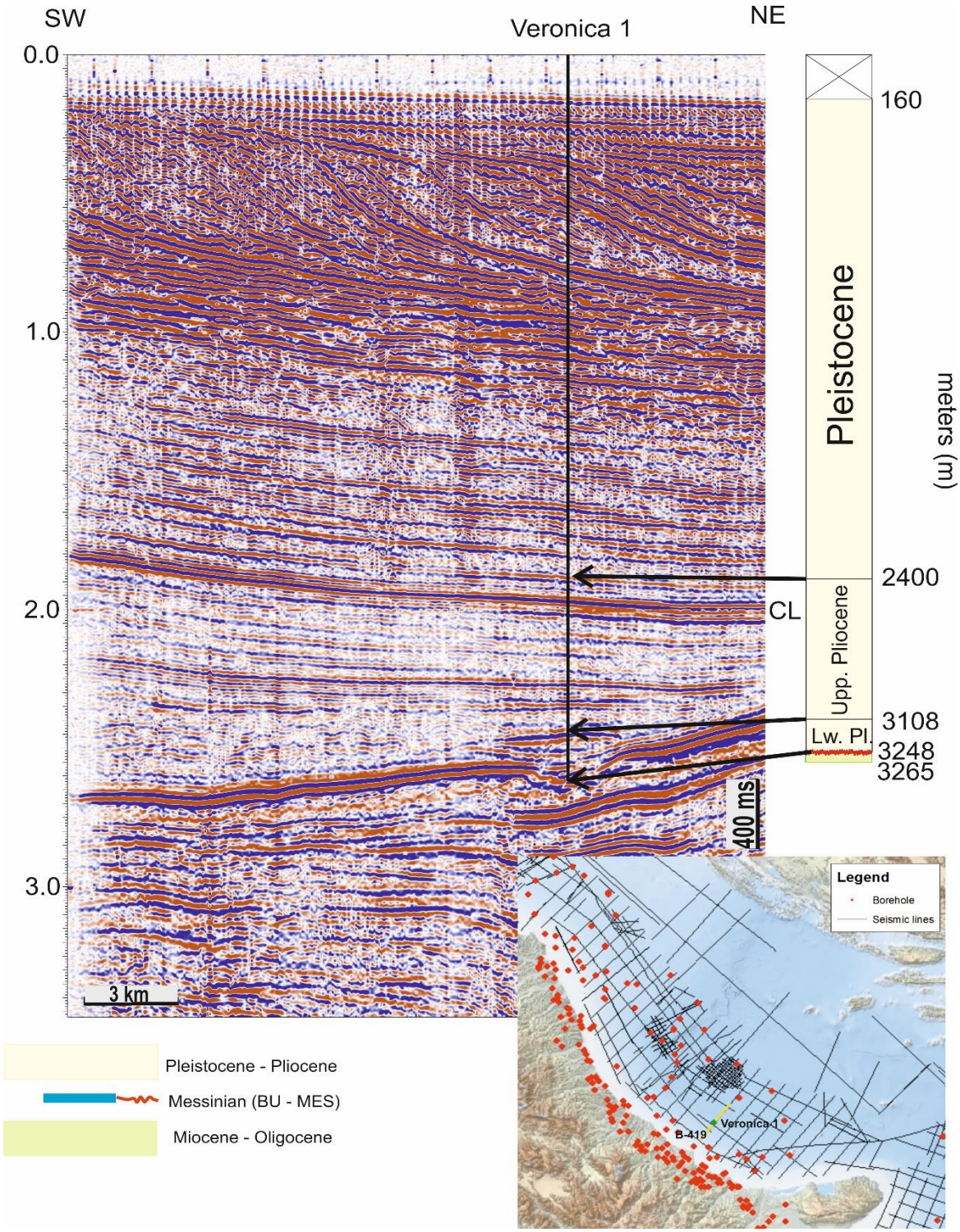


*Figure 4.3: Calibration of the Pliocene and Pleistocene considering an average velocity of about 1800 m/s in the PQ succession, lithological information from the ViDEPI database. The profile and Veronica 1 boreholes arelocated in the position map.*

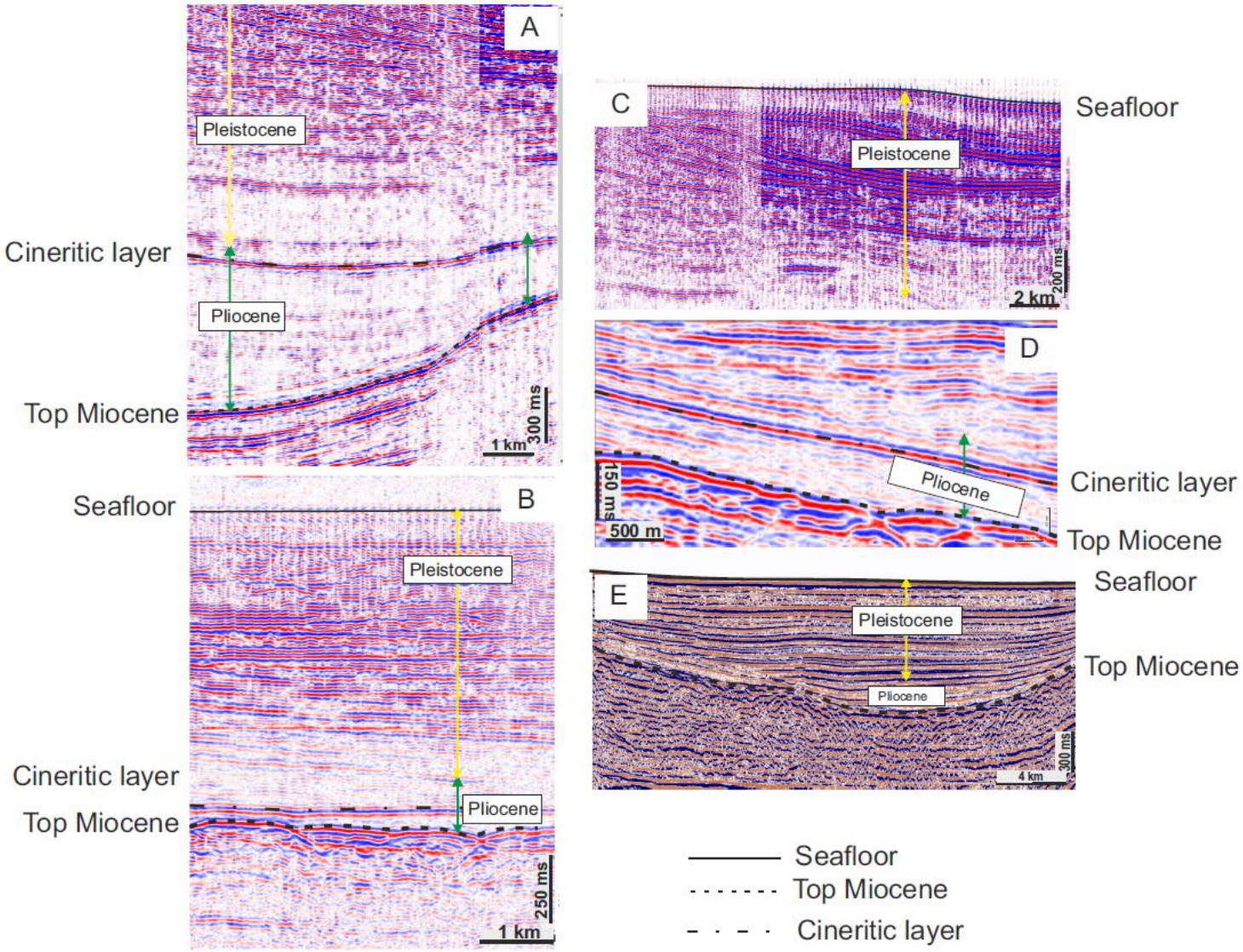


*Figure 4.4: Different seismic expression of the Plio-Pleistocene succession in the Adriatic Sea: A) a gradually westward thickness of Pliocene sediments in the Central Adriatic Sea; B) a thin Pliocene unit; C) the Pleistocene clinoform geometries of the Mid Adriatic Depression; D) an approximately constant thickness of Pliocene in the mid axis of the Adriatic Sea area; E) the Plio-Pleistocene succession in the Southern Adriatic basin.*

### 4.2.2 Miocene Succession

*The Messinian Salinity Crisis unit and surfaces*

The MSC surfaces are generally represented by a single clear reflector (MES) or by a seismic package: both allow to identify the base of the PQ sequence with good confidence (Fig. 4.4).
The previously described surfaces and units (see Chapter 1 and Chapter 3) include the surfaces MES, TES, TS, BS, and the unit BU (Lofi et al., 2011; Lofi 2018).

- MES unconformity (Fig. 4.5) is a high amplitude erosional truncation, representing a sedimentary hiatus between the PQ sequence and the pre-MSC units. The MES surface generates canyon and valley geometries (Fig. 4.5 C, F). The hiatus is mainly due to the Messinian erosion but, especially in the Croatian offshore, not to deposition, testified by the onlapping termination of the Plio-Quaternary units on the westward tilted Adriatic foreland.

- TES (Fig 4.6) is a high amplitude erosional truncation surface at the top of the Messinian evaporites (BU). Different rates of erosion caused difference in the BU thicknesses.

- TS (Fig. 4.7) is a high amplitude continuous reflector at the top of the evaporite without erosion, and the evaporites appear to be conformable with the underlying and overlying units.

- BS (Fig. 4.6; 4.7) is a high amplitude continuous reflector at the bottom of the Messinian evaporites (BU), which are conformable to the late Miocene unit.

The BU (Fig. 4.6; 4.7) represents the MSC units between TES or TS and BS. Internal reflections can be composed of one or more parallel high-amplitude reflectors. The maximum thickness of BU reaches 233 m (Table 1.1).

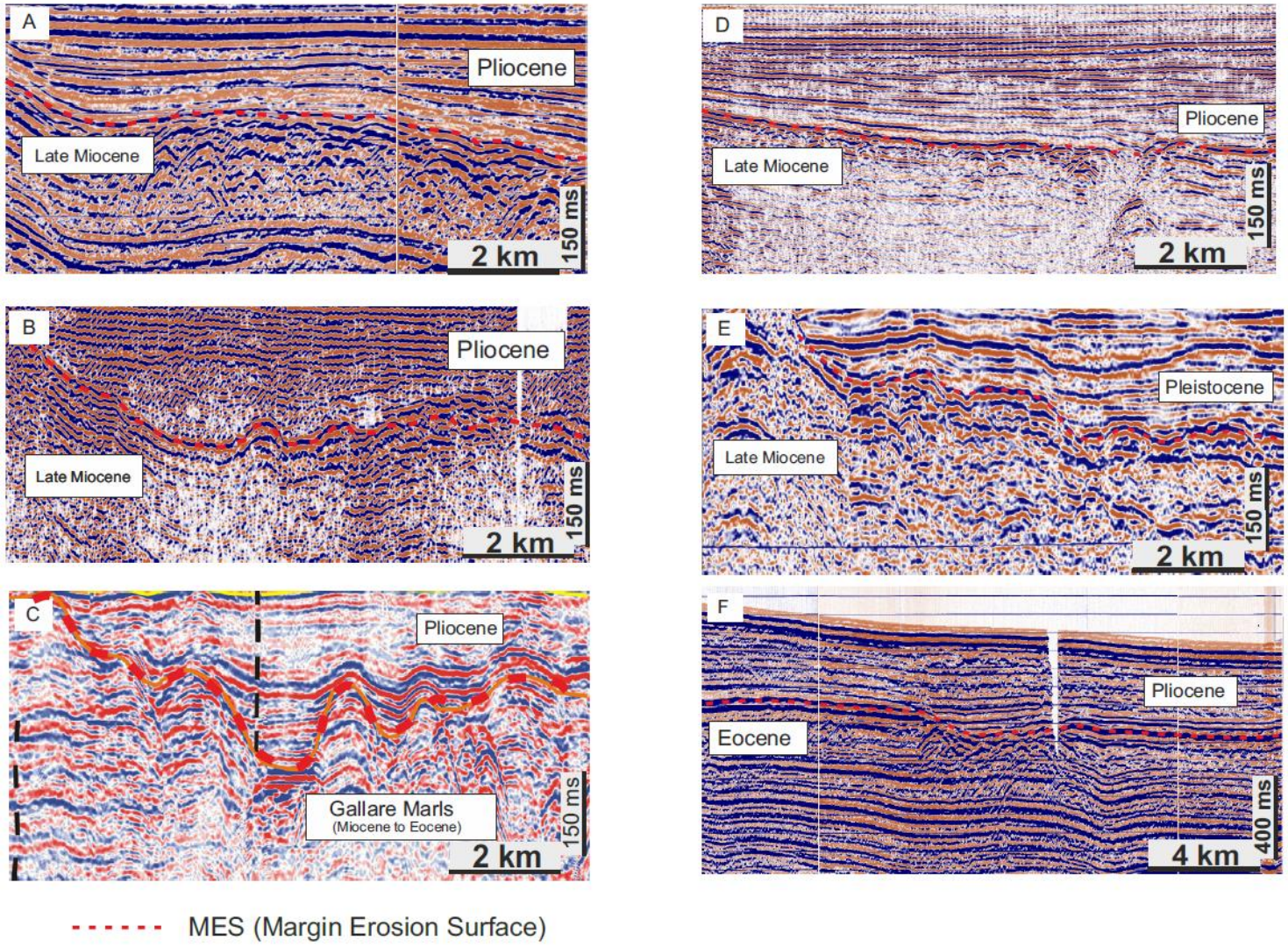


*Figure 4.5: Examples showing the MES surface in different portions of the Adriatic Sea: A) Line F004 from the southern Adriatic Sea; B) Line B412 from the Central Adriatic Sea; C) Line Stenap 09 from the Northern Adriatic Sea; D) line B420 from the Central Adriatic Sea; E) Line D448 from the Central Adriatic Sea; F) Line F004 from the Southern Adriatic Sea.*

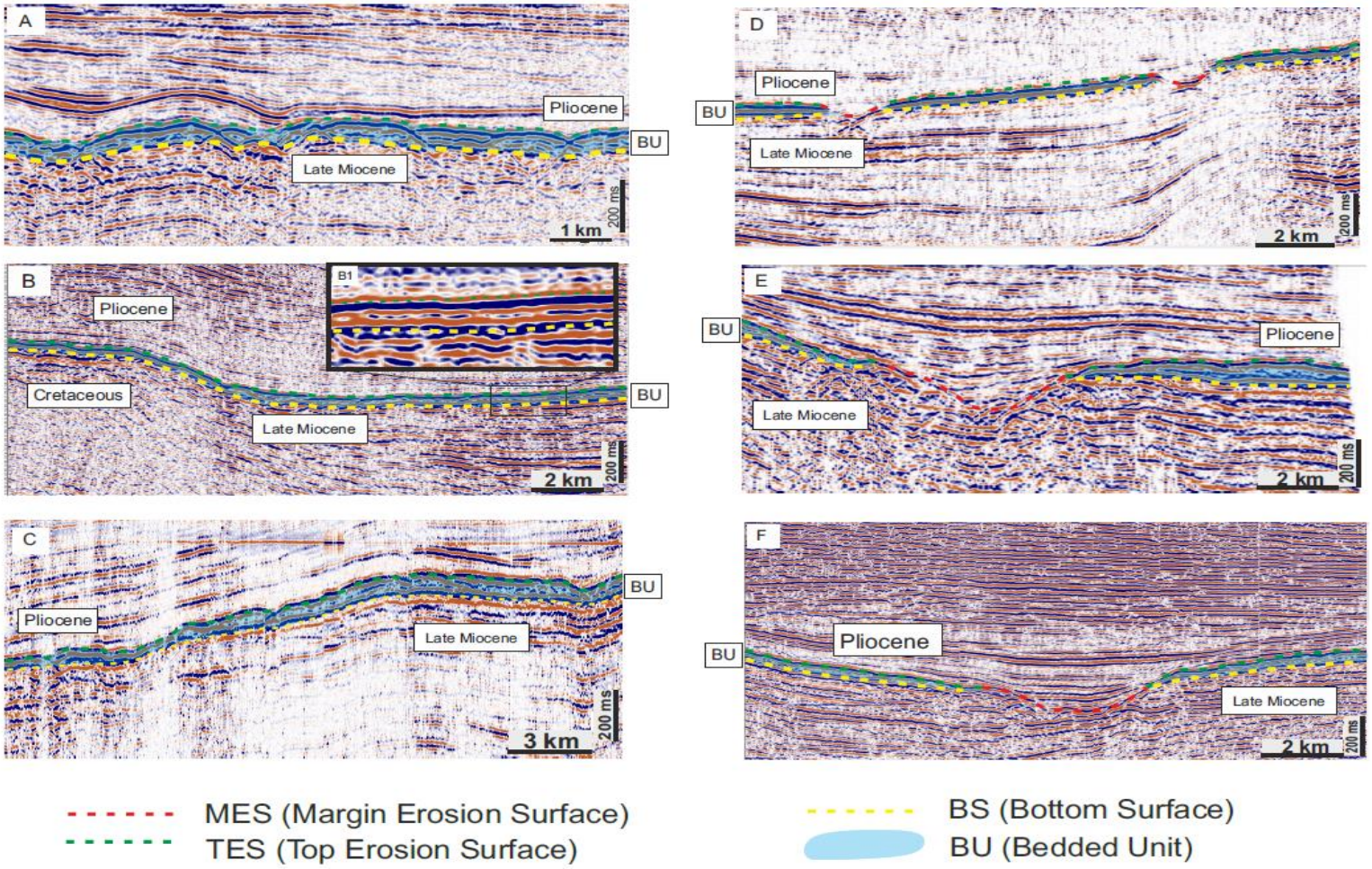


*Figure 4.6: Examples showing the TES surface in different portions of the Adriatic Sea: A) TES surface above an 80 ms TWT thick BU; B) TES above the ApCP and near basin, BU thick toward the basin as shown in the zoomed details B1 where the second internal BU reflection is visible; C) TES surface above an 80 ms TWT thick BU; D) BU reaches a total thickness of about 50 ms TWT and it is cut by two different channelized systems (MES); E) the BU (120 ms TWT thick) is partially eroded at the top (TES) and is cut by a channelized system (MES); F) the BU (80 ms TWT thick) is partially eroded at the top (TES) and cut by a channelized systems (MES).*

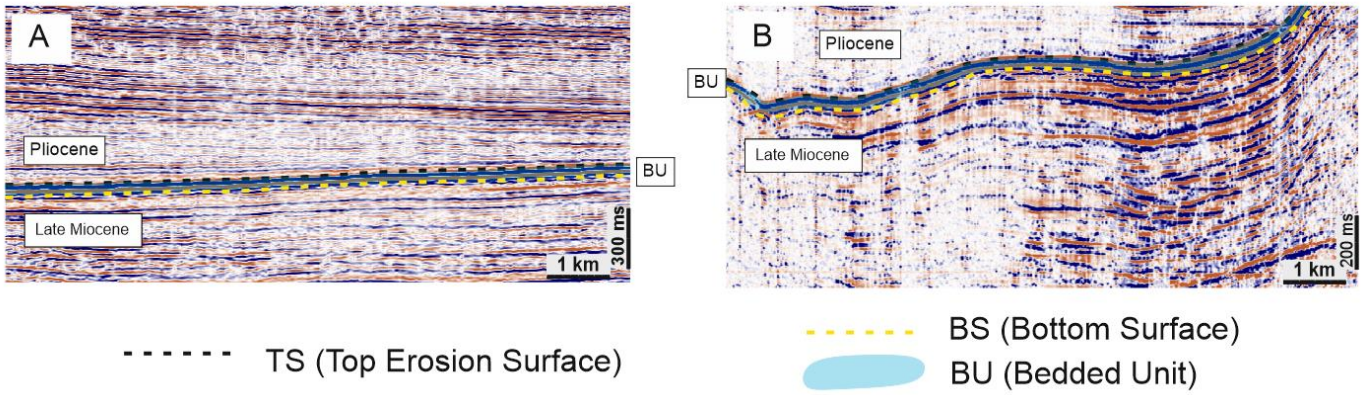


*Figure 4.7: Examples of the BU (thin) sequence topped by the TS surface in different portions of the Adriatic Sea: A) Un-deformed TS with a thin BU (20 ms TWT); B) TS deformed by the Apennine tectonics.*

*Schlier and Bisciaro Formation*

In the Central and Southern Adriatic Sea, the Messinian unit overlies the Schlier formation (Upper Miocene) and the Bisciaro Formation (Lower Miocene). When the Messinian unit is absent, the Schlier formation is often truncated by the MES (Fig.4.4B). The seismic responses of the Schlier and Bisciaro Formations are similar and are characterized by thin discontinuous medium to high amplitude reflections underlying the MSC reflector(s) (Fig. 4.8). A difference in their total thickness is noticeable, passing from 150 ms TWT to more than 600 ms TWT form the Central to the Southern Adriatic Sea (Fig. 4.8**)**. Transition to the underlying succession is evident, due to amplitude decrease inside the Scaglia Succession (Fig. 4.8A, B).

### 4.2.3 Oligocene-Lower Jurassic Succession

*Flysch*

The pre-MSC Flysch (Fig. 4.8 C, D) represents the distal turbidite sediment infilling the external Dinaric foredeep (Morelli and Mosetti, 1968; Cati et al., 1987b), produced by the dismantlement of the AdCP (Busetti et al., 2010a,b) only recognized in the Northern Adriatic Sea. The seismic response of the unit shows a medium to low continuous amplitude reflector, while few areas present

a transparent aspect (Fig. 4.8 C, D). The MES surface truncates the flysch unit, generating an angular unconformity.

*Scaglia Succession*

This unit is composed of deep-water carbonate sediments with a terrigenous input. The unit shows lower amplitude then the Bisciaro Formation. The thickness varies between different basins (e.g., about 1000 m in the Alessandra 1, about 350 m in the Ernesto 1 Nord, Fig. 3.9), and calibration through boreholes was fundamental to interpret it (Fig. 4.8 A, B, C, D).

*Marne a Fucoidi*

This formation separates the Cretaceous to Eocene Scaglia Succession from the Cretaceous – Jurassic Carbonate Pleagic Succession. This formation shows a different acoustic impedance from the overlying and underlying successions due to its different lithology (see Chapter 3.3). Being very thin (about 30-50 m), it appears as a continuous horizon represented by a medium to high amplitude reflection (Fig. 4.8 A, B).

*Carbonate Pelagic Succession*

This unit is composed of deep-water carbonate succession, overlayed by the Marne a Fucoidi marker. The internal reflectors are discontinuous and show a low amplitude and semi-transparent seismic facies (Fig.4.8 A, B). The bottom corresponds to the top of the Triassic Dolomia Principale formation, and is not always clear.

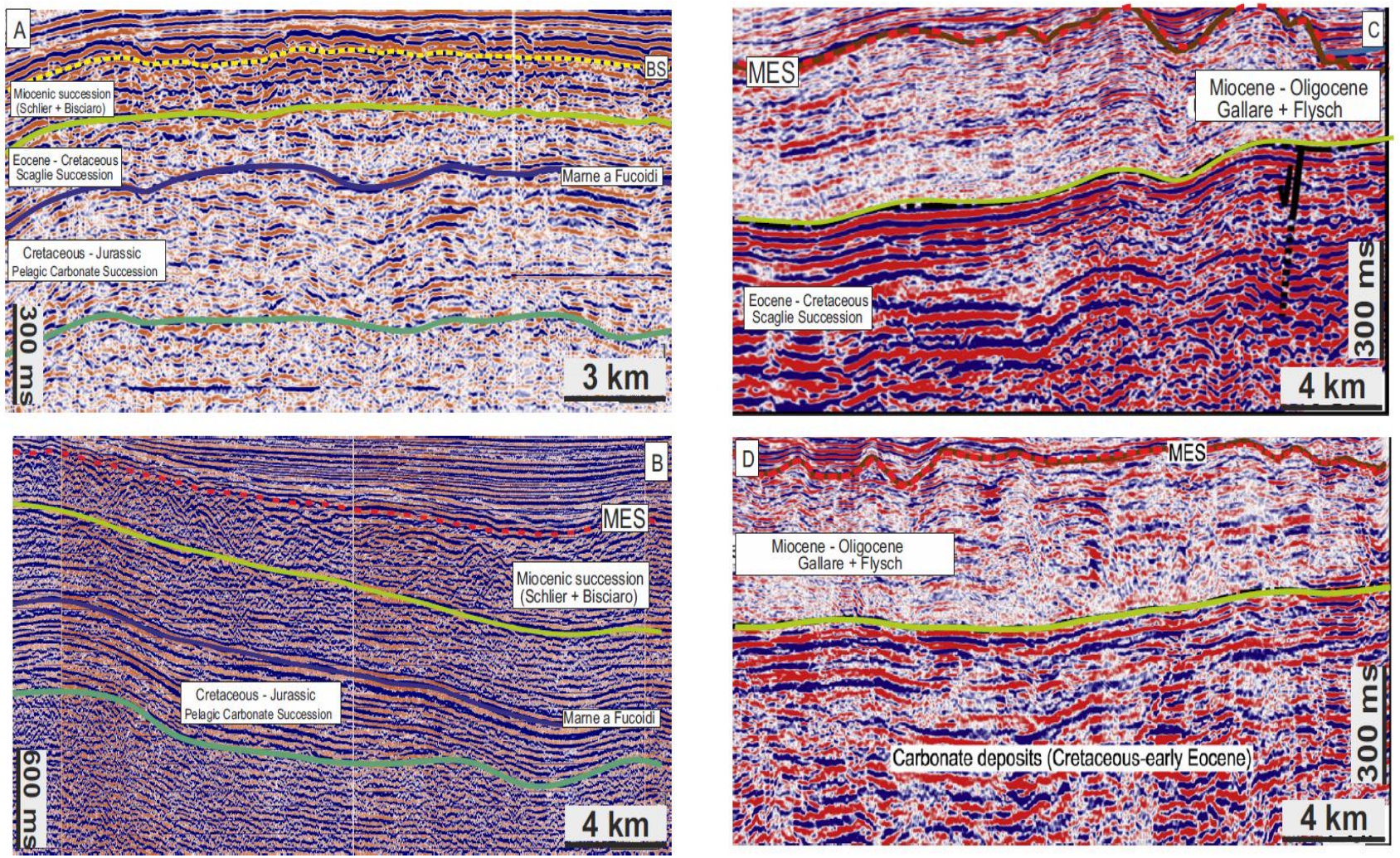


*Figure 4.8: Example of the pre-MSC sequences: A) Located in the Central Adriatic Sea, shows the Bisciaro and Schlier formation underneath the BS; B) Located in the Southern Adriatic Sea; C) and D) Located in the Northern Adriatic Sea, the MES truncates the Flysch succession.*

*Carbonate platforms (AdCP and ApCP)*

In this work: 1) the Adriatic Carbonate platform (AdCP) is the regional shallow-water succession, bordering the eastern coast of the Northern Adriatic Sea (Velic et al., 1995; Busetti et al., 2010a, 2010b; Vlahovic et al., 2005) it is differently called Friuli, Istrian, and Dalamtian carbonate platform. 2) The Apulia Carbonate Platform (ApCP), the Ombrina-Rospo plateau, and the Pre-Apulia carbonate platform outcropping in the Ionian Islands of Greece (Nicolai and Gambini, 2007; Del Ben et al., 2010, 2015; Santantonio et al., 2013) can be observed in the Southern Adriatic Sea. The seismic response of the carbonate platforms results in low amplitude and semi-opaque or transparent discontinuous reflectors (Fig. 4.9A). A clear high-amplitude continuous reflector, often truncated by the MSC sequences, is present at the top (Fig. 4.9A).

### 4.2.4 Triassic Unit

*Dolomia Principale and Burano Evaporite*

The Dolomia Principale and Burano evaporites represent the Triassic Units. It is a very thick unit located in the lower portion of the seismic section with a transparent facies. The Burano formation, composed of Triassic evaporites (mainly salt), presents several diapiric structures produced by halokinetic movements (Fig. 4.9B). Calibration of diapiric structures in several boreholes (Mizar-2, Ernesto-Nord-1, Edgar-1, Fig. 3.9.) indicates their Triassic age.

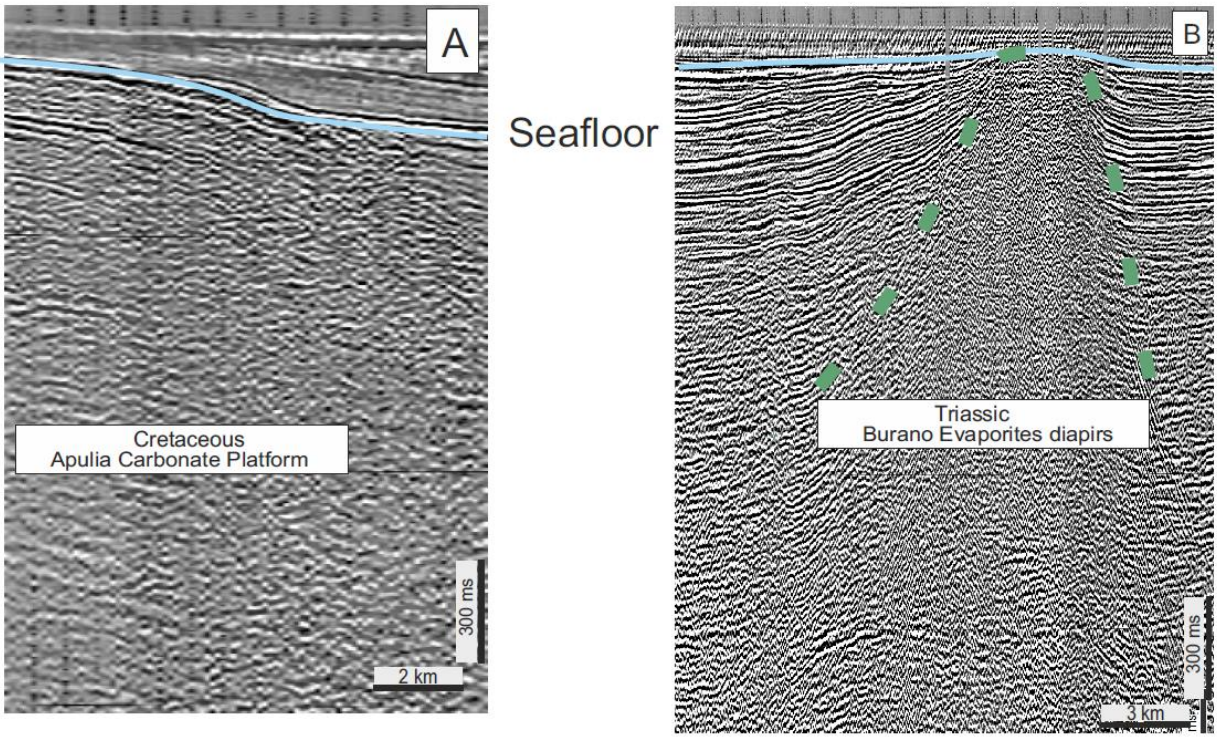


*Figure 4.9: A) Southern Adriatic Sea: the profile shows the semitransparent seismic facies of the Carbonate Platforms; B) Southern Adriatic Sea: the profile shows a diapir cutting the overlying sedimentary sequence and deforming the seafloor.*

A summary of the above-mentioned seismic facies and horizon in the Adriatic Sea is shown in figure 4.10.

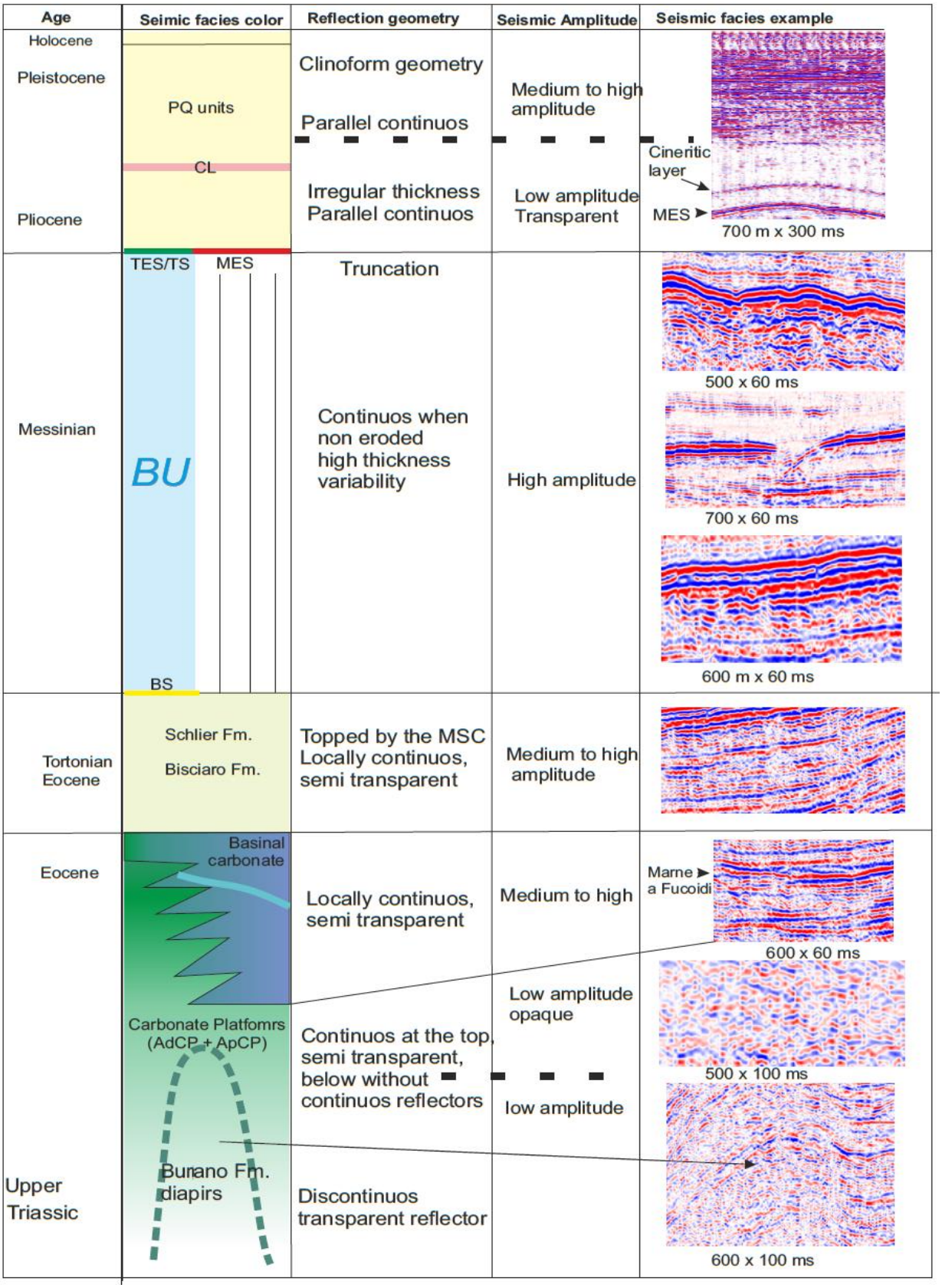


*Figure 4.10: Schematic summary of the seismic facies and horizons recognized and used in this work.*

# Chapter 5 - Results

## 5.1 Seismic interpretation

The interpreted seismic dataset shows evidence of the MSC event in the Adriatic Sea. Some regional composite profiles representative of the heterogeneous domains which have been interpreted following the seismo-stratigraphy principles described in Chapter 4 are present in this section.

I propose several lines which allow to observe the different geodynamic settings of the Adriatic Sea. In particular, a main NW-SE transect, from the Gulf of Trieste to the Albanian offshore, and nine SW-NE perpendicular transects (from the Italian to the Croatian offshore) will be described (transect G to A location in Fig. 5.1) to depict the sedimentary units and the difference in the MSC surfaces and units.

The seven perpendicular transects are produced by merging ViDEPI lines with other seismic lines previously published in other quoted works and projects. The quality of 2D seismic lines is often very different, and the data from other authors sometimes present a different interpretation than the one I applied. However, this approach allows the interpretation of the MSC unit and surfaces. With exception of the regional composite line, I propose the double version of un-interpreted and interpreted profiles.

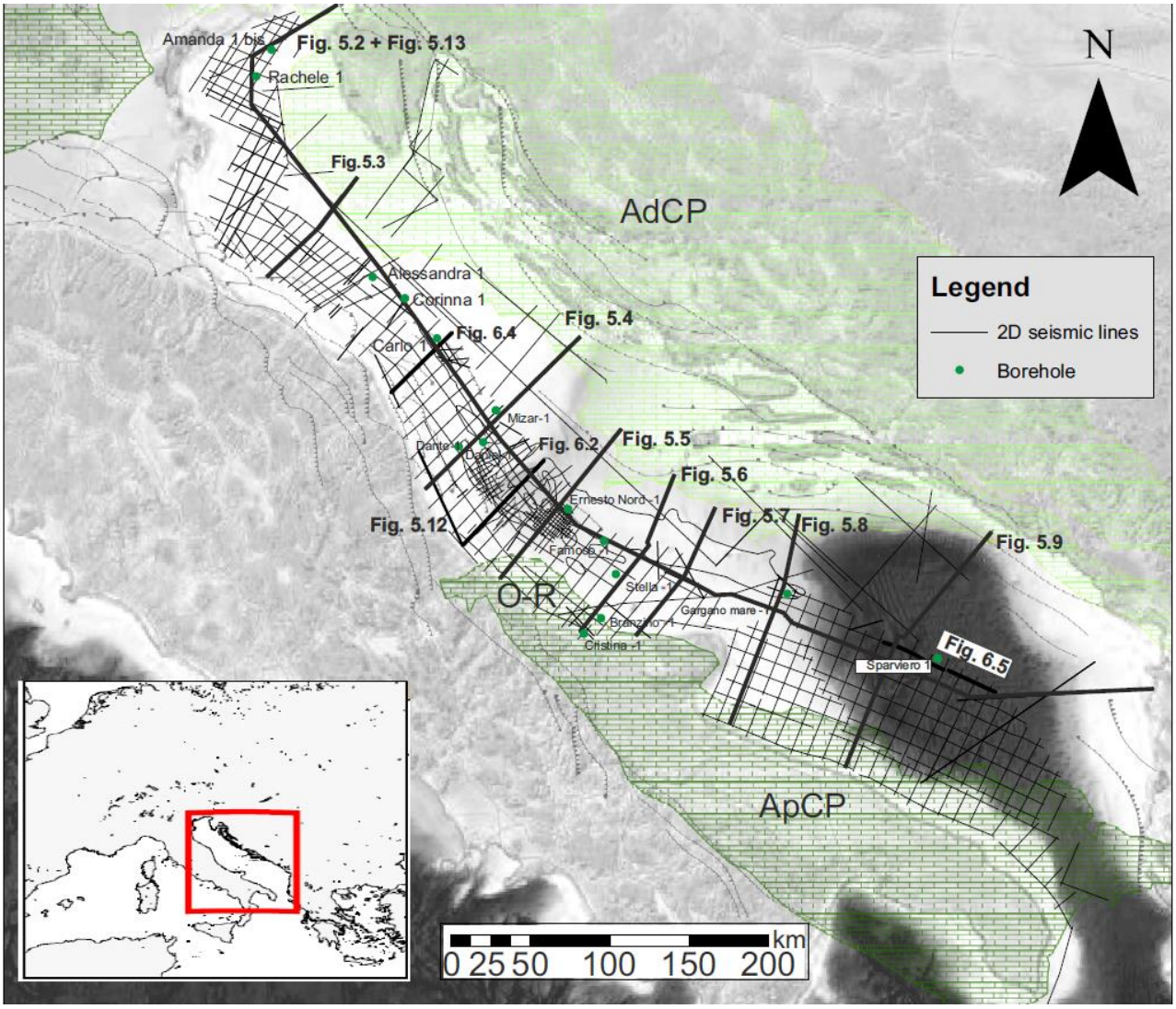


*Figure 5.1: Location map of the profiles interpreted in this work; O-R: Ombrina Rospo plateau; ApCP: Apulia Carbonate Platform; AdCP: Adriatic Carbonate Platform. Bold lines are the profiles shown in the figures; boreholes are used for calibrating the seismic profile and collected in figure 3.9.*

### 5.1.1 Transect 0

The composite NW-SE profile (Fig. 5.2) comprises parts of 15 different seismic lines, calibrated by nine projected exploration wells (Fig. 3.9).

From the NE extremity of the profile (km 0) to km 30, the MES lays at shallow depth from 90 ms TWT to 250 ms TWT, at the top of the Eocene Flysch unit (Busetti et al., 2010a). The Plio-Pleistocene unit is very thin above the AdCP between 10 and 30 km to more than 1200 m in the Adriatic foreland, reaching 1495,40 m as calibrated by Rachele-001 (Fig. 3.9). The Flysch unit documented the effect of the external Dinaric, which deformed and uplifted the AdCP in the onshore area, not analysed in this work, generating erosion and deposition on the accommodation space produced by NE-ward tilting of the Adria foreland: The Eocene succession passes from a depth of almost 1 s (TWT) to 10 ms (TWT) at the AdCP's margin (km 30). Above the MSC surface, the Plio-Quaternary unit thickens southward. From the platform edge, we observe the MES deepening toward the basin, reaching a maximum depth of 1.5 s (TWT). It is recorded by Amanda-001bis well (Fig. 3.9) at 1197,37 m (1.2 s TWT) below seafloor (km 60, Fig. 5.2). The MES appears as an irregular reflector truncating the Eocene-Oligocene succession (Fig. 5.2A, and 5.2). From km 80 to km 120 (Fig. 5.2). The MES deepens to ~1596m (1.55 s TWT) as calibrated in the Rachele-001 borehole (Fig. 3.9), where it truncates the late Miocene marl sequence. The thickness of the Plio-Quaternary units remains about constant above the Istrian Plateau (km 120 to 170).

Along this sector of the transect, the Alessandra-001 well (Fig. 5.2, km 180; Fig. 3.9) calibrates the MES at 1603.5 m (1.3 s TWT), representing a hiatus between the onlapping Late Pliocene and the eroded Schlier formation. A few kilometers apart, Corinna-001 well (Fig. 2 km 185; Fig. 3.9) crosses a thin MSC evaporitic unit (30 m of BU), eroded at its top (TES). This is the first appearance of evaporites in this section of th transrect, and roughly corresponds to the boundary between the Northern and the Central Adriatic Sea. The BU presents a variable thickness between km 180-420 (Fig. 5.2), ranging between 0 and 120 ms TWT. Due to the lack of exploration boreholes in the area, estimation of BU thickness is obtained from recognition of the MSC seismic package: from the Corinna-001 well, a southward thinning is observable until km 228, where a localized erosion origin the MES (228-235 km) as well as several canyons-like forms (e.g., km 245, km 273, km 310, Fig. 5.2) crossing the profile. They were successively filled by Early Pliocene sediments, characterized by low amplitude reflectors with onlapping terminations (Fig. 4.6). From km 200, halokinetic movement of the Permo-Triassic evaporites of the Burano Formation produced the diapiric structures characterizing the MAR. Above those structures, the BU was partially (TES)

or completely eroded (MES). Moreover, Burano halokinetic structures pierce and fold the upper sedimentary sequence, even deforming the Pleistocene layers. At km 232, we observe the highest accumulation of the Plio-Quaternary succession in the section, reaching 2 s (TWT).

Moving southward of km 270, (Fig. 5.2), other high structures have been calibrated as deep diapirs: for instance, Ernesto-1 Nord, at km 320, calibrated Burano evaporites at 3450m below seafloor (Fig. 3.9) are documented. Above the diapiric uplift, the BU is calibrated by Edgard-002 and Ernesto Nord-001 wells, both recovering 40 m of evaporites. Such thickness remains approximately constant on the sides of the structures, except for the incision at km 294 and 310 (Fig. 5.2), where the entire thickness of gypsum is eroded, and the MES deeply engraves the Miocene unit (Fig. 5.2E). From km 330, the MSC unit reaches almost 100 m, calibrated by the Famoso-001 well (Fig. 3.9). Considering seismic interpretations and the Famoso-001 exploration well (Fig. 3.9) calibrating 98 m of Messinian evaporites, in this portion of the transect, between km 330 and km 350 (100-120 ms TWT, Fig. 5.2), we may observe an accumulation of more than 150 m of BU (considering the velocity of gypsum of about 2500 m/s) topped by a high-amplitude TES. Famoso-001 records a Plio-Quaternary unit which reaches a thickness of 622 m.

Between km 350 and 400 (Fig. 5.2), the BU tapers to less than 10 ms above two neighboring MAR structures (Fig. 5.2F), and thinning of BU can be observed along the N-S profile to the south of km 380 (Fig. 5.2). Its complete absence and the corresponding hiatus is evidenced by the MES, beyond the slope of the Tremiti and Gargano highs.

It is to notice that in the Central Adriatic Sea, the MSC unit is always present above the Late Miocene succession. The Schlier and Bisciaro formations show a variable thickness, partially coeval and heavily deformed by the Burano halokinetic tectonics. In contrast, the thickness of the Scaglia Succession appears more regular even when deformed. The Marne a Fucoidi layer highlights the geometry of the underneath structures.
Above the Tremiti and Gargano structures (Fig. 4), the MES lays in a shallow position (0.3 s TWT), reaching the Scaglia Succession (respectively between km 415 – 425 and km 495-500). Gargano Mare-001 (km 480, Fig. 5.2; Fig. 3.9) calibrates the MES at 348 m below seafloor. The deformation related to the Gargano structure is interpreted as a strike-slip fault (Finetti and Del Ben, 2005) or as a salt diapir (Festa et al., 2014). The shallow position of the MSC surface remains stable until the edge of the continental platform at km 515.

In the SE-offshore of the Gargano Promontory, a regional dipping toward the South Adriatic Basin marks the continental slope (km 520 to 690, Fig.5.2), where a widespread MSC erosional surface is emphasized by the presence of a canyon-like incision (km 620). The Sparviero-1bis, at km 660, calibrates about 10 m of BU (Fig. 3.9). The seismic profile suggests a non-erosional surface at the top (TS). From km 667 to 700 the MES is observed, and laterally passes to a thick BU succession, reaching 200 ms TWT.

BU is partially onlapped by the lower Plio-Pleistocene sequence of the Dinarides dismantlement. Even the pre-Messinian succession thickens east-ward from the Gargano high, passing from 20 ms TWT (km 510) to 1 s (TWT) in the Dinaric-Albanides foredeep (km 750) and below the Albanian continental slope. In the last right part of the section (km 800–845), the BU is covered by a thick (almost 3 s TWT) Plio-Pleistocene sedimentary column.

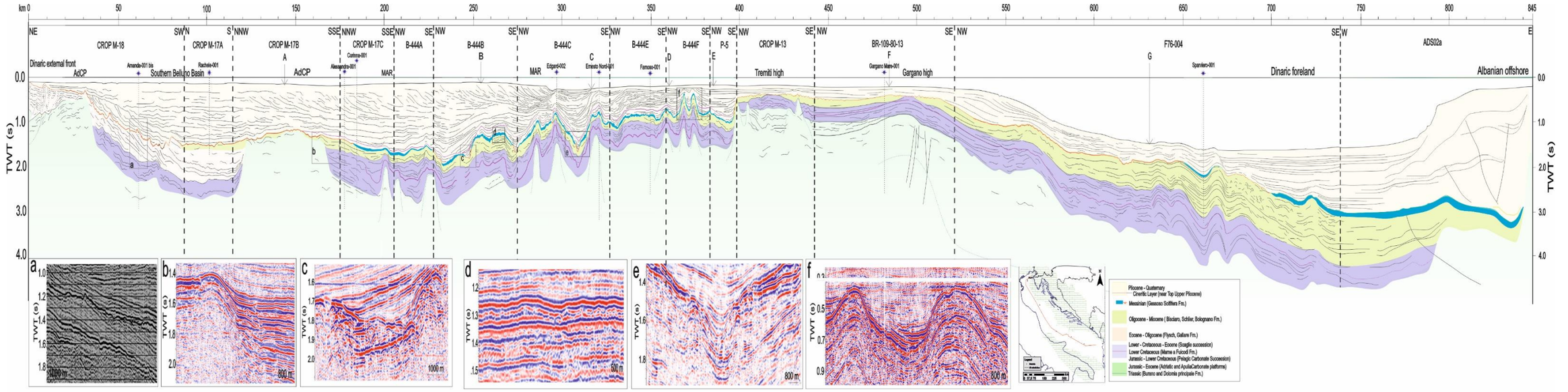


*Figure 5.2: The Transect 0 (a composite profile) crosses the Adriatic Sea from the Trieste Gulf (Italy) to the Albanian offshore. The Messinian surfaces MES and TES and the BU are highlighted in the section. A) seismic zoom highlighting the MES which truncates the Eocene Flysch Formation; B) seismic zoom displaying the MES above the AdCP and the pre-Messinian Schlier - Bisciaro Formation; C) seismic zoom highlighting the MES incision in the pre-MSC units, covered by downlapping Pliocene sediments; D) seismic zoom displaying the BU (range between 0.2 s TWT and 0.1 s TWT), slightly eroded at the top (TES); E) seismic zoom highlighting the incised system (MES), laterally affecting the evaporites unit (BU); F) seismic zoom displaying the presence of a thin BU above the two anticline structures.*

### 5.1.2 Transect A

The SW-NE Transect A crosses the Transect 0 at km 142 (Fig. 5.3). It shows the External Apennine front (SW portion) and the westernmost sector of the Istrian Plateau, NE sector of the AdCP. In correspondence of the outermost deformation of the Apennine Chain (km 0 – 15), the MSC surface is covered by 4.3 s TWT of Plio-Quaternary sediments. As shown in figure 5.2, the sedimentary cover of the Istrian Plateau is almost completely represented by Pleistocene deposits. The MSC produced total (MES) or partial (TES) erosion of the BU, testified by an irregular discontinuous surface. The MES is more largely distributed on the Istrian platform (AdCP) and on the carbonate slope (Grandic et al., 2001, 2010; Spelic et al., 2021), where the onlapping terminations, mainly referred to Pleistocene, testify a long period of emersion, suggesting a MES related to erosion and mainly non deposition. MSC sediments are probably present with a very thin unit (Fig. 5.3C), and overthrusted by the Apennine chain. Plio-Quaternary sediments decrease in thickness from more than 4.5 s TWT in the SW sector to less than 1 s TWT onlapping the AdCP.

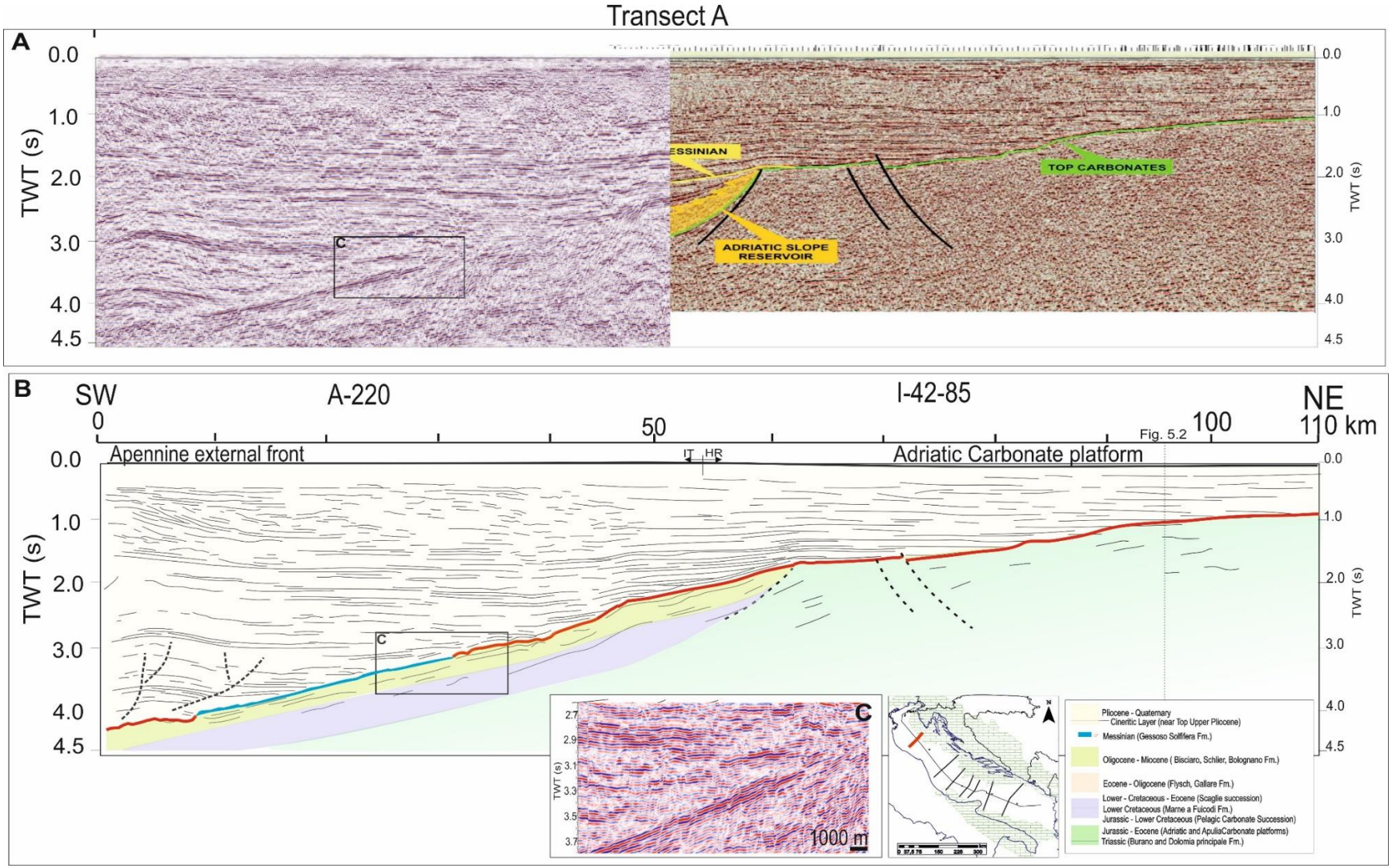


*Figure 5.3: SW-NE composite transect A, from Rimini (Italy) to the Pola (Croatia). In the western part (A-220 profile by ViDEPI) the buried outermost Apennine thrust and the related foreland tilting, less pronounced in the eastern part (I-42-85, modified from Grandic and Kolbha, 2009) where it involves the AdCP. The MES in the AdCP slope has been interpreted differently than how proposed by Grandic et al. (2010). A) Non-interpreted profiles; B) Line drawing; C) Seismic details of the onlapping Pleistocene sediments above the BU.*

### 5.1.3 Transect B

Transect B, in the Central Adriatic Sea, cuts the Transect 0 at km 255. It displays the external thrust of the Apennine Chain (SW), the halokinetic tectonics of the MAR and the western portion of the AdCP. The BU is interpreted (km 0 - 22) below the External Apennine front, where it seems to be not eroded. Even the V-shaped channel highlighted in Figure 5.4C (km 18 - 22) shows a high deformation of the BU, while it does show signs of folding rather than MSC erosion. In any case, it must be considered that the seismic profile has not been migrated, and therefore diffractions and incorrect position of the reflectors could partially deform their actual geometries. This depocenter was filled with post-Messinian deposits marked by a high-amplitude reflector (Fig. 5.4C). The MAR folding occurred during Pleistocene age as evidenced by an approximately constant thicknesses of BU (Messinian) and of the layer between LC and TES (Upper Pliocene), as also calibrated by the wells Dante-1, Daniel-1 and Mizar-1 (Fig. 5.4; 3.9). The BU locally shows the typical irregular and discontinuous seismic facies due to erosion on the top (TES reflector). The increasing thickness of BU toward NE (Dante-1 calibrates 50 m; Daniel-1 100 m; Mizar-1 116 m) suggests a decrease of erosion in the less deformed area between 60 and 100 km. The high position of the TES is due to the uplift of the MAR structures. At km 110, the BU is completely lacking: the hiatus is produced by Messinian and Pliocene erosion and non-deposition.

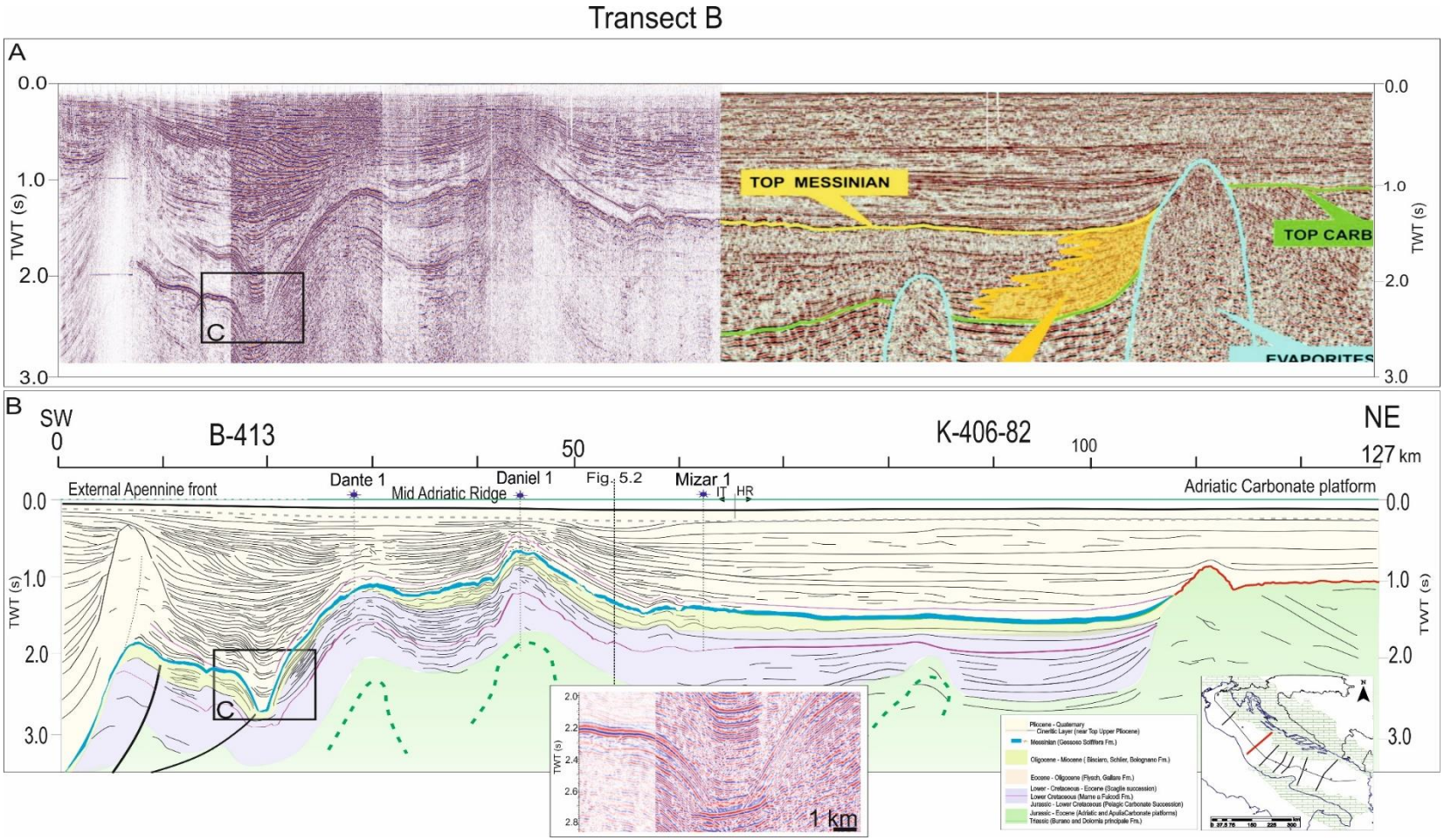


*Figure 5.4: SW-NE composite Transect B from the Teramo (Italy) to the Dugi Otok (Croatia) offshores. The line B413 (ViDEPI) shows the buried outermost thrust of the Apennine Chain and the Mid-Adriatic Ridge. The K-106-82 (by Grandic et al., 2010) shows the transition from the pelagic to the shallow water AdCP domains. Halokinetic structures produced by the Triassic Burano evaporites affected the sedimentary cover since the Paleogene age. A) Non-interpreted profiles; B) Line drawing; C) Seismic details folded BU into a V-shaped channel, the structural low seems to be due to the Pleistocene compressive tectonics, where BU is folded but continuous, that is, not affected by erosion.*

### 5.1.4 Transect C

The SW-NE Transect C cuts the Transect 0 at km 316. It explores the north-eastern part of the ApCP (at the Ombrina-Rospo plateau), the south-western part of the AdCP and the intermediate pelagic domain. Diapiric structures of the MAR have been interpreted as carbonate platform inside the pelagic domain, likely deformed by buried Burano diapirs, at least partially related to subvertical strike-slip faults (Grandic et al., 2001). The BU and the CL are largely folded, testifying that the main deformation occurred during Pleistocene. Above the ApCP, BU has a thickness of about 20 m, as calibrated by the well Rombo-Mare-1, projected from a distance of 2.2 km. The high-amplitude BU gypsum has been completely incised (MES) at km 20 and 29 (erosional channels are documented in the seismic detail of figure 5.5C. Above the MAR, the BU has been partially eroded at the top (TES) while it shows an approximately constant thickness in the NE sectors of both profiles. At km 104, a diapiric structure cuts and deforms the AdCP. The Plio-Pleistocene sequence shows a thickening toward SW, reaching almost 2 s (TWT) at km 20, while only Pleistocene sediments directly overly the AdCP with a thickness of 0.6 s TWT.

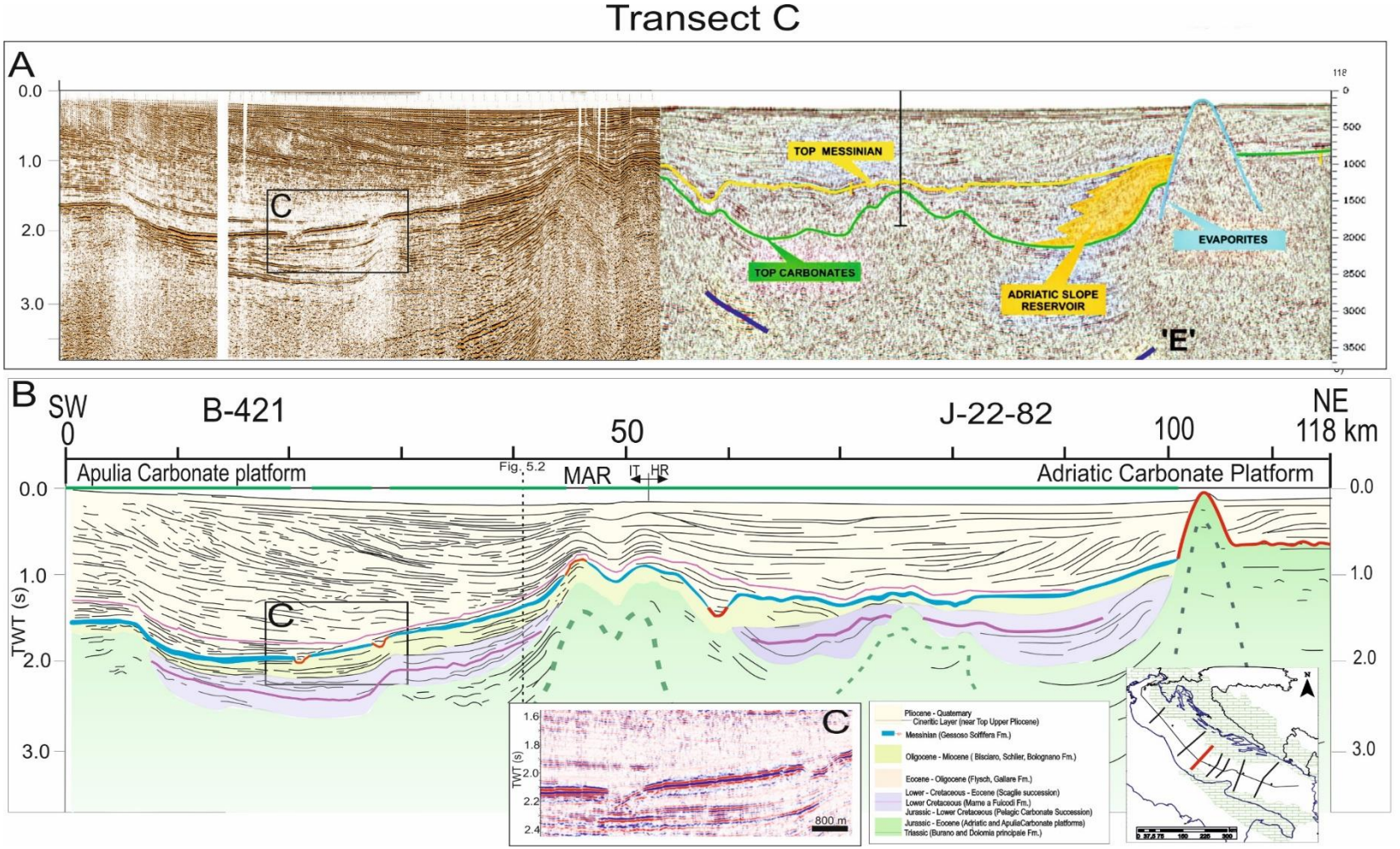


*Figure 5.5: SW-NE composite Transect C from the Ombrina Rospo Plateau (ApCP) to the AdCP near Jabuka (Croatia offshore). The western part (line B-421 by ViDEPI) shows the buried ApCP and the Mid Adriatic Ridge. The eastern part (J-22-82 by Grandic et al., 2010) points out the transition from the basin to the shallow water domain of the AdCP. Burano halokinetic structures affected the sedimentary cover since the Paleogene age. Messinian evaporites (BU) are calibrated above the ApCP and interpreted above the MAR. A) Non-interpreted profiles; B) Line drawing; C) in the seismic detail the BU presents an erosional top (TES) and two incisions that cut through the BU.*

### 5.1.5 Transect D

The Transect 0 is crossed by the Transect D at km 360. In the SW, sector the profile cuts the ApCP (the Ombrina-Rospo plateau) and the diapiric structures of the MAR, where they are at least partially related to strike-slip faults (Grandic et al., 2001) also affecting the halokinetic resurgence in the Tremiti anticline (Festa et al., 2014). The BU is calibrated by Cristina-001 (152 m of evaporites, 130 ms TWT) and Branzino-001 well (65 m), which are both located above the ApCP (Fig. 5.6 C), where it shows some local thickening caused by normal faulting. In the pelagic domain, the Stella-001 well (projected; Fig. 3.9) calibrates 150 m of the Messinian evaporites (128 ms TWT), partially eroded at the top (TES). At km 30-35 (Fig 5.6D) a canyon system seems to be over-imposed on a fault system. From the Stella-001 well, the BU is uplifted by the MAR, where it thins. At the km 70, the MSC surface appears erosive, truncating the Late Miocene. NE-ward, from km 80, the MES sinks toward the Dinaric front, out of profile. Between km 90 – 110, the high amplitude reflector suggests a BU thickness of some tens of meters. The Plio-Pleistocene sequence reaches almost 1.5 s (TWT) at km 30 and thins NE ward, with a total accumulation of 0.9 s TWT recorded above the AdCP.

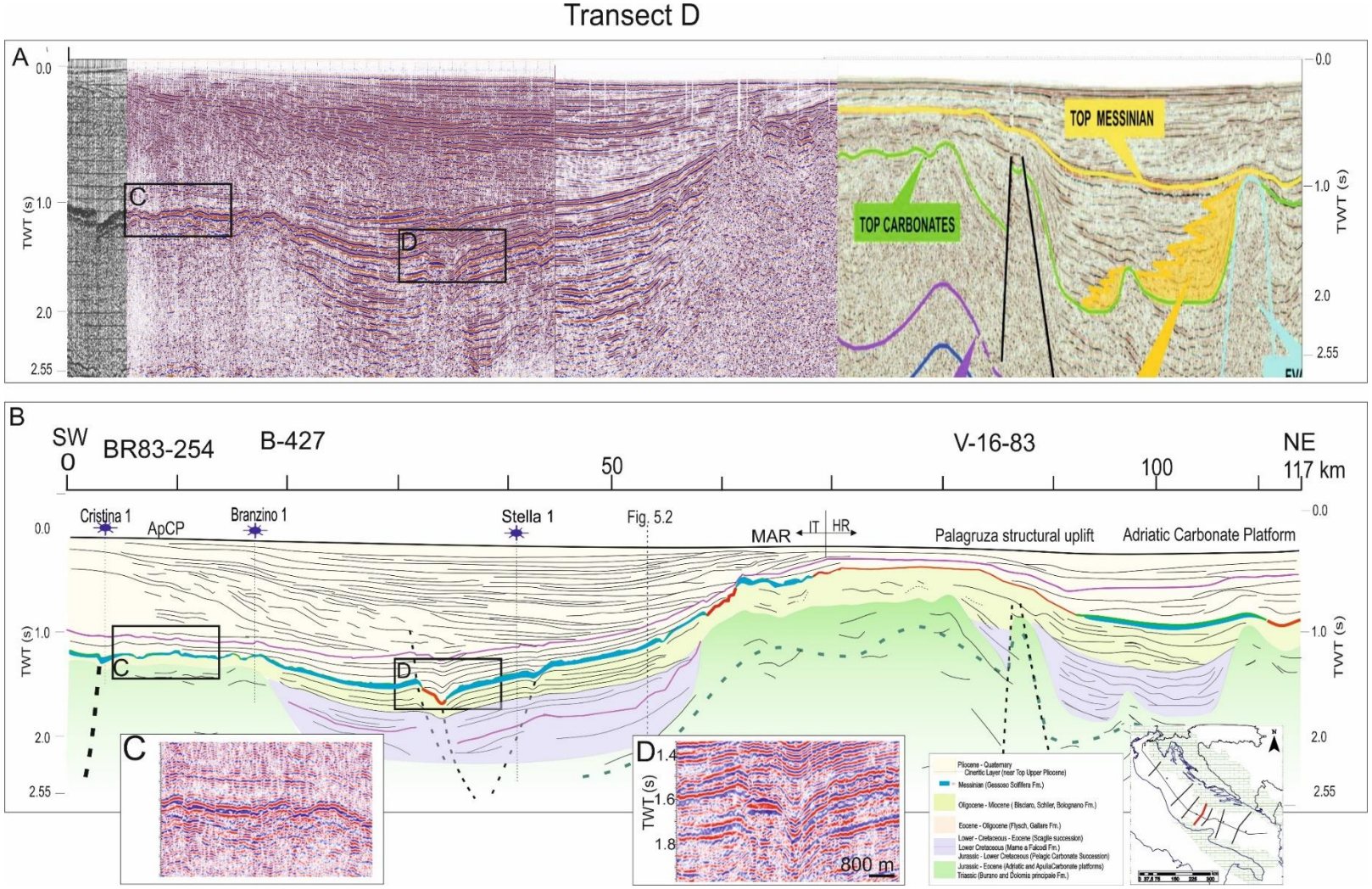


*Figure 5.6: SW-NE composite Transect D, from the Ombrina Rospo plateau (ApCP) to the AdCP in front of the Vis Island (Croatia offshore) The line B-427 (ViDEPI) crosses the buried ApCP and its transition to the deep basin, where the MAR seems to be represented by a Mesozoic carbonate platform uplifted by halokinetics. The profile V-16-83 (by Grandic et al., 2001) crosses the buried external portion of the AdCP. Messinian evaporites present a variable thickness; C) seismic detail shows the ApCP displaying thin eroded BU; D) seismic detail of the BU in the deep domain, documents thicker evaporites (BU).*

### 5.1.6 Transect E

Transect E, located at the boundary between the Central and Southern Adriatic Sea, cut the composite transect 0 at km 362. BU is preserved (20 - 10 ms TWT) above the ApCP (Fig 5.7C) even if appears partially eroded and then becomes null toward NE, from km 47. Plio-Quaternary sediments above the Gargano structure show deformation as well, indicating activation of the anticline structure between Pliocene and Pleistocene (Morsilli et al., 2017). Above the pelagic domain, the TES is covered by almost 1 s (TWT) of Plio-Quaternary sediments. In the central portion, a depositional hiatus (MES) is present above the Palagruza structure, where a thickness of about 200 ms TWT of Plio-Pleistocene succession directly covers the Cretaceous carbonate platform. Toward NE, the MES is overlayed by almost 1 s (TWT) of Plio-Quaternary sediments.

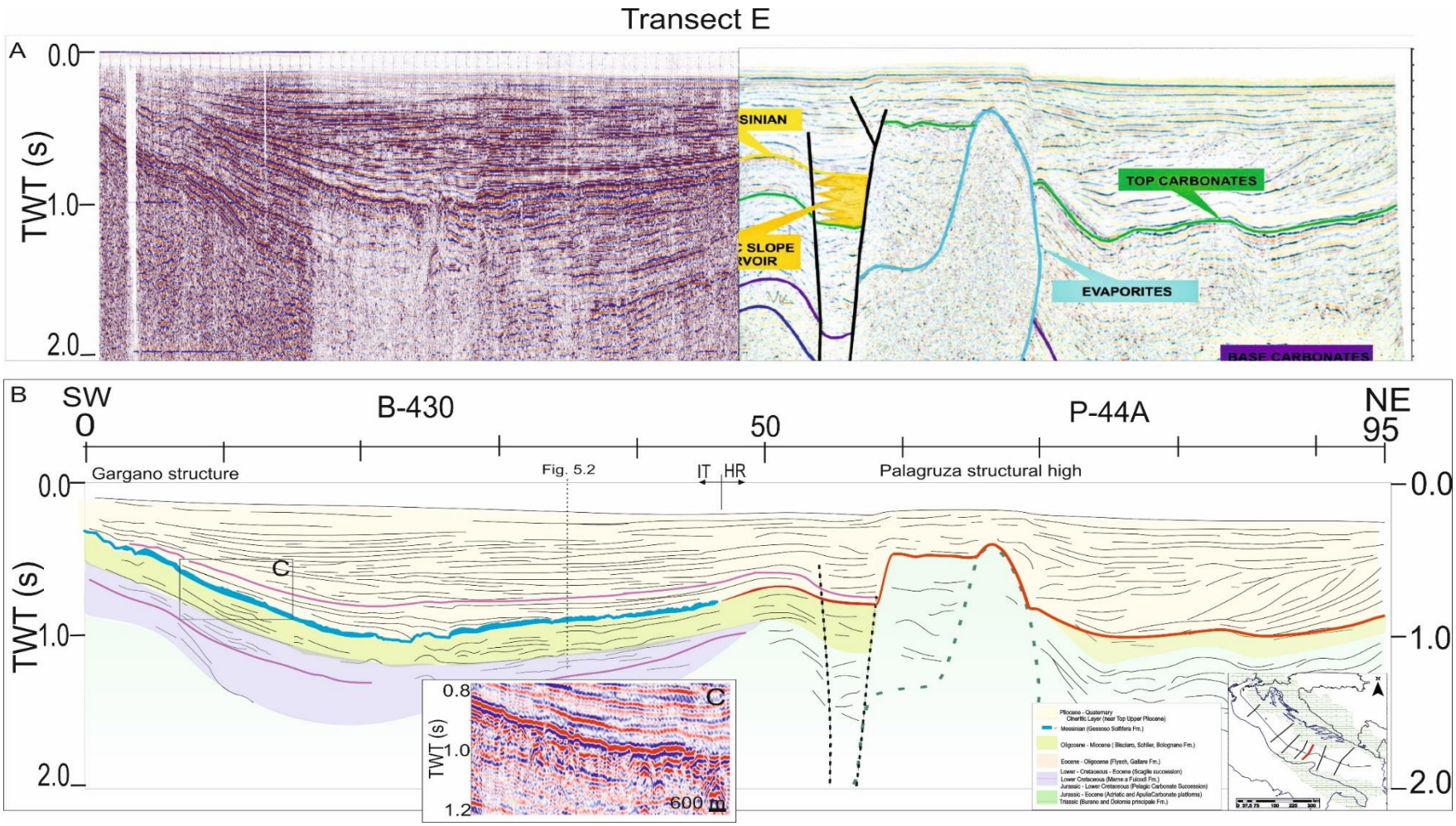


*Figure 5.7: SW-NE composite profile E, from the Gargano anticline to the AdCP near Palagruza Island (Croatia offshore). The line B-430 (ViDEPI) shows the buried ApCP, displaying the transition from the pelagic to the shallow water ApCP. The eastern part (P-44A by Grandic et al., 2001, 2009) shows the buried portion of the AdCP. BU presents a variable thickness, thinning toward NE from 15 ms (TWT) and laterally passing to a hiatus (MES) above the Palagruza structure. C) seismic detail shows the thin eroded BU. Interpretation of the Croatian 2D seismic line is different from the one proposed by Grandic et al. (2010) by placing the MSC surface in the high-amplitude reflector above the Top Carbonate, where the downlapping Clinoform of the Plio-Pleistocene succession ends.*

### 5.1.7 Transect F

The orthogonal Transect F (Fig.5.8) crosses the transect 0 (Fig. 5.2) at km 482. It is located to south-east of the Gargano Promontory, in a SW - NE direction. It is calibrated by the Gargano Mare-001 well (Fig. 5.8), which crosses the MES at 348 m below the seafloor. The MES affects the Oligo-Miocene unit overlying the ApCP and is buried by a thin (0.3 s TWT) Plio-Pleistocene succession. From km 10 to 20, a thin seismic package suggests the presence of the BU, as also from km 85 to 95, with a thickness of 10-20 ms (TWT). These localized MSC evaporites are located in syncline structures produced by the deep migration of salt toward the diapirs. While the MES lays generally in a shallow position, the BU deepens between the Gargano Mare structure and the AdCP, reaching more than 1.5 s TWT in-depth, and a thickness of about 20 ms TWT. Effects of erosion (TES) are visible from km 103 to km 138. The MSC surface is downlapped by the Plio-Pleistocene succession, showing clinoform geometries sourced by the AdCP.

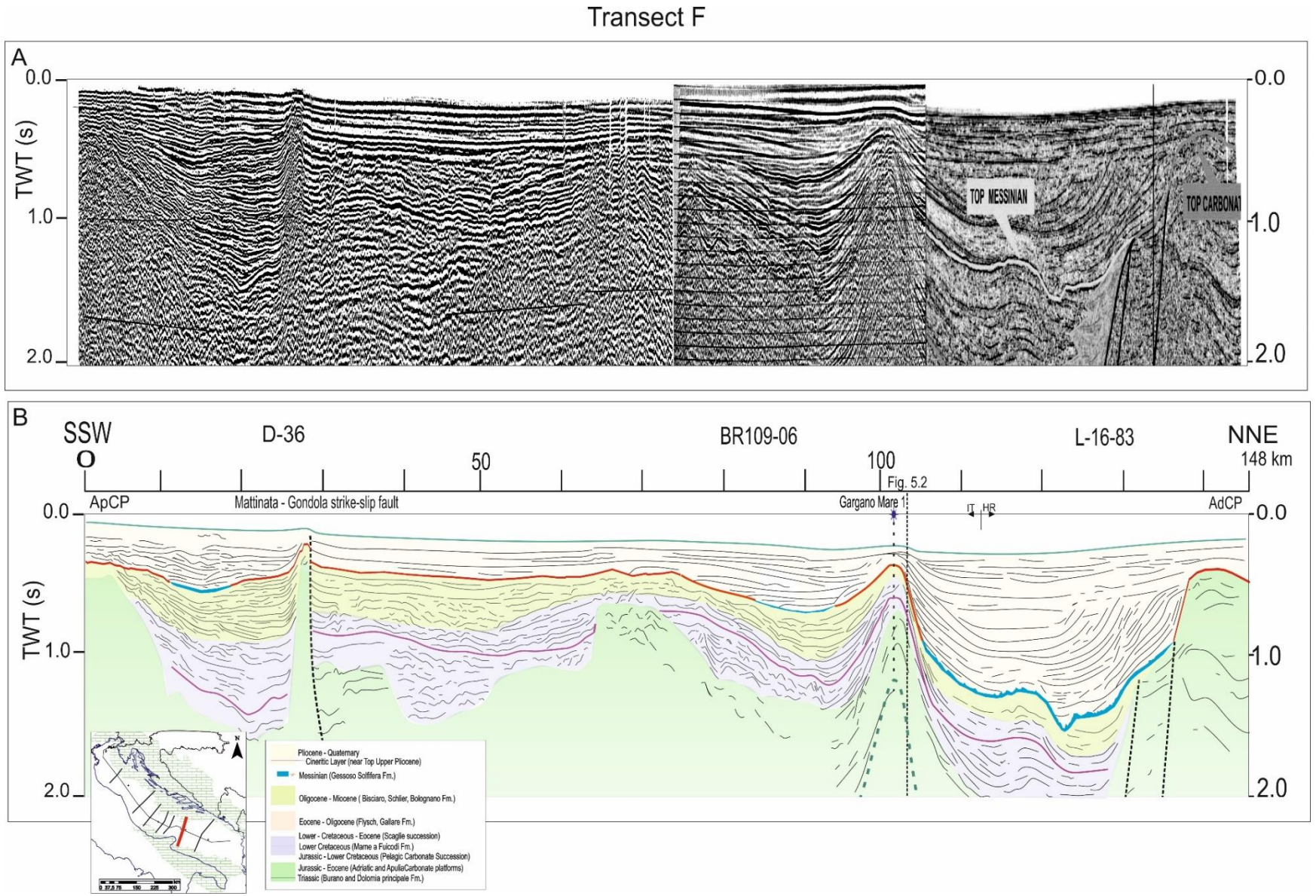


*Figure 5.8: SSW-NNE composite Transect F, from the ApCP to the AdCP margins. The pelagic domain is irregular and deformed by the Gondola-Mattinata strike-slip fault and by other halokinetic structures. D-36 and BR 109-06 profiles by ViDEPI, L-16-83 by Grandic et al. (2010). A) Non-interpreted profiles; B) Line drawing.*

### 5.1.8 Transect G

Transect G crosses the transect 0 at km 610 (Fig. 5.2) and extends from the ApCP, almost outcropping, to the deeply buried AdCP margins. Above the ApCP, the MES unconformity is laterally substituted by the TES, where a thin BU shows to be more (completely above the Gondola structure and partially above the AdCP) or less eroded. The thickness of BU is evidenced in the seismic details of Figure 5.9 C, D and E respectively at the foot of the ApCP slope (km 20 – 50) eroded at the top (TES); at the NE flank of the Gondola fault (from km 70 – 90), not eroded (TS); in the Dinaric foredeep, where an eroded scattered top BU is visible (km 122 – 160). The area overlying the Gondola strike-slip fault appears and the pre-Messinian sequence is uplifted reaching and also deforming the seafloor. At the eastern edge of the profile, the MSC unit is onlapped by a thick Plio-Quaternary sequence which shows the clinoform geometries already observed along the Transect F in its upper part, feed by the Dinaric Chain erosion.

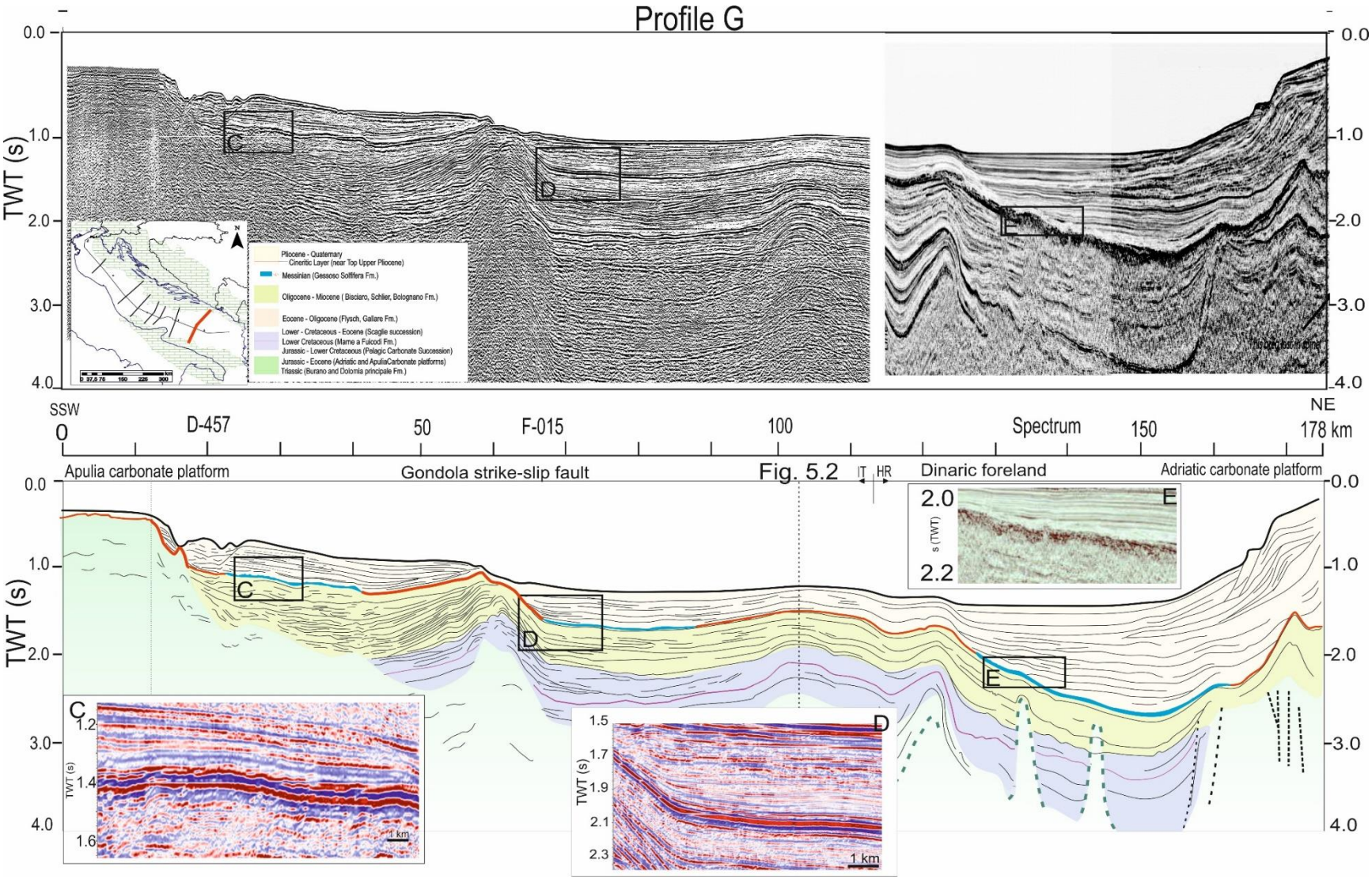


*Figure 5.9: SSW-NNE composite Transect G, from the ApCP to the deeply buried AdCP. The profile merges lines D-457, F-015 (ViDEPI) and a Spectrum profile by Mazzuca et al, (2015). Deformation of the Gondola strike-slip fault reaches the seafloor, while the AdCP is overlaid by thick Plio-Quaternary sediments. Seismic details with a thin BU in (C) and (D); E) Seismic detail in the Dinaric foredeep, with clear evidence of erosion (TES).*

## 5.2 Time structural map of the MSC surfaces

To produce the time structural map of the Messinian surface / Plio-Quaternary base (Fig. 5.10), I considered the surface at the top of the MSC events. These events produced, from time to time, complete hiatus (TES) or complete survival (TS) or partial survival (TES) of the Messinian unity (BU).

The interpreted horizons were interpolated through the GMT mapping tool.

On the western part of the study area, the map shows two main structural lows near the Italian coast and divided by the Conero high. They correspond to the Apennine foredeep, already evidenced on the Transect A (Fig. 5.3) and B (Fig. 5.4) filled with sediments produced by the dismantlement of the surrounding chains.

The maximum depth of the MSC surface in the Adriatic offshore, is reached in the Northern Adriatic Sea at 4.6 s TWT by Transect A (Fig. 5.3), while the maximum depth is calibrated by the Afrodite-001 well (Fig. 3.9) that reaches the Messinian unit at 3680 m below seafloor. The surface gradually rises toward ENE on the wide structural high of the Istrian Plateau, which extends from the Trieste Gulf to the Kvarner area and the northern Dalmatian Islands, where the pre-Messinian sequences largely outcrops (Vlahovic et al., 2005; Spelic et al., 2021). In the Northern Adriatic Sea, the seismic resolution does not allow to visualize the MSC surface below the Apennine chain, even if boreholes calibration suggests the presence of the BU (e.g., Afrodite-001, Rita-001, Table 1.1).

In the Central Adriatic Sea, the Fratello-001 well (Fig. 3.9) calibrates the top of BU at the maximum depth in the area at 4298.2 m below seafloor, that on the map of figure 5.10, corresponds to a maximum depth of 3.1 s TWT. In the Pescara foredeep, seismic profiles point out the occurrence of uneroded evaporites (TS surface).

A system of realtively small structural highs in the Central Adriatic Sea axis corresponds to the MAR, produced by halokinetic tectonics of the Triassic evaporites and aligned in a NW-SE direction, from the Ancona offshore to the Palagruza structure.

A third depocenter, located in the South Adriatic Basin (Fig. 5.2, 5.8, 5.9), reaches a depth of about 2.5 s TWT below the seafloor in the Montenegro/Albanian offshore. On the western opposite side, the Gargano Apulia offshore documents a structural high related to the ApCP.

The MSC surface position in the sediment column is strongly controlled by:

- The carbonatic platforms (specifically, AdCP and ApCP) brought the MES surfaces to a shallow position. In the Northern Adriatic Sea, from the AdCP, we observe a gentle tilting toward the Apennine chain, which highly affected and tilted the Adriatic foreland. This trend continues in the

Central Adriatic Sea, where the Messinian total hiatus (MES) passes to be a preserved (TS), or partly eroded (TES) Messinian unit (Fig. 5.2).

The Gargano-Palagruza threshold, constituted by a complex diapirs system, represents the boundary between the Central and Southern Adriatic Sea. The transition toward the Mesozoic deep basin marks the NE and SW steps respectively with the AdCP and ApCP (Figs. 5.2, 5.8, 5.9).

Above the MAR, the MSC unit (BU) is topped by the TES, while in the Gargano-Palagruza structure there are no BU, but a widespread hiatus evidenced by MES.

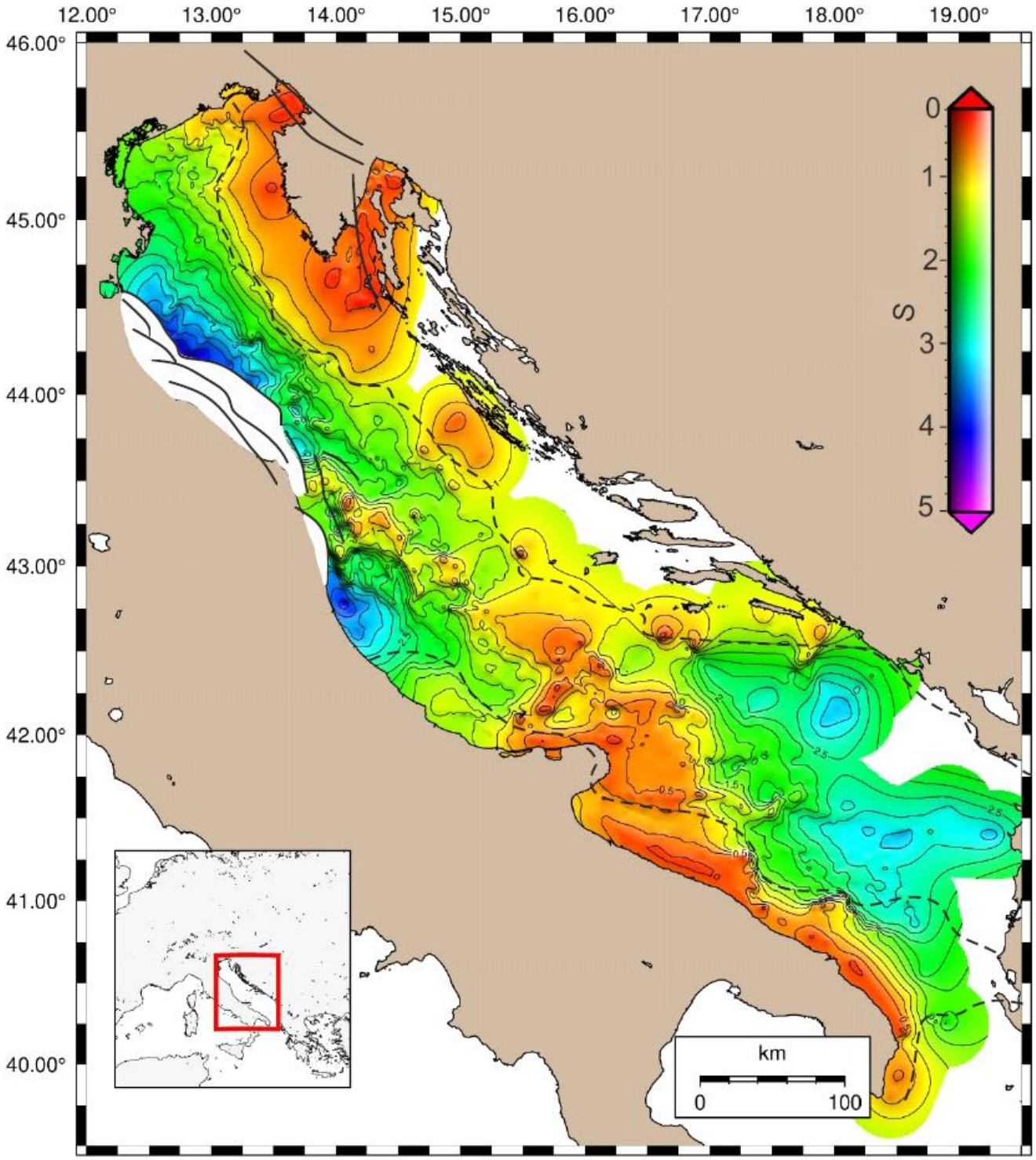


*Figure 5.10: Time structural map of the Top Messinian/Base Plio-Quaternary*

## 5.3 Isopach map of the Evaporites (BU)

In the study area several profiles have seismic resolution suitable to distinguish top and base of the BU (Fig. 5.12). On the other hand, some old profiles, characterized by lower resolution, show a single high amplitude reflector due to interference between the two discontinuities, that masks the thickness of the presence BU (Fig. 5.2). For this reason, I have integrated information from both seismic profiles and wells to obtain the best available thickness distribution, which allows us to produce the isopach map (Fig. 5.10).
Large yellowish areas have been recognized, where the BU is not present: in particular, this occurs in the North Adriatic Sea and above the two carbonate platforms, where an erosional surface has calibrated and interpreted (Fig. 5.2, 5.3, 5.4, 5.8, 5.9).

Accumulation of evaporites occurs from the Conero to the Gargano – Palagruza high, where the BU maximum thickness reaches 180 ms (TWT), indicated as the purple colors in figure 5.11. High thickness of BU is calibrated by boreholes (e.g., Edgard-001; Cristina-001, ViDEPI). In particular, the map of figure 5.11 shows scattered areas with maximum thicknesses preserved along the middle axis of the Central Adriatic Sea, locally truncated by incision through narrow valleys, reaching the pre-Messinian units (Veronica-001, Fig. 3.9) (MES). Moreover, the area is highly affected by the salt diapirs, which deformed and uplifted the BU and pre-Messinian units. Above the northern ApCP, a high thickness of BU is observed, partly eroded.

A peculiar BU accumulation is observed in the Pescara foredeep, where more than 250 ms (TWT) of Evaporites are observed in Line B439 (Fig. 5.12) buried below more than 3000 m of Plio-Pleistocene sediments, marked by four high-amplitude reflectors. In the proximity of this high-amplitude package of reflectors, the MSC surface appears not eroded (top interpreted as TS).

The Central and Southern Adriatic Sea are separated by an area with a thin or lacking BU, as recorded by Gargano Mare-001, Cigno Mare-001 wells (ViDEPI, Fig. 5.2 and 5.10). Widespread Messinian erosional surface (MES) dominates the ApCP and the South Adriatic Sea's continental slope. Erosion decreases in the deep basin where Sparviero-001 (Fig. 3.9, 5.2, 5.9) calibrates a few meters (about 40 meters) of gypsum (BU). Few lines are available in the Croatian and Albanian offshore; the AdCP shows a similar pattern to the ApCP (widespread erosional surface), while a

thickening evaporites succession (BU) is observed toward the Albanian margin where it is buried below the Albanides thrust front (Finetti et al., 1987; Del Ben et al., 1994; Argnani, 2013).

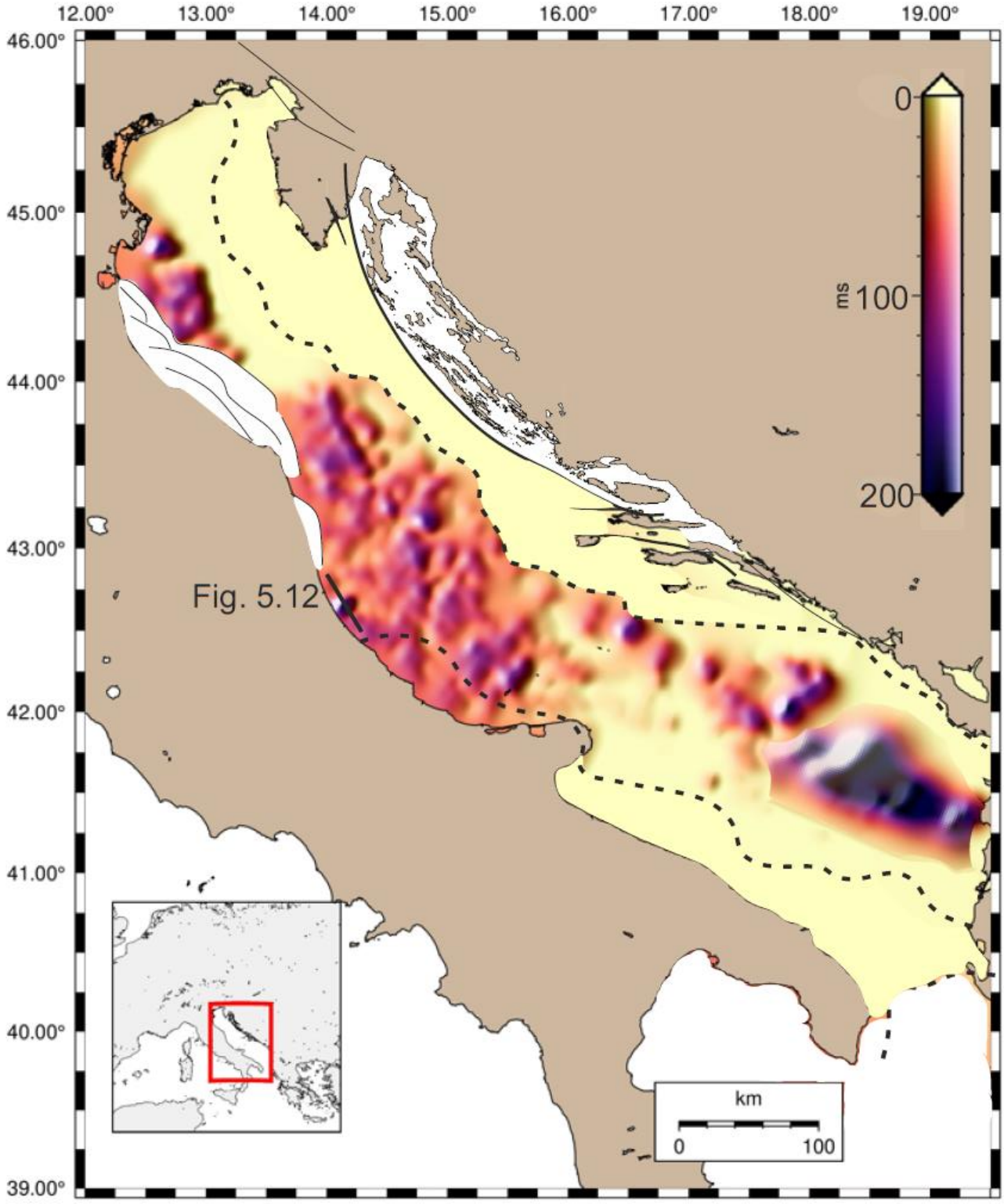


*Figure 5.11: Isopach map of the BU. The yellow area corresponds to the absence of evaporites (MES). Black dashed lines represent the AdCP and ApCP margin.*

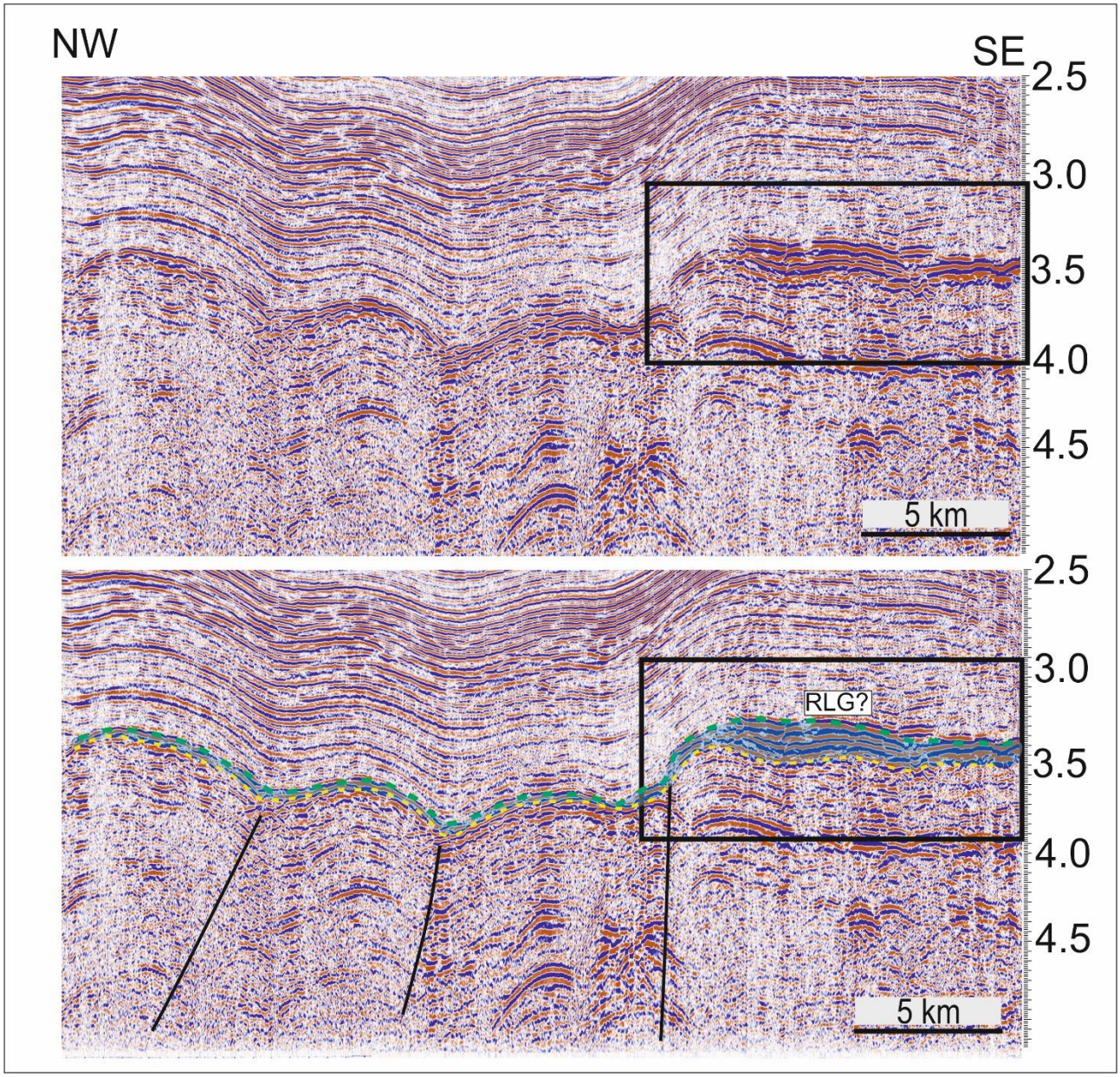


*Figure 5.12: Line B 439 zoom of the unusual accumulation of BU in the Pescara Foredeep. Position in figure 5.11.*

## 5.4 Summary of the MSC surfaces and unit

The main focused MSC unit and surfaces are summarized in figure 5.13 which shows a schematic section along the Adriatic Sea axis, displaying the distribution of the MSC MES, TES, TS, and BU.

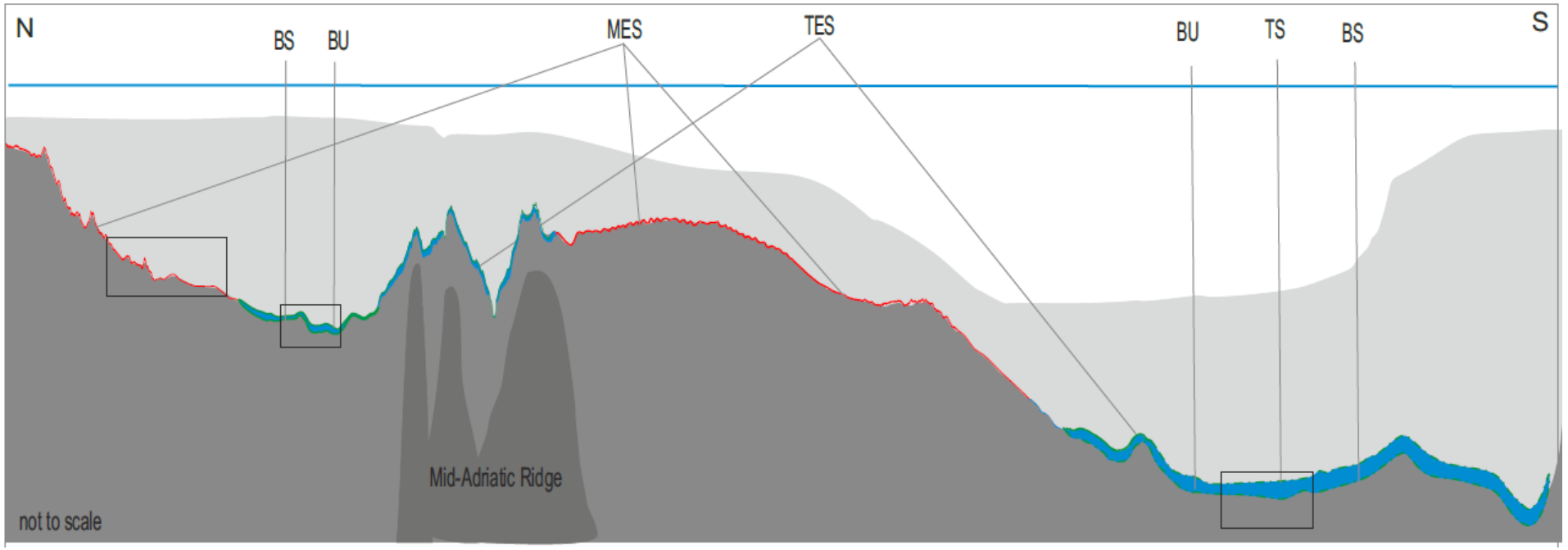


*Fig. 5.13: Schematic section of the Adriatic Sea from N to S: the main units and surfaces belonging to the MSC, interpreted and described in this chapter, are highlighted.*

# Chapter 6 - Discussion

The isopach and structural maps regionally point out the structural highs and lows of the MSC surfaces resulting from the MS, by the related sea-level drop (Hsü et al., 1978; Lofi, 2018), and the post-Messinian tectonics. The Sea level drawdown caused two main effects: i) emersion of the continental margin and slope, exposing to subaerial erosion a large portion of the paleo seafloor, which underwent incision (canyon-like and alluvial plain); ii) in case of the favorable condition, deposition of a variable thickness of Messinian related evaporites, in the specific case of the Adriatic Sea represented by Gypsum of the Gessoso-solfifera Formation also known as Bedded Unit - BU (Lofi et al., 2011; Lofi, 2018; Manzi et al., 2020). The time-structural map represents the surface at the base of the Plio-Quaternary sequence, differently called TS, TES or MES, on the base of the different conditions: uneroded BU (TS); partially eroded BU (TES) or completely absent BU due to erosion and/or non-deposition (MES). The yellow area in figure 5.11 indicates the presence of the MES, that means that the Plio-Quaternary sequence directly covers the pre-Messinian sediments.

The isopach map is produced by interpreting the BU occurrence and the MSC bottom surface BS. The isopach map shows the different thicknesses of the BU, deposited during the Messinian, and locally eroded during the Late Messinian and possibly post-Messinian age; in this latter case, a paleo-drainage system may occurr.

In particular, in the study area, on the base of aspects and distribution of MSC surfaces and units, three different areas, can be recognized:

i) The Northern Adriatic Sea, where a MES with high erosional grade is dominant;
ii) The Central and Southern Adriatic Sea, where mixed eroded evaporites are present with overlaying TES unconformity;
iii) The Central Adriatic Sea, where the erosion is absent and the evaporites are preserved and the overlying sediments conformably lie on the evaporites (TS).

## 6.1 Northern Adriatic Sea

In the North Adriatic Sea, the prevalent pattern is the deep erosion of BU which differently affects the Miocene and Oligocene sediments, the Flysch sequence, the AdCP, (Fig. 5.2 and 5.3). Several exploration wells (e.g., Amanda-001bis; Rachele-001, Fig. 3.7, 3.9) drilled in front of the Gulf of Venice, highlight a depositional hiatus between the Lower Pliocene and the pre-MSC units. Several works performed in the northern area (among others, Ghilemi et al., 2010, 2013; Donda et al. 2013; Amadori et al., 2018; Zecchin et al., 2017; Spelic et al., 2021) indicate the presence of a widespread erosional surface, combined with a canyon-like system in the modern North Adriatic Sea. Even the AdCP underwent subaerial exposure during the MSC.

Incised paleo-valley in the carbonates and clinothemes in the Kvarner area (Spelic et al., 2021) and from the Istrian plateau (Ghielmi et al., 2013; Rossi et al., 2015) suggest the development of a subaerial drainage system facing SW (Fig. 6.1). Deep Messinian incisions are present also in the Dalmatian portion of the AdCP (Wrigley et al., 2015; Scisciani and Esestime., 2017). At the same time, drainage system of the Alps was southward oriented, creating a large incision at the base of the modern Po plain foredeep (Ghielmi et al., 2013; Rossi et al., 2015; Amadori et al., 2018). The Eastward migration of the Apennine affected the shape of the foredeep depocenter. Most of the drainage of the Alps during the Oligo-Miocene flowed along a narrow and S-ward elongate basin in front of the Apennine chain, while from the Early Pliocene, a thick sequence of turbidites deposited in a deep-marine environment covering the Messinian surface in the northern Adriatic Sea and Po Plain (Ghielmi et al., 2013; Rossi et al., 2015).

Deposition of evaporites (BU) occurred in the modern Ravenna/Rimini foredeep. Unfortunately, few exploration wells were able to reach the MSC. The seismo-stratigraphy technique however, allows to interpret a consistent thickness of BU in the Area (Fig. 5.6, 5.11) where the External Apennine chain did not obliterate the MSC. Due to the presence of the external Apennine chain was not possible to reconstruct the entire extension of the MSC event in the Ravenna/Rimini foredeep. Considering the framework of the area, two distinct sectors were discriminate: 1) The Ravenna/Rimini foredeep, where BU deposition occurred; 2) the Venice and Trieste Gulfs and AdCP, where only a MES is recognized.

It is debated if deposition of evaporites (BU) occurred in the entire north Adriatic Sea. On the base of the framework of the area, I consider two different hypotheses, both according to the three stages development of the MSC proposed by many Authors:

scenario i) deposition of BU during stage 1 of the MSC, subsequently eroded in stages 2 and 3 due to the combined effect of the sea-level drop and the isostatic adjustments until the reflooding event in the Zanclean;

scenario ii) partial evaporites (BU) deposition, except for the localized portion where water remains feed by paleo-drainage systems (Fig. 6.1). Widespread erosion of the Adriatic foreland and AdCP has occurred since MSC stage 1 where the entire basin was already laying above sea level.

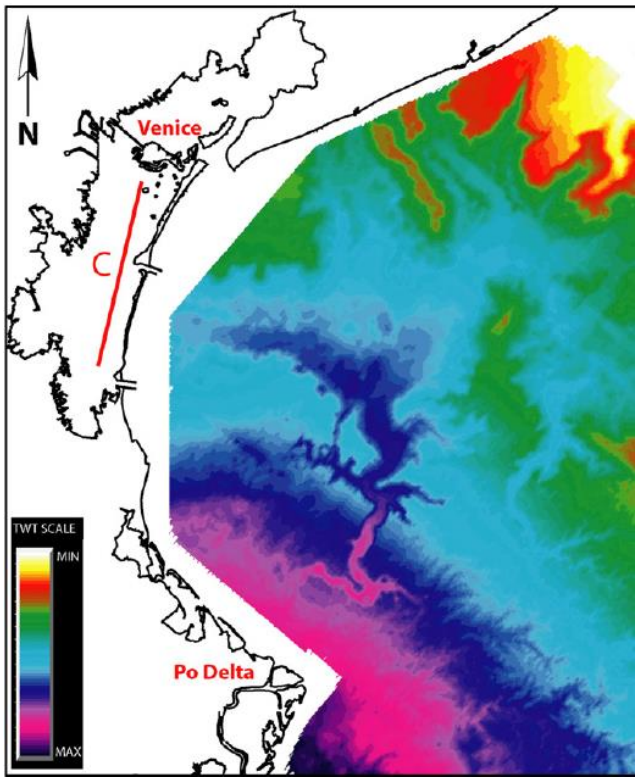


*Figure 6.1: Structural map of the MES in the Northern Adriatic Sea (modified from Ghielmi et al., 2013).*

**Scenario i** (BU deposition): during MSC stage 1, evaporites deposition, with a total thickness of more than 200 meters, occurred in the entire Adriatic Sea area except at the top of the carbonate platforms. Ghielmi et al. (2013) hypothesized more than 900 m of sea-level drop during MSC stage 2. Thus, considering the pre-existing shallow marine condition of the area, this drop would allow the complete erosion of the BU and part of the pre-Messinian sequence. A severe sea-level drop is recorded in the nearby AdCP, where incised paleo-valley reached 500 m of depth, subsequently filled by Pliocene sediments (Spelic et al., 2021). Moreover, the presence of BU is attested, as

observed by Ghielmi et al. (2010, 2013) in onlap on the AdCP. Toward the Central Axis of the Adriatic Sea, evaporites are not preserved due to a hypothetical peripheral Dinaric bulge that exposed the evaporites (Ghielmi et al., 2013; Rossi et al., 2015). Hence, the combination between the paleo-drainage from the Po Plain and the eastward migration of the Apennine chain which tilted the Adriatic foreland allowed the preservation of BU, which was subsequently covered by more than 1000 m of terrigenous Plio-Pleistocene sediments.

**Scenario ii** (partial gypsum deposition): Considering the extent of the MSC stage 2, spanning in time only for about 50 ky (Clauzon et al., 1996b; Roveri et al., 2014b), the widespread MES, and paleo-drainage systems in the area, it could be hypothesized that the Gulfs of Venice and Trieste and the AdCP where already exposed since the beginning of the crisis. Tectonic configuration of the external Dinarides bulge and Alps combined with the sea-level drawdown and evaporation, along with mechanisms of isostatic adjustment in the subsequent phases, brought a widespread incision of the Adriatic foreland and AdCP with several incised valleys (Ghielmi et al., 2015; Amadori et al., 2018). Infilling of this valley occurred in the Lago Mare and Zanclean phases, characterized by marine ingression in the entire basin (Zecchin et al., 2017). On contrast, in Ravenna/Rimini foredeep deposition of BU occurred, due to an initial tilting or a differencial subsidence of the foredeep which brought evaporites in a deeper position. Moreover, paleo-drainage from the Po Plain, allowed the preservation of the BU.

## 6.2 Central Adriatic Sea

The prevalent pattern in the Central Adriatic is characterized by the BU deposition. However, in the entire area, differences in the BU top expressed as TES and TS are observed. In order to explain what are the relationships between the MSC and the basin, the morphological features (e.g., diapirs, canyon) described in Chapter 5 have been considered.

### 6.2.1 Mid Adriatic Ridge and MSC

Above the MAR, the TES is rarely substituted by the MES (Fig. 5.4, 5.5, 5.7, 6.2). According to observation made in the area, the line B-417 (Fig. 6.2) was selected to perform the flattening technique, in order to visualize a pre- and post-MSC evolution of the Adriatic Sea.

Line B-417, located in the central Adriatic Sea, shows the Adriatic foreland tilted becoming the Pescara foredeep. Three different structures, interpreted as diapirs producing the MAR, are visible along the tilted foreland. Fratello-001 (located outside the line in Fig. 3.9) calibrates the MSC unit below 400 m of Plio-Pleistocene sediments. At the same time, Esmeralda-001 and Edmond Ter-001 (Fig. 6.2) calibrate the northeastward thickening of the BU, from 50 m to 117 m. The MSC unit is recognized at 0.5 s TWT below the seafloor in the north-eastern anticline structure.

Flattening the Cineritic Layer (Fig. 6.2C), approximately dated near the top Pliocene, may allow some results about the diapirs activity: BU is generally present with a variable thickness (Fig. 5.3, 5.4, 5.5) only locally completely eroded (Fig. 5.6, 5.7, 6.2) at the top of diapirs or in the canyons. Completely eroded BU at the diapir top, indicates that the structure was already active during the MSC (Fig. 6.2C), while preserved and constant thickness above the diapir, indicates that its activation occurred after the MSC.

It is significant to highlight that some diapirs activation occurred throughout the Pliocene and Pleistocene and could have brought the BU in subaerial exposure (Fig. 6.2C) after the MSC. Overall, I consider that portions of the evaporites could be affected by post-MSC emersion and erosion due to halokinetic movement. Consequently, erosion was not only related to the sea-level fluctuation.

In contrast with the high grade of erosion shown in the Central Adriatic axis, the BU in front of the Apennine presents a smooth surface without evidence of erosion (TS) (Fig. 6.2). This should indicate the presence of a relative deep basin, never exposed to subaerial erosion and filled by sediments coming thank to the paleo drainage surrounding the basin (Dinarides and Alpine chains).

Far effect of the Apennine chain during the MSC creating an initial tilting of the Adriatic foreland and the future Pescara foredeep basin is doubtful. Seismic evidence of a thin layer above the MSC unit, laterally eroded by a TES, was observed by Del Ben and Oggioni (2016). A flat-lying reflector above the MSC surface and unit indicates an undeformed foreland during the Late Messinian and Early Pliocene; deformation and tilting in the current Central Adriatic Sea occurred later, in the Pliocene. Nevertheless, a Messinian depocenter was present in the Pescara basin area, located between the two platforms, and collecting the water from the surrounding orogens. The continuous TS is present only in a localized area and laterally changes in the TES on the MAR, indicating an exhumation condition for this structure (Fig. 6.2).

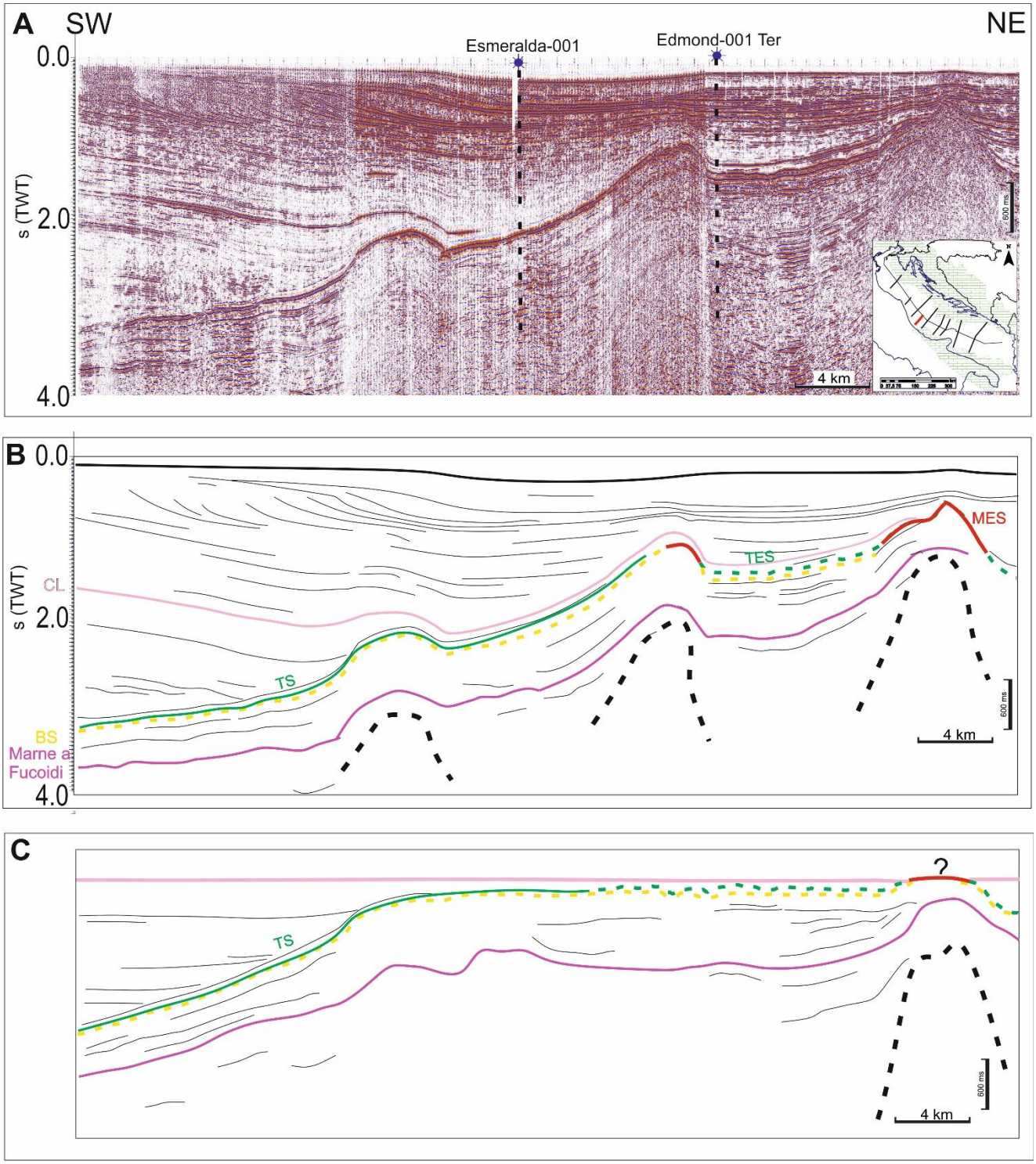


*Figure 6.2: Line B417 (position in figure 5.1) shows the Central Adriatic Sea evolution of diapirs using the flattening of the Cineritic Layer (CL), boreholes are described in figure 3.9. A) Line without interpretation; B) Line drawing, the CL horizon is in pink; dashed green MES; dashed yellow BS; red MES; purple Marne a Fucoidi marker; C) Flattening of the CL shows that not all the diapirs were active at the same time. Tilting linked to the E-ward migration of the Apennine Chain is evident in the SW portion of the section.*

### 6.2.2 Paleo-drainage

Several incisions related to canyon systems (MES) were observed in the Central Adriatic Sea (Fig. 6.3). Even in absence of data about the development of a drainage systems, cannot be excluded that subaerial exposure could have been occurred. This work has documented for the first time the presence of at least three new channelized systems (Fig. 5.2, 5.5, 5.6, and 6.3). Their peculiar paths were mainly conditioned by the MAR diapirs that have directed and deviated the water stream. The streams cut through the MAR structure (Fig. 6.3A), following the shape of the diapiric resurgence (Channel 6.3B). This could indicate which structures of the MAR were already active during the MSC and which were belatedly activated. As shown in the structural time map (Fig. 6.3) channel-1A bordered the NW-SE isolated platform calibrated by Carlo 2 (ViDEPI), while it changed direction southward, cutting two smaller MAR structures. Differently, Channel 2A and 3A cut different MAR sectors and presented a transverse drainage network, suggesting that the structure probably uplifted after the MSC. Moreover, we can observe that Channel 3A changes direction at the foot of the AdCP margin.

The channelized systems end in front of the External Apennine chain; however, we doubt the possibility of an Apennine proto-foredeep or an Apennine far effect in the area of the modern Pescara foredeep. In support of the thesis of the paleo-drainage ending in the modern Pescara foredeep, the geometry of the high-amplitude package reflectors (Fig. 5.12) may indicate the presence of a small fan-lobe at the end of the paleo-canyon. Part of the eroded gypsum was transported and re-sedimented in the fan, creating a strong amplitude signal (Fig. 5.12).

#### *Hypothesis of paleodrainage water flows*

Flow direction is hypothesized considering:

1. The AdCP, already exposed in the pre-MSC, with a large paleo-valley incision above it (Wrigley et al., 2015; Scisciani and Esestime, 2017), and this suggests a freshwater input in the Adriatic Sea from the Dinaric Chain. Similar morphologies were also recognized in the Kvarner area (Spelic et al., 2021);
2. The SE boundary between the Central and South Adriatic basin, corresponding to the Gargano-Palagruza threshold (Bache et al., 2012; Pellen et al., 2017, 2022) and the structural high of the Ombrina-Rospo plateau (ApCP), would have represented a threshold for the paleo-drainage;

3. The documented non-eroded BU (TS) in the Pescara foredeep suggests that water drainage preserves it.
4. The seismic evidence of a thin Lower Pliocene strata which parallelly covers the MSC parallel reflectors (Del Ben and Oggioni, 2016), indicates that no deformation occurred during and immediately after the Messinian;
5. The high-amplitude seismic package (Fig. 5.12) observed at the end of the study area would suggest the presence of small lobes that convey eroded gypsum (RLG);

Moreover, theories of mixed freshwater and seawater condition are upheld by Sr isotopic analysis of gypsum fluid inclusions and gypsum-bound water (Muller and Mueller, 1991), previously discovered in the Piedmont Basin (Dela Pierre et al., 2011; Natalicchio et al., 2014). These suggest that marginal basin gypsum formed from low-to moderate-salinity water masses (5 - 60 ‰) rather than from high-salinity brines (130 - 320 ‰) (Aloisi et al., 2022, Guibourdenche et al., 2022). Low salinity fluid inclusion supports the hypothesis of a paleo-drainage system which might indicate that the evaporites sedimented in a close basin, where the hydrological budget of freshwater runoff was higher than evaporation, supporting the possibility of a never exposed area, even if it was in restricted conditions.

Considering the points and the hypothesis mentioned above, I interpreted the flow path as SW-directed, from the structural high of the AdCP, forced by the SE structural high of the Gargano-Palagruza and ApCP. In the Pescara foredeep, due to constant freshwater flow, evaporites never underwent subaerial exposure.

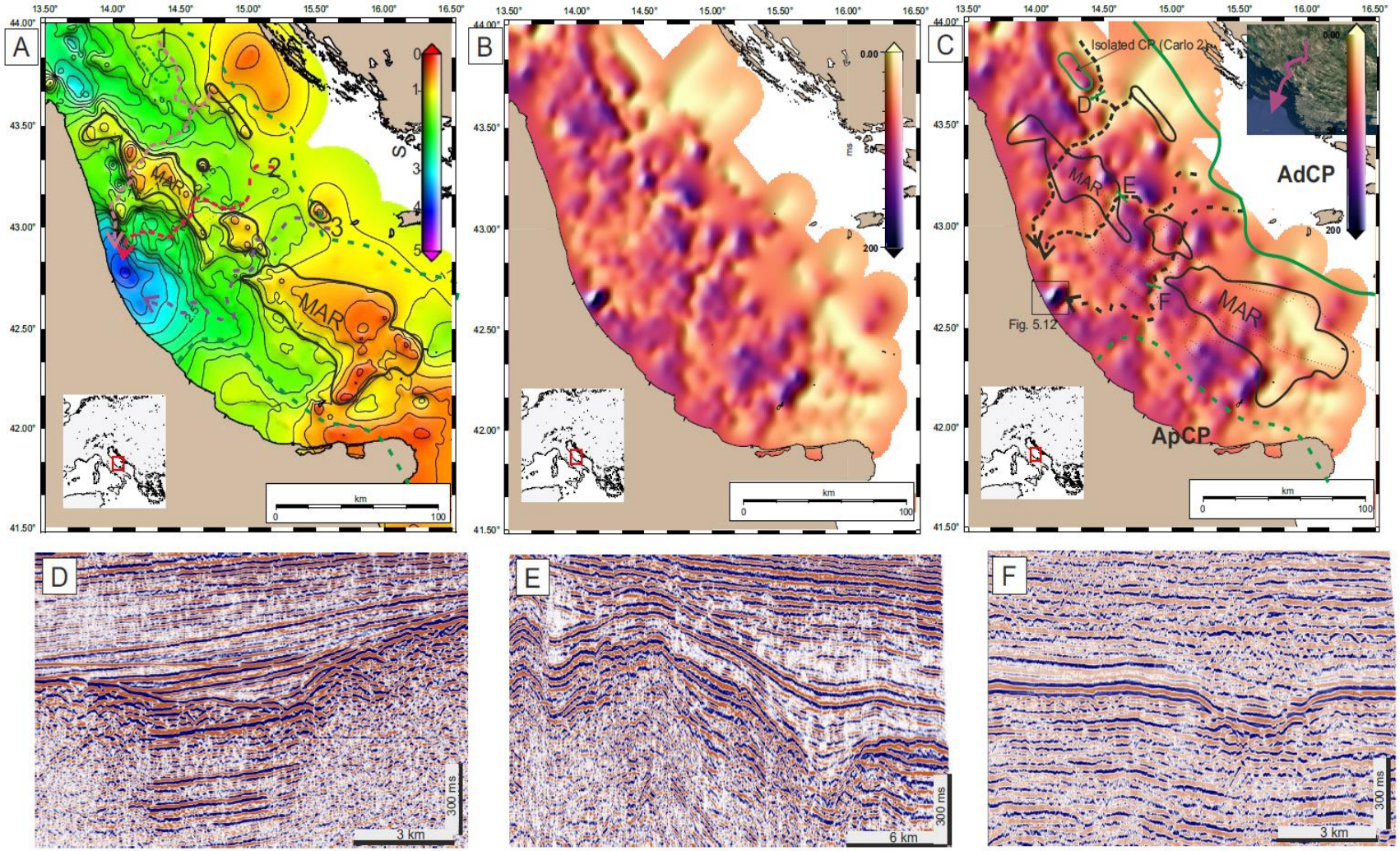


*Figure 6.3: Channel systems defined in the Central Adriatic Sea show clear erosional truncation of BU; A) channel 1 follows the flank of the Carlo-001 isolated platform, then turns westward toward the Apennine front; Channel 2 is deviated by the central portion of the MAR, and prosecute Southwest ward; Channel 3 cuts the MAR and changes direction in the proximity of the northern margin of the ApCP (Ombrina Rospo Plateau) flowing toward the Apennine front. B) BU isopach map; C) BU isopach map interpreted; D, E, F) seismic zooms of the interpreted channelized systems.*

### 6.2.3 Ombrina Rospo plateau

The Ombrina Rospo plateau (Fig. 2.11) represents the north-eastern part of the AdCP (Santantonio et al., 2013), corresponding to the SE edge of the Central Adriatic Sea. It is characterized by the presence of BU above the carbonate platform, as shown by the: Cristina-001 well that records more than 100 m of evaporites (Fig. 3.9, 5.5, 5.6). The platform shows tectonic re-activation during the Late Cretaceous, when a NW-SE normal fault system originated a fault-bounded through called "Casalbordino Corridor" by Santantonio et al. (2013). The western part of the Ombrina-Rospo plateau developed as foredeep basin before the MSC because of the eastward migration of the Apennine Chain (Patacca and Scandone, 2007, Patacca et al., 2008). Tectonic activity and sea-level changes during the MSC may have disconnected the Ionian basin from the Central Adriatic Sea (Manzi et al., 2020). Eastward migration of the Apennine chain and the flexure of the plateau produced, as a conseguence the flysch deposits occurred before the MSC. This is followed by a shallow marine environment during stage 1 of MSC, allowing the BU deposition above the plateau. Nevertheless, the seismic signal shows erosion of the evaporites (Fig. 5.5, 5.6). In contrast, in the deeper pelagic domain, the thickening of the evaporites is evident (Fig. 5.5, 5.10). Moreover, East migration of the Apennine re-activated pre-existing fault during stage 1. This effect is recorded by the Cristina-001 well (Fig. 3.9) with an extraordinary Messinian evaporites thickness of 112 m above the thin Miocene sequence covering the ApCP. The nearby borehole above the platform (Simona-001, Branzino-001, Stella-001 Fig. 3.9, 5.6) indicates a thickness of BU calibrated in some tens of meters (respectively: 60 m, 52 m, 123 m).

### 6.2.4 Post-MSC evolution (example from line B408)

The Plio-Quaternary events in the Adriatic Sea was mainly influenced by Apenninic tectonics, showing some localized structural complexity due to the Conero structure (Fig. 2.11). Line B-408 (Fig. 6.4) is 53 km long with SW –NE direction in the Italian offshore. It crosses the external Apennine front and, toward west, an isolated carbonate platform calibrated by Carlo-001 well (Fig. 3.9). TS surface in the SW portion of the line tops a BU thinner than 20 ms TWT. Deformation due to compression of the chain creates a depocenter in the SW part of the profile that in the area captured a canyon. In the central part, the MSC surface sinks into the basin, displaying a thickening of the BU to 100 ms partially eroded (TES). Proceeding NE-ward, ramping above the Carlo

structure, a thinning of BU with an incision above the structural high seems to be sited on a horst bounded by faults.
The Plio-Pleistocene succession shows some interesting features that allow us to understand the step of the basin deformation after the MSC. Fig. 6.4A highlights some main Pleistocene horizons, which were interpreted (in B) as P3 (yellow horizon), P2 (light blue horizon) and P1 (orange horizon), and the Late Pliocene high-amplitude negative polarity Cineritic Layer (pink horizon).

Overall, the Plio-Pleistocene succession shows clinoforms geometry downlapping toward NE, while underlying layers, included P2, onlaps the P1 horizon. In figure 6.4A, the orange layer topped by P1 and the blue layer topped by P2 represent two sedimentary wedges with opposite (respectively northeast ward and southwest ward) pinchout direction. From these results, we can assume that i) the orange layer deposited during the Apennines migration, when the frontal chain had not yet reached the current position and only produced a westward tilting of the foreland; ii) the blue layer deposited during the frontal chain deformation which uplifted the western part of the area crossed by the profile. This uplift also continued after P2 and P3 and terminated before the deposition of the clinoform.

The flattening of the P3 (Fig. 6.4 C) allows us to confirm that at that time deformation of the Apennine front was already active, uplifting the SW portion of the section. However, the NE portion was in a higher position than the chain front. BU experienced a mild deformation.

Flattening of the Cineritic Layer (Fig. 6.4 F) gives a broader look in the entire section, showing only initial faulting of the External Apennine front, suggesting that at the end of the Pliocene the BU was only mildly deformed. Deposition during the MSC unit was flat in the Central Adriatic Sea, as testified by parallel internal reflectors of BU.

Performing the flattening technique, I can infer some main evolutionary steps of the Apennine migration:
At P1 time, the front was far from the position observed in the section; however, the initial SW-ward tilting induced by the chain migration, created the accommodation space for the P1 wedge in the paleo-foredeep.
At P2 time, an initial uplifting of the frontal thrust is observed, generating an inversion of the tilting, and the discharge of sediments toward east in the Adriatic basin.

At P3 time, the external Apennine front was affecting the BU, uplifting the SW portion of the section and deforming the area.
All the Pleistocene sediments onlap the Carlo structure along the Mesozoic-Eocene isolated platform margin, while the huge uplift of the Apennine chain produced its erosion and deposition (1114 m of Pleistocene sediments in the Carlo-001 well) that overcomes the isolated carbonate platform.

In summary, in this portion of the Central Adriatic Sea, the effect of the Apennine chain migration and consequent tilting was active since the Pliocene, while faulting and uplift occurred during the Pleistocene time.

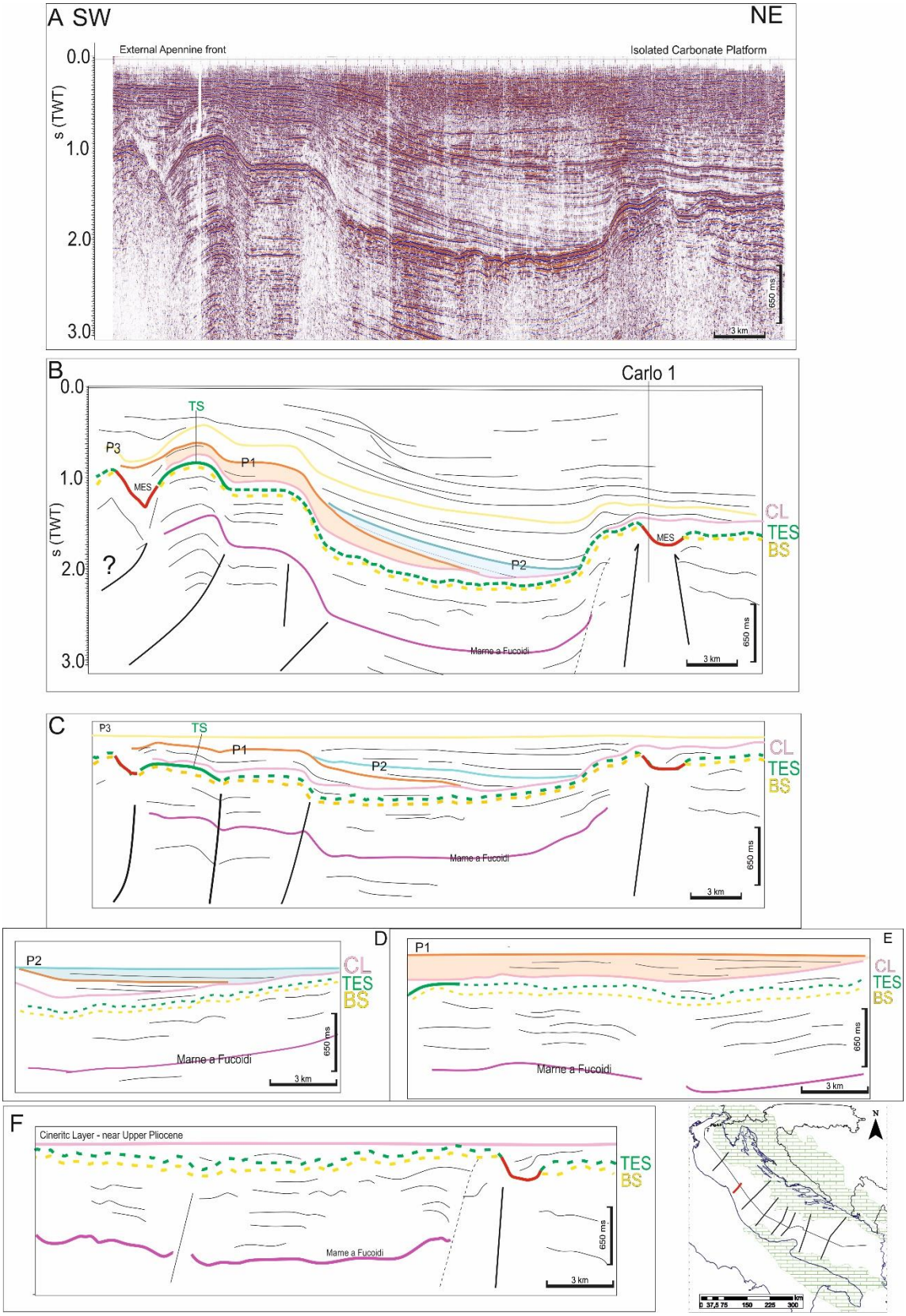


*Figure 6.4: Line B408, used as example of evolution in Central Adriatic Sea. A) Seismic profile B408, from the Ancona offshore toward NE, position in Fig. 5.1; B) Line drawing of the line; the main interpreted horizons are: P3 in yellow color, P1 in light blue, P2 in orange, Cineritic Layer CL in pink; TES in dashed green; BS in dashed yellow; MES in red; Marne a Fucoidi in purple; C) Flattening of the horizon P3; D) Flattening of horizon P2; E) Flattening of horizon P1; F) Flattening of the CL.*

## 6.3 Southern Adriatic Sea

The separation between the Central and Southern Adriatic Sea is represented by the Gargano promontory, an anticline structure related to Dinaric and Apennine contraction produced during the Neogene (Bertotti et al., 1999; Morsilli et al., 2017). Primary deformation and uplift occurred between the Late Miocene and Pliocene (Morsilli et al., 2017); a widespread erosional surface (MES) is evident above the Gargano-Palagruza high, which gently deepens southward (Fig. 5.7, 5.8, 5.9). Above the continental slope, MES is located in the shallowest position. In deeper domain, the BU is partially eroded (TS); from the middle axis of the South Adriatic Basin, it thickens toward the Albanian margin (Fig. 5.8, 5.9). Unlike the northern Ombrina-Rospo plateau, the ApCP in the Southern Adriatic Sea presents a different flexural response to the Apennine, related to the farther position of the Apennine chain and a possible forebulge effect of the platform (Patacca and Scandone, 2008). It is heavily eroded and covered by a thin Quaternary sequence without MSC deposits. MES documents a long-lasting exposure of the ApCP and the carbonatic slope.

In contrast, erosion is visible in the deep portion of the South Adriatic Basin (Fig. 5.8, 5.9) in the Italian and a few Croatian profiles. Widespread erosion in the ApCP and in the deep basin may indicate subaerial erosion during stages 2 and 3, while stage 1 deposition of BU evaporites thicken eastward, from 10 m in Sparviero-001 (Fig. 3.9) reaching more than 200 m in the Albanian offshore (Argnani, 2013). Anyway, we have to consider the strong eastward tilting of the Adria Basin due to the Dinaric compression during the Plio-Quaternary age, as well depicted by figures 5.8 and 5.9, suggesting that eventual emersion was due to a reduced sea level drop. Few exploration wells are available, and only one of these, Sparviero-001 bis (Fig. 3.9), intercepts a 10 meters of Messinian evaporites.

On the contrary, BU is recognized in the deeper eastern portion of the basin (Argnani, 2013), where more than 200 ms TWT of BU are recognized (Finetti, 1985).

Moreover, the tilted MSC surface and unit present a peculiar seismic response in the Croatian offshore (scattered, low to medium–amplitude reflector; Fig. 5.8) interpreted as possible karstification of the Messinian evaporites, which occurred when combined chemical and mechanical weathering dissolved the dense structure of gypsum. Opaque and transparent appearance may indicate the presence of minor density in the evaporites sediments produced by sinkholes in the gypsum succession. The high solubility of the gypsum ranges between 0.4 mm/yr and 1.0 mm/yr (Cucchi et al., 1998) and is enhanced by the weathering, which heavily affects the

structure of the gypsum. In the framework of the MSC, BU evaporites deposition most likely occurred in a shallow-water domain, which progressively decreased into a sabhka environment, with cyclic variation between humid and arid periods (Manzi et al., 2011, 2016; Roveri et al., 2014a; Perri et al., 2017; Borrelli et al., 2021), where drainage did not provide enough fresh water supply. To note that, Calligaris et al. (2019) demonstrate that in the fluctuating condition of the water level, the evaporite dissolution rate rises to 2.8 mm/yr, allowing the formation of fractures in the evaporites.

Erosion in the deepest portion of the Southern Adriatic Basin suggests that, before the Pliocene Albanides E-ward tilting of the South basin foreland, the paleo seafloor was in subaerial/shallow marine condition even in the southern Adriatic Basin. Configuration of a disconnected South Adriatic basin from the Ionian basin during the MSC comes from considering the geometry of the ApCP and its south-eastward extension toward the modern Albanian margin, outcropping in the Karaburun peninsula (Argnani et al., 1996; Ballauri et al., 2002; Nicolai and Gambini, 2007; Del Ben et al., 2015). Mocnik (2008) delineated a complex outline around the Merlo-001 well (ViDEPI, Fig. 2.12) where Messinian non-evaporitic sediments have been calibrated. Del Ben et al. (2015) and Brancatelli et al. (2022) hypothesize a threshold between the Ionian and Adriatic Seas during the Messinian, represented by the eastward ApCP extension to the Karaburun peninsula in Albania, across the Otranto Channel.

On the western side of the ApCP, Del Ben et al. (2015) highlighted a very similar stratigraphy of the eastern side, without evidence of BU but with a MES regionally distributed. To the west of the ApCP and of the Adria continental margin, the Ionian Basin and the Calabrian Arc present a different onset of the MSC characterized by the Calcare di Base formation (Rouchy, 1982, Rouchy and Caruso, 2006) and halite as main evaporitic lithology deposition during the MSC event.

### 6.3.1 Line F004 as model for the Southern Adriatic Sea

The effect of the Albanides/Dinarides chain, producing E-ward tilting of the foreland, is represented in figure 6.5 which exemplifies the evolution of the Southern Adriatic Sea. The Plio-Pleistocene succession onlaps the MSC surface, affected by tilting due to 40–45° of clockwise rotation of the Albanides / Hellenides front (Mauritsch et al., 1995; Speranza et al., 1995, van Hinsbergen et al., 2006; Argnani, 2013; Del Ben et al., 2015).

The MES, except for a small area in the middle of the section, is calibrated by Sparviero-001 (Fig. 3.9). Even in the deeper portion of the section, the horizon appears erosive, suggesting the condition of subaerial erosion during the MSC. The pink horizon onlaps the MSC surface in Figure 6.5 suggesting that the Adria foreland tilting occurred after the MSC when the W-ward migrating Albanides orogens created more accommodation space for the Pliocene deposits, which show a pinch-out geometry (Fig. 5.12, 6.5).

However, previous accommodation space appears to be generated in pre-MSC time. In particular, through the flattening of the TES, a thickening wedge of the Early Miocene succession toward the Albanides/Dinarides is visible (Fig. 6.5B, C). The wedge geometry is emphasized by the onlapping green horizon, interpreted as the top of Bisciaro Formation, which thickens in the Southern Adriatic Basin. Changes in the Schlier and Bisciaro thicknesses suggest a far effect of the Dinarides chain or differential subsidence affecting the Southern Basin creating more accommodation space before the MSC, allowing the higher accumulation of MSC evaporites in the Albanian offshore (e.g., Finetti, 1985; Argnani et al., 2013).

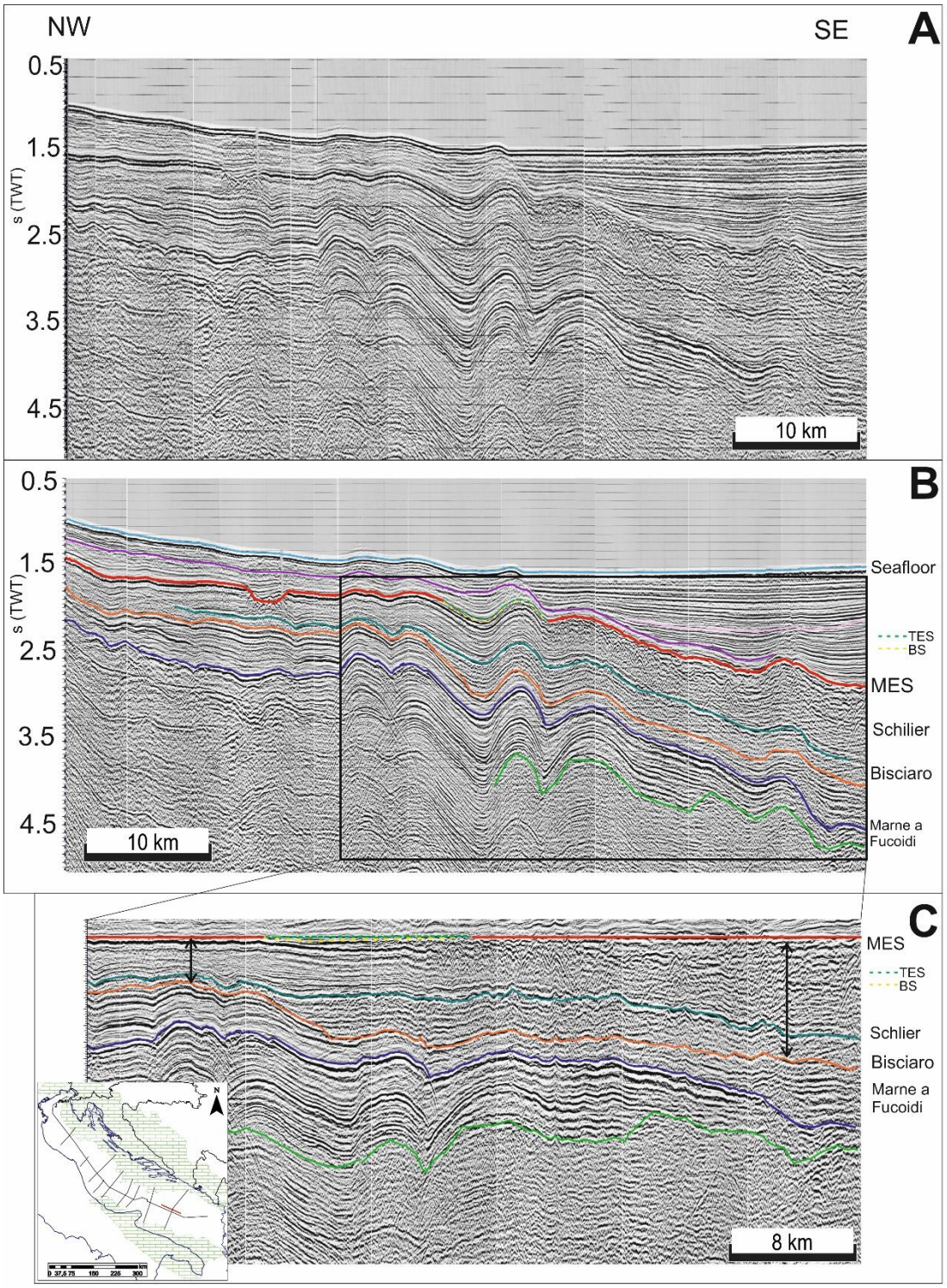


*Figure 6.5: Line F004, located in figure 5.1, describes the evolution in the central axis of the Southern Adriatic Sea through the flattening technique. A) Interpreted Line F004: light blue as the seafloor; red as the MES; green Schlier base; Orange Bisciaro Base, Blue Marne a Fucoidi; the pink horizon highlights the onlapping geometries of the Pliocene succession above the MES, indicating the foreland tilting toward the Albanides; C) Flattening of the MES highlights the SE-ward thickening of the Pre-MSC unit, this suggests that the basin was already influenced by the far effect of the Dinarides/Albanides.*

## 6.4 The Lago Mare Formation

In the framework of this work, I primarily focused on Stages 1 and 2 of the MSC event, ignoring the last stage of the event and the reflooding of the Adriatic Basin.

Bache et al. (2012; 2015) proposed a three steps model for the Mediterranean Sea, characterized by a "low-salinity crisis," showing (bio)geochemical evidence of substantial brine dilution and brackish biota-bearing terrigenous sediments (sub-stage 3.2 or Lago-Mare phase, 5.42-5.33 Ma) deposited in the Mediterranean Sea. This was characterized by relatively large amounts of riverine and Paratethys-derived low-salinity waters (Andreetto et al., 2021). Unfortunately, the seismic data available for this work did not reach the necessary seismic resolution needed for recognized the presence of the Stage 3 formation. However, the large amount of borehole data suggests that this phase is present in the Adriatic Sea and as in the rest of the Mediterranean realm. Figure 6.6 collects the information from the exploration well drilled in the Adriatic offshore that calibrated the presence of the Colombacci or Fusignano Formations that I associate to the Lago-Mare formation. However, it is essential to highlight that the Lago Mare phase is not consistently recognized by previoous authors, and this could be due to the scarce interest of these sequences in the past (e.g., early 60’s): few boreholes recognized the brackish environment above the evaporites, but early stage of the MSC debate did not suggest to correlate their formation to Stage 3.

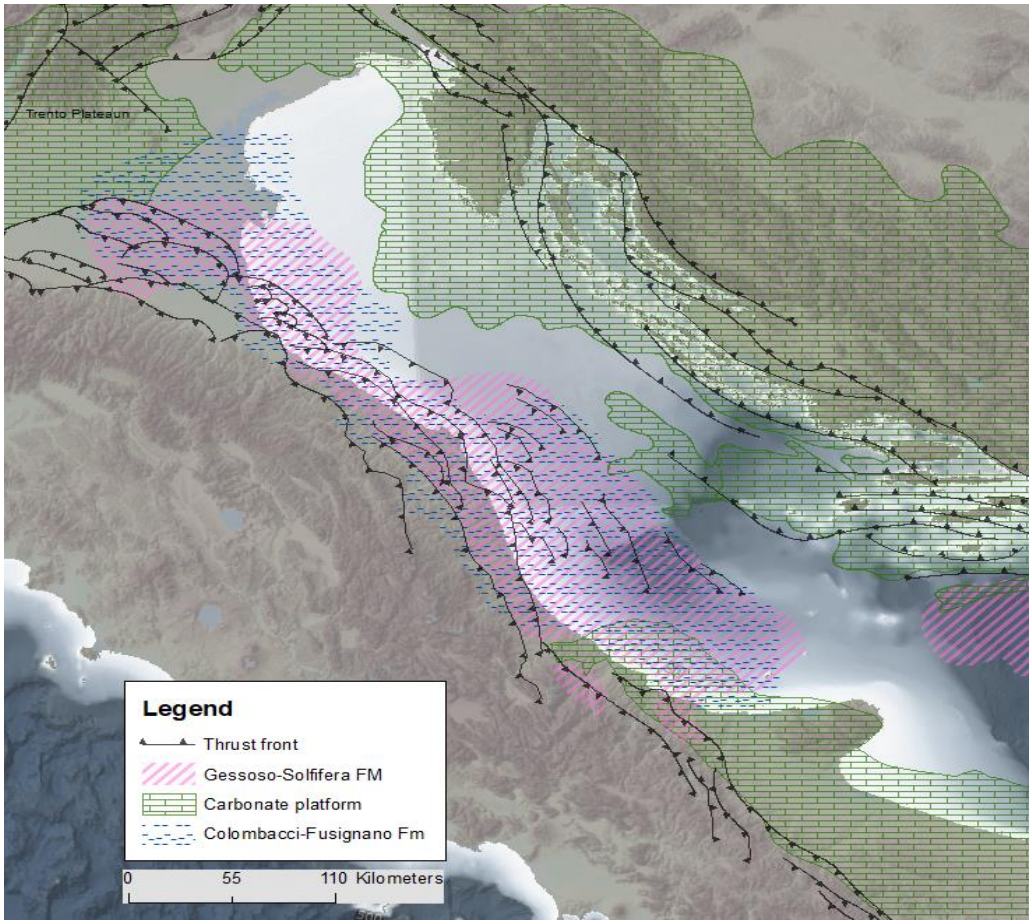


***Figure 6.6*** *The boreholes analysis have allowed to reconstruct the spatial distribution of the Fusignano/Colombacci formations in the Adriatic Sea.*

## 6.5 Role of the Adriatic Sea in the Mediterranean MSC

I propose a new paleogeographic map where the Adriatic Sea was never completely drowned; instead, continental runoff from the surrounding orogens (Dinardes and Alps) created a mixed marine and freshwater basin in the area of the modern Pescara foredeep. Continental runoff maintained the basin in underwaer condition, "protecting" the BU from subaerial erosion throughout the MSC until it was flooded in the Zanclean.

**pre-MSC**: The Adriatic Sea was connected to the Mediterranean, particularly to the Ionian basin, through the current Otranto strait, and the Casalbordino corridor between the Apennine chain and the ApCP (Fig. 6.7A). This corridor is recognized in several works (e.g., Santantonio et a., 2013; Manzi et al., 2020) as an intra-platform basin that subsides during the E-migration of the Apennine chain (Manzi et al., 2020). Restoration of the original position of the Apennine chain (Patacca and Scandone 2007, Del Ben et al., 2008) indicates a retrodeformation of more than 100 km in front of the ApCP. Nevertheless, Manzi et al. (2020) reported the presence of Messinian deposit in the Bradanic Through, interpreted as a shallow-to-deep marine basin connected to the Central Adriatic Sea. The Northern Adriatic Sea and the Po Plain were in underwater condition, as well as the Umbria-Marche basin and the Ombrina Rospo-Plateau. The drainage system from the Alps brought freshwater in the Po Plain and along a narrow foredeep of the Apennine chain, where silico-clastic deposits of the Marnoso-Arenacea Fm. (Ricci Lucchi, 1975) and Laga Fm. (Ricci Lucchi, 1975) sedimented. From the eastside, the freshwater runoff was supplied by the Dinarides. During this phase, a mixing of marine and continental water characterized the signature of the water.

**Stage 1 of the MSC**: initial sea-level drawdown, partially disconnected the Adriatic Sea from the Mediterranean Sea (Fig. 6.7B). The Gessoso-solfifera formation (BU) started to sediment, leaving the peculiar isotopic Sr and S signature (Natalicchio et al., 2014, Aloisi et al., 2022, Guibourdenche et al., 2022), indicating the presence of mixed water. As highlighted by the seismic signal of the MES, high-grade erosion and absence of evaporites may promote the hypothesis that part the northern Adriatic Sea, the Gulf of Trieste and Gulf of Venice areas, were already exposed to subaerial erosion during Stage 1 (Fig. 6.8). On contrast, in the Rimini and Ravenna foredeep (Fig. 2.9), deposition of BU occurred. Paleo-drainage of the Po Plain (Ghielmi et al., 2013; Amadori et al., 2018), contribute to the freshwater input. Contemporaneously, in the Central and Southern Adriatic Sea, evaporites were deposited (Fig. 6.8), in the area that extends from the Conero (Fig.

2.11) to the South Adriatic Basin (Fig. 2.12). Further sea-level drawdown triggered the restriction and disconnection with the Mediterranean, isolating the Adriatic Sea from the Ionian basin. The Ionian underwent different evaporite precipitation, mostly halite, indicating a different sedimentological environment.

**Stage 2+3 of the MSC:** Hypothesis of a sea-level drowning between 1000 – 2000 m (Amadori et al., 2019, Ghielmi et al., 2018, Camerlenghi et al., 2019, Heida et al., 2022) and consequent isostatic rebound, would suggest a complete disconnection from the Mediterranean basin during stage 2 and 3 (Fig. 6.7C). Isostatic adjustment enhances the erosion of the accumulated BU evaporites in the central axis of the Adriatic Sea (MAR, AdCP and the Ombrina Rospo plateau) and in the South Adriatic Basin. However, portion of the Central Adriatic Sea (modern Pescara foredeep) was never completely desiccated, due to the continental runoff from the AdCP and the Umbria Marche Basin.

With the progressively sea level drop, evaporation, isostatic adjustment, and disconnection of the Adriatic Sea basins occurred, dividing the water mass (Bache et al., 2012; Pellen et al., 2017, 2022). The northern Adriatic Sea and portion of the Po Plain remained exposed to subaerial erosion; Alpine and Dinaric fluvial system drainage brought water into the Ravenna/Rimini foredeep and in the Central Adriatic Sea, following the Pre-Messinian Apennine and Laga foredeep path. The Central Adriatic Sea was separated from the Southern Adriatic Sea through the Gargano-Palagruza structure, which represented a threshold (Pellen et al., 2017, 2022). The Central Adriatic Sea was partially exposed, in its central axis, while, due to continental runoff, part of it was protected from the subaerial erosion, as testified by the TS.

The south Adriatic Sea underwent partial subaerial exposure as TES, and eroded evaporites are recognized (Fig. 5.9). The connection between the Southern and Central Adriatic Sea may be possible due to one incised system in the continental slope, which may indicate occasional spilling of water in the deeper basin, where the seismic signal of the MSC surfaces appears less erosive. A second threshold, disconnecting the Adriatic Sea from the Ionian basin, may be recognized in the southern ApCP margin (Del Ben et al., 2015; Fig. 6.7C), representing a sill between the South Adriatic Basin and the South Apulia Basin. The sea-level drawdown also exposed the Western margin of the AdCP, represented by shallow marine domains and isolated platforms (e.g., Monte Alpi), and subsequently incorporated into the Apennine thrust belt (Del Ben et al., 2015; Manzi et al., 2020). The end of the MSC occurred with the refilling of different depocenters in more than one pulse.

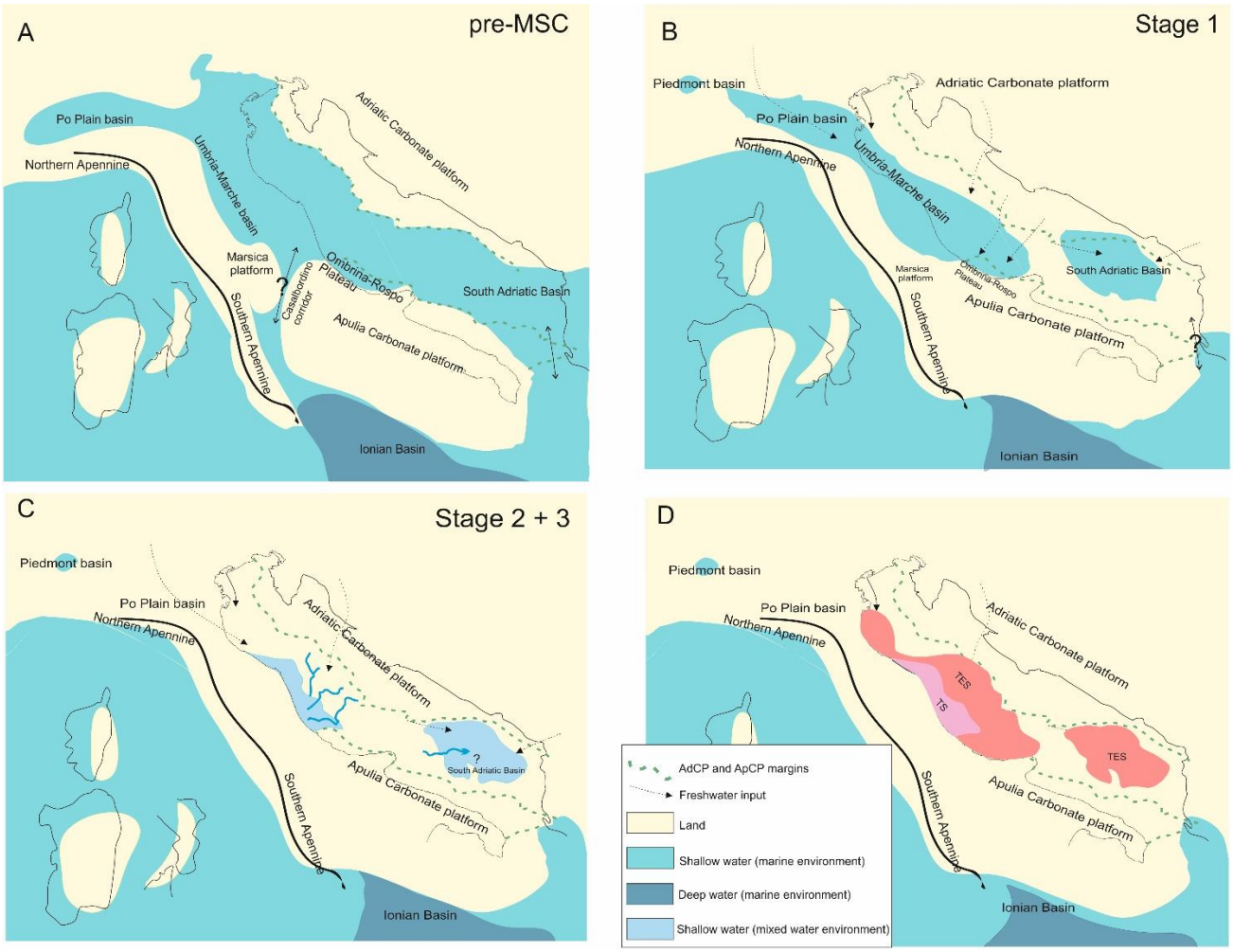


*Figure 6.7: Paleogeographic evolution of the Adriatic Sea before and during the MSC. The map is obtained by combining paleogeographic information from Stampfli (2005), Nicolai and Gambini (2007), Patacca and Scandone (2007), Del Ben et al. (2010). A) Pre-MSC time illustrates a connection between the Adriatic Basin and the Ionian Sea through the proto-Otranto strait and the Casalbordino corridor. Freshwater supplies were flowing from the Alps S-ward inside the Marche-Umbria basin. B) with the MSC stage 1 the sea-level drawdown started, connection with the Ionian Sea gradually decreases, disconnecting the Adriatic Basin from the rest of the Mediterranean, and freshwater inputs from the Alps and Dinarides continued and fill the Po Plain and Central Adriatic Sea. C and D) MSC acme leaves the Adriatic Basin with several small disconnected basins, which did not go to subaerial exposure due to the freshwater input; this area is recognized thanks to the TS above the MSC evaporites.*

To summarize the different results discussed in this work, we use the three different maps represented in Figs. 5.10, 5.11, 6.8. These maps are complementary because they describe different points:

Fig. 5.10 is the structural map of the base of Plio-Quaternary: it depicts the regional deformation of the top Messinian occurred during the Plio-Quaternary;

Fig. 5.11 is the isopach of the Messinian sequence, that is the thickness in TWT: it depicts the deformation occurred during the MSC added to the effect of erosion;

Fig. 6.8 depict the depositional domains more or less affected by erosion.

The comparison of these maps evidences the different paleogeographic realms present in the Adriatic Sea during the MSC (Fig. 6.8):

- In the northern portion, where a widespread MES is observable (Fig. 5.11), subaerial exposure is testified. In the area the Alpine and Apennine Chains face each other toward a common foreland. Except for the AdCP (i.e., Istrian Plateau), which was in uplift due to the External Dinarides (Vlahovic et al., 2005) and shows large incisions and paleo-valleys (Spelic et al., 2021), during the MSC erosion affected a flat-lying foreland. In the Trieste Gulf (NE extremity of the section in Gig. 5.2) before the MSC, the Dinaric compression produced the NE-ward tilting of the foreland and the deposition of the Eocene Flysch, while, after the MSC, the Northern Apennine's migration caused the SW-ward foreland tilting. The tilting was followed by the Plio-Quaternary sedimentary wedge and brought the MSC surfaces to the current deep position (blue color in the North Adriatic Sea in Fig. 5.10). In the Rimini and Ravenna foredeep, still during the MSC, the Apennine foreland tilting produced a deeper domain, where the BU and the Upper Messinian Colombacci-Fusignano Fm. deposited (Figs. 5.3, 5.11, 6.6) as calibrated by boreholes. More than 3000 m of Plio-Quaternary sediments covered the Messinian evaporites with deposits sourced from the Po Plain drainage system (Fig. 5.10).

- In the Central Adriatic Sea, a more extensive evaporite deposition occurred. The MSC seismic package with sub-parallel reflectors suggests that the Messinian evaporites deposited in a flat-lying external foreland. Structural highs are observable in the AdCP and partially in the MAR (Fig. 5.10, 5.11, 6.8), where the MES is present. The highest accumulation of BU occurred in the NE flank of the deep salt structures of the MAR (Fig. 5.11) due to erosion of the anticlines top, already uplifting before, but also during and after the MSC. The MAR, better defined than previously published, shows a complex structural

pattern specially produced during the Plio-Quaternary (as testified by Fig. 5.10), but hardly depending by the MSC erosional effect. Also above the Ombrina-Rospo plateau a large thickness of BU is calibrated by boreholes (Fig. 5.11), partially reduced by subaerial erosion occurred during stages 2 and 3 (Fig. 6.8). In the western area the deep salt structure of the MAR is not observed, so that no uplift occurred and absence of erosion (TS) is interpreted (Fig. 6.8), due to a never exposed portion of the Adria foreland. In support of this hypothesis is the presence of the canyon systems sourced from the AdCP and directed toward SW (Figs. 6.3, 6.8): freshwater input in a endorheic lake (Fig. 6.7) preserved the BU from being eroded during the MSC acme. Interpretation of a thin package of parallel horizons of Early Pliocene sediments, directly overlying the MSC surface (Del Ben and Oggioni, 2013), corroborates this hypothesis. Tilting of the Adria foreland due to the East-ward migration of the Apennine Chain, creating the Pescara Foredeep, occurred during the Pliocene. The MSC surface are intact here observed in a deep position (Fig. 5.10).

- The Gargano promontory represents a structural high which uplifted during the Pliocene (Festa et al., 2014). The wide Messinian erosion interpreted in this work would confirm the Bache et al. (2012) and Pellen et al. (2017) suggestion of a sill already present during the MSC, separating the Central and the Southern Adriatic Sea.

- On the base of the abovementioned, the Southern Adriatic Sea would be disconnected from the rest of the Adriatic Sea (by the Gargano promontory) and from the Ionian Sea (by the ApCP). Above the ApCP, a widespread MES is observed, suggesting that the carbonate platform underwent subaerial exposure during the MSC. At the same time, Messinian evaporite deposition occurred in large amounts in the deepest portion of the basin (Fig. 5.11, 6.8). However, even in the South Adriatic Basin, evaporites appear to be eroded (Fig. 5.9), hypothesizing that the sea level drop during the MSC acme was several hundred meters. The absence of a large freshwater drainage system, able to maintain a brackish environment such as in the Central Adriatic, could have contribute to the temporary desiccation.

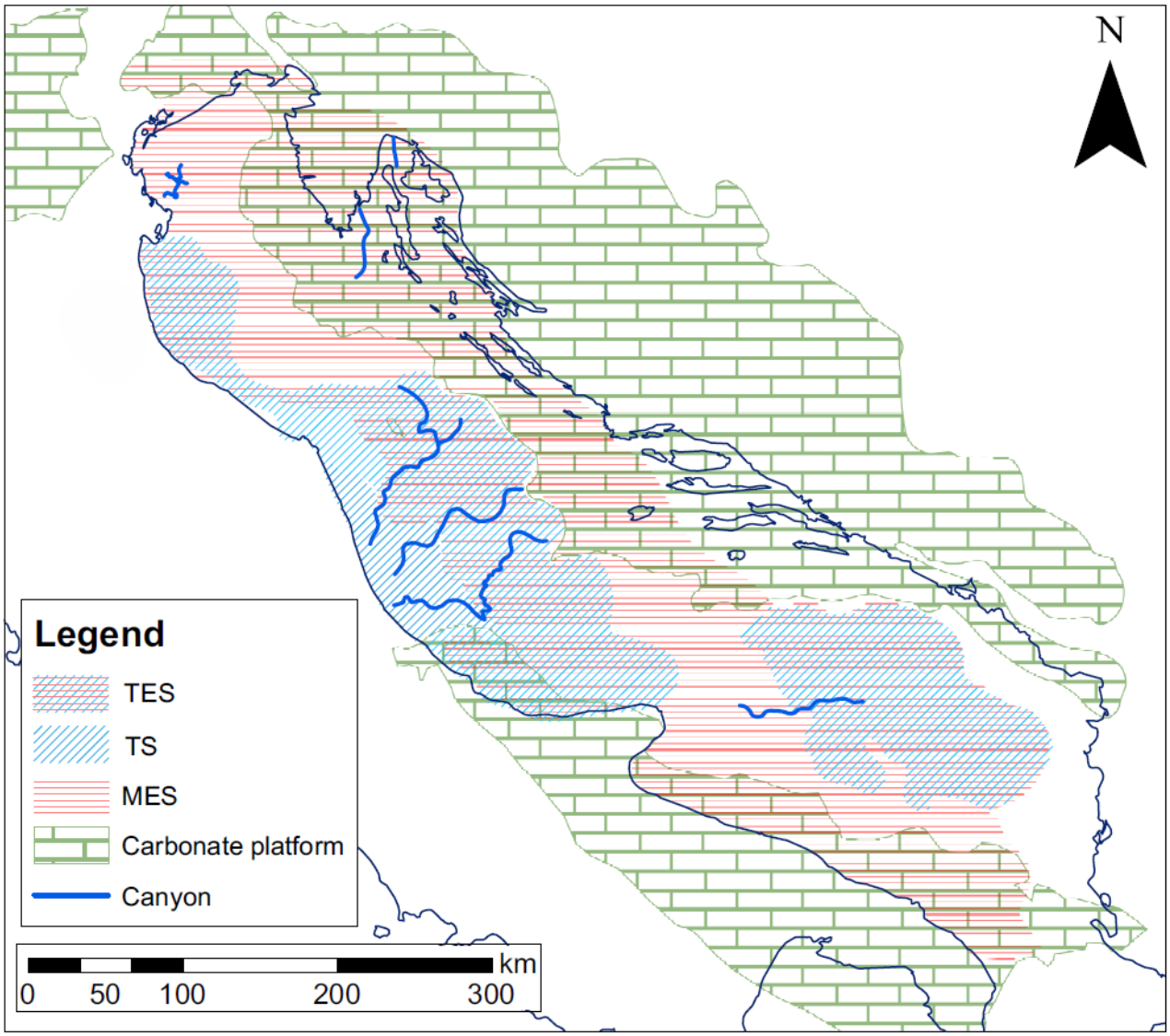


*Figure 6.8: Summarized map of the MSC surfaces and channelized systems in the Adriatic Sea. In the Northern Adriatic Sea, the two mapped canyons are from Ghielmi et al. (2013) and Spelic et al. (2021).*

# Conclusion

In this work I focus on the effects of the Messinian Salinity Crisis (MSC) in the Adriatic Sea, interpreting more than 10000 km of 2D seismic reflection lines, calibrated with a large amount of boreholes drilled in the study area since the ’50s.

The first objective of the PhD thesis was to analyze the MSC surfaces and units in the entire Adriatic Sea using the Kingdom Suite interpretation software. Ten transects have been selected in order to represent the different structural and tectonic evolution acting since the Mesozoic in the study area with their effect on the extreme events occurred during the MSC.

I divided the Adriatic Sea in three main areas based on the occurrence of the MSC on the dataset, which are:

- **Northern Adriatic Sea**: during the MSC it was mainly affected by subaerial erosion and formation of channel systems, where the widespread MES incised the AdCP and the Po Plain foreland, in particular in front of the Trieste and Venice Gulfs. Evaporite deposition occurred in the Rimini foredeep.
- **Central Adriatic Sea:** it was affected by the combined effect of deposition and erosion. In the area of the Pescara foredeep a TS is recognized above a regional constant thickness of the Messinian gypsum (non-erosional surface above the BU). Several channel incisions in this area are related to paleo-drainage systems.
- **Southern Adriatic Sea:** it was affected by a strong erosion on the ApCP. Evaporites (BU) are present and eroded (TES) along the margins of the South Adriatic Basin, whereas they are preserved with no evident erosion (TS) in the deeper basin.

Paleo-geographic reconstruction of the Adriatic Sea suggests that the Northern Adriatic Sea experienced subaerial exposure even at the beginning of the MSC, except for the area of the Rimini foredeep where BU deposition occurred due to the presence of a paleo-drainage system from the Po Plain and Alpine chain.

In the Central Adriatic Sea, three channelized systems (directed from NE to SW) were mapped in this work. The presence of paleo-drainage allowed to hypothesize that part of the Central Adriatic Sea never underwent subaerial exposure, preserving the BU from subaerial exposure.

Moreover, it can be hypothesized that the Central and Southern Adriatic Sea were disconnected from each other, due to the widespread MES along the lineament of the Gargano-Palagruza sill. The BU in the Southern Adriatic Sea shows a thickening toward the Albanian offshore, caused by the differential subsidence rate which started in pre-MSC time. Here however, the BU shows evidence of erosion on the basin margin.

Due to the geographic configuration of the Apulia Carbonate Platform and magnitude of the sea-level drawdown, I support the theory of a disconnection between the Southern Adriatic and the Ionian Seas.

Following the MSC, it is possible to affirm that the Adriatic Sea underwent different evolutionary steps. Boreholes calibration highlight the presence of a locally very thin Pliocene succession in the entire Adriatic Sea. The eastward-migration of the Apennine Chain covered and obliterated part of the MSC from the Late Pliocene (as inferred from the Cineritic Layer). The main effect of the Apennines eastward migration occurred during the Lower Pliocene, as testified by the regional tilting of the MSC reflectors, onlapped by Plio-Quaternary parallel reflectors. In the Conero offshore, which approximately separates the Northern from the Central Adriatic Sea, the deformation acme took place during the Pleistocene, when strong uplift of the external thrust brought up the pre-Pleistocene sequence including the Messinian layer. The Southern Adriatic Sea was affected by the Albanides orogenesis, as testified by the eastward foreland tilting during the Pliocene, where PQ sediments onlap the MSC unconformity.

A regional map describing the distribution of the different conditions of the Messinian layer BU in the study area is presented and can be summarized as follows:

- A wide area where BU is completely absent (MES), mainly due to non-deposition, mainly in the North Adriatic Sea and above the AdCP, or to non-deposition and erosion, mainly in the western part of the South Adriatic Sea.
- An area where BU is present and affected by partial erosion (TES) occurred in the last phase of the MSC, in the Northern Apennines foredeep, on the MAR and in the western flank of the South Adriatic Basin and on the Ombrina-Rospo Plateau.
- An area of preserved BU which, after deposition in deeper areas, was covered by Pliocene sediments and protected from erosion even when uplifted by compressive deformation, as in the Conero offshore.

Several Messinian channel systems have been reconstructed: they engrave the BU or, if this latter is absent, the pre-MSC sediments, with an east to west direction, testifying that the main drainage system went from the Dinaric Chain.

The presence of BU in the Northern Apennines foredeep suggests that there was a westward tilting in that area during the MSC. Despite the deep position of the MSC horizons, the same evidence is not found for the Central Adriatic foreland, which was almost horizontal, as shown by the regional constant thickness of BU in the study area, only laterally modified, due to the effect of deposition in an irregular basal horizon or due to the erosion that occurred during the last MSC phases.

# References


Aloisi, G., Guibourdenche, L., Natalicchio, M., Caruso, A., Haffert, L., El Kilany, A., and Pierre, F. D. (2022). The geochemical riddle of "low-salinity gypsum" deposits. *Geochimica et Cosmochimica Acta*, *327*, 247-275.

Amadori, C., Toscani, G., Di Giulio, A., Maesano, F. E., D'Ambrogi, C., Ghielmi, M., and Fantoni, R. (2019). From cylindrical to non-cylindrical foreland basin: Pliocene–Pleistocene evolution of the Po Plain–Northern Adriatic basin (Italy). *Basin Research*, *31*(5), 991-1015.

Amadori, C., Garcia-Castellanos, D., Toscani, G., Sternai, P., Fantoni, R., Ghielmi, M., and Di Giulio, A. (2018). Restored topography of the Po Plain-Northern Adriatic region during the Messinian base-level drop—Implications for the physiography and compartmentalization of the palaeo-Mediterranean basin. *Basin Research*, *30*(6), 1247-1263.

Andreetto, F., Aloisi, G., Raad, F., Heida, H., Flecker, R., Agiadi, K., Lofi, J., Blondel, S., Bulian, F., Camerlenghi, A., Caruso, A., Ebner, R., Garcia-Castellanos, D., Gaullier, V., Guibourdenche, L., Gvirtzman, Z., Hoyle, T. M., Meijer, P. T., Moneron, J., … Krijgsman, W. (2021). Freshening of the Mediterranean Salt Giant: Controversies and certainties around the terminal (Upper Gypsum and Lago-Mare) phases of the Messinian Salinity Crisis. *Earth Science Reviews*, 216, 103577.

Andreetto, F., Matsubara, K., Beets, C. J., Fortuin, A. R., Flecker, R., and Krijgsman, W. (2020). High Mediterranean water-level during the Lago-Mare phase of the Messinian Salinity Crisis: Insights from the Sr isotope records of Spanish marginal basins (SE Spain). *Palaeogeography, Palaeoclimatology, Palaeoecology*, 562, 110139.

Argnani, A., (2013). The influence of Mesozoic paleogeography on the variations I structural style along the front of the Albanide thrust-and-fold belt. *Ital. J. Geosci. (Boll. Soc. Geol. It.)*, Vol. 132, No. 2 (2013), pp. 175-185.

Argnani, A., and Frugoni, F. (1997). Foreland deformation in the Central Adriatic and its bearing on the evolution of the Northern Apennines. *Annals of Geophysics*, *40*(3).

Argnani, A., Favali, P., Frugoni, F., Gasperini, M., Ligi, M., Marani, M., and Mele, G. (1996). Tettonica dell'Adriatico meridionale. *Mem. Soc. Geol. It.*

Aubouin, J., Blanchet, R., Cadet, J. P., Celet, P., Charvet, J., Chorowicz, J., ... and Rampnoux, J. P. (1970). Essai sur la géologie des Dinarides. *Bulletin de la Société géologique de France*, *7*(6), 1060-1095.

Bache, F., Gargani, J., Suc, J. P., Gorini, C., Rabineau, M., Popescu, S. M., ... and Aslanian, D. (2015). Messinian evaporite deposition during sea level rise in the Gulf of Lions (Western Mediterranean). *Marine and Petroleum Geology*, *66*, 262-277.

Bache, F., Popescu, S. M., Rabineau, M., Gorini, C., Suc, J. P., Clauzon, G., J.L. Olivet, J.L. Rubino, M.C. MelinteDobrinescu, F. Estrada, L. Londeix, R. Armijo, B. Meyer, L. Jolivet, G Jouannic, E. Leroux, D. Aslanian, A.T.D. Reis, L. Mocochain, N. Dumurdžanov, I. Zagor chev, V. Lesić, D. Tomić, N. NamikCağatay, J.P. Brun, D. Sokoutis, I. Csato, G. Ucarkus, Z. Çakir, (2012). A two-step process for the reflooding of the Mediterranean after the Messinian Salinity Crisis. *Basin Research*, *24*(2), 125-153.

Bache, F., Olivet, J. L., Gorini, C., Rabineau, M., Baztan, J., Aslanian, D., and Suc, J. P. (2009b). Messinian erosional and salinity crises: view from the Provence Basin (Gulf of Lions, Western Mediterranean). *Earth and Planetary Science Letters*, *286*(1-2), 139-157.

Badley, M. E. (1985). Practical seismic interpretation.

Bahrouni, N., Masson, F., Meghraoui, M., Saleh, M., Maamri, R., Dhaha, F., & Arfaoui, M. (2020). Active tectonics and GPS data analysis of the Maghrebian thrust belt and Africa-Eurasia plate convergence in Tunisia. *Tectonophysics*, *785*, 228440.

Bailey, J. V., Orphan, V. J., Joye, S. B., and Corsetti, F. A. (2009). Chemotrophic microbial mats and their potential for preservation in the rock record. *Astrobiology*, *9*(9), 843-859.

Ballauri, A., Bega, Z., Meehan, P., Gambini, R., and Klammer, W. (2002). Exploring in structurally complex thrust belt: Southwest Albania Case. In *AAPG Hedberg Conference.*

Battaglia, M., Murray, M. H., Serpelloni, E., and Bürgmann, R. (2004). The Adriatic region: An independent microplate within the Africa-Eurasia collision zone. *Geophysical Research Letters*, *31*(9).

Bellucci, M., Aslanian, D., Moulin, M., Rabineau, M., Leroux, E., Pellen, R., ... and Camerlenghi, A. (2021). Salt morphologies and crustal segmentation relationship: New insights from the Western Mediterranean Sea. *Earth-Science Reviews*, *222*, 103818.

Bernoulli, D. (2001). Mesozoic-Tertiary carbonate platforms, slopes and basins of the external Apennines and Sicily. In *Anatomy of an orogen: The Apennines and adjacent Mediterranean basins* (pp. 307-325). Springer, Dordrecht.

Bertello, F., Fantoni, R., Franciosi, R., Gatti, V., Ghielmi, M., and Pugliese, A. (2010, January). From thrust-and-fold belt to foreland: hydrocarbon occurrences in Italy. In *Geological society, london, petroleum geology conference series* (Vol. 7, No. 1, pp. 113-126). Geological Society of London.

Bertotti, G., Picotti, V., Chilovi, C., Fantoni, R., Merlini, S., Mosconi, A., (2001). Neogene to Quaternary sedimentary basins in the south Adriatic (Central Mediterranean): foredeeps and lithospheric buckling. *Tectonics* 20, 771–787.

Bertotti, G., Casolari, E., and Picotti, V. (1999). The Gargano Promontory: a Neogene contractional belt within the Adriatic plate. *Terra Nova-Oxford*, *11*(4), 168-173.

Bigi, D., Lugli, S., Manzi, V., and Roveri, M. (2022). Are fluid inclusions in gypsum reliable paleo-environmental indicators? An assessment of the evidence from the Messinian evaporites. *Geology*, *50*(4), 454-459.

Boccaletti, M., Ciaranfi, N., Cosentino, D., Deiana, G., Gelati, R., Lentini, F., ... and Tortorici, L. (1990). Palinspastic restoration and paleogeographic reconstruction of the peri-Tyrrhenian area during the Neogene. *Palaeogeography, Palaeoclimatology, Palaeoecology*, *77*(1), 41-IN13.

Borrelli, M., Perri, E., Critelli, S., Gindre-Chanu, L. (2021). The onset of the Messinian Salinity Crisis in the Central Mediterranean recorded by the pre-salt carbonate/evaporite deposition. *Sedimentology 68*, 119-1197.

Bosellini F., Russo A. and Vescogni A. (2001). Messinian reef-building assemblages of the Salento Peninsula (southern Italy): palaeobathymetric and palaeoclimatic significance. *Palaeogeography, Palaeoclimatology, Palaeoecology*, 175, 7-26.

Bosellini, A., Masetti, D., Sarti, M. (1981). A jurassic "toungue of the Ocean" infilled with oolitic sand: The Belluno Trough, Venetian Alps, Italy. *Marine Geology 44*, Issues 1-2, 59-95.

Bosellini, A., Neri, C., and Luciani, V. (1993). Platform margin collapses and sequence stratigraphic organization of carbonate slopes: Cretaceous–Eocene, Gargano Promontory, southern Italy. *Terra Nova*, *5*(3), 282-297.

Bougrine, A., Yelles-Chaouche, A. K., & Calais, E. (2019). Active deformation in Algeria from continuous GPS measurements. *Geophysical Journal International*, *217*(1), 572-588.

Bouyahiaoui, B., Sage, F., Abtout, A., Dèverchère, J., Yelles, A., Beslier, M.O., Kherroubi, A., Schenini, L., Marok, A., Klingelhoefer, F., Bracene, R., Collor, J.Y., Arab, M., Lepretre, A., Mercier de Lepinay, B. (2018). -10A- East Algeria Margin. In J. Lofi (Ed.), *Seismic atlas of the Messinian salinity crisis markers in the Mediterranean Sea*. Volume 2. - Mémoires de la Société géologique de France, n.s., 2018, t. 181, and Commission for the Geological Map of the World, pp. 36

BRAMBATI, A., CIABATTI, M., FANZATTI, G., MARABINI, F., and MAR-occo, R. (1983). A new sedimentological textural map of the northern and central Adriatic Sea: Bolettino di Oceanologia Teorica ed Applicata, v. 1.

Brancatelli, G., Forlin, E., Bertone, N., Del Ben, A., and Geletti, R. (2022). Time to depth seismic reprocessing of vintage data: A case study in the Otranto Channel (South Adriatic Sea). In *Interpreting Subsurface Seismic Data* (pp. 157-197). Elsevier.

Brancolini, G., Civile, D., Donda, F., Tosi, L., Zecchin, M., Volpi, V., ... and Forlin, E. (2019). New insights on the Adria plate geodynamics from the northern Adriatic perspective. *Marine and Petroleum Geology*, *109*, 687-697.

Brown, A. R., (1999), Iterpretation of three-dimnsion seismic data.

Busetti, M., Volpi, V., Nicolich, R., Barison, E., Romeo, R., Baradello, L., Ramella, R. (2010a). Dinaric tectonic features in the Gulf of Trieste (Northern Adriatic). In: D. Slejko (Ed.), *Novelties in Geophysics, Select paper from the 27th Annual Conference of the Italian Group for Solid Earth Geophysics, Trieste. Bollettino di Geofisica Teorica e Applicata, 51*(2-3), 117-128.

Busetti, M., Volpi, V., Barison, E., Giustiniani, M., Marchi, M., Ramella, R., Zanolla, C. (2010b). Cenozoic seismic stratigraphy and tectonic evolution of the Gulf of Trieste (Northern Adriatic). *Proceedings of the "ADRIA 2006 – International Geological Congress on Adriatic area*", GeoActa, Special Publication, 3, 1-14.

Butler, R.W.H., Lickorish, W.H., Grasso, M., Pedley, H.M., Ramberti, L. (1995). Tectonics and sequence stratigraphy in Messinian basins, Sicily: Constrain on the initiation and termination of the Mediterranean salinity Crisis. *GSA Bulletin*, 107(4), 425-439.

Calamita, F., Satolli, S., Scisciani, V., Esestime, P., and Pace, P. (2011). Contrasting styles of fault reactivation in curved orogenic belts: Examples from the Central Apennines (Italy). *Bulletin*, *123*(5-6), 1097-1111.

Calamita, F., Cello, G., Invernizzi, C., and Paltrinieri, W. (1990). STILE STRUTTURALE E CRONOLOGIA DELLA DEFORMAZIONE LUNGO LA TRAVERSA MS-VICINO-POLVERIGI (APPENNINO MARCHIGIANO ESTERNO).

Calligaris, C., Ghezzi, L., Petrini, R., Lenaz, D., and Zini, L. (2019). Evaporite dissolution rate through an on-site experiment into piezometric tubes applied to the real case-study of Quinis (NE Italy). *Geosciences*, *9*(7), 298.

Camerlenghi, A., Wardell, N., Mocik, A., Del Ben, A., Geletti, R., Urgeles, R. (2018). -2 A,BC,D-Algero-Balearic Basin. In J. Lofi (Ed.), *Seismic atlas of the Messinian salinity crisis markers in the Mediterranean Sea*. Volume 2. - Mémoires de la Société géologique de France, n.s., 2018, t. 181, and Commission for the Geological Map of the World, pp. 14-16.

Camerlenghi, A., Del Ben, A., Hübscher, C., Forlin, E., Geletti, R., Brancatelli, G., Micallef, A., Saule, M., Facchin, L., (2019). Seismic markers of the Messinian salinity crisis in the deep Ionian Basin. *Basin Res*. 32 (4)

Camerlenghi, A., and Aloisi, V. (2020). Uncovering the Mediterranean Salt Giant (MEDSALT)-Scientific networking as incubator of cross-disciplinary research in Earth Sciences. *European Review*, *28*(1), 40-61.

Carminati, E., Doglioni, C., & Scrocca, D. (2004). Alps vs apennines. *Special volume of the Italian Geological Society for the IGC*, *32*, 141-151.

Carminati, E., Doglioni, C., and Scrocca, D. (2003). Apennines subduction-related subsidence of Venice (Italy). *Geophysical Research Letters*, *30*(13).

Carminati, E., and Doglioni, C. (2012). Alps vs. Apennines: The paradigm of a tectonically asymmetric Earth. *Earth-Science Reviews*, *112*(1-2), 67-96.

Carruba, S., Casnedi, R., Perotti, C. R., Tornaghi, M., and Bolis, G. (2006). Tectonic and sedimentary evolution of the Lower Pliocene Periadriatic foredeep in Central Italy. *International Journal of Earth Sciences*, *95*(4), 665-683.

Carulli, G. B., Carobene, L., Cavallin, A., Martinis, B., and Onofri, R. (1980). Evoluzione strutturale plio-quaternaria del Friuli e della Venezia Giulia.

Casero, P., Rigamonti, A., and Iocca, M. (1990). Paleogeographic relationships during Cretaceous between the Northern Adriatic area and the Eastern Southern Alps. *Memorie della Societa Geologica Italiana*, *45*, 807-814.

Casero, P., Roure, F., Moretti, I., Muller, C., Sage, L., and Vially, R. (1988). Evoluzione geodinamica neogenica dell'Appennino meridionale. *Mem. Soc. Geol. It*, *41*, 109-120.

Castellarin, A., Nicolich, R., Fantoni, R., Cantelli, L., Sella, M., and Selli, L. (2006). Structure of the lithosphere beneath the Eastern Alps (southern sector of the TRANSALP transect). *Tectonophysics*, *414*(1-4), 259-282.

Castellarin, A., Cantelli, L., Fesce, A. M., Mercier, J. L., Picotti, V., Pini, G. A., ... and Selli, L. (1992). Alpine compressional tectonics in the Southern Alps. Relationships with the N-Apennines. In *Annales tectonicae* (Vol. 6, No. 1, pp. 62-94).

Cati, A., Sartorio, D., and Venturini, S. (1987b). Carbonate Platforms in the Subsurface of the Northern Adriatic Area. Mem. Soc. Geol. It., 295-308.

Cazzini, F., Zotto, O. D., Fantoni, R., Ghielmi, M., Ronchi, P., and Scotti, P. (2015). Oil and gas in the Adriatic foreland, Italy. *Journal of Petroleum Geology*, *38*(3), 255-279.

Cello, G., and Mazzoli, S. (1998). Apennine tectonics in southern Italy: a review. *Journal of Geodynamics*, *27*(2), 191-211.

Chanell, J. E. T., D'Argenio, B., & Horvath, F. (1979). Adria, the African Promontory in Mesozoic Mediterranean paleogeography. *Earth Sci. Rev.*, *15*, 213-292.

Chun, J.H. and Jacewitz, C.A. (1981). Fundamentals of frequency domain migration. *Geophysics*, 45(5), 717-733.

Chumakov, I. (1973). Pliocene and Pleistocene deposit od the Nile valley in Nubia and upper Egypt

CIESM, - Anton, J., Cagatay, M.N., De Lange, G., Flecker, R., Gaullier, V., Gunde-Cimerman, N., Hubsher, C., Krijgsman, W., Lambregts, P., Lofi, J., Lugli, S., Manzi, V., McGenity, T.J., Roveri, M., Sierro, F.J., and Suc, J. -P. (2008) Executive Summary, in: Briand, F. (Ed.), The Messinian Salinity crisis from mega -deposits to microbiology - A consensus report. *CIESM Workshop Monographs*, Monaco, 7 -28.

Cita, M.B. and Corselli, C. (1990) Messinian paleogeography and erosional surfaces in Italy: an overview. *Palaeogeography, Palaeoclimatology, Palaeoecology*, 77, 67 -82.

Clauzon, G., Suc, J. P., Gautier, F., Berger, A., and Loutre, M. F. (1996b). Alternate interpretation of the Messinian salinity crisis: Controversy resolved? *Geology*, 24, 363– 366.

Cucchi, F., Forti, P., Finocchiaro, F. (1998). Gypsum degradation in Italy with respect to climatic textural and erosional conditions. *Geogr. Fis. Din. Quat. 1998*, 3, 41–49.

Cuffaro, M., Riguzzi, F., Scrocca, D., Antonioli, F., Carminati, E., Livani, M., and Doglioni, C. (2010). On the geodynamics of the northern Adriatic plate. *Rendiconti Lincei*, *21*(1), 253-279.

de Alteriis, G. (1995). Different foreland basins in Italy: examples from the central and southern Adriatic Sea. *Tectonophysics*, *252*(1-4), 349-373.

de Alteriis, G., and Aiello, G. (1993). Stratigraphy and tectonics offshore of Puglia (Italy, southern Adriatic Sea). *Marine Geology*, *113*(3-4), 233-253.

Decima, A., Wezel, J.A. (1971). Osservazioni sulle evaporiti messinain della Sicilia centro-meridionale. *Rivista Mineraria Siciliana*, 130-134, 172-187.

Degobbis, D., Precali, R., Ivancic, I., Smodlaka, N., Fuks, D., and Kveder, S. (2000). Long-term changes in the northern Adriatic ecosystem related to anthropogenic eutrophication. *International journal of environment and pollution*, *13*(1-6), 495-533.

Dela Pierre, F., Bernardi, E., Cavagna, S., Clari, P., Gennari, R., Irace, A., Lozar, F., Lugli, S., Manzi, V., Natalicchio, M., Roveri, M., and Violanti, D. (2011). The record of the Messinian salinity crisis in the Tertiary Piedmont Basin (NW Italy): The Alba section revisited. *Palaeogeography, Palaeoclimatology, Palaeoecology*, 310, 238– 255.

Dela Pierre, F., Natalicchio, M., Ferrando, S., Giustetto, R., Birgel, D., Carnevale, G., Gier, S., Lozar, F., Marabello, D. and Peckmann, J. (2015). Are the large filamentous microfossils preserved in Messinian gypsum colorless sulfide-oxidizing bacteria? *Geology*, *43*(10), 855-858.

Del Ben A., Geletti R., Mocnik, A., Castagner, R., (2018). – 13. A, B, C- Central Adriatic Basin. *In. J. Lofi, Ed., Seismic atlas of the Messinian salinity crisis markers in the Mediterranean Sea.* Volume 2 – Mem. Soc. geol. Fr., n.s, 2018, t 181, and Commission for the Geological Map of the World, p. 45-47.

Del Ben, A., Oggioni, F., (2016). Seismic evidence of the rebound of the Adria foreland and the current geodynamics of the Central and Southern Apennines (Italy). *J. Geodyn*. 99, 51–63.

Del Ben, A., Mocnik, A., Volpi, V., Karvelis, P., (2015). Old domains in the South Adria plate and their relationship with the West Hellenic front. *J. Geodyn*. 89, 15–28.

Del Ben, A., Geletti, R., and Mocnik, A. (2010). Relation between recent tectonics and inherited Mesozoic structures of the central-southern Adria plate. *Bollettino di Geofisica Teorica ed Applicata, 51*.

Del Ben, A., Barnaba, C., Taboga, A., (2008). Strike-slip systems as the main tectonic features in the Plio-Quaternary kinematics of the Calabrian Arc. Mar. *Geophys.Res*. 29, 1–12

Del Ben, A., Finetti, I., Mongelli, F., & Zito, G. (1994). Seismic and heat flow study of the southern Adriatic Basin. *Bollettino di Geofisica Teorica ed Applicata*, *36*(141-44), 29-44.

Devoti, R., Riguzzi, F., Cuffaro, M., and Doglioni, C. (2008). New GPS constraints on the kinematics of the Apennines subduction. *Earth and Planetary Science Letters*, *273*(1-2), 163-174.

Dewey, J. F., Helman, M. L., Knott, S. D., Turco, E., and Hutton, D. H. W. (1989). Kinematics of the western Mediterranean. *Geological Society, London, Special Publications*, *45*(1), 265-283.

Di Stefano, R., Kissling, E., Chiarabba, C., Amato, A., and Giardini, D. (2009). Shallow subduction beneath Italy: Three-dimensional images of the Adriatic-European-Tyrrhenian lithosphere system based on high-quality P wave arrival times. *Journal of Geophysical Research: Solid Earth*, *114*(B5).

Diviacco, P., Firetto Carlino, M., and Busato, A. (2019). Enhancing the value of public vintage seismic data in the Italian offshore. *Geoscience Data Journal*, *6*(1), 6-15.

Diviacco, P., Pshenichny, C., Carniel, R., Khrabrykh, Z., Shterkhun, V., Mouromtsev, D., ... and Pascolo, P. (2015). Organization of a geophysical information space by using an event-bush-based collaborative tool. *Earth Science Informatics*, *8*(3), 677-695.

Do Couto, D., Popescu, S.-M., Suc, J.-P., Melinte-Dobrinescu, M. C., Barhoun, N., Gorini, C., … Auxietre, J.-L. (2014). Lago Mare and the Messinian salinity crisis: Evidence from the Alboran Sea (S. Spain). *Marine and Petroleum Geology*, 52, 57– 76.

Doglioni, C., Carminati, E., Cuffaro, M., and Scrocca, D. (2007). Subduction kinematics and dynamic constraints. *Earth-Science Reviews*, *83*(3-4), 125-175.

Donda, F., Forlin, E., Gordini, E., Panieri, G., Buenz, S., Volpi, V., ... and De Santis, L. (2015). Deep-sourced gas seepage and methane-derived carbonates in the Northern Adriatic Sea. *Basin research*, *27*(4), 531-545.

Donda, F., Civile, D., Forlin, E., Volpi, V., Zecchin, M., Gordini, E., Merson, B., and De Santis, L. (2013). The northernmost Adriatic Sea: a potential location for CO2 geological storage?. *Marine and petroleum geology*, *42*, 148-159.

Faccenna, C., Speranza, F., Caracciolo, F. D. A., Mattei, M., and Oggiano, G. (2002). Extensional tectonics on Sardinia (Italy): insights into the arc–back-arc transitional regime. *Tectonophysics*, *356*(4), 213-232.

Faccenna, C., Funiciello, F., Giardini, D., and Lucente, P. (2001b). Episodic back-arc extension during restricted mantle convection in the Central Mediterranean. *Earth and Planetary Science Letters*, *187*(1-2), 105-116.

Faccenna, C., Mattei, M., Funiciello, R., and Jolivet, L. (1997). Styles of back-arc extension in the central Mediterranean. *Terra Nova*, *9*(3), 126-130.

Fantoni, R., and Franciosi, R. (2010). Tectono-sedimentary setting of the Po Plain and Adriatic foreland. *Rendiconti Lincei*, *21*(1), 197-209.

Fantoni, R., Bersezio, R., and Forcella, F. (2004). Alpine structure and deformation chronology at the Southern Alps-Po Plain border in Lombardy. *Bollettino della Società geologica italiana*, *123*(3), 463-476.

Fantoni, R., Della Vedova, B., Giustiniani, M., Nicolich, R., Barbieri, C., Del Ben, A., ... and Castellarin, A. (2003). Deep seismic profiles through the Venetian and Adriatic foreland (Northern Italy).

Festa, V., Teofilo, G., Tropeano, M., Sabato, L., Spalluto, L. (2014). New insights on diapirism in the Adriatic Sea: the Treniti salt structure (Apulia offshore, southeastern Italy). *Terra Nova, 26*, 169-178.

Finetti, I., and Del Ben, A. (2005). Crustal tectono-stratigraphic setting of the Adriatic Sea from new CROP seismic data. *In I. Finetti, and I. Finetti (Ed.), CROP Project: Deep Seismic Exploration of the Central Mediterranean and Italy* (pp. 519-547). Elsevier.

Finetti, I. R. (Ed.). (2005). *CROP project: deep seismic exploration of the central Mediterranean and Italy*. Elsevier.

Finetti, I.R., Bricchi, G., Del Ben, A., Pipan, M., Xuan, Z., (1987). Geophysical study ofthe Adria Plate. Mem. Soc. Geol. Italy 50, 335–344.

Finetti, I.R. (1985). Structure and evolution of the central Mediterranean (Pelagian and Ionian Seas). *Geological evolution of the Mediterranean Basin*, 215-230.

Finetti, I.R., (1982). Structure, stratigraphy and evolution of central Mediterranean. *Boll. Geof. Teor. Appl.* 24, 247–312.

Finetti, I.R., Lentini, F., Carbone, S., Del Ben, A., Di Stefano, A., Guarnieri, P., Pipan, M., (2005b). Crustal tectono-Stratigraphy and geodynamics of the southernapennine form CROP and other integrated Geophysical-Geological data. In: Finetti, I.R. (Ed.), CROP Project: Deep Seismic Exploration of the CentralMediterranean and Italy, 1. Elsevier, Atlases in Geoscience, pp. 225–262.

Fortuin, A. R., Kelling, J. M. D., and Roep, T. B. (1995). The enigmatic Messinian-Pliocene section of Cuevas del Almanzora (Vera Basin, SE Spain) revisited—erosional features and strontium isotope ages. *Sedimentary Geology*, *97*(3-4), 177-201.

Gačić, M., Lascaratos, A., Manca, B. B., and Mantziafou, A. (2001). Adriatic deep water and interaction with the Eastern Mediterranean Sea. In *Physical oceanography of the Adriatic Sea* (pp. 111-142). Springer, Dordrecht.

Garcia-Castellanos, D., Estrada, F., Jimenez-Munt, F., Gorini, C., Fernandez, M., Verges, J., De Vincente, R. (2009). Catastrophic flood of the Mediterranean after the Messinian Salinity Crisis. *Nature*, 462, 778-782.

Garcia-Castellanos, D., Micallef, A., Camerlenghi, A., Abril, J. M., Periañez, R., Estrada, F., and Ercilla, G. (2018, April). A fast refill of the Mediterranean after the Messinian salinity crisis? Looking for independent evidence. In *EGU General Assembly Conference Abstracts* (p. 9520).

Garcia-Castellanos, D., Micallef, A., Estrada, F., Camerlenghi, A., Ercilla, G., Periáñez, R., and Abril, J. M. (2020). The Zanclean megaflood of the Mediterranean – Searching for independent evidence. *Earth Science Reviews*, 201, 103061.

García-Veigas, J., Cendón, D. I., Gibert, L., Lowenstein, T. K., and Artiaga, D. (2018b). Geochemical indicators in Western Mediterranean Messinian evaporites: Implications for the salinity crisis. *Marine Geology*, 403, 197– 214.

Geletti, R., Del Ben, A., Busetti, M., Ramella, R., Volpi, V., (2008). Gas seeps linked to salt structures in the Central Adriatic Sea. *Basin Res. 20*, 473–487.

Geletti, R., Zgur, F., Del Ben, A., Buriola, F., Fais, S., Fedi, M., … Pipan, M. (2014). The Messinian salinity crisis: New seismic evidence in the West-Sardinian Margin and Eastern Sardo-Provençal basin (West Mediterranean Sea). *Marine Geology*, 351, 76– 90.

Ghielmi, M., Minervini, M., Nini, C., Rogledi, S., Rossi, M., and Vignolo, A. (2010). Sedimentary and tectonic evolution in the eastern Po-Plain and northern Adriatic Sea area from Messinian to Middle Pleistocene (Italy). *Rendiconti Lincei*, *21*(1), 131-166.

Ghielmi, M., Minervini, M., Nini, C., Rogledi, S., and Rossi, M. (2013). Late Miocene–Middle Pleistocene sequences in the Po Plain–Northern Adriatic Sea (Italy): the stratigraphic record of modification phases affecting a complex foreland basin. *Marine and Petroleum Geology*, *42*, 50-81.

Gordini, E., Falace, A., Kaleb, S., Donda, F., Marocco, R., and Tunis, G. (2012). Methane-related carbonate cementation of marine sediments and related macroalgal coralligenous assemblages in the Northern Adriatic Sea. In *Seafloor Geomorphology as Benthic Habitat* (pp. 185-200). Elsevier.

Grandic, S., Krakatovic, I., and Rusan, I. (2010). Hydrocarbon potential assesment of the slope deposits along the SW Dinarides carbonate platform edge. *Nafta*, *61*, 325-338.

Grandić, S., and Kolbah, S. (2009). New commercial oil discovery at Rovesti structure in South Adriatic and its importance for Croatian part of Adriatic basin. *Nafta*, *60*(2), 83-86.

Grandic, S., Biancone, M., and Samarzija, J. (2001). Geophysical and stratigraphic evidence of the Triassic rift structuration in the Adriatic offshore area. *Nafta (Zagreb)*, *52*(12), 383-396.

Grandić, S., Boromisa-Balas, E., Sustercic, M., and Kolbah, S. (1999). Hydrocarbon possibilities in the eastern Adriatic slope zone of Croatian offshore area. *Nafta (Zagreb)*, *50*(2), 51-73.

Guennoc, P., Gorini, C., and Mauffret, A. (2000). Geological history of the Gulf of Lions: mapping the Oligocene-Aquitanian rift and Messinian surface. *Géologie de la France*, *3*, 67-97.

Guibourdenche, L., Cartigny, P., Pierre, F. D., Natalicchio, M., and Aloisi, G. (2022). Cryptic sulfur cycling during the formation of giant gypsum deposits. *Earth and Planetary Science letters, 593*, 117676

Gvirtzman, Z., Manzi, V., Calvo, R., Gavrieli, I., Gennari, R., Lugli, S., … Roveri, M. (2017). Intra-Messinian truncation surface in the Levant Basin explained by subaqueous dissolution. *Geology*, 45, 915– 918.

Haq, B., Gorini, C., Baur, J., Moneron, J., and Rubino, J. L. (2020). Deep Mediterranean's Messinian evaporite giant: how much salt? *Global and Planetary Change*, *184*, 103052.

Hardie, L.A. (1984). Evaporites: marine or Non-Marine. Am. J. Sci., 284 (1984), pp. 193-240.

Hardie, L. A., Lowenstein, T. K. (2004). Did the Mediterranean Sea dry out during the Miocene? A reassessment of the evaporite evidence from DSDP Legs 13 and 42A cores. *Journal of Sedimentary Research*, *74*(4), 453-461.

Harvie, C.E., Weare, J.H., Hardie, L.A., Eugster, H.P. (1980). Evaporation of Seawater: Calculated Mineral Sequences. *Science*, 208 (1980), pp. 498-500.

Hatton, L., Worthington M. H. and Makin J., (1986), Seismic data processing: theory and practice., Merlin Profiles Ltd.

Heida, H., Raad, F., Garcia-Castellanos, D., Jiménez-Munt, I., Maillard, A., and Lofi, J. (2022). Flexural-isostatic reconstruction of the Western Mediterranean during the Messinian Salinity Crisis: Implications for water level and basin connectivity. *Basin Research*, *34*(1), 50-80.

Hermann, A.G., Knake, D., Schneider, J., Peters, H. (1973), Geochemistry of modern seawater and brines from salt pans: main components and bromine distributions. *Contr Mineral. Petrol*., 40 (1973), pp. 1-24.

Hilgen, F. J., Krijgsman, W., Langereis, C. G., Lourens, L. J., Santarelli, A., and Zachariasse, W. J. (1995). Extending the astronomical (polarity) time scale into the Miocene. *Earth and Planetary Science Letters*, *136*(3-4), 495-510.

Hilgen, F.J. and Krijgsman, W. (1999) Cyclostratigraphy and astrochronology of the Tripoli diatomite formation (pre-evaporite Messinian, Sicily, Italy). *Terra Nova*, 11, 16-22.

Hilgen, F.J., K. Kuiper, W. Krijgsman, E. Snel, E. van der Laan. (2007) Astronomical tuning as the basis for high resolution chronostratigraphy: the intricate history of the Messinian salinity crisis. *Stratigraphy*, 4, pp. 231-238.

Hsü, K. J. (1972). Origine of saline ginats: A critical review after the discovery of the Meiterranean Evaporite. *Earth-Science Reviews*, 8(4), 371-396.

Hsü, K. J. (1973). The dessicated deep-basin model for the Messinian events. *Drooger, C.W. (ed.), Messinian Events in the Mediterranean. North-Holland Publ. Co., Amsterdam*, 60-67.

Hsü, K. J., Ryan, W. B. F., and Cita, M. B. (1973b). Late Miocene dessication of the Mediterranean. *Nature*, 242, 240– 244.

Kearey, P., Brooks, M., and Hill, I. (2002). An introduction to geophysical exploration (3rd). *Great Britain: Blackwell Science Ltd*.

Kherroubi, A., Deverchere, J., Yelles, K., Sage, F., Bouyahiaoui, B., Grandorge, D., Mercier de Lepiany, B. (2018). -10B- East Algeria Margin. In J. Lofi (Ed.), *Seismic atlas of the Messinian salinity crisis markers in the Mediterranean Sea*. Volume 2. - Mémoires de la Société géologique de France, n.s., 2018, t. 181, and Commission for the Geological Map of the World, pp. 37.

Koulali, A., Ouazar, D., Tahayt, A., King, R. W., Vernant, P., Reilinger, R. E., ... & Amraoui, N. (2011). New GPS constraints on active deformation along the Africa–Iberia plate boundary. *Earth and Planetary Science Letters*, *308*(1-2), 211-217.

Krijgsman, W., Capella, W., Simon, D., Hilgen, F. J., Kouwenhoven, T. J., Meijer, P. T., ... and Flecker, R. (2018). The Gibraltar corridor: Watergate of the Messinian salinity crisis. *Marine Geology*, *403*, 238-246.

Krijgsman, W., Hilgen, F. J., Raffi, I., Sierro, F.J. and Wilson, D.S., (1999b). Chronology, causes and progression of the Messinian salinity crisis. *Nature*, 400, 652 –655.

Le Goff, J., Reijmer, J. J. G., Cerepi, A., Loisy, C., Swennen, R., Heba, G., ... and De Graaf, S. (2019). The dismantling of the Apulian carbonate platform during the late Campanian–early Maastrichtian in Albania. *Cretaceous Research*, *96*, 83-106.

Lipizer, M., Partescano, E., Rabitti, A., Giorgetti, A., and Crise, A. (2014). Qualified temperature, salinity and dissolved oxygen climatologies in a changing Adriatic Sea. *Ocean Science*, *10*(5), 771-797.

Lofi, J. (2018). *Seismic Atlas of the Messinian salinity crisis markers in the Mediterranean Sea*. Vollume 2 - Mémoires de la Société géologique de France, n.s., 2018, t. 181, and Commission for the Geological Map of the World, 72 p. + DVD.

Lofi, J., Sage, F., Déverchère, J., Loncke, L., Maillard, A., Gaullier, V., … Gorini, C. (2011). Refining our knowledge of the Messinian salinity crisis records in the offshore domain through multi-site seismic analysis. *Bulletin de la Société géologique de France*, 182(2), 163– 180.

Lofi, J., Gorini, C., Berné, S., Clauzon, G., Dos Reis, A. T., Ryan, W. B., and Steckler, M. S. (2005). Erosional processes and paleo-environmental changes in the Western Gulf of Lions (SW France) during the Messinian Salinity Crisis. *Marine Geology*, *217*(1-2), 1-30.

Lymer, G., Lofi, J., Gaullier, V., Maillard, A., Thinon, I., Sage, F., ... and Vendeville, B. C. (2018). The Western Tyrrhenian Sea revisited: New evidence for a rifted basin during the Messinian Salinity Crisis. *Marine Geology*, *398*, 1-21.

Lugli, S., Gennari, R., Gvirtzman, Z., Manzi, V., Roveri, M., and Schreiber, B. C. (2013). Evidence of clastic evaporites in the canyons of the Levant Basin (Israel): Implications for the Messinian salinity crisis. *Journal of sedimentary research*, *83*(11), 942-954.

Lugli, S., Manzi, V., Roveri, M., Schreiber, B.C. (2010). The Primary Lower Gypsum in the Mediterranean: a new facies interpretation for the first stage of the Messinian salinity crisis. *Palaeogeography, Palaeoclimatology, Palaeoecology*, 297, 83–99.

Lugli, S., Schreiber, B.C., Triberti, B. (1999b). Fiant polygons in the Realmont Mine (Agrigento, Sicily): evidence for the desiccation of a Messianian halite basin. *Journal of Sedimentary Ressearch*, 69(3), 764-771.

Malinverno, A., and Ryan, W. B. (1986). Extension in the Tyrrhenian Sea and shortening in the Apennines as result of arc migration driven by sinking of the lithosphere. *Tectonics*, *5*(2), 227-245.

Maillard, A., Gaullier, V., Lézin, C., Chanier, F., Odonne, F., and Lofi, J. (2020). New onshore/offshore evidence of the Messinian Erosion Surface from key areas: The Ibiza-Balearic Promontory and the Orosei-Eastern Sardinian margin. *BSGF-Earth Sciences Bulletin*, *191*(1), 9.

Maillard, A., Gorini, C., Mauffret, A., Sage, F., Lofi, J., and Gaullier, V. (2006). Offshore evidence of polyphase erosion in the Valencia Basin (Northwestern Mediterranean): Scenario for the Messinian Salinity Crisis. *Sedimentary Geology*, 188–189, 69– 91.

Mancinelli, P., and Scisciani, V. (2020). Seismic velocity-depth relation in a siliciclastic turbiditic foreland basin: a case study from the Central Adriatic Sea. *Marine and Petroleum Geology*, *120*, 104554.

Manzi, V., Lugli, S., Ricci Lucchi, F. and Roveri, M. (2005b). Deep -water clastic evaporites deposition in the Messinian Adriatic foredeep (northern Apennines, Italy): did the Mediterranean ever dry out? *Sedimentology*, 52, 875 -902.

Manzi, V., Roveri, M., Gennari, R., Bertini, A., Biffi, U., Giunta, S., Iaccarino, S. M., Lanci, L., Lugli, S., Negri, A., Riva, A., Rossi, M. E., and Taviani, M. (2007). The deep-water counterpart of the Messinian Lower Evaporites in the Apennine foredeep: The Fanantello section (Northern Apennines, Italy). *Palaeogeography, Palaeoclimatology, Palaeoecology*, 251, 470– 499.

Manzi, V., Lugli, S., Roveri, M., Schreiber, C.B. (2009a). A new facies model dot the Upper Gypsum of Siciy (Italy): Chronological and paleo-environmental constrains for the Messiani salinity crisis in the Mediterranean. *Sedimentology*, 56(7), 1937-1960.

Manzi, V., Lugli, S., Roveri, M., Schreiber, B. C., and Gennari, R. (2011). The Messinian "Calcare di Base"(Sicily, Italy) revisited. *Bulletin*, *123*(1-2), 347-370.

Manzi, V., Gennari, R., Lugli, S., Roveri, M., Scafetta, N., and Schreiber, B. C. (2012). High-frequency cyclicity in the Mediterranean Messinian evaporites: evidence for solar–lunar climate forcing. *Journal of Sedimentary Research*, *82*(12), 991-1005.

Manzi, V., Gennari, R., Hilgen, F., KRijgsman, W., Lugli, S., Roveri, M. and Sierro, F.J. (2013). Age refinement of the Messinian salinity crisis onset in the Mediterranean. *Terra Nova*, 25, 315 - 322.

Manzi, V., Lugli, S., Roveri, M., Pierre, F. D., Gennari, R., Lozar, F., ... and Turco, E. (2016). The Messinian salinity crisis in Cyprus: a further step towards a new stratigraphic framework for Eastern Mediterranean. *Basin Research*, *28*(2), 207-236.

Manzi, V., Argnani, A., Corcagnani, A., Lugli, S., and Roveri, M. (2020). The Messinian salinity crisis in the Adriatic foredeep: evolution of the largest evaporitic marginal basin in the Mediterranean. *Marine and Petroleum Geology*, *115*, 104288.

Marabini, S., Vai, G.B., (1985). Analisi di facies e macrotettonica della Vena del Gesso in Romagna. *Bollettino della Societa` Geologica Italiana 104*, 21–42.

Mattavelli, L., Novelli, L., Anelli, L., (1991). Occurrence of hydrocarbons in the Adriatic basin. *In: Spencer, A.M. (Ed.), Generation, Accumulation, and Production of Europe's Hydrocarbon*. Special Publication of the European Association of Petroleum Geoscientists, pp. 369–380.

Mattei, M., Cipollari, P., Cosentino, D., Argentieri, A., Rossetti, F., Speranza, F., and Di Bella, L. (2002). The Miocene tectono-sedimentary evolution of the southern Tyrrhenian Sea: stratigraphy, structural and palaeomagnetic data from the on-shore Amantea basin (Calabrian Arc, Italy). *Basin Research*, *14*(2), 147-168.

Mauritsch, H. J., Scholger, R., Bushati, S. L., and Ramiz, H. (1995). Palaeomagnetic results from southern Albania and their significance for the geodynamic evolution of the Dinarides, Albanides and Hellenides. *Tectonophysics*, *242*(1-2), 5-18.

Mazzuca, N., Bruni, A., and Joppen, T. (2015). Exploring the potential of deep targets in the South Adriatic Sea: insight from 2D basin modeling of Croatian offshore. *Geologia Croatica*, *68*(3), 237-246.

McKenzie, J.A. (1985). Stable-isotope mapping in Messinian evaporative carbonates of central Sicily. *Geology*, 13, 851-54.

Meghraoui, M., & IGCP-601 Working Group. (2016). The seismotectonic map of Africa. *Episodes Journal of International Geoscience*, *39*(1), 9-18.

Meghraoui, M., & Pondrelli, S. (2012). Active faulting and transpression tectonics along the plate boundary in North Africa. *Annals of Geophysics*, *55*(5), pp-955.

Mele, G. (2001). The Adriatic lithosphere is a promontory of the African plate: Evidence of a continuous mantle lid in the Ionian Sea from efficient Sn propagation. *Geophysical research letters*, *28*(3), 431-434.

Merlini, S., and Mostardini, F. (1986). Appennino centro-meridionale: sesioni geologiche e proposta di modello strutturale. In *Geologia dell'Italia centrale. Congresso nazionale. 73* (pp. 147-149).

Micallef, A., Camerlenghi, A., Garcia-Castellanos, D., Cunarro Otero, D., Gutscher, M. A., Barreca, G., Spatola, D., Facchin, L., Geletti, R., Krastel, S., Gross, F., and Urlaub, M. (2018). Evidence of the Zanclean megaflood in the eastern Mediterranean Basin. *Scientific Reports*, 8, 1– 8.

Milia, A., and Torrente, M. M. (2014). Early-stage rifting of the Southern Tyrrhenian region: the Calabria–Sardinia breakup. *Journal of Geodynamics*, *81*, 17-29.

Mitchum Jr, R. M., and Vail, P. R. (1977). Seismic stratigraphy and global changes of sea level: Part 7. Seismic stratigraphic interpretation procedure: Section 2. Application of seismic reflection configuration to stratigraphic interpretation.

Mocnik, A. (2008). Metodologie geofisiche integrate per la correlazione tra strutture superficiali e profonde nel Canale di Otranto (MD thesis), University of Trieste.

Morelli, C., and Mosetti, F. (1968). Rilievo sismico continuo nel Golfo di Trieste. Andamento della formazione arenacea (Flysch) sotto il fondo marino nella zona tra Trieste, Monfalcone e Grado. *Boll. Soc. Adr. Sc*, *56*(1), 42-57.

Morsilli, M., Hairabian, A., Borgomano, J., Nardon, S., Adams, E., Bracco Gartner, G. (2017). The Apulia Carbonate Platform-Gargano Promontory, Italy (Upper Jurassic – Eocene). *AAPG Bullettin, v. 101*, No. 4, 523-531.

Müller, D. W., and Mueller, P. A. (1991). Origin and age of the Mediterranean Messinian evaporites: implications from Sr isotopes. *Earth and Planetary Science Letters*, *107*(1), 1-12.

Natalicchio, M., Dela Pierre, F., Lugli, S., Lowenstein, T. K., Feiner, S. J., Ferrando, S., Manzi, V., Roveri, M. and Clari, P. (2014). Did Late Miocene (Messinian) gypsum precipitate from evaporated marine brines? Insights from the Piedmont Basin (Italy). *Geology*, *42*(3), 179-182.

Natalicchio, M., Pellegrino, L., Clari, P., Pastero, L., and Pierre, F. D. (2021). Gypsum lithofacies and stratigraphic architecture of a Messinian marginal basin (Piedmont Basin, NW Italy). *Sedimentary Geology*, *425*, 106009.

Nesteroff, W.D. (1973). Un modele pur les evaporites messiniennes en Mediterranee: Des bassins pei profonds avec depots d'avaporites lagunaires. In Messinian events in the Mediterranean (Vol. 7, pp. 68-81). North-Holland Amsterdam.

Nicolai, C., Gambini, R., (2007). Structural architecture of the Adria platform-and-basin system. *In: Mazzotti, A., Patacca, E., Scandone, P. (Eds.), Bollettino Della Società Geologica Italian*a. CROP-04, pp. 21–37 (Spec. IssueN.7).

Nicolosi, I., Speranza, F., and Chiappini, M. (2006). Ultrafast oceanic spreading of the Marsili Basin, southern Tyrrhenian Sea: Evidence from magnetic anomaly analysis. *Geology*, *34*(9), 717-720.

Nocquet, J. M., and Calais, E. (2003). Crustal velocity field of western Europe from permanent GPS array solutions, 1996–2001. *Geophysical Journal International*, *154*(1), 72-88.

Panieri, G., Lugli, S., Manzi, V., Roveri, M., Schreiber, B. C., and Palinska, K. A. (2010). Ribosomal RNA gene fragments from fossilized cyanobacteria identified in primary gypsum from the late Miocene, Italy. *Geobiology*, *8*(2), 101-111.

Patacca, E., Scandone, P., and Mazza, P. (2008). Oligocene migration path for Apulia macromammals: the Central-Adriatic bridge. *Bollettino della Società Geologica Italiana*, *127*, 337-355.

Patacca, E., and Scandone, P. (2007). Geology of the southern Apennines. *Bollettino della Società Geologica Italiana*, *7*, 75-119.

Patacca, E., Sartori, R., and Scandone, P. (1990). Tyrrhenian basin and Apenninic arcs: kinematic relations since late Tortonian times. *Memorie della Società Geologica Italiana*, *45*, 425-451.

Pellegrino, L., Natalicchio, M., Abe, K., Jordan, R. W., Longo, S. E. F., Ferrando, S., Carnevale, G., and Dela Pierre, F. (2021). Tiny, glassy, and rapidly trapped: The nano-sized planktic diatoms in Messinian (late Miocene) gypsum. *Geology*, *49*(11), 1369-1374.

Pellen, R., Aslanian, D., Rabineau, M., Suc, J. P., Cavazza, W., Popescu, S. M., & Rubino, J. L. (2022). Structural and sedimentary origin of the Gargano-Pelagosa gateway and impact on sedimentary evolution during the Messinian Salinity Crisis. *Earth-Science Reviews*, 104114.

Pellen, R., Popescu, S. M., Suc, J. P., Melinte-Dobrinescu, M. C., Rubino, J. L., Rabineau, M., ... and Aslanian, D. (2017). The Apennine foredeep (Italy) during the latest Messinian: Lago Mare reflects competing brackish and marine conditions based on calcareous nannofossils and dinoflagellate cysts. *Geobios*, *50*(3), 237-257. PICHA F.J. (2002) - Late orogenic strike-slip faulting and escape tectonics in frontal Dinarides-Hellenides, Croatia, Yugoslavia, Albania, and Greece. AAPG Bull., 86, 1659-1671.

Perri, E., Gindre-Chanu, L., Caruso, A., Fefalà, M., Scopelliti, G. and Tucker, M. (2017) Microbial-mediated pre-salt carbonate deposition during the Messinian salinity crisis (Calcare di Base fm., Southern Italy). *Mar. Petrol. Geol.*, *88*, 235-250.

Raad, F., Lofi, J., Maillard, A., Tzevahirtzian, A., and Caruso, A. (2021). The Messinian Salinity Crisis deposits in the Balearic Promontory: an undeformed analog of the MSC Sicilian basins?. *Marine and Petroleum Geology*, *124*, 104777.

Reghizzi, M., Lugli, S., Manzi, V., Rossi, F. P., and Roveri, M. (2018). Orbitally forced hydrological balance during the Messinian Salinity Crisis: Insights from strontium isotopes (87Sr/86Sr) in the Vena del Gesso Basin (Northern Apennines, Italy). *Paleoceanography and Paleoclimatology*, *33*(7), 716-731.

Renz, C. (1940). *Die Tektonik der griechischen Gebirge* (Vol. 8). Grapheion Dēmosieumatōn tēs Akadēmias Athēnōn.

Ricci Lucchi, F. (1975). Miocene palaeogeography and basin analysis in the Periadriatic Apennines. *C. Squyres (Ed.), Geology of Italy, vol. 2, PESL, Castelfranco-Tripoli* (1975), pp. 129-236.

Rosenbaum, G., and Lister, G. S. (2004b). Neogene and Quaternary rollback evolution of the Tyrrhenian Sea, the Apennines, and the Sicilian Maghrebides. *Tectonics*, *23*(1).

Rossi, M., Minervini, M., Ghielmi, M., and Rogledi, S. (2015). Messinian and Pliocene erosional surfaces in the Po Plain-Adriatic Basin: Insights from allostratigraphy and sequence stratigraphy in assessing play concepts related to accommodation and gateway turnarounds in tectonically active margins. *Marine and Petroleum Geology*, *66*, 192-216.

Rouchy, J.M. and Caruso , A. (2006) The Messinian salinity crisis in the Mediterranean basin: a reassessment of the data and an integrated scenario. *Sedimentary Geology*, 188, 35 -67.

Rouchy, J.-M., and Saint Martin, J.-P. (1992). Late Miocene events in the Mediterranean as recorded by carbonate-evaporite relations. *Geology*, 20, 629– 632.

Rouchy, J.M. (1982) La genèse des évaporites messiniennes de Méditerranée. B. Mus. Natl. His. Nat., pp. 1-280.

Roveri, M., Bassetti, M.A., Ricci Lucchi, F., (2001). The Mediterranean Messinian salinity crisis: an Apennine foredeep perspective. Sedimentary Geology 140, 201–214.

Roveri, M., Manzi, V., Lucchi, F. R., and Rogledi, S. (2003). Sedimentary and tectonic evolution of the Vena del Gesso basin (Northern Apennines, Italy): Implications for the onset of the Messinian salinity crisis. *Geological Society of America Bulletin*, *115*(4), 387-405.

Roveri, M., A. Landuzzi, M.A. Bassetti, S. Lugli, V. Manzi, F. Ricci Lucchi, G.B. Vai, (2004). The record of Messinian events in the northern Apennines foredeep basins. *B19 Field Trip Guidebook. 32nd International Geological Congress*, Firenze, 20-28Agosto 2004

Roveri, M., Manzi, V., Lugli, S., Schreiber, B., Caruso, A., Rouchy, J.M., Iaccarino, S., Gennari, R., Vitale, F., Lucchi, F. (2006). Clastic vs. Primaty precipitate evaporites in the Messinian Sicilian basins. L'ateneo Parmense. *Acta Naturalia: Organo Della Società Di Medicina e Scienze Naturali Di Parma*, 42, 125-199.

Roveri, M., Manzi, V., Gennari, R., Iaccarino, S.M., Lugli, S., (2008). Recent advancements in the Messinian stratigraphy of Italy and their Mediterranean scale implications. *Bollettino della Società Paleontologica Italiana* 47, 71–85.

Roveri, M., Manzi, V., Bergamasco, A., Falcieri, F.M., Gennari, R., Lugli, S. and Schreiber, C. (2014a). Dense shelf water cascading and Messinian canyons: a new scenario for the Mediterranean salinity crisis. *American Journal of Science, 34*, 751 -784.

Roveri, M., Flecker, R., Krijgsman, W., Lofi, J., Lugli, S., Manzi, V., Sierro, F.J., Bertini, A., Camerlenghi, A., De Lange, G., Govers, R., Hilgen, F.J., Hübscher, C., Meijer, P.T.H. and Stoica, M. (2014b). The Messinian Salinity Crisis: Past And Future Of A Great Challenge For Marine Sciences. *Marine Geology*, 352, 25 –58.

Roveri, M., Gennari, R., Lugli, S., Manzi, V., Minelli, N., Reghizzi, M., ... and Schreiber, B. C. (2016). The Messinian salinity crisis: open problems and possible implications for Mediterranean petroleum systems. *Petroleum Geoscience*, *22*(4), 283-290.

Roveri, M., Lugli, S., Manzi, V., Reghizzi, M., and Rossi, F. P. (2020). Stratigraphic relationships between shallow-water carbonates and primary gypsum: insights from the Messinian succession of the Sorbas Basin (Betic Cordillera, Southern Spain). *Sedimentary geology*, *404*, 105678.

Ryan, W. B. F. (1973). Geodynamic implication of the Messinian crisis of salinity. *Messinian events in the Mediterranean*.

Ryan, W.B.F. (1976). Quantitative evaluation of the depth of the western Mediterranean before, during and after the Late Miocene salinity crisis. *Sedimentolog*y, 23(6), 791-813.

Ryan, W. B. F., and Cita, M. B. (1978). The nature and distribution of Messinian erosional surfaces — Indicators of a several-kilometer-deep Mediterranean in the Miocene. *Marine Geology*, 27, 193–230.

Santantonio, M., Scrocca, D. AND Lipparini, L. (2013). The Ombrina -Rospo Plateau (Apulian Platform): Evolution of a Carbonate Platform and its Margins during the Jurassic and Cretaceous. *Marine Petroleum Geology*, *42*, 4 -29.

Satolli, S., Speranza, F., and Calamita, F. (2005). Paleomagnetism of the Gran Sasso range salient (central Apennines, Italy): Pattern of orogenic rotations due to translation of a massive carbonate indenter. *Tectonics*, *24*(4).

Scisciani, V., and Esestime, P. (2017). The Triassic evaporites in the evolution of the Adriatic Basin. In *Permo-Triassic Salt Provinces of Europe, North Africa and the Atlantic Margins* (pp. 499-516). Elsevier.

Scisciani, V. and Calamita, F. (2009). Active intraplate deformation within Adria: Examples from the Adriatic region. *Tectonophysics, 476*, 57 -72.

Scrocca, D. (2006). Thrust front segmentation induced by differential slab retreat in the Apennines (Italy). *Terra Nova*, *18*(2), 154-161.

Scrocca, D., Carminati, E., Doglioni, C., and Marcantoni, D. (2007). Slab retreat and active shortening along the central-northern Apennines. In *Thrust belts and foreland basins* (pp. 471-487). Springer, Berlin, Heidelberg.

Sekulić, B., and Vertačnik, A. (1997). Comparison of anthropological and "natural" input of substances through waters into Adriatic, Baltic and Black Sea. *Water Research*, *31*(12), 3178-3182.

Selli, R., (1954). Su un livello-guida nel Messiniano romagnolo-marchigiano. Atti del VII Convegno Nazionale del Metano e Petrolio, Taormina 1, 192–195.

Selli, R. (1960) Il Messiniano Mayer -Eymar, 1867, Proposta di un neostratotipo. Giornale di Geologia, 28, 1 - 3.

Serpelloni, E., Vannucci, G., Pondrelli, S., Argnani, A., Casula, G., Anzidei, M., ... & Gasperini, P. (2007). Kinematics of the Western Africa-Eurasia plate boundary from focal mechanisms and GPS data. *Geophysical Journal International*, *169*(3), 1180-1200.

Sheriff, R. E. (1976). Inferring stratigraphy from seismic data. *AAPG Bulletin*, *60*(4), 528-542.

Sheriff, R. E., and Geldart, L. P. (1995). *Exploration seismology*. Cambridge university press.

Sonnenfeld, P., Finetti, I. (1985). Messinian evaporites in the Mediterranean: a model of continuous inflow and outflow. In *Geological evolution of the Mediterranean Basin* (pp. 347-353). Springer, New York, NY.

Spelic, M., Del Ben, A., Petrinjak., K. (2021). Structural setting ang geodynamic of the Kvarner area (Northen Adriatic). *Marine and Petroleum Geology*, 125, 104857.

Speranza, F., Adamoli, L., Maniscalco, R., and Florindo, F. (2003). Genesis and evolution of a curved mountain front: paleomagnetic and geological evidence from the Gran Sasso range (central Apennines, Italy). *Tectonophysics*, *362*(1-4), 183-197.

Speranza, F., Sagnotti, L., and Mattei, M. (1997). Tectonics of the Umbria-Marche-Romagna arc (central northern Apennines, Italy): New paleomagnetic constraints. *Journal of Geophysical Research: Solid Earth*, *102*(B2), 3153-3166.

Speranza, F., Islami, I., Kissel, C., and Hyseni, A. (1995). Paleomagnetic evidence for Cenozoic clockwise rotation of the external Albanides. *Earth and Planetary Science Letters*, *129*(1-4), 121-134.

Stampfli, G.M., (2005). Plate tectonics of the Apulia-Adria microcontinents. *In: Finetti, I.R. (Ed.), CROP Project: Deep Seismic Exploration of the Central Mediterranean and Italy, 1.* Elsevier, Amsterdam, pp. 447–470 (Elsevier, Atlases in Geoscience).

Stampfli, G. M., and Höcker, C. F. W. (1989). Messinian paleorelief from a 3-D seismic survey in the Tarraco concession area (Spanish Mediterranean Sea). *Geologie en Mijnbouw*, *68*(2), 201-210.

Stumm, W., Morgan, J. J., and Drever, J. I. (1996). Aquatic chemistry. *Journal of environmental quality*, *25*(5), 1162.

Tišljar, J., Vlahović, I., Velić, I., and Sokač, B. (2002). Carbonate platform megafacies of the Jurassic and Cretaceous deposits of the Karst Dinarides. *Geologia Croatica*, *55*(2), 139-170.

Tomljenović, B., Csontos, L., Márton, E., and Márton, P. (2008). Tectonic evolution of the northwestern Internal Dinarides as constrained by structures and rotation of Medvednica Mountains, North Croatia. *Geological Society, London, Special Publications*, *298*(1), 145-167.

Tomljenović, B., and Csontos, L. (2001). Neogene–Quaternary structures in the border zone between Alps, Dinarides and Pannonian Basin (Hrvatsko zagorje and Karlovac basins, Croatia). *International Journal of Earth Sciences*, *90*(3), 560-578.

Topper, R. P. M., Lugli, S., Manzi, V., Roveri, M., and Meijer, P. T. (2014). Precessional control of Sr ratios in marginal basins during the Messinian Salinity Crisis?. *Geochemistry, Geophysics, Geosystems*, *15*(5), 1926-1944.

Toscani, G., Bonini, L., Ahmad, M. I., Di Bucci, D., Di Giulio, A., Seno, S., and Galuppo, C. (2014). Opposite verging chains sharing the same foreland: Kinematics and interactions through analogue models (Central Po Plain, Italy). *Tectonophysics*, *633*, 268-282.

Trincardi, F., Campiani, E., Correggiari, A., Foglini, F., Maselli, V., and Remia, A. (2014). Bathymetry of the Adriatic Sea: The legacy of the last eustatic cycle and the impact of modern sediment dispersal. *Journal of Maps*, *10*(1), 151-158.

Trincardi, F., and Correggiari, A. (2000). Quaternary forced regression deposits in the Adriatic basin and the record of composite sea-level cycles. *Geological Society, London, Special Publications*, *172*(1), 245-269.

Trincardi, F., Correggiari, A., & Roveri, M. (1994). Late Quaternary transgressive erosion and deposition in a modern epicontinental shelf: the Adriatic semienclosed basin. *Geo-marine letters*, *14*(1), 41-51.

Urgeles, R., Camerlenghi, A., Garcia-Castellanos, D., De Mol, B., Garcés, M., Vergés, J., ... and Hardman, M. (2011). New constraints on the Messinian sealevel drawdown from 3D seismic data of the Ebro Margin, western Mediterranean. *Basin Research*, *23*(2), 123-145.

Usuglio, J. (1849). Analyse de l'eau de la Mediterranee sur la c**ô**tes de France. *Ann, Chim*., 27 (92-107) (1849), pp. 172-191.

Vai, G. B., and Ricci Lucchi, F. (1977a). The Vena del Gesso Basin in Northern Apennines. In *Field Trip Guidebook, Messinian Seminar n. 2, Gargano 1976, IGCP Pr. No 96 STEM-Mucchi Modena* (pp. 1-16).

Vai, G.B. (1994). Crustal evolution and basement elements in the Italian Area: palaeogeography and characterization. Boll. Geof. Teor. Appl., 36 (141–144) (1994), pp. 411-434

Vai G.B. (1997b). Cyclostratigraphic estimate of the messinian stage duration. *Montanari, G.S. Odin, R. Coccioni (Eds.), Miocene Stratigraphy: an Integrated Approach, vol. 15*, Developments in Paleontology and Stratigraphy (1997), pp. 463-476

Valyashko M.G. (1972). Playa lakes – a necessary stage in the development of a salt-bearing basin G. Richter-Bernburg (Ed.), Geology of Saline deposits, UNESCO, Paris (1972), pp. 41-52.

van Couvering, J.A., D. Castradori, M.B. Cita, F.J. Hilgen, D. Rio (2000). The base of the zanclean stage and of the Pliocene series- Episodes, 23–3 (2000), pp. 179-187.

van Hinsbergen, D. J., Torsvik, T. H., Schmid, S. M., Maţenco, L. C., Maffione, M., Vissers, R. L., ... and Spakman, W. (2020). Orogenic architecture of the Mediterranean region and kinematic reconstruction of its tectonic evolution since the Triassic. *Gondwana Research*, *81*, 79-229.

van Hinsbergen, D. J., and Meulenkamp, J. E. (2006). Neogene supradetachment basin development on Crete (Greece) during exhumation of the South Aegean core complex. *Basin Research*, *18*(1), 103-124.

van Hinsbergen, D. J. J., Hafkenscheid, E., Spakman, W., Meulenkamp, J. E., and Wortel, R. (2005). Nappe stacking resulting from subduction of oceanic and continental lithosphere below Greece. *Geology*, *33*(4), 325-328.

Velić, I., Tišljar, J., Vlahović, I., Velić, J., Koch, G., and Matičec, D. (2002a). Palaeogeographic variability and depositional environments of the Upper Jurassic carbonate rocks of Velika Kapela Mt. (Gorski Kotar Area, Adriatic carbonate platform, Croatia). *Geologia Croatica*, *55*(2), 121-138.

Velić, I., Tišljar, J., Atičec, and Vlahović, I. (1995). A review of the Geology of Istria. *Field Trip Guide Book The first Croatian Geol*. Cong., 21-30.

Velić, I., and Vlahović, I. (1994). Foraminiferal assemblages in the Cenomanian of the Buzet-Savudrija area (northwestern Istria, Croatia). *Geologia Croatica, 47*(1), 25-43.

Vlahović, I., Tišljar, J., Velić, I., and Ačec, D. (2005). Evolution of the Adriatic Carbonate Platform: Paleogeography main events and depositional dynamics. *Paleogeography, Paleoclimatology, Paleoecology*, 220, 333-360.

ViDEPI Project (Visibilità Dati Esplorazione Petrolifera in Italia) 2009http://unmig.sviluppoeconomico.gov.it

Warren, J. K. (2006). Depositional chemistry and hydrology. *Evaporites: sediments, resources and hydrocarbons*, 59-138.Wrigley, R., N. Hodgson, P. Esestime (2015). Petroleum geology and hydrocarbon potential of the Adriatic basin, offshore Croatia. J. Petrol. Geol., 38/3 (2015), pp. 301-316.

Wessel, P., Luis, J. F., Uieda, L., Scharroo, R., Wobbe, F., Smith, W. H., and Tian, D. (2019). The generic mapping tools version 6. *Geochemistry, Geophysics, Geosystems*, *20*(11), 5556-5564.

Wessel, P., and Smith, W. H. (1998). New, improved version of Generic Mapping Tools released. *Eos, Transactions American Geophysical Union*, *79*(47), 579-579.

Wessel, P., and Smith, W. H. (1995). New version of the generic mapping tools. *Eos, Transactions American Geophysical Union*, *76*(33), 329-329.

Wortmann, U. G., Weissert, H., Funk, H., and Hauck, J. (2001). Alpine plate kinematics revisited: the Adria problem. *Tectonics*, *20*(1), 134-147.

Wrigley, R., Hodgson, N., and Esestime, P. (2015). Petroleum geology and hydrocarbon potential of the Adriatic basin, offshore Croatia. *Journal of Petroleum Geology*, *38*(3), 301-316.

Yilmaz, O. (1987). Seismic data processing: Soc. *Expl. Geophys*, *252*.

Zappaterra, E., (1992). Regional distribution models of source rocks in the Periadriatic region. *Mem. Soc. Geol. Italy 45*, 817–822.

Zecchin, M., Donda, F., and Forlin, E. (2017). Genesis of the Northern Adriatic Sea (Northern Italy) since early Pliocene. *Marine and Petroleum Geology*, 79, 108-130.

Žibret, L., and Vrabec, M. (2016). Paleostress and kinematic evolution of the orogen-parallel NW-SE striking faults in the NW External Dinarides of Slovenia unraveled by mesoscale fault-slip data anaysis. *Geologia Croatica*, *69*(3), 295-305.